

# Microplastics as a vector for micropollutants in aquatic environments.

SOUZA MOURA, D.

2023

*The author of this thesis retains the right to be identified as such on any occasion in which content from this thesis is referenced or re-used. The licence under which this thesis is distributed applies to the text and any original images only – re-use of any third-party content must still be cleared with the original copyright holder.*

**Microplastics as a vector for micropollutants in  
aquatic environments**

**Diana Souza Moura**

**PhD**

**2023**

# **Microplastics as a vector for micropollutants in aquatic environments**

**Diana Souza Moura**

A thesis submitted in part fulfilment of the requirement of Robert Gordon  
University for the degree of Doctor of Philosophy

September 2023

# TABLE OF CONTENTS

TITLE PAGE .....	I
TABLE OF CONTENTS .....	III
DECLARATION.....	V
DEDICATION.....	VI
ACKNOWLEDGMENTS.....	VII
LISTS OF ABBREVIATIONS.....	VIII
ABSTRACT .....	XIII
THESIS STRUCTURE.....	XIIV
<b>CHAPTER 1: INTRODUCTION.....</b>	<b>1</b>
1.1 Water pollution .....	5
1.2 Natural pollutants.....	6
1.3 Anthropogenic pollutants in freshwater .....	7
1.4 Interaction of micropollutants with microparticles .....	21
1.5 Thesis aim and objectives .....	28
<b>CHAPTER 2: MICROPLASTIC SELECTION AND CHARACTERISATION.....</b>	<b>32</b>
2.1 Introduction .....	35
2.2 Materials and methods .....	47
2.3 Results and discussions .....	55
2.4 Conclusion and recommendation for the pre-experimental characterisation of microplastic particles .....	96
<b>CHAPTER 3: ADSORPTION OF CYANOTOXIN (MICROCYSTINS) ONTO MICROPLASTICS.....</b>	<b>98</b>
3.1 Introduction .....	100
3.2 Materials and methods .....	108
3.3 Results and discussion.....	119
3.4 Conclusions and environmental implications.....	140
<b>CHAPTER 4: ADSORPTION AND DESORPTION MECHANISM OF PHARMACEUTICALS ONTO AND FROM MICROPLASTICS .....</b>	<b>143</b>
4.1 Introduction .....	145
4.2 Materials and methods .....	153
4.3 Results and discussions .....	164
4.4 Conclusion and environmental implications .....	198

<b>CHAPTER 5: ECOTOXICITY OF MICROPLASTIC PARTICLES AND POLLUTANT-LOADED MICROPLASTIC PARTICLES TO DAPHNIA MAGNA.....</b>	<b>202</b>
5.1 Introduction .....	204
5.2 Materials and methods .....	210
5.3 Results and discussion .....	221
5.4 Conclusions and environmental impact.....	233
<b>CHAPTER 6: CONCLUSIONS AND FUTURE WORK.....</b>	<b>236</b>
6.1 Conclusions.....	237
6.2 Future work .....	241
REFERENCES .....	243
APPENDIX .....	276

## **DECLARATION**

I declare that the work presented in this thesis is my own, except where otherwise acknowledged, and has not been submitted in any form for another degree or qualification at any other academic institution.

Information derived from published or unpublished work of others has been acknowledged in the text and a list of references is given.

Diana S. Moura

## **DEDICATION**

Aos meus incomparáveis pais  
Rômulo e Lene

## **ACKNOWLEDGMENTS**

I am extremely grateful for the constant support, guidance, encouragement and excellent mentorship of my supervisory team, Dr Carlos Pestana, Professor Linda Lawton and Professor Colin Moffat. It was truly a pleasure to learn from them during this PhD. I am also deeply grateful to the Hydro Nation Scholar Programme funded by the Scottish Government through the Scottish Funding Council and managed by the Hydro Nation International Centre for funding this research.

The other members of CyanoSol in RGU were hugely helpful so thanks go to Professor Christine Edwards, Dorothy McDonald, Len Montgomery, Jane Moore, and Colin Sloan for all their help and advice at every stage of the process. In special, I would like to thank Indira Menezes for not only the immense support but her true friendship during this PhD.

I am also very grateful for the support provided by the RGU staff, especially Dr Colin Thompson and Andrea McMillian. I also would like to thank Dr Jianing Hui and Dr Nikoletta Gkoulemani from University of St Andrews for the characterisation of the microplastics and collaboration.

I am also extremely grateful for my friends who made this PhD and my time in Aberdeen an experience that will never forget. Huge thanks to Kai, Kam, Kwadjo, Eduardo, Teo, Nuruddin, Shubhada, and Katie.

Finally, I want to thank my family for the constant love and support that they have given me over the last few years. More importantly, I would like to thank my parents who I own everything. Their unconditional love and support made everything that I have accomplished possible. Thank you, dad, for showing me how is the dad I want for my kids. Thank you, mum, for showing me what is dedication and how is to have a best friend in my life. I am also grateful to my husband Leandro for believing in me and for being always by my side. Last but not least, I would like to thank my siblings Aline, César e Nara for being such an important part of my life that helped shaping who I am now.



## LIST OF ABBREVIATIONS

$\Sigma_{MC}$	Total amount of microcystin
$\Sigma_{PHA}$	Total amount of pharmaceuticals
AF	Assessment factor
AFW	Artificial freshwater
AMWPE	Average density polyethylene
ATR	Attenuated Total Reflectance
BET	Brunauer-Emmett-Teller
BMAA	$\beta$ -Methylamino-L-alanine
$C_{CTRL}$	Control concentration
$C_e$	Concentration at equilibrium
CI	Carbonyl index
<i>D. magna</i>	<i>Daphnia magna</i>
$D_{50}$	Median size
$D_{90}$	90% of the total volume of material in the sample is in the stated size range
DAB	2,4-diaminobutyric acid
DSC	Differential Scanning Calorimetry
$EC_{50}$	Half maximal effective concentration
EU	European Union
FT-IR	Fourier Transform Infrared

GF/F	Glass fibre filter category F (0.7 $\mu\text{m}$ )
HDPE	High density polyethylene
HPLC	High Performance Liquid Chromatography
LC <sub>50</sub>	Half maximal lethal concentration
LDPE	Low density polyethylene
MC	Microcystin
NOEC	No observed effect concentration
PA	Polyamide
PCB77	3,3',4,4'-tetrachlorobiphenyl
PDA	Photodiode array
PE	Polyethylene
PET	Polyethylene terephthalate
pKa	Acid dissociation constant
PNEC	Predicted no effect concentration
PP	Polypropylene
PPCP	Pharmaceuticals and personal care product
PS	Polystyrene
PSA	Particle Size Analysis
PVC	Polyvinyl chloride
Py-GCMS	Pyrolysis-gas chromatograph mass spectrometry
Q <sub>0</sub>	Maximum adsorption capacity

$q_e$	Amount of compound adsorbed per mass of adsorbent at equilibrium
$r$	Pearson correlation coefficient
$S_{BET}$	$N_2$ -Brunauer-Emmett-Teller adsorption-desorption surface area
SD	Standard deviation
SEM	Scanning Electron Microscopy
$S_{PSA}$	Simulated surface area
STGE	Shanghai Guanbu Electromechanical Technology Co. Ltd.
$t$	Time
$T_c$	Cold crystallisation exotherm temperature
TFA	Trifluoroacetic acid
$T_m$	Melting endotherm temperature
UHMWPE	Ultra-high molecular weight polyethylene
UK	United Kingdom
USEPA	United States Environmental Protection Agency
UV	Ultraviolet
v/v	Volume/volume
w/v	Weight/volume
WHO	World health organisation
WWTP	Wastewater treatment plant
$X_c$	Degree of crystallinity

XRD	X-Ray Diffraction
$\Delta H_c$	Enthalpy change associated to the cold crystallisation exotherm temperature
$\Delta H_m$	Enthalpy change associated to the melting endotherm temperature
$\Delta H_{m(100\%)}$	Reference value considering 100% crystalline polymer
$\zeta$	Zeta potential

## ABSTRACT

Poor water quality has been of increasing environmental concern, particularly related to man-made contaminants. It is becoming evident that microplastics can interact with micropollutants when co-existing in the environment. The aim of this thesis was to elucidate the potential role of microplastics as a vector for cyanotoxins (microcystins) and anthropogenic contaminants (pharmaceuticals) in freshwater. To this end, polypropylene (PP), polyethylene (PE), polyethylene terephthalate (PET), polyamide (PA), polystyrene (PS), and polyvinyl chloride (PVC) microparticles were acquired commercially in two sizes (described in this thesis as small,  $D_{50} < 35 \mu\text{m}$ , and large,  $D_{50} 95\text{-}157 \mu\text{m}$ ). The virgin microplastics were also artificially aged to achieve more environmentally relevant particles for experimentation. The virgin and artificially aged particles were fully characterised. The characterisation of the material received from the supplier led to a publication that highlights the importance of a detailed characterisation of commercially acquired microplastics for reliable interpretation of data. The analytical findings uncovered inconsistencies in the supplier stated purity and size of the commercial microplastics. Furthermore, eight microcystin analogues (MC-RR, -YR, -LR, -WR, -LA, -LY, -LW, and -LF), and five pharmaceuticals (ibuprofen, carbamazepine, venlafaxine, fluoxetine, and ofloxacin) were selected to evaluate their interaction with microplastics. The selected micropollutants were placed in contact with microplastics in a range of pollutant combinations (in mixtures and individually). Later, fluoxetine was selected to evaluate the adsorption and desorption mechanisms onto/from virgin and artificially aged, small PP, PA, and PVC. Finally, *Daphnia magna* neonates were exposed to the virgin and aged particles of fluoxetine-loaded small PP, PA, and PVC. Results demonstrated that the microplastic type, weathering of the microplastics, the

size of the particles, and the properties of the compound were all key factors affecting the adsorption onto microplastics. Among the microplastic types evaluated, small PP stood out with the greatest adsorption of microcystins (80-100%) and pharmaceuticals (16-97%). More worrying if available to aquatic life, the more toxic compounds (MC-LW, -LF, and fluoxetine) adsorbed in greater amounts onto the microplastics. For the microcystin analogues, results demonstrated the more toxic and more hydrophobic microcystin analogues (MC-LW and -LF) competed with the more hydrophilic analogues (MC-RR and -LR) for the binding sites on the microplastics. Furthermore, the aging of the microplastics for 72 h increased up to 30-fold the adsorption of pharmaceuticals onto microplastics, while decreasing the adsorption of microcystin onto small PP, PE, and PS. The bioavailability of the fluoxetine loaded onto microplastics also varied according to the microplastic type. Despite of the significant adsorption, almost no desorption was observed from small PP. On the other hand, up to 20% of the adsorbed fluoxetine desorbed from the small PA and PVC particles under freshwater environment conditions (pH 7, 25 °C). *D. magna* demonstrated to ingest PP, PA, and PVC particles when exposed to microplastics for 48 h. More importantly, all three microplastic types investigated either unloaded or when loaded with fluoxetine had a negative impact on the *D. magna* neonate's survival in a short period of exposure (48 h). This thesis has demonstrated that the ingestion of microplastics loaded with micropollutants can be a route for micropollutants into the food web with potentially hazardous effects to wildlife.

**Keywords:** Water Pollutants; Cyanobacteria; Pharmaceuticals; Polymer; Characterisation; Plastic weathering; Adsorption; Desorption; Ecotoxicity

## THESIS STRUCTURE

This thesis is divided into six chapters that consist of: the rationale for this research (chapter 1), the selection and characterisation of the microplastics investigated (chapter 2), the interaction of the natural toxin, microcystins, with microplastics (chapter 3), the interaction of pharmaceuticals with microplastics, the adsorption and desorption kinetics and mechanisms of a selected compound with selected microplastics types (chapter 4), and the evaluation of whether microplastics can act as a vector for micropollutants into the food chain and have toxic effects to *D. magna* (chapter 5). Finally, the last chapter consists of a conclusion of the findings of this thesis and proposal for future work (chapter 6).

The content of three publications contributed with this thesis. Pestana et al. (2021), provides foundational insights that underpin the entire thesis, however the data from Pestana et al. (2021) is not presented within. The publications Moura et. al (2023) and Moura et al. (2022) are integrated in the chapters 2 and 3, respectively. Together, these publications serve as essential pillars upon which this thesis is built.

# **Chapter 1**

## **Introduction**



<b>1 INTRODUCTION</b> .....	<b>1</b>
<b>1.1 Water pollution</b> .....	<b>4</b>
<b>1.2 Natural pollutants</b> .....	<b>5</b>
1.2.1 Cyanobacteria .....	6
<b>1.3 Anthropogenic pollutants in freshwater</b> .....	<b>7</b>
1.3.1 Pharmaceuticals .....	8
1.3.2 Plastic as a sub-set of polymers .....	10
1.3.3 Plastic applications world-wide .....	10
1.3.4 Plastic in the aquatic environment .....	12
1.3.5 Microplastics definition.....	14
1.3.6 Quantification and identification of microplastics in environmental samples .....	15
1.3.7 Microplastics in the aquatic environment .....	18
<b>1.4 Interaction of micropollutants with microparticles</b> .....	<b>21</b>
<b>1.5 Thesis aim and objectives</b> .....	<b>28</b>

## 1.1 Water pollutants

The deterioration of water quality has become a mounting environmental concern. Water pollutants can be classified as organic pollutants, inorganic pollutants, pathogens, suspended solids, nutrients and agriculture pollutants, thermal, radioactive, and other pollutants (Figure 1.1, Wasewar, Singh and Kansal 2020).

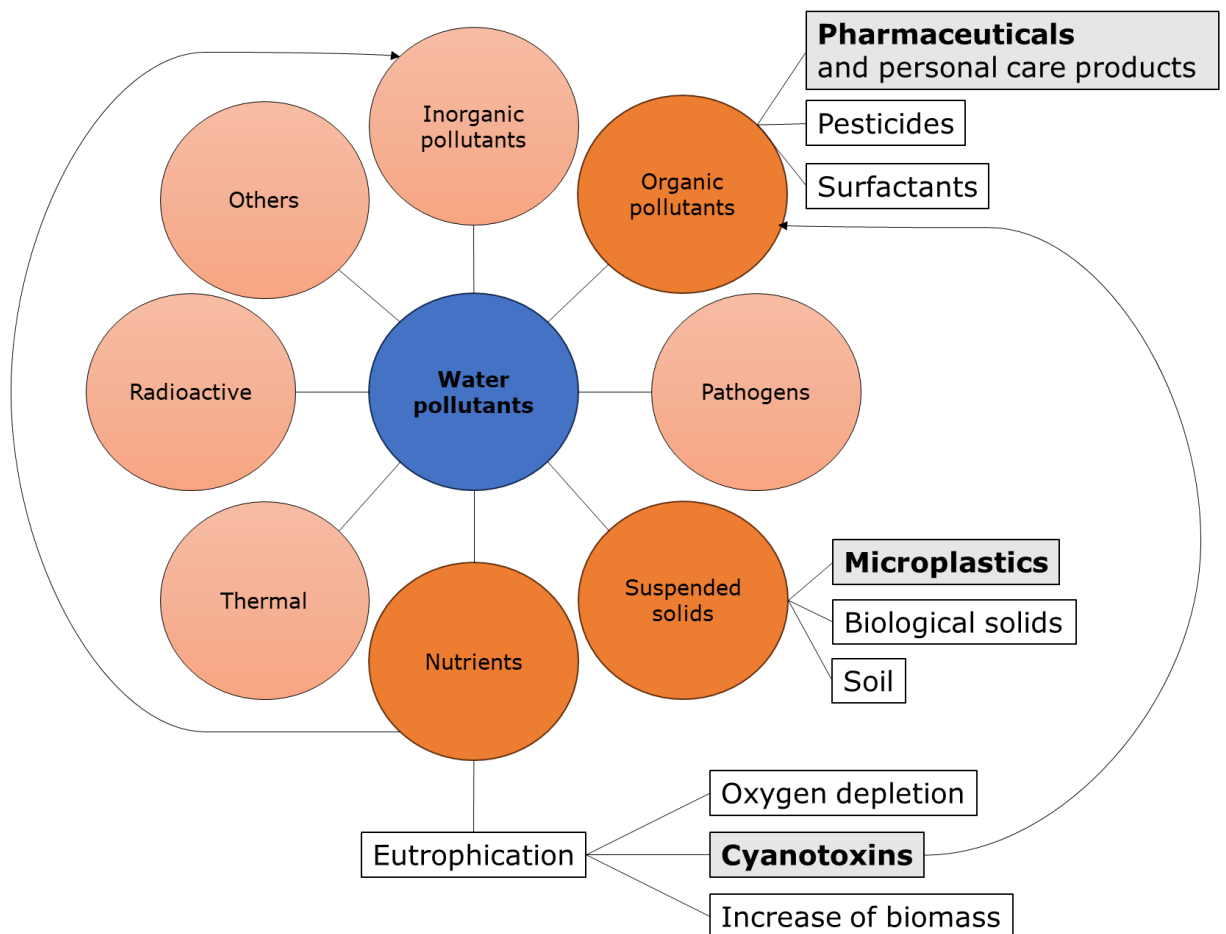


**Figure 1.1:** Types of water pollutants and some examples of water pollutants that can co-occur in the environment. The arrow represents that although the presence of cyanotoxins in water are led by the increase of nutrients, cyanotoxins also fit the organic pollutants category of water pollutants. Nutrients (e.g., phosphates and nitrates) can also fit the inorganic pollutants category.

Water pollutants can be derived from both natural and anthropogenic causes. For instance, the presence of nutrients (e.g., phosphates and nitrates), suspended solids (e.g., soil), and pathogens (e.g., parasites) in aquatic systems are

naturally part of an ecosystem. However, human activities can exacerbate the presence of these natural elements in the environment which can affect the equilibrium of the ecosystem. The discharge of untreated industrial and domestic wastewater and wastewater treatment (WWTP) effluents in aquatic environments are an important source of several water pollutants such as inorganic pollutants (e.g., mercury), organic pollutants (e.g., pharmaceuticals), pathogens (e.g., *Escherichia coli*), suspended solids (e.g., (nano, micro) plastics) and nutrients (e.g., nitrogen and phosphorus). The discharge of untreated wastewater effluents can also cause thermal pollution. Thermal pollution is the degradation of water quality by any process that changes the ambient water temperature. The temperature change can be caused by natural and/or anthropogenic activities, such as increased water system temperature due to solar radiation and heated industrial effluents (Speight 2020). Radioactive pollution occurs when radioactive materials are present or deposited in the atmosphere or environment. While there are several man-made sources of radiation pollution, natural sources such as cosmic rays, terrestrial rays, and the radiation found internally in every human can also cause radioactivity (The American Nuclear Society 2020).

## **1.2 Natural pollutants**

Increasing the concentration of nutrients in water bodies, either naturally or caused by human activities, can lead to eutrophication. Eutrophication is the earth's most widespread water quality problem (Schindler 2012). Initially, the term was mainly used to describe the natural aging of lakes, where a large, deep, nutrient-deficient lake gradually becomes more productive with plant and animal life and transforms into a pond, followed by a marsh as it becomes more nutrient-rich over time (Anderson, Glibert and Burkholder 2002). The availability

of nutrients in water bodies is not uniform and can range from very scarce to extremely abundant. This spectrum of water bodies includes those that are ultra-oligotrophic (very low food and nutrients), oligotrophic, mesotrophic (moderate food and nutrients), eutrophic, ultra-eutrophic, and hyper-eutrophic (very high food and nutrients, Boyd 2016). Potential effects of eutrophication, caused by the excessive input of phosphorus and, to a lesser extent, nitrogen to lakes, reservoirs, rivers and coastal oceans include (Dokulil and Teubner 2011):

- Increase of phytoplankton and macrophyte biomass
- Shift to bloom-forming algal species that might be toxic or inedible to wildlife
- Increase of biomass of benthic and epiphytic algae
- Change in macrophyte species composition
- Increase of biomass of consumer species
- Increase of fish kill incidences
- Reduction in species diversity
- Reduction in harvestable fish biomass
- Decrease in water transparency
- Oxygen depletion in the water body
- Increased drinking water treatment cost due to the presence/algal production of taste and odour compounds
- Decrease in the perceived aesthetic value of the water body

Although, eutrophication can be considered a natural process in aquatic systems, it has been accelerated by anthropogenic activities. According to the World Health Organisation (WHO), in large parts of the world, waterbody eutrophication started accelerating in the middle of the 20th century, in the wake of urbanisation and industrialisation (WHO 2021). During the 1960s and 1970s,

algal blooms were linked to nutrient enrichment resulting from anthropogenic activities such as agriculture, industry, and sewage disposal (Schindler 1974). Blue-green algae tend to dominate phytoplankton communities in eutrophic waters (Boyd 2016).

### **1.2.1 Cyanobacteria**

Blue-green algae is a term often used to refer to cyanobacteria. The term cyanobacteria was coined in 1977 by Stanier (Stanier 1977; Garcia-Pichel et al. 2020). This term was adopted instead of 'blue-green algae' to accurately classify and differentiate these photosynthetic organisms based on their bacterial nature rather than incorrectly associating them with algae. The term cyanobacteria reflects their characteristic blue-green colour (cyan) and their classification as bacteria (bacteria). Cyanobacteria are the most ancient phytoplankton on the planet and can form harmful algal blooms in freshwater, estuarine, and marine ecosystems (O'Neil et al. 2012). Cyanobacteria have left fossil remains as old as 2-3.5 billion years, and they are believed to be ultimately responsible for the oxygenation of Earth's atmosphere (Garcia-Pichel 2009). Today cyanobacteria make a significant contribution to the global primary production of the oceans and become locally dominant primary producers in many extreme environments, such as hot and cold deserts, hot springs, and hypersaline environments. Due to their highly adaptative nature, cyanobacteria have been detected in all continents across the globe (Hernández-Prieto, Semeniuk and Futschik 2014).

Cyanobacteria can form a great variety of secondary metabolites, which exhibit various types of biological or biochemical activities with some having been identified as potent toxins (cyanotoxins). The cyanotoxins are a diverse group of

compounds, both from the chemical and the toxicological points of view. In terms of their toxicological target, cyanobacterial toxins can act as hepatotoxins, neurotoxins, cytotoxins, dermatotoxins, and irritants (Bláha, Babica and Maršálek 2009).

### **1.3 Anthropogenic pollutants in freshwater**

Along with natural pollutants such as cyanotoxins, in the last decades, anthropogenic organic micropollutants have gained increased attention due to the ineffective removal in conventional drinking water treatment and WWTP, and consequential detection in the receiving waters (Luo et al. 2014). In 1995, the United Nations Environmental Programme Governing Council was aware of the concerns of the international community regarding the risks posed by an initial list of twelve persistent organic pollutants. In 1997, international action was deemed necessary to protect human health and the environment (United Nations Environment Programme 1997; Zimmerman, Thurman and Bastian 2000). Micropollutants are defined by their occurrence at low concentrations, but with concentrations remaining at trace levels, i.e. up to the microgram per litre range (Stamm et al. 2016). Micropollutants in aquatic systems include several classes of substances, such as pharmaceuticals and personal care products, including steroid hormones, industrial chemicals, pesticides, among others (Gorito et al. 2018). To date, WWTPs have been identified as the main source of micropollutants in water bodies (Abbasi et al. 2022). The occurrence of micropollutants in the aquatic environment has been frequently associated with a number of negative effects, including short-term and long-term toxicity, endocrine disrupting effects and antibiotic resistance in microorganisms (Luo et al. 2014).

### 1.3.1 Pharmaceuticals

Pharmaceutical compounds are highly bioactive, and therefore, undesired effects in organisms cannot be excluded after their discharge into the aquatic environment, where, owing to their polarity, they tend to be quite mobile (Schwarzenbach et al. 2010). Due to inefficient removal of pharmaceuticals and personal care product compounds, the release of WWTP effluent into surface waters has been considered the main cause of the presence of micropollutants in receiving watercourses (Kasprzyk-Hordern et al., 2009). Due to the increasing detection of micropollutants in aquatic environments, priority pollutant lists have been developed both by the European Union (EU) and the United States Environmental Protection Agency (USEPA) identifying a wide variety of chemicals present in wastewaters and storm water runoff that may pose a threat to receiving water bodies (Ebele, Abdallah and Harrad 2017). In the 2022 EU watch list of substances for world-wide monitoring in surface water, 12 out of 26 substances, are pharmaceutical compounds, including the antidepressant venlafaxine and the antibiotic ofloxacin. The main issues related to pharmaceutical residues in wastewater effluents are connected to their ecotoxicological effects, however there is also a growing concern about human health because of the presence of some of these compounds in drinking water derived from indirect or direct potable reuse (Schwarzenbach et al. 2010).

A study has demonstrated that an anxiolytic drug (oxazepam) altered behaviour and feeding rate of wild European perch (*Perca fluviatilis*) at concentrations encountered in effluent-influenced surface waters. The fish exposed to water with dilute drug concentrations ( $1.8 \mu\text{g L}^{-1}$ ) exhibited increased activity, reduced socialisation, and higher feeding rate (Brodin et al. 2013). Furthermore, a review

conducted by Bahamonde, Munkittrick and Martyniuk (2013), found that at least 37 fish species from 17 families have been identified with intersex gonads in 54 field survey studies, probably due to exposure to hormone-disrupting water pollutants. Intersex is defined by the authors as the simultaneous presence of male and female gonadal tissue in a gonochoristic (fixed sex) species.

Among the toxicity thresholds, predicted no effect concentration (PNEC) is usually adopted for risk assessment of pharmaceuticals. The estimation of PNECs is mainly based on two methods, including the assessment factor method and the statistical extrapolation method based on species sensitivity distributions. In the assessment factor method, PNECs are obtained based on the toxicity endpoints divided by an assessment factor. Both acute toxicities and chronic toxicities have been used as toxicity endpoints, such as the median lethal concentration ( $LC_{50}$ ), the median effect concentration ( $EC_{50}$ ) and no observed effect concentration (NOEC, Zhao et al. 2017) using test organisms such as the water flea, *Daphnia magna*.

In addition to dissolved organic compounds such as pharmaceuticals, another anthropogenic pollution is the presence of plastic in water. Plastic waste, composed of various synthetic polymers, poses a serious threat to aquatic ecosystems. Plastics, including microplastics and macroplastics, find their way into water bodies through improper waste disposal, runoff from landfills, and accidental or intentional spills.



### **1.3.2 Plastic as a sub-set of polymers**

Plastics are a synthetic or semisynthetic sub-set of polymers that are typically lightweight, strong, inexpensive, durable, and corrosion resistant (Napper and Thompson 2019). Plastics can also provide societal benefits: they play a critical role in maintaining food quality, safety and reducing food waste (Ritchie and Roser 2018), along with a wide range of medical applications. Polymers can be natural or synthetic and consist of a long string of repeating chemical units called a monomer (Wagner et al., 2014). Polymerisation is the name given to the types of reactions where many monomer units are chemically linked to form polymers (Brandau 2012). Every polymer, that forms plastics, has different properties such as density, crystallinity and rubberiness. The term plastics applies to a wide range of materials that at some stage in manufacture are capable of flow such that they can be extruded, moulded, cast, spun or applied as a coating (Thompson et al. 2009). For Cowie and Arrighi (2007), the main criterion is that plastic materials can be formed into complex shapes, often by the application of heat or pressure. Plastics can be subdivided into thermosetting and thermoplastic materials. Thermosetting materials become permanently hard once heated above a critical temperature and will not soften again on reheating (Cowie and Arrighi 2007). While, thermoplastics are from a family of plastics that can be reheated, reshaped and cooled repeatedly and represented 83.1% of the world plastic production in 2021 (Plastic Europe 2022).

### **1.3.3 Plastic applications world-wide**

Plastics are used for multiple applications world-wide. Leo Baekeland invented Bakelite, the first fully synthetic plastic that was used in electrical insulators, radio and telephone casings, kitchenware, jewellery, pipe stems, children's toys,

and firearms (Baekeland 1909). This marked the start of the modern plastics industry. Plastics are versatile, flexible, resistant, and cheap materials, widely used in modern society (Bertoldi et al. 2021). In 2021, approximately 352 million tonnes of fossil fuel-based plastics were produced in the world (Plastic Europe 2022). The single-use applications of plastics for sterile packaging, storage, transportation, and disposable medical parts play a significant role in its contribution to global waste (Zhao et al. 2022b). During the Covid-19 pandemic, plastics entered into the top three of the most widely manufactured materials in the world together with cement and steel (Williams and Rangel-Buitrago 2022). Plastics are often categorised by their polymer-based material. Every polymer has different properties, which makes plastics suitable for multiple applications (Table 1.1).

**Table 1.1:** List of most used polymer types in the world/European Union and a summary of their most common uses (Adapted from Plastics Europe 2020).

<b>Polymer type</b>	<b>Example of uses</b>
Polypropylene (PP)	Carrier bags, food packaging, sweet and snack wrappers, hinged caps, microwave containers, pipes, automotive parts, bank notes
Low density polyethylene (LDPE)	Reusable bags, trays and containers, agricultural film, food packaging film
High density polyethylene (HDPE)	Toys, milk bottles, shampoo bottles, pipes, houseware
Polyethylene terephthalate (PET)	Drink bottles, cleaners
Polyamide (PA)	Textiles, automotive industry, carpets, kitchen utensils and sportswear
Polystyrene (PS)	Food packaging (dairy, fish), building insulation, electrical and electronic equipment, inner liner for fridges, eyeglasses frames
Polyvinyl chloride (PVC)	Window frames, floor and wall coverings, pipes, cable insulation, garden hoses, inflatable pools

The production of plastic destined for packaging has dominated global primary plastic (plastics made from crude oil or gas) production since 1950, and polyolefins such as high- and low-density polyethylene (HDPE and LDPE,

respectively) and polypropylene (PP) account for 50% of total production (Hurley et al. 2020). Other types of polymers, e.g., polyvinyl chloride (PVC), polyethylene terephthalate (PET), polystyrene (PS), and polyamide (PA) represent approximately 30% of the combined plastic production (Plastic Europe 2022). The majority of monomers used to make plastics (i.e., ethylene and propylene) are derived from fossil hydrocarbons, therefore are not readily biodegradable. As a result, they accumulate, rather than decompose, in landfills or the natural environment (Geyer, Jambeck and Law 2017).

#### **1.3.4 Plastic in the aquatic environment**

Prior to 1980, recycling and incineration of plastic was negligible, therefore nearly 100 percent was discarded (Ritchie and Roser 2018). From the 1950s to 2015, it was estimated that approximately 8,300 million tonnes of plastic have been manufactured with 4,900 million tonnes (60%) residing in a landfill or the environment (Geyer, Jambeck and Law 2017; Sorensen and Jovanović 2021). In 2015, an estimated 55% of global plastic waste was discarded, 25% was incinerated, and 20% recycled (Ritchie and Roser 2018). In the United Kingdom (UK), 19% of post-consumer plastic waste was sent to landfill in 2020 (Plastic Europe 2022). In 2010, a study estimated, that 8 million tonnes of plastic (3% of the global annual plastic waste) entered the oceans through multiple outlets, including rivers, annually (Ritchie and Roser 2018). A study conducted by Greenpeace (2019) has found that all of the 13 surveyed rivers throughout the UK contained plastic pollution (Greenpeace 2019), including river Clyde in Scotland (Figure 1.2).



**Figure 1.2:** River Clyde in Glasgow, UK, where plastic pollution is visible on the banks of the river.

When plastics enter the environment, plastics can easily be transported due to their light weight (Zhang et al. 2021). Precipitation, surface runoff, and riverine transport are the potential main routes that transfer plastics from land to waters (van Emmerik et al. 2019). In the aquatic environment, plastic debris is exposed to continuous photo-oxidation and/or mechanical abrasion that can lead to plastics being fragmented into smaller sized particles (Kyoung Song et al. 2017). Photo-oxidation is the degradation and fragmentation of plastic when exposed to sunlight, especially due to ultraviolet radiation (100-400 nm). This process is a result of the absorbance of high-energy wavelengths of the ultraviolet spectrum by the polymers (Napper and Thompson 2019), resulting in thermal- and photo-oxidation which ultimately leads to fragmentation. Due to fragmentation, plastics can enter the aquatic environment in a wide range of sizes.

### **1.3.5 Microplastics definition**

Typically, there are three categories used to describe plastics according to their size: macroplastic (> 20 mm diameter), mesoplastic (5-20 mm) and microplastic (< 5 mm, Napper and Thompson 2019). Currently, the European Marine Strategy Framework Directive Working Group on Good Environmental Status defines large microplastics as size from 1 to 5 mm, and small microplastics, from 20 µm to 1 mm (Hanke et al. 2013). The term nanoplastics is still under debate, and some authors set the upper size limit at 1,000 nm while others at 100 nm (Gigault et al. 2018).

Microplastics (< 5 mm in all dimensions) are divided into primary, i.e., manufactured small plastic particles, and secondary, plastics fragmented due to physical, chemical, and biological interaction (Thompson et al. 2009). The most abundant type of microplastics in the environment (Weithmann et al. 2018) are secondary plastics, typically derived from fragmentation of larger plastic debris items either during use of products or due to weathering degradation of plastic litter (Andrady 2017). In the literature, the term microplastic is used to describe either polymer particles or plastic particles with a size smaller than 5 mm. To avoid confusion and because it is the more common term, "microplastic(s)" will be used in this thesis to describe all plastic and polymer particles that measure less than 5 mm in all dimensions.

### 1.3.6 Quantification and identification of microplastics in environmental samples

The identification of microplastic in environmental samples is challenging and yet not standardised. There are several approaches to detect and quantify microplastics in environmental samples. According to Sarijan et al. (2021), at least four steps are usually employed based on the literature reviewed by these authors. The steps consist of collection of the samples, separation of microplastics from other particles, visual inspection of the particles, and analysis of the material collected (Figure 1.3).

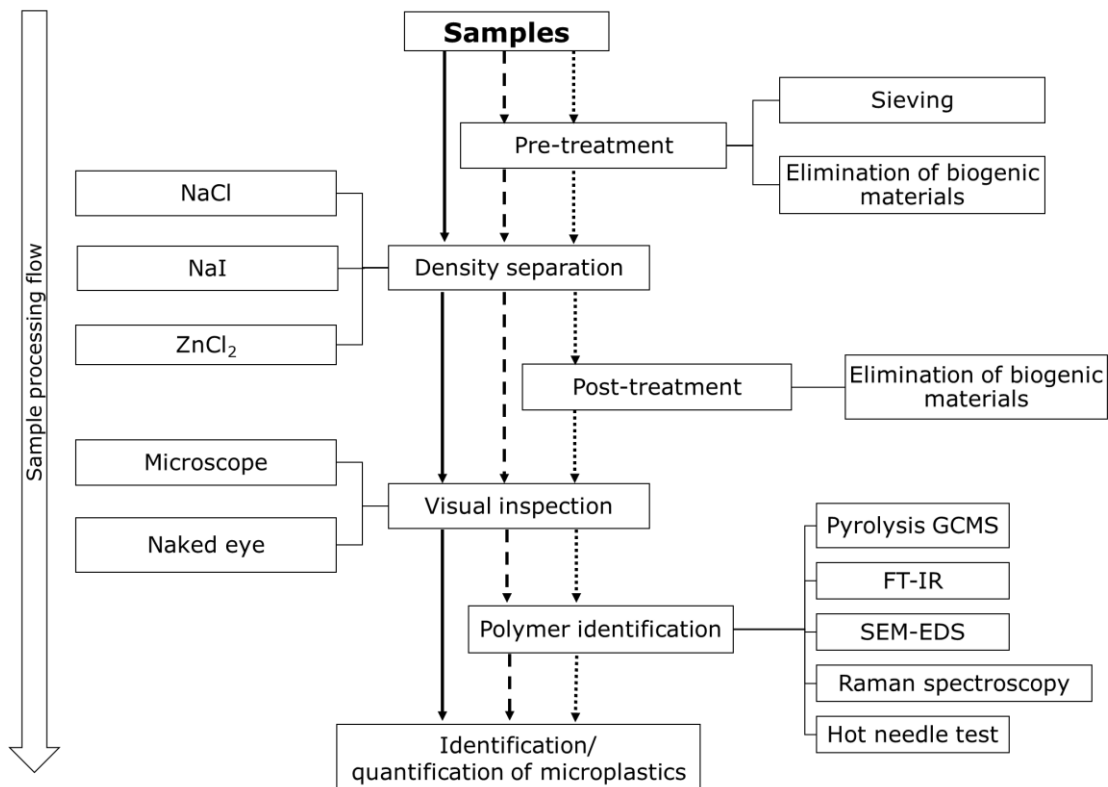


**Figure 1.3:** Strategies to analyse microplastics in the environment reported in the literature. Each arrow represents a possible analysis route published (Adapted from Sarijan et al. 2021).

A great challenge in the identification of microplastics in environmental samples, is cross contamination. To minimize the presence of microplastics in environmental samples, including airborne particles, it is important to implement

certain precautions during the sampling process. According to Prata et al. (2019), the precautions are: (1) opt for glass and metal tools, (2) avoid the use of synthetic textiles and prefer 100% cotton lab coats, (3) clean surfaces using 70% ethanol and paper towels, wash equipment with acid followed by ultrapure water, use consumables directly from packaging, and filter all working solutions, (4) use open petri dishes, procedural blanks, and replicates to monitor and control for airborne contamination, (5) keep samples covered as much as possible and handle them in clean rooms with controlled air circulation, (6) limit access by keeping doors and windows closed, and preferably carry out the process in a laminar airflow hood or an algae-culturing unit. Alternatively, cover the equipment while handling the samples. A laminar airflow hood can reduce contamination by 50%, and covering the samples during filtration, digestion, and visual identification can reduce contamination by over 90% (Prata et al. 2019).

Neuston, manta and plankton nets, sieving, pumps, and filtration are common sampling methods used to collect microplastic in aquatic environments, including freshwater. Pump sampling consist of pumping water manually or using a motor through an inline filter. Sieving can be used as both sampling method and pre-treatment to reduce volume of samples on-site as it gives a promising specimen volume without the need to transfer the whole to the laboratory. In a study that reviewed 150 investigations for sampling microplastics in surface water and sediments demonstrated that manta nets (often with a mesh size of 333  $\mu\text{m}$ ) are the main sampling tool for microplastic separation from surface water (Razeghi et al. 2021). However, the authors suggested that by using manta nets, a significant fraction of small microplastic particles is very likely to be underestimated because they might pass through the net. Especially, fibres are

typically small (Cole 2016), hence easily missed when using a manta net trawl to sample (Eriksen et al. 2013; Koelmans et al. 2019).

Density separation is a commonly used technique to separate microplastics from samples. Differences in density can be used to separate plastics from other suspended solids, usually by carefully mixing the water sample with salt saturated solutions and collecting the supernatant containing microplastics for further filtration. The common salt used for density separation is sodium chloride (NaCl,  $\rho = 1.2 \text{ g cm}^{-3}$ ) since this salt is low-cost, highly available, and ecofriendly. Other salt solutions used are potassium formate (KF,  $\rho = 1.91 \text{ g cm}^{-3}$ ), sodium iodide (NaI,  $\rho = 1.6\text{--}1.8 \text{ g cm}^{-3}$ ), zinc bromide ( $\text{ZnBr}_2$ ,  $\rho = 1.7 \text{ g cm}^{-3}$ ), and zinc chloride ( $\text{ZnCl}_2$ ,  $\rho > 1.6 \text{ to } 1.7 \text{ g cm}^{-3}$ ). NaI,  $\text{ZnBr}_2$ , and  $\text{ZnCl}_2$  have higher densities than NaCl. Hence, these salt solutions can offer consistent separation for higher density microplastic types such as PET and PVC. However, NaI and KF are expensive salts, thus they are not viable for large volume and/or high number of samples. Moreover, the ecological hazards (reported toxic effects to wildlife) of  $\text{ZnCl}_2$  and  $\text{ZnBr}_2$  also complicate their disposal (Sarijan et al. 2021). As result, there is a possibility that high-density plastics may not have been sufficiently considered in the analysis of microplastics, which use low-density separation solutions such as NaCl (Kye et al. 2023).

The manual counting under a stereomicroscope is the most simple and thus widely used method to count microplastics collected in the environment (Li, Liu and Chen 2018). However, according to Dris et al. (2015), identification by visual observation is less reliable due to this method subjectivity, which may produce wide variations between observers and is highly time consuming. To assure



reliable assessment of plastic particles, Koelmans et al. (2019) suggested that the polymer identity needs to be confirmed, preferably by using (micro) FT-IR or Raman spectroscopy, pyrolysis-gas chromatograph mass spectrometry (Py-GCMS) or thermogravimetry-GCMS techniques. Characterising microplastics using (micro) FT-IR or Raman spectroscopy offers non-destructive chemical identification but may be surface-sensitive and struggle with mixed plastics. Pyrolysis-GCMS, on the other hand, provides a chemical fingerprint and high sensitivity but is destructive and requires complex data analysis. Meanwhile, thermogravimetry-GCMS reveals thermal behaviour and volatile products but can lack detailed chemical information and involves complex data interpretation.

### **1.3.7 Microplastics in the aquatic environment**

Microplastics are an abundant type of plastic debris in some locations, e.g. the North Pacific, the Gulf of Alaska, the Bering Sea, and Southern California (Shaw 1977; Gilfillan 2009; Goldstein, Rosenberg and Cheng 2012). In recent years, the presence of microplastics in the environment has been globally reported (Li, Liu and Chen 2018). Microplastics were widely detected in environments such as sediments (Blair et al. 2019), lakes (Bertoldi et al. 2021), rivers (Cera et al. 2022), ground water (Mintenig et al. 2019), seawater (Wang et al. 2021), and glaciers (Ambrosini et al. 2019). However, most research efforts have been focused on monitoring microplastics in seawater. Tyre debris and WWTP are important sources of microplastics in freshwater systems (Mani et al. 2015). Studies have identified microplastics in varied freshwater systems across continents (Eerkes-Medrano et al. 2015). Rivers act as a major pathway to transport most of the plastic debris from land to the marine environment, therefore the knowledge on the occurrence of microplastics in the freshwater

environment is crucial to understand its sources and transport into the ocean (Sarijan et al. 2021). Until 2018, less than 4% of microplastic-related studies were focused on freshwaters (Li, Liu and Chen 2018). In the past five years (2018 and end of 2022), there was an increase of microplastic research in freshwater environments (approximately 1,300 published studies), while approximately 6,000 publications focussed on the marine environment (Web of Science, 2023). Further, according to Li, Busquets and Campos (2019), freshwater environments are often nearer humans activities, thus the potential threat of pollution can be higher than in the marine environment. Freshwater systems are also often used as catchments for wastewater effluents and sewage overflows, which can make these environments susceptible to the co-occurrence of various pollutants in higher concentrations. Taking into account the significant role of freshwater ecosystems in microplastic pollution, the limited attention given to them previously, and their vulnerability to pollution, investigating microplastics in these environments, the focus of the current thesis will be the freshwater ecosystem.

Usually, the plastic particles reported in the environment are categorised on the basis of their size, shape (Table 1.2) and colour. Fragments are the dominant shapes reported in the majority of literature cited for this thesis which concurs with the review of Koelmans et al. (2019), who also state that fragments are the most reported microplastic encountered in the freshwater environment. Fibres were also an abundant microplastic shape reported in freshwater systems (Baldwin et al., 2016). Recently, fibres were also the predominant microplastic reported in glaciers (Ambrosini et al. 2019).

**Table 1.2:** Category definition of microplastics forms commonly reported in freshwater environment around the world and a summary of their potential source.

Category	Definition	Potential Source	Reference
Fragment	Secondary plastic broken down from larger debris	Bottles, hard, sturdy plastics	Cable et al. (2017)
Film	Thin plastic from bags and wrappers	Plastics bags, wrappers, or sheeting	
Fibre	Individual filaments of textile threads, very thin and frequently curled	Clothing or textiles	
Line	Fishing line, straighter, and thicker than fibre	Fishing line/nets	
Foam	Lightweight, sponge-like	Foam floats, Styrofoam	Miller et al. (2017)
Sphere/ Spherules	Particles with a homogeneous sphere. E.g., Pellet: Hard, rounded plastic particles. Nurdle is a sub-set of pellets.	Primary plastics, virgin pellets, cosmetic products	Mani et al. (2015)

The size and colours of the microplastics reported in the freshwater environment are heterogeneous and the range of the sizes investigated in the literature is varied. However, Koelmans et al. (2019) show that studies aimed at smaller particles, generally find higher particle numbers. The shape of microplastics can be divided into fragments, fibres, films, lines, pellets, and spherules. The most common types of microplastics reported in freshwater are PP and PE particles (Figure 1.4). Greenpeace (2019) has found microplastics in 28 out of 30 locations tested throughout the UK, with PE (46%), PS (23%), and PP (17%) making up more than 80% of the microplastic types found. It is expected that buoyant microplastics, such as PP and PE (density < 1 g cm<sup>-3</sup>), are more easily detected when sampling methods such as a manta net (Bertoldi et al. 2021) and density separation using NaCl (Ambrosini et al. 2019) are used. However, PP and PE were also the microplastic types most reported in the sediment samples from a stormwater pond in Denmark (Molazadeh et al. 2022). The dominant presence of PP and PE in freshwater is predictable since PP and PE are the most used plastics according to Plastics Europe (2020), also PP and PE are mainly used in

Europe for 'single-use' purposes, e.g. packing. Following PP and PE; PET, PA, PS, and PVC are in the top 8 of the microplastic types detected in freshwater bodies (Figure 1.4, Koelmans et al. 2019).

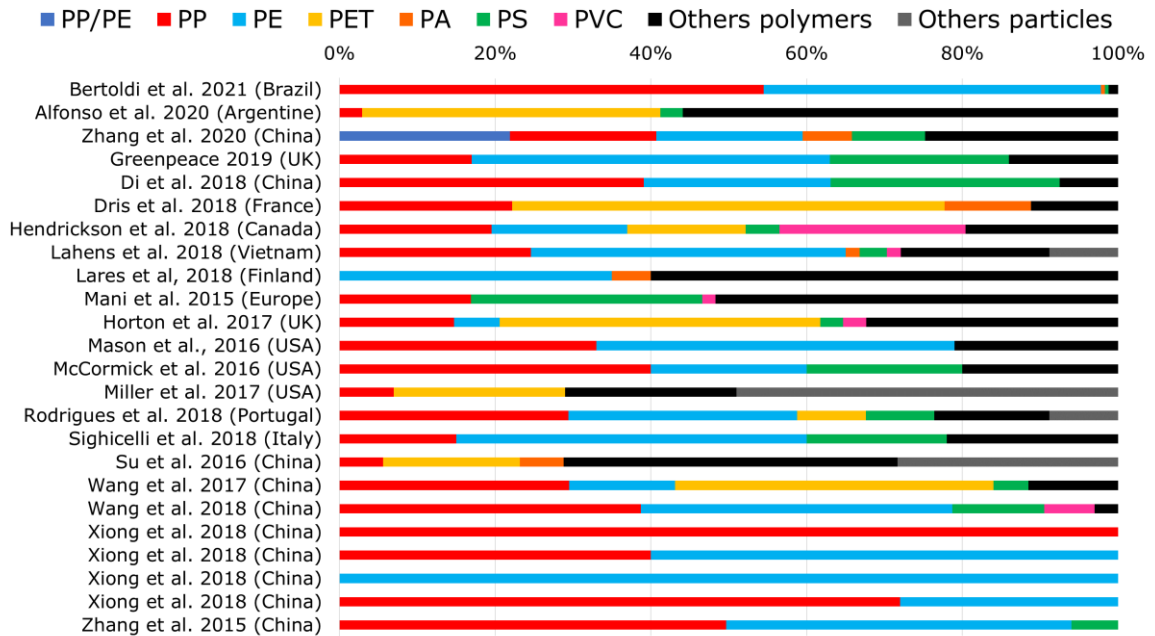


**Figure 1.4:** Percent distribution of microplastic types detected in freshwater environments world-wide reported by 19 studies. Polypropylene (PP, ■), polyethylene (PE, ■), polyethylene terephthalate (PET, ■), polyamide (PA, ■), polystyrene (PS, ■), and polyvinyl chloride (PVC, ■). The microplastics that could not be distinguished as either PP or PE was defined by the authors as polypropylene/polyethylene (PP/PE, ■). Other polymers (■) included other polymeric particles such as unspecified polyester and poly (methyl methacrylate) a.k.a. acrylic. Other particles (■) relate to non-polymeric particles smaller than 5 mm.

## 1.4 Interaction of micropollutants with microparticles

It is expected that freshwater bodies with poor water quality have multiple micropollutants, such as cyanotoxins and pharmaceuticals, co-occurring with microplastics. Several studies have demonstrated micropollutants can interact with microplastics when in the same environment (Table 1.3). The studies were selected mainly according to the media used to evaluate the interaction of microplastics and the selected compounds (freshwater). Studies published in the past five years (2018-2022) or highly cited (over 250 citations) were selected.

Furthermore, two publications that this author has contributed to were selected (Pestana et al. 2021; Petrie et al. 2023).

**Table 1.3:** Selection of studies that investigated the adsorption of chemicals onto microplastics in freshwater medium per polymer type, polymer size (as stated by the authors), octanol-water partition coefficient (log K<sub>ow</sub>) and main adsorption results reported by the studies.

Chemical	Plastic	Plastic concentration (mg L <sup>-1</sup> )	Medium	Particle size (µm)	log K <sub>ow</sub>	Adsorption preference	Reference
Pyrene (Pyr)	HDPE PS PVC	200	Artificial Freshwater	100-150	-	PVC<PS<HDPE	Wang and Wang (2018a)
Carbamazepine (CBZ) 4-methylbenzylidene camphor (4MBC) Triclosan (TCS) 17α-ethinyl estradiol (EE2)	LDPE debris	200; 1,000	Water + CaCl <sub>2</sub> + NaN <sub>3</sub>	250-280	CBZ - log K <sub>ow</sub> 2.45 4MBC - log K <sub>ow</sub> 5.1 TCS - log K <sub>ow</sub> 4.76 EE2 - log K <sub>ow</sub> 3.67	CBZ<EE2<TCS<4MBC	Wu et al. (2016)
Perfluorinated alkylated substances (PFAS)	HDPE micro spheres, PS PS-COOH <sup>a</sup>	2; 5	Natural freshwater	3-16	-	HDPE<PS-COOH<PS	Llorca et al. (2018)
Sulfadiazine (SDZ) Amoxicillin (AMX) Tetracycline (TC) Ciprofloxacin (CIP) Trimethoprim (TMP)	PS PP PS PA PVC	0.5; 1; 5; 10; 15	Ultrapure water	75-180	SDZ - log K <sub>ow</sub> -0.06 AMX - log K <sub>ow</sub> 0.87 TC - log K <sub>ow</sub> -1.37 CIP - log K <sub>ow</sub> 1.32 TMP - log K <sub>ow</sub> 0.91	PVC≈PS<PP≈PE<PA TC<SDZ<TMP<AMX<CIP	Li et al. (2018)
Ag, Cd, Co, Cr, Cu, Hg, Ni, Pb, Zn	Virgin PE and Aged PE pellets	10; 400	River water	4,000	-	Virgin PE<aged PE (Others metals) <Cu<Ag<Zn<Hg<Pb	Turner and Holmes (2015)
n-Hexane (nHex) - Cyclohexane (cHex) Benzene (Ben) Toluene (Tol) Chlorobenzene (ClBen) Ethylbenzoate (eBenz) Naphthalene (Naph)	PE PS PVC PA	2,000-6,000	Water + CaCl <sub>2</sub> + NaN <sub>3</sub>	< 250	nHex - log K <sub>ow</sub> 3.9 cHex - log K <sub>ow</sub> 3.44 Ben - log K <sub>ow</sub> 2.18 Tol - log K <sub>ow</sub> 2.72 ClBen - log K <sub>ow</sub> 2.84 eBenz - log K <sub>ow</sub>	PA<PE<PVC<PS (Others compounds) <Naph<cHex<nHex	Hüffer and Hofmann (2016)

Chemical	Plastic	Plastic concentration (mg L <sup>-1</sup> )	Medium	Particle size (µm)	log K <sub>ow</sub>	Adsorption preference	Reference
					2.64 Naph - log K <sub>ow</sub> 3.36		
Cadmium (Cd)	HDPE	28, 571	Distilled water	1,000-2,000 600-1,000 100-154	-	1,000-2,000 <600-1,000 <100-154	Wang et al. (2019)
Ciprofloxacin	PS PVC Aged PS Aged PVC	400	Not reported	75	log K <sub>ow</sub> 0.4	PS<PVC< Aged PVC <Aged PS	Liu et al. (2019)
Phenanthrene (Phe)	PE PS PVC Natural sediment	400	Artificial freshwater + NaN <sub>3</sub>	100-150	-	Natural sediment< PVC<PS<PE	Wang and Wang (2018b)
Sulfamethoxazole (SMX) Sulfamethazine (SMT) Cephalosporin C (CEP-C)	Naturally aged PS, Naturally aged PE	2,000	Freshwater	500-1,000 100-200	SMX - log K <sub>ow</sub> 0.89 SMT - log K <sub>ow</sub> 0.14 CEP-C - log K <sub>ow</sub> - 2.4	PE<PS CEP-C<SMT< SMX	Guo and Wang (2019)
Propranolol hydrochloride (PNL) Fluoxetine hydrochloride (FLX)	Bioplastics PA Cellulose	2,500	Ultrapure + CaCl <sub>2</sub>	Bioplastic: 1-310 PA: 4-211 Celulose: 11-352	PNL: log D <sub>ow</sub> <sup>b</sup> (pH 7.5) - 1.55 FLX: log D <sub>ow</sub> <sup>b</sup> (pH 7.5) - 1.75	Cellulose<polyamide <bioplastics FLX>PNL	Petrie et al. (2023)
Microcystin - LR (MC-LR) Microcystin - LF (MC-LF)	PET debris LDPE debris PVC debris PS debris	10,000	Artificial freshwater	90-125 250-500 1,000-5,000	MC-LR - log D <sub>ow</sub> <sup>b</sup> (pH 7) - 1.2 MC-LF - log D <sub>ow</sub> <sup>b</sup> (pH 7) - 0.06	MC-LR<MC-LF PET<LDPE≈ PVC <PS 1,000-500< 250-500< 90-125	Pestana et al. (2021)

<sup>a</sup> PS-COOH: polystyrene carboxylate

<sup>b</sup> Log D<sub>ow</sub> is the pH dependent octanol-water partition coefficient

'Sorption' is the generic term that is often used to refer to the interaction between a micropollutants (sorbate) and microplastics (sorbent), on the other hand, the term 'adsorption' refers when surface interaction is taking place (Velez et al. 2018). Adsorption can occur because of physical forces or by chemical bonds (Artioli 2008). Many studies show that adsorption, either mono or multilayer, dominates the interaction of organic compounds with microplastics. The results in this thesis also support that adsorption takes place regarding the interaction of selected micropollutants onto microplastic. For this reason, the term 'adsorption' will be adopted from now on.

Due the potential of plastic particles to act as a vector for micropollutants in aquatic systems, several studies have been performed to evaluate the adsorption of micropollutants onto microplastics. Characteristics, such as the microplastic type, pollutant hydrophobicity, and media seemed to affect the adsorption behaviour. For instance, according to Guo and Wang (2019), the surface roughness of microplastics can significantly influence the adsorption capacity. External factors, such as temperature, pH, salinity, and composition of the water phase can also influence the adsorption capacity (Wang and Wang, 2018a). The log  $K_{ow}$  is a measure of hydrophilicity/lipophilicity of compounds (Leo, Hansch and Elkins 1971; Mackay et al. 1980; Cumming and Rucker 2017). A chemical with a high log  $K_{ow}$  will have a lower water solubility than less hydrophobic substances, with a lower log  $K_{ow}$ . This means that hydrophobic substances will preferentially bind to a hydrophobic particulate, such as microplastics (Horton et al. 2018). The hydrophobicity of organic contaminants is important in the determination of their adsorption onto microplastics (Huffer and Hofmann 2016). Several studies have shown that plastics have clear selectivity



towards hydrophobic organic contaminants (Moura et al. 2022; Pestana et al. 2021; Razanajatovo et al. 2018; Wang et al. 2018). However, organic compounds can be ionisable, with the extent of their ionisation varying with the pH of the media (Wagstaff, Lawton and Petrie 2021). This needs to be taken into account when considering the environmental fate of such compounds and is done using the pH dependent octanol-water partition coefficient ( $\log D_{ow}$ ).

Aged microplastics have been shown to have a high adsorption capacity for hydrophobic organic pollutants (Zhang 2019). Turner and Holmes (2015) demonstrated that aged microplastics had a higher adsorption coefficient for metal cations and oxyanions (anion containing oxygen), than metal anions without oxygen. According to the authors, there is evidence that weathered microplastics could adsorb a greater amount of hydrophilic pollutants because aged pellets tend to acquire an inherent surface charge and a greater surface area through photo-oxidation.

The investigation of the interaction of micropollutants in contact with microplastics has gained momentum over the past years. However, the effect of the interaction of microplastics with micropollutants in the environment is still undetermined. Furthermore, the body of research focussed on this topic still lacks understanding of important aspects regarding this interaction. For instance, micropollutants are often detected as mixture of contaminants in freshwater environments (Moura et al. 2022). However, most research has focused on the evaluation of individual compounds onto microplastic types which often do not represent those found in the freshwater environment. Commonly found

freshwater pollutants in contact with microplastics have been under-investigated. For instance, the adsorption of pharmaceuticals on suspended particulate matter has been much less investigated than that of more hydrophobic micropollutants such as polychlorinated biphenyls, a class of chlorinated organic chemicals that are used for a variety of industrial and commercial purposes (Johnson et al. 1964), or polycyclic aromatic hydrocarbons, compounds found in crude oil and often produced as a result of combustion (Boulard et al. 2020). Furthermore, while some work has been undertaken to understand the adsorption of synthetic compounds onto microplastics, little work has explored the adsorption of natural pollutants present in freshwater systems.

The microplastic types, shapes, and sizes most commonly used in research, on occasion does not represent what is found in freshwater systems. Meng et al. (2019) affirm that, often, the microparticles used in experiments are not representative of the polymer types and shapes detected in the environment, since there is a focus on spherical particles rather than fragments and fibres. Furthermore, due to the difficulty to either produce in the laboratory or to commercially acquire microplastics smaller than 100  $\mu\text{m}$ , the impact of such small particles in the environment is under-investigated. This is of concern since smaller particles are more likely to be ingested by the wildlife (Nematdoost Haghi and Banaee 2017). Moreover, the study of virgin microplastics over aged particles can lead to an underestimation of the amounts of the studied compounds adsorbed onto microplastics.

Along with the interaction of micropollutants, microplastics are reported to be ingested by wildlife when in the environment. The effects of the ingestion of

microplastic itself has been reported in the literature (Roman et al. 2020). However, the impact of micropollutant-loaded microplastics ingested by aquatic organisms has not yet been evaluated.

## **1.5 Thesis aim and objectives**

The aim of this thesis is to elucidate the potential role of environmentally relevant microplastics as a vector for natural and anthropogenic contaminants, both as individual compounds and as mixtures, and to assess the bioavailability (availability of the compound adsorbed onto microplastics to wildlife) and the potential toxicity of the compounds adsorbed onto the particles should they desorb in the digestive track of biota. Therefore, the objectives are:

### *Objective 1: Selection and microplastic characterisation (chapter 2)*

- 1.1 This thesis will select the microplastic types and the particle sizes most reported in the freshwater environment for experimentation.
- 1.2 This thesis will develop an accelerated artificially aging protocol to achieve more environmentally relevant microplastics.
- 1.3 Information such as polymer composition, particle size, surface area, crystallinity, and weathering of microplastics is essential to ensure a reliable interpretation of data and key factors affecting the interaction of organic compounds with microplastics. Therefore, a detailed characterisation of the acquired microplastics and the artificially aged microplastics will be performed to fully understand the physico-chemical properties of the microplastics investigated.

*Objective 2: Evaluation of the interaction of micropollutants with microplastics (chapter 3 and chapter 4)*

Microplastics often co-occur with cyanotoxins and anthropogenic contaminants such as pharmaceuticals in freshwater environments.

2.1 This thesis will determine whether different selected cyanotoxins (chapter 3) and selected, commonly occurring, poorly or non-biodegradable pharmaceutical (chapter 4) compounds adsorb to different types of microplastics, particle size, and weathering, and under typical freshwater environment conditions.

2.2 The bioavailability of the adsorbed micropollutants from different microplastic types and weathered microplastics will be evaluated (chapter 4).

2.3 This will include determination of the adsorption and desorption kinetics and the adsorption mechanisms (chapter 4).

*Objective 3: Investigation of the toxic effects of micropollutant-loaded microplastics on Daphnia magna (chapter 5)*

Microplastics are reported to be ingested by wildlife in the freshwater environment, which can be loaded with co-occurring micropollutants. The micropollutant adsorbed onto the microplastics can be bioavailable when ingested and pose toxic effects to wildlife. This thesis will investigate the biological effect of microplastics loaded with selected compounds on the ecological indicator organism *Daphnia magna*.

This thesis will be divided into six chapters (Table 1.4) that consist of: the rationale for this research (chapter 1), the selection and characterisation of the microplastics investigated (chapter 2), the interaction of the natural toxin, microcystins, with microplastics (chapter 3), the interaction of pharmaceuticals

with microplastics, the adsorption and desorption kinetics and mechanisms of a selected compound with selected microplastics types (chapter 4), and the evaluation of whether microplastics can act as a vector for micropollutants into the food chain and have toxic effects to *D. magna* (chapter 5). Finally, the last chapter consists of a conclusion of the findings of this thesis and proposal for future work (chapter 6). In this thesis, three key publications play a role in shaping the research. Pestana et al. (2021) serves as a proof-of-principle study, providing foundational insights that underpin the entire thesis. While the data from Pestana et al. (2021) is not presented within this thesis, its significance is acknowledged throughout the text. The subsequent two publications, result from studies carried out in this thesis, each integrate into chapter 2 (Moura et al. 2023) and chapter 3 (Moura et al. 2022), further contribute to the overarching narrative of this work, offering valuable empirical support and expanding upon critical concepts.

**Table 1.4:** Structure of the thesis according to the content of each chapter.

---

<b>Section of the thesis</b>	<b>Content of the chapter</b>
Chapter 1	Rationale, environmental background, aims and objectives.
Chapter 2	Selection and characterisation of the microplastics used in this thesis.
Chapter 3	Evaluation of the interaction of the natural toxin, microcystins and its analogues, with microplastics widely detected in the freshwater environment.
Chapter 4	Investigation of the interaction of selected pharmaceuticals with microplastics and evaluation of the bioavailability of the micropollutant that showed greatest adsorption when in contact with selected microplastics.
Chapter 5	Evaluation whether microplastics can act as a vector for micropollutants loaded onto the microplastics, and subsequently pose toxic effects on water quality indicator organism, <i>Daphnia magna</i> .
Chapter 6	Conclusion and future work

---

# **Chapter 2**

## **Microplastic selection and characterisation**

<b>2</b>	<b>MICROPLASTIC SELECTION AND CHARACTERISATION .....</b>	<b>32</b>
<b>2.1</b>	<b>Introduction .....</b>	<b>35</b>
2.1.1	Microplastics research.....	35
2.1.2	Sources of microplastics in scientific research .....	37
2.1.3	Selection of microplastics .....	39
2.1.4	Artificially aging microplastics for research purposes.....	41
2.1.5	Characterisation of microplastics .....	42
2.1.6	Chapter aim and objectives .....	46
<b>2.2</b>	<b>Materials and methods.....</b>	<b>47</b>
2.2.1	Commercially acquired microplastics .....	47
2.2.2	Particle size standardisation of the commercial microplastics.....	50
2.2.3	Method development for accelerated artificially aging of the microplastics 51	
2.2.4	Evaluation of polymer composition of virgin and aged microplastics ....	52
2.2.5	Evaluation of the surface area of virgin and aged microplastics.....	52
2.2.6	Particle size and surface morphology of the virgin and aged microplastics 53	
2.2.7	Crystallinity pattern and degree of crystallinity of microplastics of virgin and aged microplastics .....	53
2.2.8	Surface charge of the virgin and aged microplastics.....	54
2.2.9	Statistics .....	55
<b>2.3</b>	<b>Results and discussions .....</b>	<b>55</b>
2.3.1	Characterisation of virgin microplastics: Identification/confirmation of the polymer composition .....	55
2.3.2	Characterisation of virgin microplastics: verification of the particle size and surface morphology of the microplastics .....	60
2.3.3	Characterisation of virgin microplastics: Evaluation of the microplastic surface area.....	69
2.3.4	Characterisation of virgin microplastics: evaluation of the crystallinity and glassiness.....	72
2.3.5	Characterisation of virgin microplastics: evaluation of the surface charge and oxidation of the particles.....	78
2.3.6	Characterisation of artificially aged microplastics: visual inspection of aged microplastics .....	80
2.3.7	Characterisation of artificially aged microplastics: evaluation of chemical structure of the aged microplastics .....	82
2.3.8	Characterisation of artificially aged microplastics: evaluation of the particle size and surface area of the aged microplastics.....	85
2.3.9	Characterisation of artificially aged microplastics: evaluation of the crystallinity and glassiness of the aged microplastics .....	88
2.3.10	Characterisation of artificially aged microplastics: evaluation of the surface charge and oxidation of the aged microplastics .....	92



<b>2.4 Conclusion and recommendation for the pre-experimental characterisation of microplastic particles .....</b>	<b>96</b>
--------------------------------------------------------------------------------------------------------------------	-----------

## 2.1 Introduction

### 2.1.1 Microplastics research

In the past 5 years, there is an increasing interest in microplastic-related topics (Figure 2.1). There has been a magnified awareness of the issues associated with microplastics in recent years due to their increased detection in the aquatic environment (Vaughan et al. 2017; Wang et al. 2018a; Xiong et al. 2018), and inside the digestive track of wild animals (Sun et al. 2017; Souza et al. 2018). Recently, microplastics were also detected in humans' organs (Horvatits et al. 2022) and placenta (Ragusa et al. 2021). In March of 2022, for the first time, microplastics were detected in the blood of four out of 22 adult volunteers in a study conducted in Netherlands (Leslie et al. 2022). The worrisome publications and uncertainties of the impact of microplastic on human health boosted the already increasing interest in microplastic-related research, as demonstrated by the peak popularity (100) of 'microplastics' as a search term worldwide in March-April 2022 in Google Trends (2023, Figure 2.1).

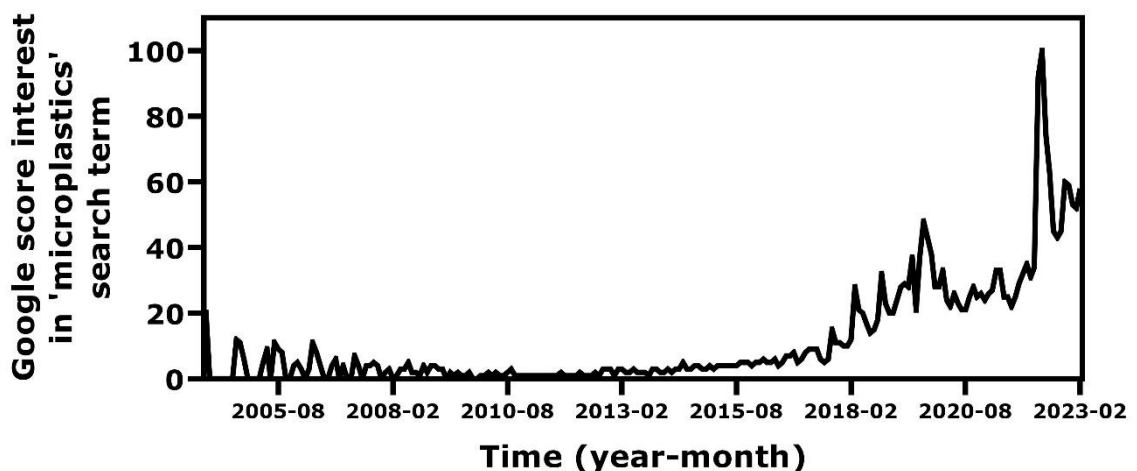


**Figure 2.1:** Increase of the worldwide trend of 'microplastics' web search according to Google Trends (2023). Numbers represent search interest relative to the highest point on the chart for the given region and time. A value of 100 is the peak popularity for the term ('microplastics'). A value of 50 means that the term is half as popular. A score of 0 means that there was not enough data for this term.

Currently, the Netherlands, Singapore, and New Zealand are top of the regions worldwide where the microplastic topic has been most popular, while Russia and Brazil have the lowest interest point among the regions that presented interest data (Figure 2.2, Google Trends 2023). Meanwhile, UK has shown a interest score of 55 for the search of the term 'microplastics'.

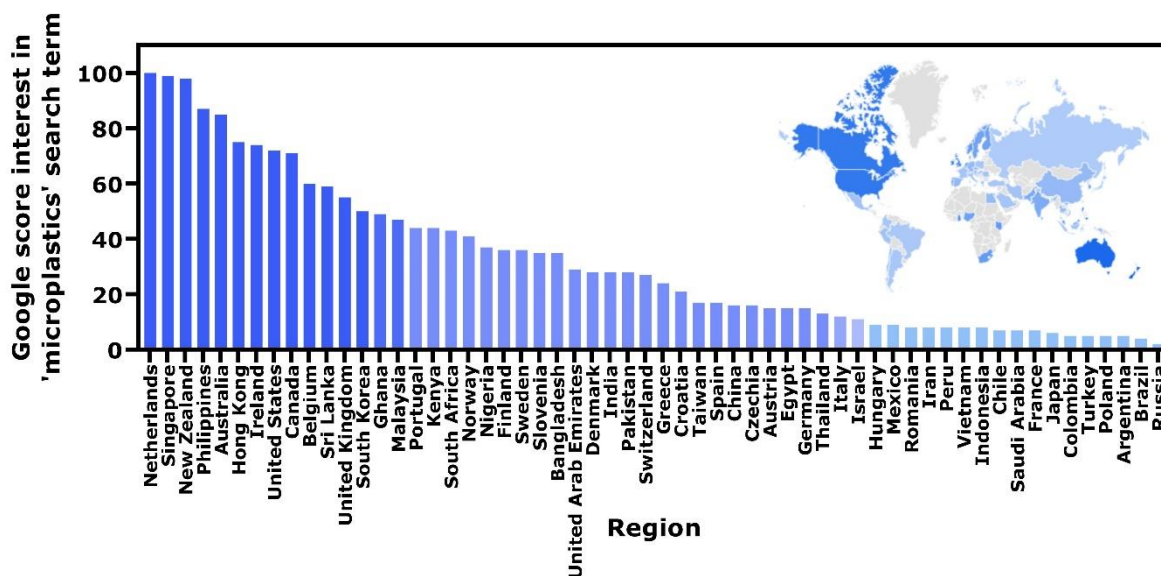


**Figure 2.2:** Interest for 'microplastics' per region based on 'microplastics' web search in February 2023 according to Google Trends (2023). All regions that data are present are shown. Numbers represent search interest relative to the highest point on the chart for the given region and time. The darker the blue colour of the bar, the greater the score. A value of 100 is the peak popularity for the term ('microplastics'). A value of 50 means that the term is half as popular. A score of 0 means that there was not enough data for this term.

The interest in microplastic pollution in scientific research has also increased over the years. Around 6,300 research publications involving microplastic pollution were published between 2018 and end of 2022 compared to 515 publications published between 2013 and end of 2017 according to Web of Science database. Due to the increased detection of microplastics co-occurring with micropollutants in the environment, the recognition that microplastics could act as a vector for chemical pollutants has also gained attention (Magadini et al. 2020; Joo et al. 2021). Almost 1,000 publications related to the adsorption of a wide range of

compounds to microplastics have been published in the past 5 years (2018-2022), while only 30 studies published between 2013 and end of 2017 are identified in the Web of Science database (2023).

### **2.1.2 Sources of microplastics in scientific research**

Researchers obtain microplastics from a range of sources and in some cases prepare their own by mechanical grinding (Wu et al. 2016b; Elizalde-velázquez et al. 2020; Pestana et al. 2021) plastic pellets, and grating large pieces of plastic (Xu et al. 2018a) to obtain the microplastic particles. Typically, the particles are then sieved to obtain a specific size range that is relevant for a particular investigation. However, preparing microplastics in the laboratory is very time-consuming, presents difficulties in obtaining particles small enough and poses the risks of exposure by those undertaking the research to fine particle dust. Furthermore, there is the risk of spills and unintentional microplastic release into the environment. Microplastics can be acquired commercially and are frequently used as received. This author evaluated 17 studies where microplastics were acquired commercially (Table 2.1). To ensure a comprehensive analysis, the current study applied the following selection criteria to identify relevant studies: (1) publications from 2018-2022, except for highly cited studies (over 250 citations); (2) inclusion of diverse microplastic properties, such as polymer composition, weathering nature, and size, as stated by the authors; and (3) selection of publications from a range of journals to ensure diversity in publishing criteria. The investigation of adsorption studies (n=17) revealed that microplastic particles were supplied by 19 different companies. The majority of the microplastic supplier companies were based in China (10 out of 17). The size of the particles used as received varied from smaller than one  $\mu\text{m}$  to 5,000  $\mu\text{m}$

according to what was stated by the authors. Approximately 80% of the microparticles used in the adsorption studies selected were conducted using microplastics greater than 100  $\mu\text{m}$  size (Table 2.1). PE (including low, average, high density, and non-specified PE) and PS were the most studied microplastic types across the literature selected (Table 2.1). In contrast, PET and polylactic acid (PLA) were the least studied types of microplastic. In 57% of the studies investigated, authors evaluated a single type of microplastic in contact with one or more organic compounds.

**Table 2.1:** Microplastic supplier information of 17 adsorption studies according to the plastic type investigated, particle size, supplier, supplier country, and microplastic treatment prior experimentation. Polypropylene (PP), polyethylene (PE), low density PE (LDPE), high density PE (UHMWPE), average density PE (AMWPE), polyethylene terephthalate (PET), polyamide (PA), polystyrene (PS), polyvinyl chloride (PVC).  $D_{90}$  means that 90% of the total volume of material in the sample is in the stated size range. Table adapted from Moura et al. (2023).

Plastic	Size ( $\mu\text{m}$ )	Suppliers	Country	Microplastic treatment	Reference
PE PS PP PA PVC	$D_{90}$ 75-180	Youngling Electromechanical Technology Co., Ltd.	China	Used as received	Li et al. (2018)
PA PE PET PS PVC PP	100-150	SinoPec	China	Sieved	Guo et al. (2019)
UHMW-PE	45-48	Sigma Aldrich	USA	Used as received	Mamitiana et al. (2018)
LDPE PVC PP HDPE	63-125	Dowlex, Krakchemia, Resinex and Sigma-Aldrich	No information	Sieved	Puckowski et al. (2021)
PE	mean size 150	Goodfellow Company	UK	Used as received	Xu et al. (2018)
PS	450-1,000	No information	No information	Sieved	Zhang et al. (2018)
PS PVC	mean size 75	Dongguan Jing Tian Raw Materials of Plastics Co. Ltd.	China	Used as received	Liu et al. (2019)
PE	mean size 100	MicroPowders	USA	Used as received	Atugoda et al. (2020)
PLA PVC	PLA 250–550 PVC 75–150	Yangli electromechanical Co. LTD	China	Used as received	Fan et al. (2021)

Plastic	Size ( $\mu\text{m}$ )	Suppliers	Country	Microplastic treatment	Reference
PVC PP PE	4,000-5,000	LG Company, Guangzhou Bofeng Chemical Technology Company	Korea China	Used as received	Lu et al. (2020)
PS	mean sizes 75.4 106.9 150.5 214.6	Shanghai Youngling Electromechanical Technology	China	Sieved	Li et al. (2019)
PVC	Small <1 Large ~100	Dongguan Jing Tian Raw Materials of Plastics Co. Ltd.	China	Used as received	Ma et al. (2019)
PE PS	PE 225 $\pm$ 41 PS 313 $\pm$ 48 Soil < 74	Nanjing Kaver Scientific Instruments Co., Ltd.	No information	Used as received	Chen et al. (2021)
PP	<180	Yangli Electromechanical Technology Co., Ltd	China	Grided and sieved	Wu et al. (2020)
PS	50.4 $\pm$ 11.9	Guanbu Electromechanical Technology Inc..	China	Used as received	Liu et al. (2020)
PE PS PP PA PVC	<250	Goodfellow Cambridge Ltd.	UK	Sieved	Hüffer and Hofmann (2016)
PS	4,000	Xingwang Dongguan Plastic Ltd.	China	Used as received	J. Wu et al. (2020)

### 2.1.3 Selection of microplastics

Microplastics can be divided into different categories, such as their type (polymer-based), shape, colour, and size. In the current study, microplastics were acquired based on their type and size. The types of microplastics selected were based on their environmental relevance based on their reported occurrence in freshwater systems. Polypropylene (PP), polyethylene (PE), polyethylene terephthalate (PET), polyvinyl chloride (PVC), polystyrene (PS) and polyamide (PA) were the microplastics types selected. In this study, fragment-shaped microplastics were preferred for a better representation of the microplastic found in freshwater environments (Zhao et al. 2022a). Spherically shaped (beads) microparticles were avoided when selecting the microplastic tested. In a review

conducted by Koelmans et al. (2019), the authors verified that the detection frequency of spheres (11) and beads (7) in freshwater was lower when compared to fragments (35) and fibres (25) from 55 records evaluated. Furthermore, studies have reported greater ecotoxicity of fragments of plastic to aquatic organisms such as the water flea *Daphnia magna* when compared to plastic beads (Ogonowski et al. 2016; An et al. 2021). In a proof-of-principle study, conducted by the author, plastic pellets were grinded in order to obtain plastic fragments at various ranges of sizes smaller than 5 mm (Pestana et al. 2021). PE, PET, and PS pellets and a PVC rod were grinded and sieved to reach three size ranges: 90-150  $\mu\text{m}$ , 250-500  $\mu\text{m}$ , and 1,000-5,000  $\mu\text{m}$  (Figure 2.3). However, due this being hazardous (risk of inhalation) and very time consuming, along with the difficulty of getting particles smaller than 90  $\mu\text{m}$ , the microplastics used in the current study were acquired commercially.

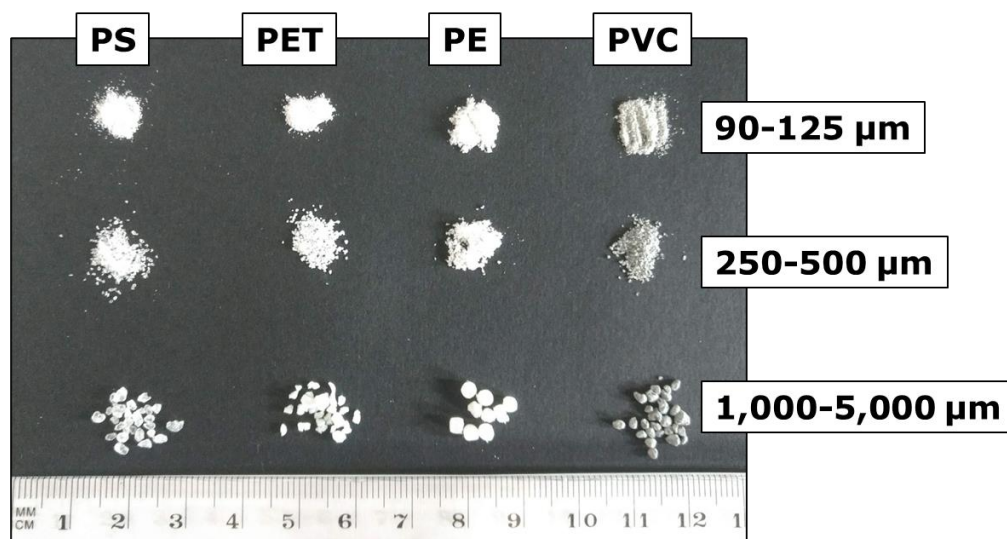


**Figure 2.3:** Microplastic type and range sizes of the particles used in the proof-of-principle study. Polyethylene (PE), Polyethylene terephthalate (PET), and polystyrene (PS) pellets and a polyvinyl chloride (PVC) rod were grinded and sieved to reach three size ranges at 90-150  $\mu\text{m}$ , 250-500  $\mu\text{m}$ , and 1,000-5,000  $\mu\text{m}$ .

The particles reported in the aquatic environment are in a wide range of size, however, microplastics less than 300  $\mu\text{m}$  were abundant in freshwater bodies in a review performed by Koelmans et al. (2019). The Pestana et al. (2021) study has demonstrated that microplastics sized 90-125  $\mu\text{m}$ , the smallest size analysed, had the greatest adsorption of a natural toxin, microcystin-LF. Li et al. (2019) also showed that the smaller the microplastics, the higher the adsorption potential of the compounds analysed. Further, smaller particles are more likely to be consumed by microscopic wildlife organisms such as zooplankton, therefore smaller microplastic particles can more readily enter the food chain. In addition, the smaller the microplastics, the greater the difficulty to either produce the microparticles or to acquire them commercially. As a result, there is a greater lack of understanding, especially regarding their interaction with micropollutants. For this reason, the current study selected microplastic size ranges 10-25  $\mu\text{m}$  and 100  $\mu\text{m}$  to investigate their interaction with freshwater micropollutants under controlled environmental conditions.

#### **2.1.4 Artificially aging microplastics for research purposes**

Researchers obtain microplastics from a range of sources in order to conduct adsorption experiments with microplastics. However, virgin microplastics may not be environmentally representative. In the environment, plastics are exposed to solar radiation that can lead to degradation by thermal and photo-oxidation of the plastics (Feldman 2002). In a proof-of-concept study, a PET plastic bottle was collected on St. Andrews beach (UK), cut, grinded, sieved (90-125  $\mu\text{m}$ ), and placed in contact with two analogues of a natural toxin, microcystin-LR (MC-LR) and microcystin-LF (MC-LF) for 48 h. While neither MC-LR nor MC-LF adsorbed



onto virgin PET (90-125  $\mu\text{m}$ ) as demonstrated by Pestana et al. (2021), MC-LF adsorbed approximately 30% on naturally weathered PET (90-125  $\mu\text{m}$ , unpublished data). However, collecting naturally weathered plastics is challenging. Naturally aged microplastics are exposed to a variety of environmental conditions that can affect the adsorption of organic compounds along with the weathering of the microplastics caused by oxidation of the particles. Furthermore, separating the microplastic types and achieving the amount of microplastics sufficient for the investigation can be limiting factors for the use of environmental samples of microplastics. Artificially weathering microplastics in the laboratory has been demonstrated to aid researchers to achieve a controlled aging of microplastics (Hüffer, Weniger and Hofmann 2018a; Guo and Wang 2019; Liu et al. 2020a). Researchers have used ultraviolet irradiation (UV, 100-400 nm) to age microplastics (Mylläri, Ruoko and Syrjälä 2015; Liu et al. 2019; Almond et al. 2020; Wu et al. 2020a; Fan et al. 2021). However, in natural sunlight irradiation, UV light only accounts for a small portion ( $\sim 7\%$ ) compared to the high amount of visible light (55%, Liu et al. 2021). The aging process of microplastics has been reported to enhance the adsorption of organic compounds onto microplastics (Zhang et al. 2018; Liu et al. 2020b). For this reason, the current study has developed a protocol to accelerate the artificial aging of virgin microplastic.

### **2.1.5 Characterisation of microplastics**

The microplastic type, degree of crystallinity, glassiness, polarity, and particle size can influence the adsorption behaviour of pollutants onto microplastics (Atugoda et al. 2021), including the degree of weathering of the particles. To fully understand the physico-chemical properties of microplastics, several

analytical techniques can be used. Fourier transform infrared (FT-IR) spectroscopy and microscopy have been widely used to confirm/identify the type (polymer-based) of microplastics. For solid samples, an attenuated total reflectance (ATR) can be used as a sampling accessory to obtain the infrared spectra. The FT-IR spectra provide a fingerprint for each of the polymers. The FT-IR spectra can be compared with those in a library to either identify or confirm the polymeric material. According to Moura et. al. (2023), among 21 studies investigated by this author, 38% (8) did not confirm the polymer composition of commercial microplastics. Moreover, FT-IR spectroscopy is one of the most common analytical techniques to monitor oxidative reactions (Almond et al., 2020). As result, most of the studies (n = 21) analysed by Moura et. al. (2023) that performed FT-IR analysis focused on evaluating the aging of the polymer rather than confirming the polymer composition and purity of the microplastics.

X-ray diffraction (XRD) and differential scanning calorimetry (DSC) are typically used to evaluate the crystallinity pattern and the degree of crystallinity, respectively, of polymeric materials. However, those analyses can also be used to identify the polymer composition of the material investigated (Li, Zhang and Zhang 2018; Elizalde-velázquez et al. 2020).

Particle size, in particular, has been shown to be a key factor for adsorption of compounds by microplastics (Ma et al. 2019; Pestana et al. 2021) and directly influence ingestion of microplastics by aquatic organism such as *Daphnia magna* (An et al. 2021). Laser diffraction particle size analysis (PSA) is an important tool to measure the particle size distribution of materials ranging from hundreds of

nanometres up to several millimetres in size. However, in the studies evaluated, authors have often relied on the particle size information provided by the supplier. Moura et al. 2023 highlighted the lack of characterisation of commercial microplastics in adsorption studies regarding the particle size, especially in microplastics used as received. Scanning electron microscopy (SEM) images have been used for various purposes such as to evaluate the surface morphology and the shape of the particles, and to verify the size of the acquired particles. However, visual analysis of the particle size using SEM images has limitations. Especially when the images are presented as either one single particle or zoomed in on a single particle making it impossible to assess the size-distribution of particles in a given sample (Chen et al. 2021; Elizalde-velázquez et al. 2020; Fan et al. 2021; Guo et al. 2018; Li et al. 2018; Liu et al. 2019, 2020; Wu et al. 2020b; Zhang et al. 2018). To ensure a certain size range of microplastics, researchers have sieved the particles received. However, when the microplastics were sieved, the studies tend to rely on the mesh size of the sieves used to describe the particle size range (Wu et al. 2016a; Guo et al. 2018; Zhang et al. 2018; Guo, Chen and Wang 2019; Pestana et al. 2021; Puckowski et al. 2021) rather than carry out subsequent size confirmation. In this thesis, results will confirm that sieving the microplastics does not guarantee a particle size range according to the mesh size of the sieves.

The surface area of the microplastics plays an important role in the interaction between organic compounds and microplastics. Morphological properties such as roughness and porosity can influence the surface area of microplastics. The greater the surface area of the material, the greater the amount of binding sites potentially available for adsorption of compounds onto microplastics (Chen,

Sawyer and Regan 2013). The surface of microplastics can be measured using N<sub>2</sub>-BET adsorption-desorption surface area analysis. Furthermore, zeta potential analysis of microplastics has been used to investigate the surface charge of the particles and contribute to the interpretation of the mechanisms involved in the adsorption of organic compounds.

In the current study, a detailed characterisation of six commercially acquired microplastic polymers in two sizes (10-25 µm and 100 µm, according to supplier) was carried out. A range of analytical methods were used to confirm the polymer composition (FT-IR), the crystallinity pattern (XRD), the degree of crystallinity (DSC), the glassiness (DSC), the size of the particles (PSA), the surface morphology (SEM), and the surface area (N<sub>2</sub> – BET adsorption-desorption analysis) of the received microparticles of polypropylene (PP), polyethylene (PE), polyethylene terephthalate (PET), polyamide (PA), polystyrene (PS), and polyvinyl chloride (PVC, Figure 2.4). The microplastics received were sieved to standardise the size of the particles using 20 and 45 µm sieves (small particles) and 90 and 150 µm (large particles). The size-standardised microplastics were used for all investigations in this thesis. The particle size can impact behaviour of the microplastics, therefore, the size-standardised microplastics were characterised again after sieving to have a true representation of the microplastics used. Finally, the size-standardised microplastics were also artificially aged to compare the properties of virgin versus artificially aged microplastics, which necessitated an additional detailed characterisation of the aged particles was performed (Figure 2.4).

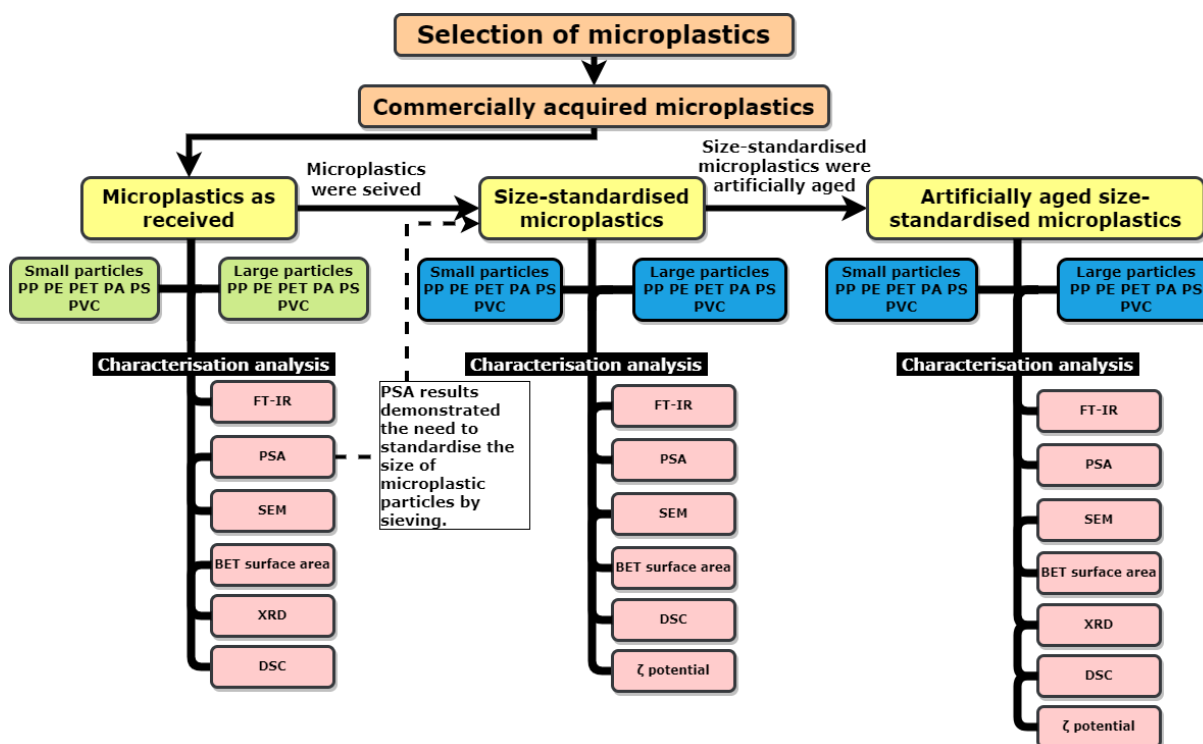


**Figure 2.4:** Diagram of the characterisation of the microplastics used in this thesis. The blue boxes represent the microplastics used for the experiments in this research. Fourier transform infrared (FT-IR), laser diffraction particle size analysis (PSA), scanning electron microscopy (SEM), N<sub>2</sub>-BET adsorption-desorption surface area analysis (BET surface area), x-ray diffraction (XRD), differential scanning calorimetry (DSC), and zeta ( $\zeta$ ) potential.

### 2.1.6 Chapter aim and objectives

Full understanding of the physico-chemical properties of microplastics is a key factor affecting the interaction of organic compounds with microplastics. More specifically, information such as polymer composition, particle size, surface area, crystallinity, and weathering of microplastics is essential to ensure a reliable interpretation of data. Therefore, the aim of this chapter is to select and characterise the commercial microplastics prior to use in subsequent chapters. This was achieved with the following objectives:

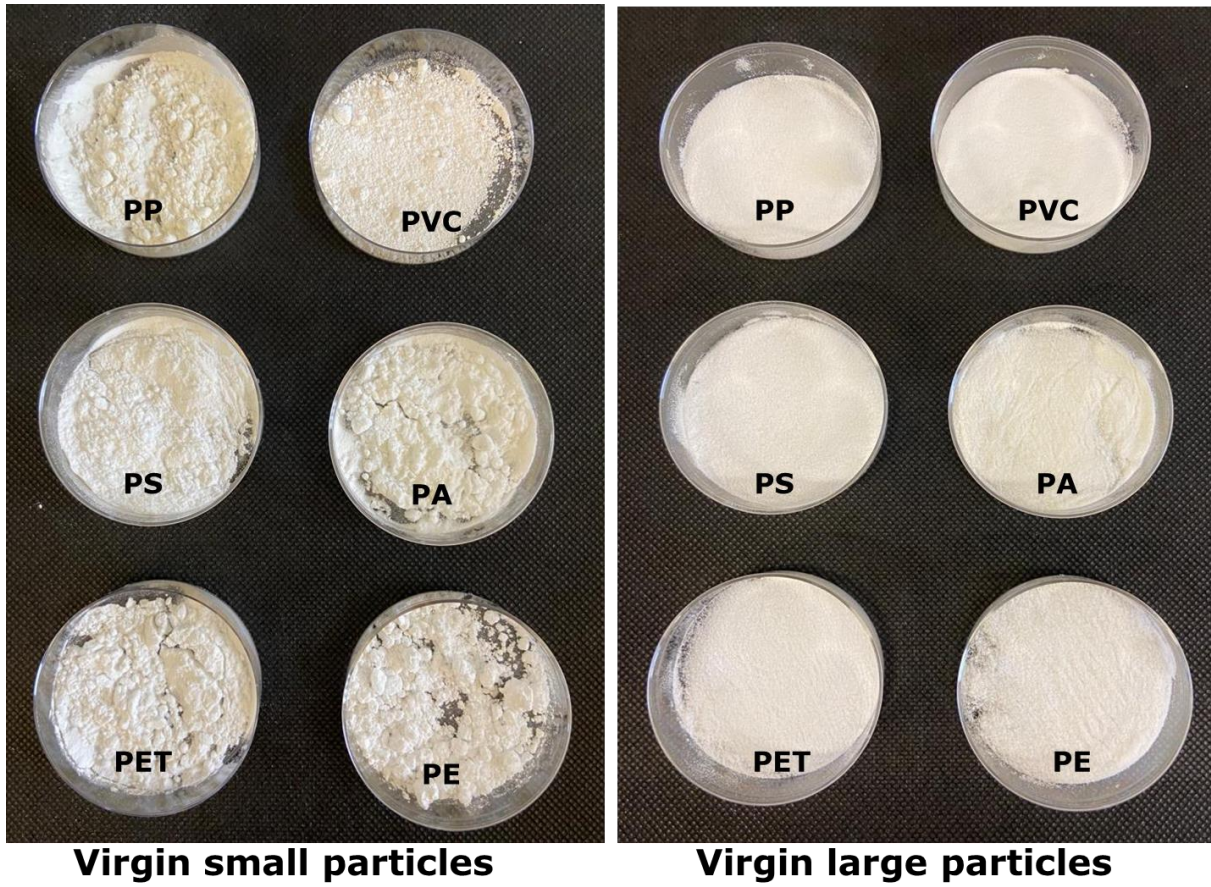
- 1) Selection of microplastics

- 2) Characterisation of microplastic (as received) using a range of analytical methods to confirm and evaluate physico-chemical properties
- 3) Standardisation of the size of commercial microplastics due to size inconsistencies revealed during characterisation
- 4) Development of an accelerated artificial aging method for microplastics
- 5) Characterisation of the artificially aged microplastics to evaluate how the aging process affected the physico-chemical properties of the particles

## **2.2 Materials and methods**

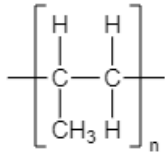
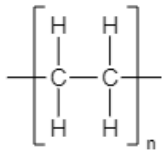
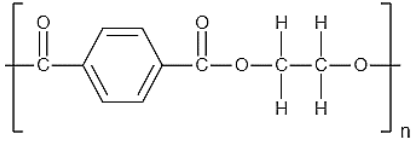
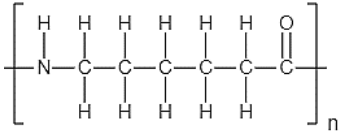
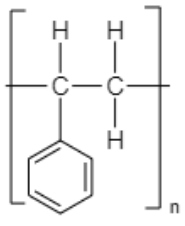
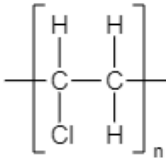
### **2.2.1 Commercially acquired microplastics**

Six microplastics types were commercially acquired from Shanghai Guanbu Electromechanical Technology Co. Ltd. (STGE, China). Microparticles of polypropylene (PP), polyethylene (PE), polyethylene terephthalate (PET), polyamide (PA), polystyrene (PS), and polyvinyl chloride (PVC) were purchased in two sizes (10-25  $\mu\text{m}$  and 100  $\mu\text{m}$ , according to supplier) described from now on as small and large particles (Figure 2.5 and Table 2.2). A volume of one litre was acquired of each microplastic type per size. To avoid repetition, from this point forward, the microplastic types (polymer-based) will be represented by their polymer composition abbreviation and described size (small and large).



**Figure 2.5:** Small material (left) with an average size between 10 and 25  $\mu\text{m}$  and large material (right) with an average size of 100  $\mu\text{m}$  according to the supplier.

**Table 2.2:** Summary of average particle sizes detailed by the supplier, chemical structure (repeat unit), and density of microplastic acquired commercially for selected microplastic types.

Polymer	Chemical structure (repeat unit)	Small particles – according to the supplier (µm)	Large particles – according to the supplier (µm)	Density <sup>a</sup> (g cm <sup>-3</sup> )
PP		25	100	0.87-0.92
PE <sup>b</sup>		15	100	0.89-0.93
PET		15	100	1.38-1.41
PA <sup>c</sup>		18	100	1.07-1.16
PS		13	100	1.04-1.08
PVC		10	100	1.40-1.42

<sup>a</sup> Grigorescu et al. (2019)

<sup>b</sup> Treated as low-density polyethylene (LDPE)

<sup>c</sup> Treated as polyamide 6 (nylon 6)



### **2.2.2 Particle size standardisation of the commercial microplastics**

To standardise the size range of the received particles they were sieved using a shaker (AS200 Control Vibratory Sieve Shaker, RETSCH, UK) at 1.5 mm amplitude for 10 min. The small material was retained between 20  $\mu\text{m}$  and 45  $\mu\text{m}$  sieves (ISO 3310/1, Fisher Scientific, UK), meanwhile the large material was retained between 90  $\mu\text{m}$  and 150  $\mu\text{m}$  sieves (ISO 3310/1, Fisher Scientific, UK). All sieves were carefully washed and dried in between sieving different polymers to avoid cross contamination. However, for small PE and PVC, the sieving method needed to be adjusted. Small PE particles clumped during the shaking, probably due to the particles' high roughness, which prevented the particles from passing through the 45  $\mu\text{m}$  sieve. For this reason, HPLC grade methanol (Fisher Scientific, UK) was used to aid the sieving of small PE. After sieving, the methanol was allowed to evaporate for a week at room temperature in a fume cupboard which resolved the issue for PE. Laser diffraction particle size analysis (PSA) results showed that small PVC contained nanoparticles ( $< 1 \mu\text{m}$ , Figure 2.8). In the later studies, it was planned to use micro centrifuge tubes with acetate filters (0.22  $\mu\text{m}$  pore size) to separate microplastics from the aqueous phase prior to injection for liquid chromatography. In an attempt to remove particles less than 0.22  $\mu\text{m}$  that could potentially pass through the filters, small PVC was suspended in methanol and passed through a GF/F filter (pore size 0.7  $\mu\text{m}$ ), and the material retained by the filter was collected. Methanol has 'excellent' compatibility with PE and PVC (Cole-Parmer 2023), therefore the solvent did not affect the properties of the particles. However, this procedure showed not to be efficient for the size separation of small PVC particles (Figure 2.10). For this reason, the small PVC was used as received. Likewise, as small PP

particle size was in the majority smaller than 20  $\mu\text{m}$ , small PP particles were also used as received.

The size analysis of the PA microplastic described by the supplier as having an average size 18  $\mu\text{m}$  was actually found to have a particle size distribution similar to the sample provided as 100  $\mu\text{m}$  (large PA, Figure 2.8). Small PA (as received) contained approximately 13% of particles at sizes between 20 and 45  $\mu\text{m}$ , while large PA (as received) consisted of approximately 22% at size range 20-45  $\mu\text{m}$ . In order to enable the study of small particles of PA (20-45  $\mu\text{m}$ ) both sizes of PA were sieved using 20  $\mu\text{m}$  and 45  $\mu\text{m}$  sieves (small particles), and 90  $\mu\text{m}$  and 150  $\mu\text{m}$  sieves (large particles). To have sufficient amount of small PA (20-45  $\mu\text{m}$ ) for all required investigation, the particles retained between the 20  $\mu\text{m}$  and 45  $\mu\text{m}$  sieves from both PA sizes were combined. From now on, small PA represents the combined sieved PA particles, unless denoted otherwise.

### **2.2.3 Method development for accelerated artificially aging of the microplastics**

The size-standardised virgin microplastics were aged using a SUNTEST XLS+ Xenon Arc weathering testing unit (ATLAS AMETEK Electronics Instrument Group, USA) equipped with a 1700 W xenon arc lamp operated at 60 W  $\text{m}^{-2}$  (300-400 nm) intensity, which is similar to the intensity of sunlight in summer ( $\sim 1000$  W  $\text{m}^{-2}$ , Liu et al. 2021). Microplastic (1 g) was placed into a 200 mL beaker. The total exposure time was 72 h. The samples were shaken every 24 h to ensure uniform exposure. No water was used during the aging process. The chamber temperature was set to 30  $^{\circ}\text{C}$  ( $29.3 \pm 3.4$   $^{\circ}\text{C}$ ,  $n = 2788$  over 72 h).

#### **2.2.4 Evaluation of polymer composition of virgin and aged microplastics**

A Nicolet iS10 Fourier Transform Infrared (FT-IR) Spectrometer from Thermo Fisher Scientific (UK) with OMNIC Spectra Software was used to confirm the polymer composition of each of the microplastics in both sizes. Further, FT-IR was also used to monitor the formation of carbonyl functional group peaks in the spectra of the aged microplastics. The FT-IR scanning wavenumber was set from 400 to 4,000  $\text{cm}^{-1}$ . Attenuated Total Reflectance (ATR) was used as a contact sampling method. Thirty-two scans at resolution of 8  $\text{cm}^{-1}$  were used to produce the spectra. No correction was applied. The carbonyl index (CI) was calculated from the ratio between the integrated band absorbance of the carbonyl (C=O) peak from 1,850 to 1,650  $\text{cm}^{-1}$  and a reference peak that is not usually affected by the oxidation process (Almond et al. 2020) according to equation 2.1:

$$CI = \frac{\text{Area under band } 1,850\text{--}1,650 \text{ cm}^{-1} (\text{C=O})}{\text{Area under band } 1,500\text{--}1,420 \text{ cm}^{-1} (\text{CH}_2)} \quad (2.1)$$

#### **2.2.5 Evaluation of the surface area of virgin and aged microplastics**

The  $\text{N}_2$ -Brunauer-Emmett-Teller (BET) adsorption-desorption surface area ( $S_{BET}$ ) was determined using a Tristar II surface area and porosity instrument (Micromeritics, UK). Prior to the analysis, the microplastics were maintained under vacuum for 24 hours using a VacPrep degasser (Micromeritics, UK) at 30 °C. This process removed surface adsorbed gas and moisture. However, the  $\text{N}_2$ -BET adsorption-desorption analysis has limitations when applied to plastic samples. The degassing of the  $\text{N}_2$ -BET adsorption-desorption analysis is normally

employed at over 130 °C (Hussain et al. 2010; Hui et al. 2021). However, due to the plastics' low melting temperature, degassing was performed at lower temperatures (30 °C; Moura et al., 2022).

### **2.2.6 Particle size and surface morphology of the virgin and aged microplastics**

Laser diffraction particle size analysis (PSA) was carried out using a Mastersizer 2000 particle size analyzer (Malvern Panalytical, UK). Water was used as a sample dispersant. However, due to the buoyancy of the microplastics, isopropanol (Fisher Scientific, UK) was also used to aid the dispersion of the microplastic in the water. The solvent was added to the water until the particles were fully dispersed in the water column. The obscuration was set from 10 to 20%. Each sample was measured at least three times. A simulated surface area ( $S_{PSA}$ ) was calculated by the PSA software (assuming perfect sphericity of the particles, not accounting for potential porosity or roughness of the material). Scanning Electron Microscopy (SEM, Scios DualBeam, Thermo Fisher Scientific, UK) was employed to investigate the morphologies and to confirm the particle size of the microplastics.

### **2.2.7 Crystallinity pattern and degree of crystallinity of microplastics of virgin and aged microplastics**

For crystallinity composition evaluation, powder X-Ray Diffraction (XRD) was carried out using an Empyrean diffractometer (Malvern Panalytical, UK) in reflection mode with a primary beam monochromator (Cu K $\alpha$ 1). The calorimetry characteristic of the microplastics was measured using differential scanning

calorimetry (DSC) on a DSC250 (TA, USA) with N<sub>2</sub> as the purge gas. Microplastic (6.0 mg) was placed into an aluminium pan (TA, USA) and, sealed with an aluminium lid (TA, USA) using a Tzero Press (TA, USA). The pan, lid, and samples were handled using tweezers to avoid external interference on the sample weight. A sample without microplastic was prepared as a reference. To erase any thermal history effects, a heating-cooling-heating method was applied. For PP, PE, PET, PA, and PS, the first heating run was performed from 40 to 290 °C with a heating rate of 20 °C min<sup>-1</sup>, followed by cooling from 290 to 0 °C with a cooling rate of 10 °C min<sup>-1</sup>. The second heating run was from 0 to 290 °C at 10 °C min<sup>-1</sup>. PVC showed degradation at 270 °C, therefore the first and second heating runs for PVC samples were limited to 250 °C. The degree of crystallinity ( $X_C$ ) was calculated using the equation 2.2:

$$X_C = \frac{\Delta H_m - \Delta H_c}{\Delta H_{m_{100\%}}} \times 100 \quad (2.2)$$

Where,  $\Delta H_m$  is the enthalpy change associated to the melting endotherm temperature ( $T_m$ ) from the second heating run.  $\Delta H_c$  is the enthalpy change associated to the cold crystallisation exotherm temperature ( $T_c$ ).  $\Delta H_{m_{(100\%)}}$  is the reference value considering a 100% crystalline polymer (Table 2.6).

### **2.2.8 Surface charge of the virgin and aged microplastics**

The zeta potential of the virgin and aged plastics in experimental medium was measured by a Malvern Zetasizer instrument (Nano ZS, UK). The experimental medium consisted of artificial freshwater (AFW), prepared as per Akkanen and Kukkonen, (2003), with 0.02% (w/v, 200 mg in 1 litre) of sodium azide (NaN<sub>3</sub>) used as a microbial inhibitor. The AFW + 0.02% NaN<sub>3</sub> with microplastics (plastic concentration of 2 g L<sup>-1</sup>) was placed into a capillary zeta cell (DTS1070) to

perform the measurements. The samples were measured from three to six times at 25 °C at a 173° scattering angle with 4 mW He-Ne laser.

### **2.2.9 Statistical analysis**

Student's t-test was carried out using Microsoft Excel to perform significance testing. For all statistical tests, a significance level of 5% was set.

## **2.3 Results and discussions**

### **2.3.1 Characterisation of virgin microplastics: Identification/confirmation of the polymer composition**

The detailed characterisation of the microplastics received by the supplier was extensively discussed as published in Moura et.al. (2023). FT-IR spectroscopy analysis was performed to confirm the chemical nature of the constituent polymers of the commercially acquired microplastics that were to be used to investigate the adsorption of a range of chemicals. The FT-IR spectra provides a fingerprint for each of the polymers that can be compared to a library to either identify or confirm the polymeric material. The polymer composition of the six microplastic types acquired matched with the description supplied by the manufacturer. The spectra of the microplastics investigated matched the library spectra (Hummel polymer sample library) and spectra presented in the literature (Geil 2017). Further investigation of the FT-IR spectra of materials can include the identification of functional groups based on the band/peak position and intensity of the peaks. Results have demonstrated the importance to analyse the spectra of the materials beyond, and not just to rely on the fair match with a

database of polymers. Despite positive correlation with library spectra, FT-IR has revealed inconsistencies in the purity of some material as received. For example, PP consist of the alkane (C-C and C-H) functional groups. Alkane functional groups result in a strong absorption band at range 3,000-2,840  $\text{cm}^{-1}$ . As would be expected, corresponding peaks were observed in the spectra of the polymer labelled as PP (Figure 2.6). However, a peak corresponding to a carbonyl functional group (C=O) was detected in the spectrum of small PP particles. Typically, neat PP should not present oxygen-bond related peaks, since it is exclusively comprised of carbon and hydrogen molecules. The carbonyl peak present in the small PP spectrum can indicate either oxidation of the small PP particles or the presence of a grafting agent. The grafting polymerisation method is utilised to alter the form, size, and structure of polymeric materials (Mandal et al. 2017). Acrylic acid and maleic anhydride, which contain carbonyl groups, are common grafting agents. Acrylic acid is commonly used in polymer compositions, including plastics such as polyacrylic acid (Brown 2014). FT-IR spectra displayed a strong peak at 1,711  $\text{cm}^{-1}$  and a weak peak at 1,200  $\text{cm}^{-1}$ , which correspond to carboxylic acid (RCOOH) and C-O (stretch) respectively (Figure 2.6), suggesting a grafting reaction of acrylic acid (AA) on PP to form the copolymer known as PP-g-AA (Cai et al. 2008; Xu et al. 2014; Mandal et al. 2017). Acrylic acid is characterised by its acidic, tart aroma which was noticed by the author when handling small PP samples, however a definitive identification was not possible. The chemical structure of small PP impacts the adsorption of organic compounds, as seen in the study conducted by Moura et al. (2022) where significant adsorption of eight variants of a group of cyanotoxins named microcystins was observed on small particles of this particular PP.

The FT-IR spectra of the small and large sizes of PA as received showed distinct peaks for N-H ( $3,292\text{ cm}^{-1}$ ) and C-H ( $2,918\text{-}2,850\text{ cm}^{-1}$ ) stretching frequencies, as expected. However, differences were noted, including higher absorbance intensity of N-H peaks in the small PA spectra compared to large PA and lower absorbance intensity of C-H peaks and amide peaks (CONH<sub>2</sub>; C=O + C-N; C-N + N-H) in the small PA spectrum compared to large PA (Figure 2.6). The differences between the two spectra, even if discreet, may suggest that small and large PA are two different forms of PA. PA can be categorised into various forms that only show IR spectra differences in the absorbance intensity, such as aromatic, cycloaliphatic, and aliphatic, based on monomer arrangement and chemistry (Kausar 2017). FT-IR spectra alone cannot precisely identify the form of PA, so further characterisation was required to confirm the specific form present. As mentioned in section 2.2.2, the material described as small PA consisted of the combination of the material retained between 20 and 45  $\mu\text{m}$  sieves from both, the material described as having an average size of 18  $\mu\text{m}$  and PA described as having an average size of 100  $\mu\text{m}$ . The combined PA particles were used throughout this study. The FT-IR spectrum of small PA differs from the spectrum of the small PA as received (Figure 2.7). In the spectra of small PA as received and small PA sieved, the N-H peak ( $3,292\text{ cm}^{-1}$ ) was similar, however a lower peak intensity of C-H ( $2,918\text{-}2,850\text{ cm}^{-1}$ ) and for the amides ( $1,635\text{ cm}^{-1}$ ;  $1,542\text{ cm}^{-1}$ ) was observed. Thus, it is likely that results for PA represent the results for a composite of two (unidentified) types of PA.



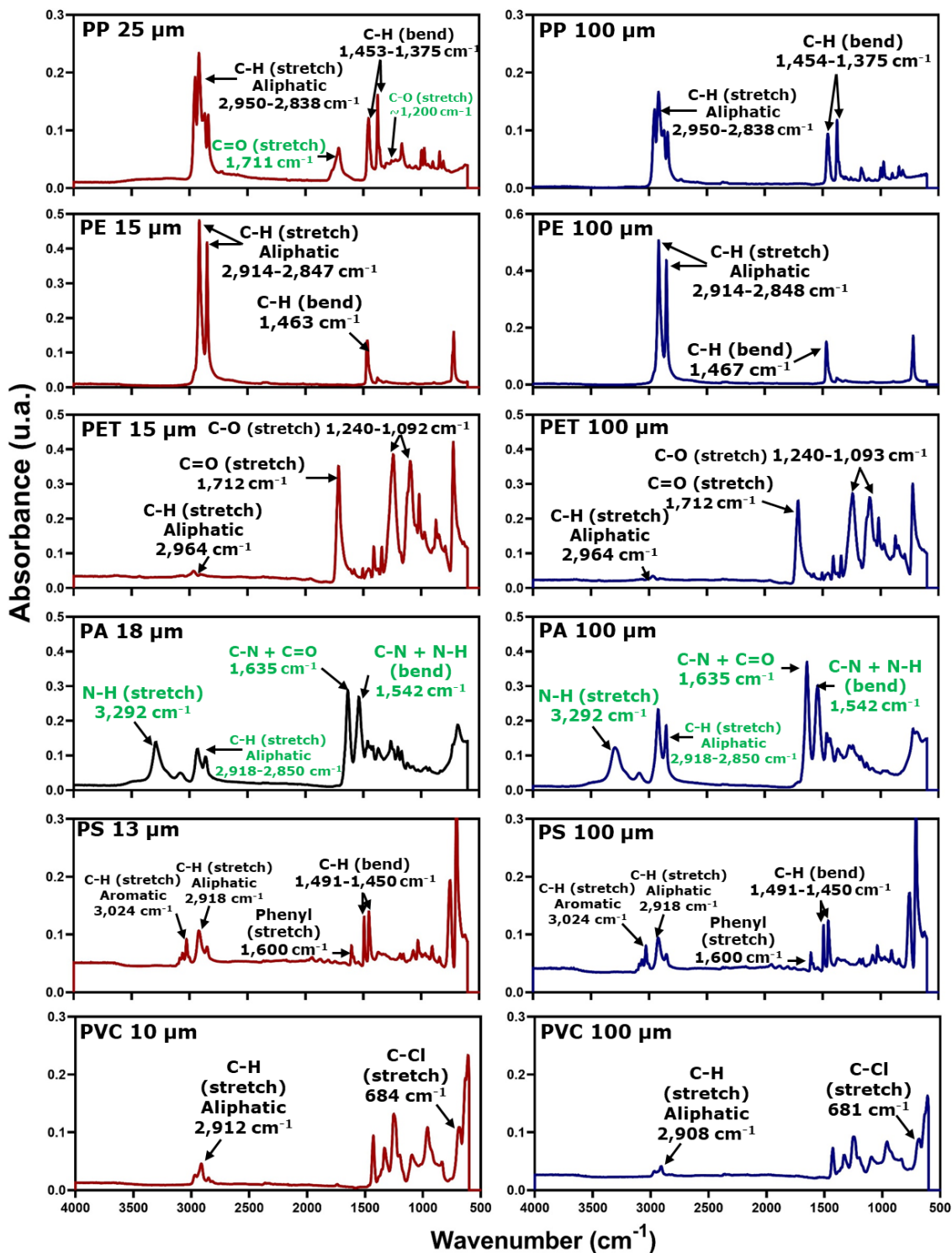


**Figure 2.6:** Polymer composition of the microplastics received from the supplier using attenuated total reflectance Fourier transform infrared (ATR FT-IR) spectra. The sizes stated are as supplied by the manufacturer. — = small particles and — = large particles represent the spectrum of the material used throughout this study. Except for the material described as PA 18  $\mu\text{m}$  (—), which the spectrum only represents the material received from the supplier. PP, PE, PET, PA, PS, and PVC main functional groups and their FT-IR absorption peaks are presented. Highlighted in green are the FT-IR peaks that showed differences between the small and large size.

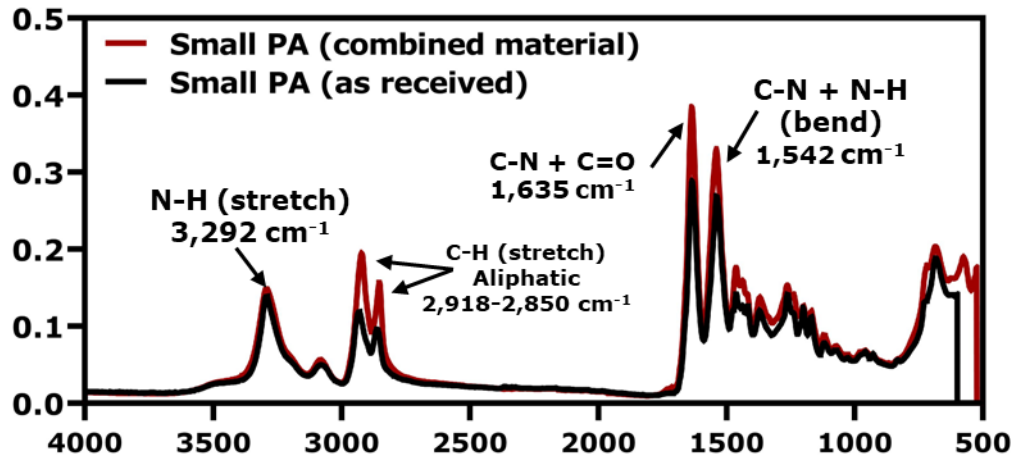


**Figure 2.7:** Polymer composition of the two formulations of small PA according to attenuated total reflectance Fourier transform infrared (ATR FT-IR) spectra. Comparison of small PA as received (—) detailed by the supplier as average size 18  $\mu\text{m}$  with the spectrum of small PA (—) which is the combination of both PA sizes. — = small PA represents the material tested throughout the current study. The main functional groups of small PA as received, and small PA sieved, and their FT-IR absorption peaks are presented.

No further discrepancies were observed in the FT-IR spectra of the other microplastic samples. Like PP, PE consists of the alkane (C-C and C-H) functional groups. Alkane functional groups result in a strong absorption band at range 3,000 – 2,840  $\text{cm}^{-1}$ . No differences were apparent for the spectra of the two sizes of PE. A strong peak at 1,712  $\text{cm}^{-1}$  was detected in the FT-IR spectra of both small and large PET. This peak is consistent with the ester functional group (RCOOR) present in PET, as indicated in Table 2.2. Additionally, both small and large PET particles showed similar spectra. PS and PVC also had matching spectra for their respective sizes. The aliphatic C-H stretching adsorption peak ( $\sim 2,910 \text{ cm}^{-1}$ ) was present in both PS and PVC spectra, with only PS showing an aromatic C-H stretching peak (3,024  $\text{cm}^{-1}$ , Table 2.2; Figure 2.6). On the other hand, PVC showed chlorine-related absorptions (C-Cl peak) at 684  $\text{cm}^{-1}$  (detailed as size 10  $\mu\text{m}$ ) and 681  $\text{cm}^{-1}$  (detailed as size 100  $\mu\text{m}$ ).

### **2.3.2 Characterisation of virgin microplastics: verification of the particle size and surface morphology of the microplastics**

Along with the polymer composition of microplastics, the size of the particles affects their ability to adsorb micropollutants (Pestana et al. 2021). To confirm the size of the microplastics received from the supplier, laser diffraction particle size analysis (PSA) was performed. Results showed that the size of the particles received from the supplier was inconsistent with their stated size. An extreme example was the small PA. The material described as having an average size of 18  $\mu\text{m}$  by the supplier (small PA 18  $\mu\text{m}$ ), PSA demonstrated to have a median size ( $D_{50}$ ) of 75  $\mu\text{m}$ , and average size of 91  $\mu\text{m}$  (Table 2.3). Furthermore, small PVC was described as having an average size of 10  $\mu\text{m}$ , but PSA revealed two distinct size distributions, one between 0.04-0.3  $\mu\text{m}$  and another between 0.5-4  $\mu\text{m}$  (Table 2.3; Figure 2.8). It was also observed that the small particles of PE (0.2-549  $\mu\text{m}$ ), PET (7-91  $\mu\text{m}$ ), and PS (1-79  $\mu\text{m}$ ) showed a wide size distribution that overlapped with the size distribution of the large particles (Figure 2.8). These discrepancies highlight the importance of performing PSA for data interpretation.

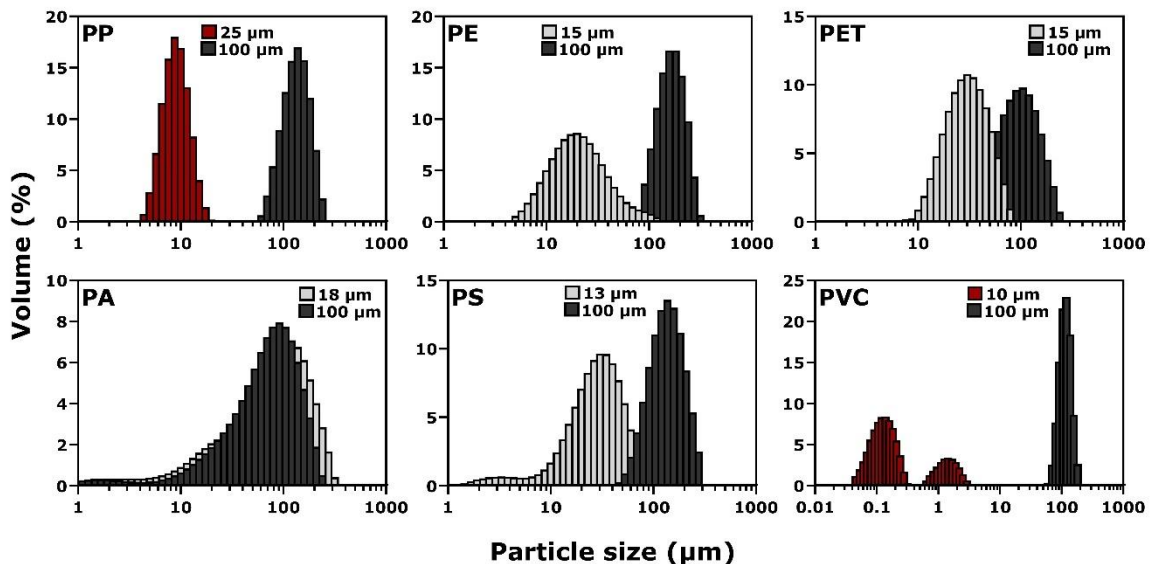
**Table 2.3:** Evaluation of the particle size of both size formulations (small and large) of the material received using laser diffraction particle size analysis (PSA) range, PSA median size of the particle size distribution ( $D_{50}$ ), and calculated average size of the microplastics.

Small particles				
Plastic	Supplier stated size	PSA range	$D_{50}$	Average size
	( $\mu\text{m}$ )	( $\mu\text{m}$ )	( $\mu\text{m}$ )	( $\mu\text{m}$ )
PP	25	4-23	8	9
PE	15	0.2-549	25	42
PET	15	7-91	28	33
PA	18	0.2-363	75	91
PS	13	1-79	21	30
PVC <sup>a</sup>	10	0.04-0.3	0.11	0.6
		0.5-4	1.3	3

Large particles				
Plastic	Supplier stated size	PSA range	$D_{50}$	Average size
	( $\mu\text{m}$ )	( $\mu\text{m}$ )	( $\mu\text{m}$ )	( $\mu\text{m}$ )
PP	100	60-275	124	137
PE	100	69-316	153	169
PET	100	4-240	81	93
PA	100	0.3-240	65	78
PS	100	40-317	125	142
PVC	100	60-209	106	116

<sup>a</sup>Note: There are two PSA ranges for PVC due to the fact that on analysis there were found to be two distinct size distributions.



**Figure 2.8:** Particle size distribution from the laser diffraction particle size analysis of microplastics investigated ■ = small particles (PP and PVC) used throughout this study as received. Light grey (▨) bars represent the particle size distribution of small particles as received, while the dark grey bars (■) represent the particle size distribution of large particles as received. The sizes stated are as supplied by the manufacturer.

The broad distribution of particle sizes would make meaningful evaluation of the impact of particle size on adsorption impossible. For this reason, the microplastic was sieved in an attempt to standardise the particle size across the microplastic types. However, sieving the microplastics did not show considerable effect on the particle size distribution of the microplastics, unless there was an extremely wide particle size distribution such as small PA (as received). For the small particles, the median size of the PE ( $D_{50}$  25  $\mu\text{m}$ ), PET ( $D_{50}$  28  $\mu\text{m}$ ), and PS ( $D_{50}$  21  $\mu\text{m}$ ) as received was very similar to  $D_{50}$  of the sieved particles (20-45  $\mu\text{m}$ ) of PE ( $D_{50}$  24  $\mu\text{m}$ ), PET ( $D_{50}$  29  $\mu\text{m}$ ), and PS ( $D_{50}$  26  $\mu\text{m}$ , Figure 2.9).

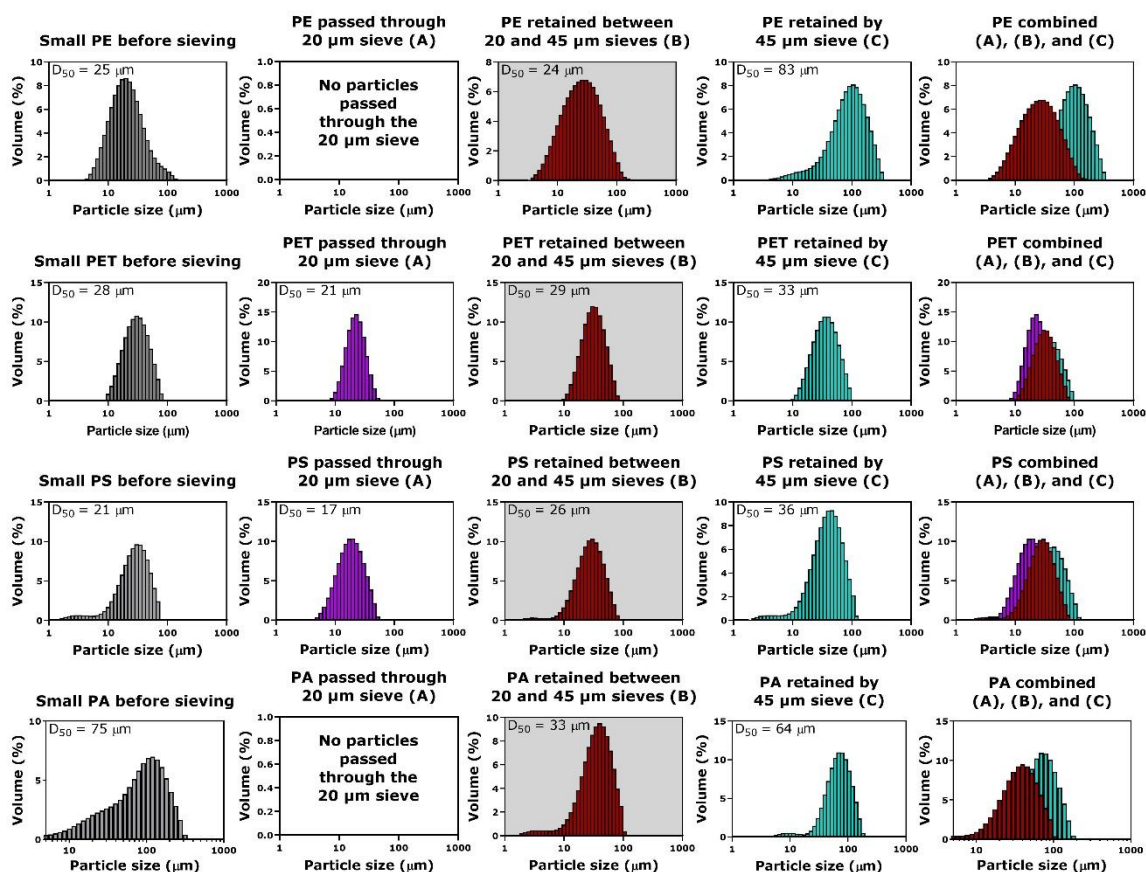


**Figure 2.9:** Particle size distribution from the laser diffraction particle size analysis of the small microplastics investigated. ■ = particles as received (also shown in Figure 2.8); ■ = particles that passed through the 20  $\mu\text{m}$  sieve; ■ = particles retained between 20  $\mu\text{m}$  and 45  $\mu\text{m}$  sieves, and ■ = particles retained by the 45  $\mu\text{m}$  sieve. The combination of the three size ranges obtained during the sieving process is presented (right end). The grey background indicates the particles that were used in the experiments of this thesis.  $D_{50}$  represents the median of the particle size distribution.

The extremely small size of the PVC particles (contrary to the information provided by the supplier) was of concern (Table 2.3). In adsorption experiments, the liquid phase is filtered to remove the microplastics before analysis of compound concentration by either injecting it into the HPLC injection port (Li, Zhang and Zhang 2018; Puckowski et al. 2021) or photo spectrophotometer (Liu et al. 2019; Ma et al. 2019; Atugoda et al. 2020). Frequently, membranes with a pore size of 0.22  $\mu\text{m}$  or greater are used for filtering samples prior analysis (Wu et al., 2016; Yu et al., 2020), which are unsuccessful in removing particles smaller than 0.22  $\mu\text{m}$ . For liquid chromatographic analysis, this can result in damage to the analytical equipment. While for photo spectrophotometer analysis, the remaining very small particles in suspension might affect absorption of the light and impact on the results. In an attempt to remove particles that could potentially pass through 0.22  $\mu\text{m}$  filters, the small PVC was dispersed in methanol. The solvent containing PVC particles was filtered through a GF/F filter (0.7  $\mu\text{m}$ ). The smallest pore size available of GF/F (0.7  $\mu\text{m}$ ) was selected due to its inert glass composition. As well as the sieving, filtering the small particles of PVC dispersed in methanol was ineffective (Figure 2.10). The filtering of small PVC was not only unable to remove the particles < 0.22  $\mu\text{m}$ , but also seemed to contaminate the material with debris of particles sized approximately 10  $\mu\text{m}$ . This contamination is possibly attributed to the glass fibres from the GF/F filter and/or microparticles suspended in the ambient air when filtering the particles. For this reason, the material described as small PVC was used as received.

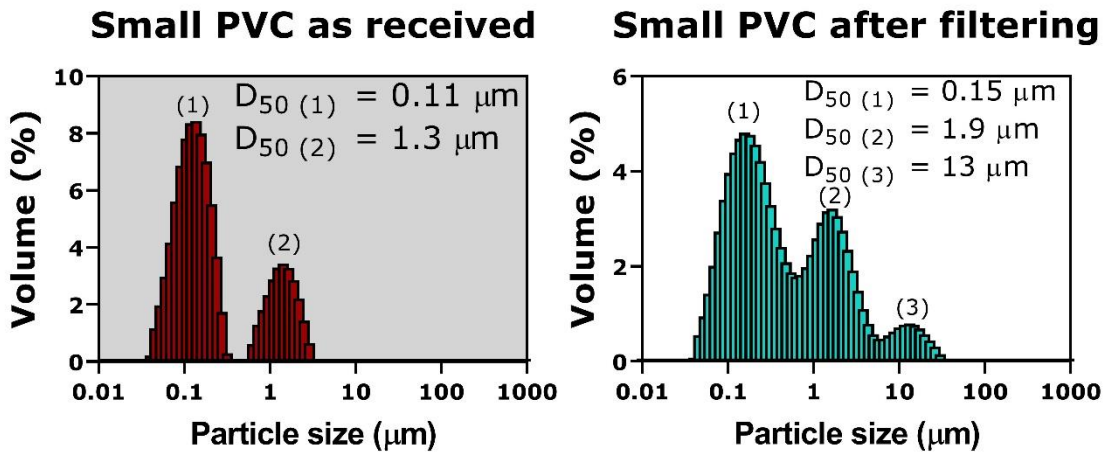


**Figure 2.10:** Particle size distribution from the laser diffraction particle size analysis of small PVC. ■ = particles as received (left); ■ = particles retained by the GF/F filter (0.7  $\mu\text{m}$ , right). The grey background indicates the particles that were used in this research.  $D_{50}$  represents the median of the particle size distribution of each peak.

Sieving of large microplastics was able to separate the small particles from the material received. For this reason, an increase in the  $D_{50}$  of the material retained between the 90 and 150  $\mu\text{m}$  sieves was observed for all microplastic types (Figure 2.11). The process of sieving the microplastics was found to have a better effect on the particle size distribution of the large microplastics when compared to the small microplastics.

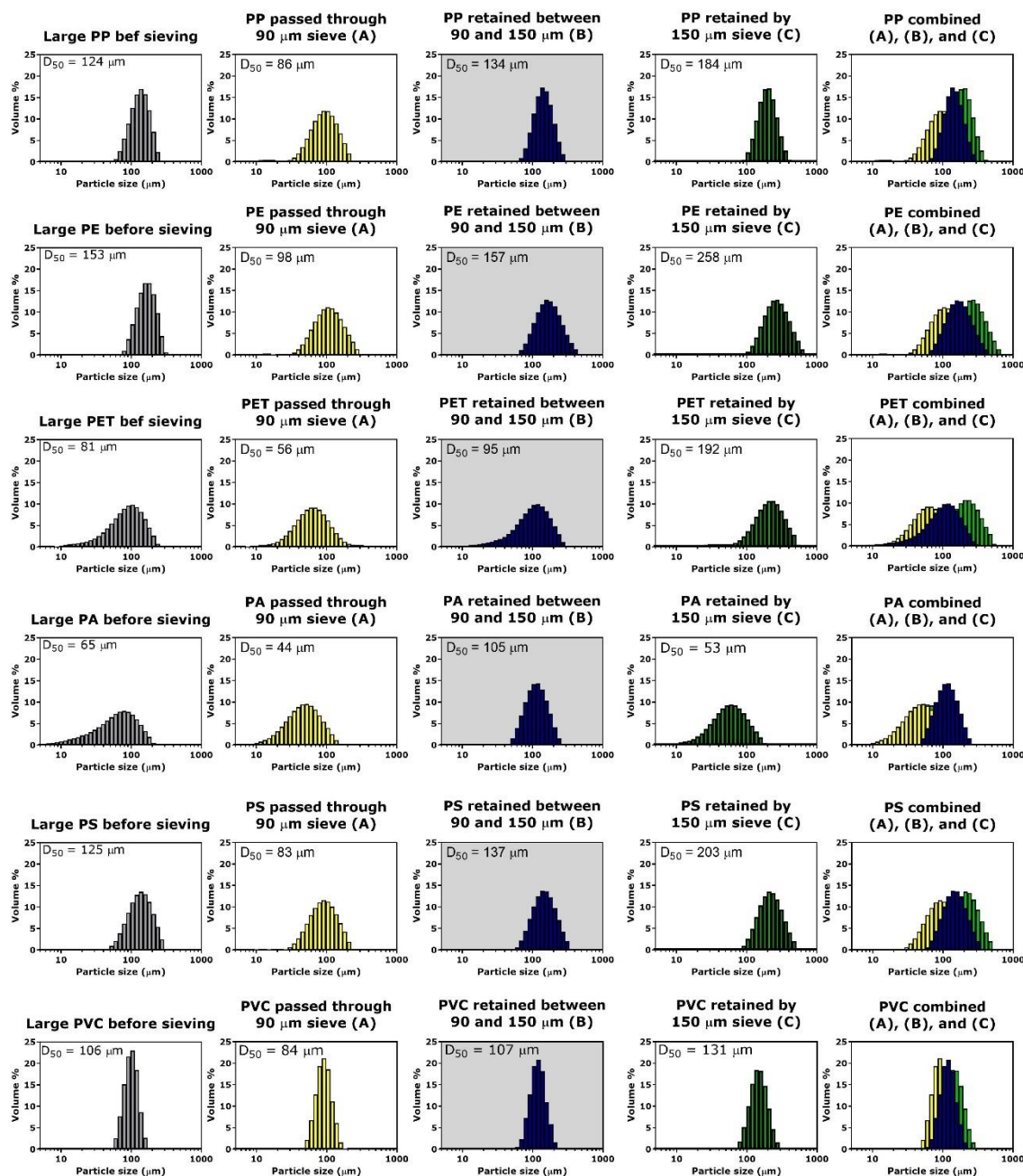


**Figure 2.11:** Particle size distribution from the laser diffraction particle size analysis of large of microplastics. ■ = particles as received; ■ = particles that passed through the 90  $\mu\text{m}$  sieve; ■ = particles retained between 90  $\mu\text{m}$  and 150  $\mu\text{m}$  sieves; and ■ = particles retained by the 150  $\mu\text{m}$  sieve. The combination of the three size ranges obtained during the sieving process is presented (right end). The grey background indicates the particles that were used for most experiments of this thesis.  $D_{50}$  represents the median of the particle size distribution.

Although the median size ( $D_{50}$ ) was very similar, the sieving of the small microplastics reduced the range for the particle sizes (Table 2.4). For instance,



the range of sizes of small PE reduced from 0.2-549  $\mu\text{m}$  to 3-209  $\mu\text{m}$ , and small PA range size have also reduced from 0.2-363  $\mu\text{m}$  to 1-105  $\mu\text{m}$ . For the large particles, the size range of the particles has also been reduced. Especially large PA that before presented a particle size range of 0.3-240  $\mu\text{m}$  ( $D_{50}$  65  $\mu\text{m}$ ), after the sieving demonstrated a particle size range of 46-240  $\mu\text{m}$  ( $D_{50}$  105  $\mu\text{m}$ , Table 2.4). The particle size distribution of the size-standardised microplastics used for experimentation is presented in Figure 2.12.

**Table 2.4:** Size range of size-standardised microplastics determined by laser diffraction particle size analysis (PSA) range and median of the particle size distribution ( $D_{50}$ ) of size-standardised microplastic of both sizes (small and large).

<b>Small particles</b>		
<b>Plastic</b>	<b>PSA range</b>	<b><math>D_{50}</math></b>
	<b>(<math>\mu\text{m}</math>)</b>	<b>(<math>\mu\text{m}</math>)</b>
PP <sup>a</sup>	4-23	8
PE	3-209	24
PET	10-91	29
PA	1-105	33
PS	2-91	26
PVC <sup>a</sup> (1)	0.04-0.3	0.11
PVC <sup>a</sup> (2)	0.5-4	1.3
<b>Large particles</b>		
<b>Plastic</b>	<b>PSA range</b>	<b><math>D_{50}</math></b>
	<b>(<math>\mu\text{m}</math>)</b>	<b>(<math>\mu\text{m}</math>)</b>
PP	60-216	134
PE	60-478	157
PET	3-216	95
PA	46-240	105
PS	60-263	134
PVC	52-240	107

<sup>a</sup> used as received.

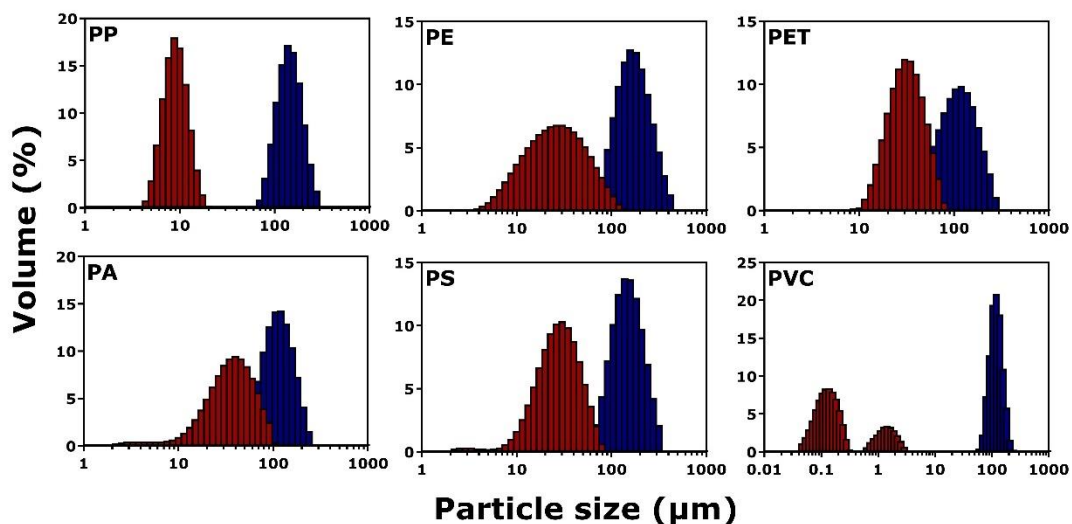


**Figure 2.12:** Summary of particle size distribution from the laser diffraction particle size analysis (PSA) of particles used in this thesis. ■ = small particles; ■ = large particles.

Scanning electron microscopy (SEM) imaging of the material received from the supplier revealed predominantly irregular surface morphologies (Figure 2.13). The SEM images allow visual verification of particle sizes determined through PSA (Figure 2.8). The SEM images displayed a diverse range of sizes in samples of large PET and small PA (as received). Additionally, the SEM images confirmed the extremely small size and broad size distribution of the small PVC sample claimed to have an average size of 10  $\mu\text{m}$  by the supplier (Figure 2.13). As for surface morphologies, small PP, small PVC, and both sizes of PE showed a rough surface, while PET, PS, PA (both sizes), and large PP presented with smooth surfaces. Small PVC was spherical in shape with a spongy appearance. SEM images of small PA (sieved) also showed the reduced size and the range of sizes (Figure 2.14) when compared to the material received from the supplier (Figure 2.13).

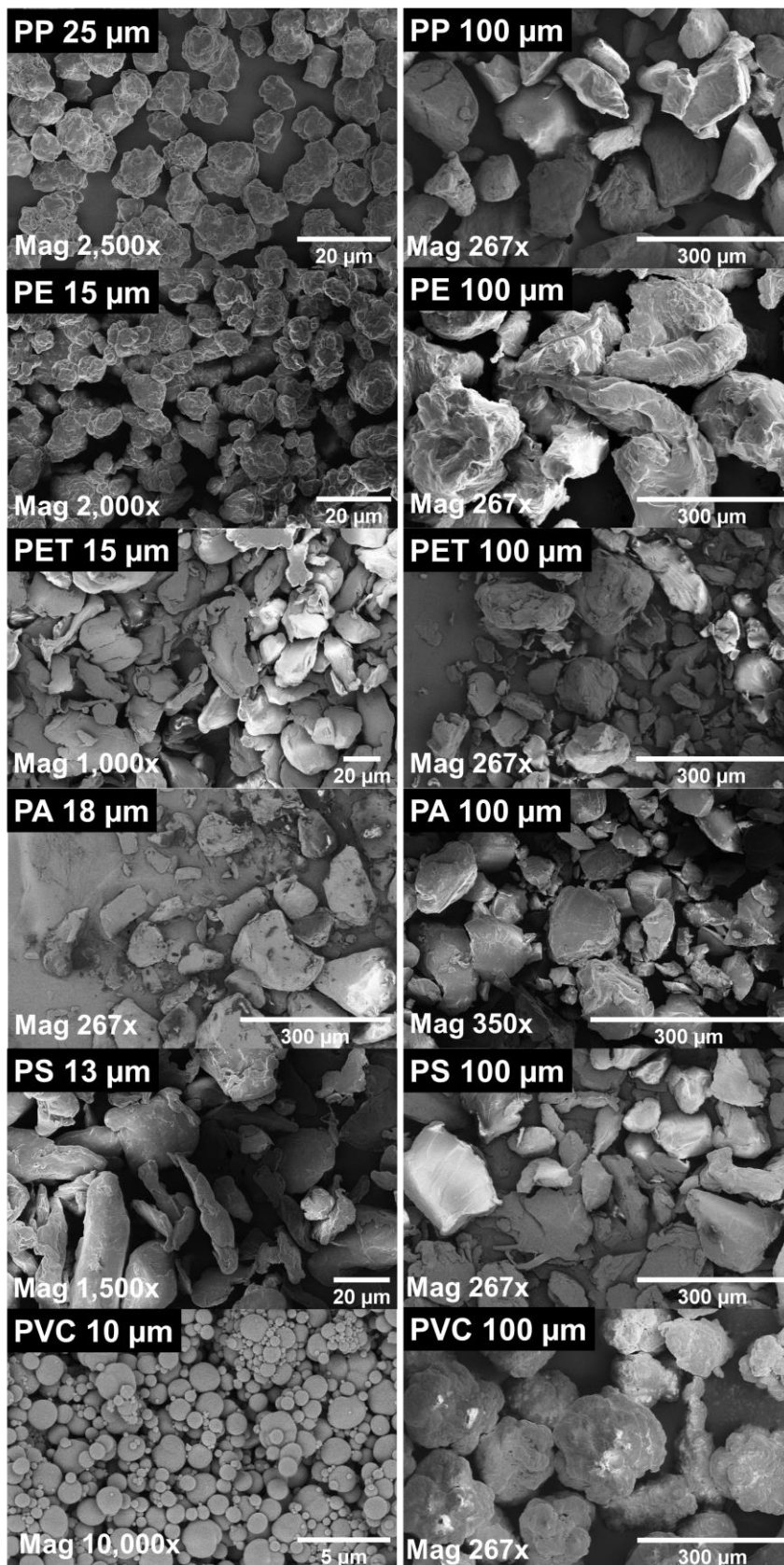


**Figure 2.13:** Surface morphology and particle size of the microplastic particles (as received) using scanning electron microscopy (SEM) imaging. The sizes as provided by the supplier are in the top left corner of each image. The magnification of the images ranged from 297x to 10,000x.

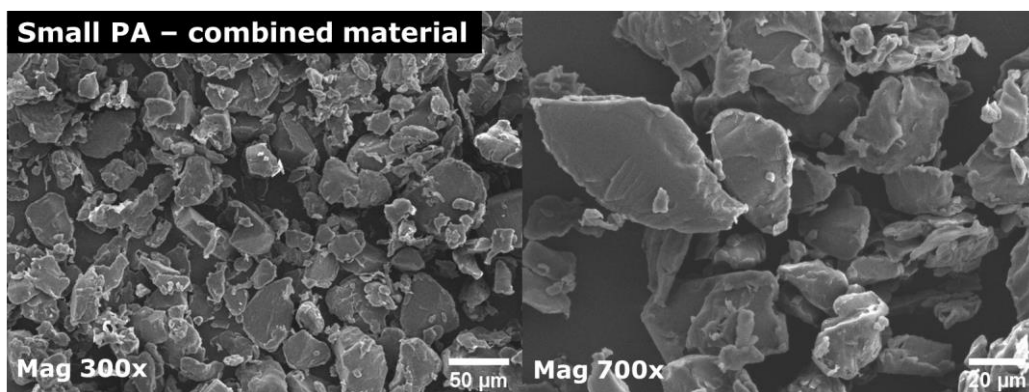


**Figure 2.14:** Surface morphology and particle size of small PA (combined material) using scanning electron microscopy (SEM) imaging. The magnification of the images was 300x and 700x.

The separation of the microplastics by the sieves depended on various factors such as the particle size distribution, shape of the particle and roughness of the microplastics. However, sieving microplastic in the laboratory can be hazardous: unintentional spills resulting in contamination of wastewater with microplastics, inhalation of microplastic by the operator, and risk of contamination of the microplastic samples. Furthermore, the time required to process samples should not be underestimated. Depending on the study question, sieving alone does not replace the need for a detailed characterisation of the material for a reliable interpretation of the data.

### **2.3.3 Characterisation of virgin microplastics: Evaluation of the microplastic surface area**

The surface area of the microplastics plays an important role in the interaction between organic compounds and microplastics. The greater the surface area of the material, the greater the amount of binding sites potentially available for adsorption of compounds onto microplastics (Chen, Sawyer and Regan 2013). The N<sub>2</sub>-BET adsorption-desorption surface area of both the material as received

from the supplier and the sieved microplastics (20-45  $\mu\text{m}$  for small and 90-150  $\mu\text{m}$  for large particles) was measured. Likewise, the simulated surface area ( $S_{PSA}$ ) of the material as received and the sieved particles was calculated (Table 2.5).

As mentioned before, small PP and small PVC were used as received.

**Table 2.5:** Simulated surface area ( $S_{PSA}$ ), and  $\text{N}_2$ -BET adsorption-desorption surface area ( $S_{BET}$ ) of both sizes (small and large) of the received microplastics and size-standardised microplastics.

<b>Small particles</b>				
<b>Plastic</b>	<b><math>S_{PSA}</math> as received</b>	<b><math>S_{BET}</math> as received</b>	<b><math>S_{PSA}</math> sieved</b>	<b><math>S_{BET}</math> sieved</b>
	<b>(<math>\text{m}^2 \text{g}^{-1}</math>)</b>	<b>(<math>\text{m}^2 \text{g}^{-1}</math>)</b>	<b>(<math>\text{m}^2 \text{g}^{-1}</math>)</b>	<b>(<math>\text{m}^2 \text{g}^{-1}</math>)</b>
PP	0.72	52.2	0.72	52.2
PE	0.22	1.58	0.31	1.47
PET	0.31	0.82	0.22	0.76
PA	0.11	0.97	0.30	0.61
PS	0.37	2.34	0.27	1.56
PVC	43.5	4.33	43.50	4.57
<b>Large particles</b>				
<b>Plastic</b>	<b><math>S_{PSA}</math> as received</b>	<b><math>S_{BET}</math> as received</b>	<b><math>S_{PSA}</math> sieved</b>	<b><math>S_{BET}</math> sieved</b>
	<b>(<math>\text{m}^2 \text{g}^{-1}</math>)</b>	<b>(<math>\text{m}^2 \text{g}^{-1}</math>)</b>	<b>(<math>\text{m}^2 \text{g}^{-1}</math>)</b>	<b>(<math>\text{m}^2 \text{g}^{-1}</math>)</b>
PP	0.05	0.73	0.05	0.01
PE	0.04	0.28	0.04	0.28
PET	0.10	0.46	0.09	0.28
PA	0.09	0.92	0.06	0.92
PS	0.05	0.39	0.05	0.39
PVC	0.06	0.59	0.053	0.41

Small PP had a very high surface area ( $S_{BET}$ ) of  $52.2 \text{ m}^2 \text{g}^{-1}$  compared to the other microplastics investigated (Table 2.5). The simulated surface area ( $S_{PSA}$ ), of small PP ( $0.72 \text{ m}^2 \text{g}^{-1}$ ) was much lower compared to its  $S_{BET}$  which indicates that small PP is a porous material. The increased surface area may be a result of the use of grafting agents in small PP, as evidenced by Yang et al. (2013). These authors discovered a correlation between the graft ratio and the surface area of PP particles. Moura et al. (2022) conducted an experiment in which a combination of eight microcystins variants were placed in contact with the same small and large PP and PET particles that are being studied in this study. The

results showed a significant adsorption of microcystins onto small PP (with a carbonyl functional group peak as determined by FT-IR, indicative of the presence of a grafting agent) in comparison to small PET. However, there was no noticeable difference in the adsorption of large PP (without a carbonyl functional group IR peak) compared to large PET.

The average size of the small PVC particles was 0.48  $\mu\text{m}$ , its  $S_{PSA}$  was 43.5  $\text{m}^2 \text{g}^{-1}$  while its  $S_{BET}$  was 4.33  $\text{m}^2 \text{g}^{-1}$  (Table 2.5). The reason for this discrepancy may be that the degassing of the  $\text{N}_2$ -BET adsorption-desorption analysis was performed at 30  $^\circ\text{C}$ , instead of the normally employed 130  $^\circ\text{C}$ , due to PVC's low melting point. Except for small PVC, all simulated surface areas calculated based on the laser diffraction particle size analysis ( $S_{PSA}$ ) were smaller when compared to the  $S_{BET}$ .  $S_{PSA}$  assumes perfect sphericity of the particles, therefore a greater  $S_{BET}$  suggests a degree of porosity/roughness for most of the microplastic particles. As expected, the  $S_{BET}$  of PA as received of both sizes were similar, since the material received from the supplier described as small and large PA were effectively the same size. Generally, the sieved microplastics showed a decreased on the  $S_{BET}$  when compared to the microplastics as received (Table 2.5). The reason might be that during the sieving process, the particles were more exposed to air, therefore due to the limitations of the degassing method, atmospheric gases potentially adsorbed onto the microplastics was not successfully removed during the degassing process during  $S_{BET}$  analysis.  $S_{BET}$  analysis can bring insights regarding the surface area when compared the surface area the microplastic types analysed, however the limitations of the method (low degassing temperature) and the lack of replicates mean that  $S_{BET}$  results should be interpreted with some caution.

#### **2.3.4 Characterisation of virgin microplastics: evaluation of the crystallinity and glassiness**

The crystalline structure of microplastics was analysed using x-ray diffraction (XRD). A greater peak height in the XRD pattern indicates a higher degree of crystallinity (Figure 2.15). The XRD patterns of PP, PE, and PET revealed clear peaks and a bumpy baseline, indicating the presence of both crystalline and amorphous regions. The presence of melting temperature <sup>TM</sup> peaks confirmed the semi-crystalline structure of PP, PE, and PET (Figure 2.16). On the other hand, the XRD patterns (Figure 2.15) and DSC analysis (Figure 2.16) of PS and PVC showed no diffraction peaks and melting peaks, respectively, confirming their amorphous structure. The glass transition temperature ( $T_g$ ) is considered the melting point of amorphous polymers.  $T_g$  refers to the temperature at which plastics become soft, and polymers with  $T_g$  below the ambient temperature of 25°C, such as PP and PE, are considered rubbery. On the other hand, polymers with  $T_g$  above 25°C, such as PET, PA, PS, and PVC, are considered glassy. The melting point is the temperature at which crystalline order is completely destroyed upon heating (Chawla 2012). Amorphous polymers like PS and PVC do not have crystalline regions and therefore, the absence of melting peaks in the DSC graphs is expected (Figure 2.16).

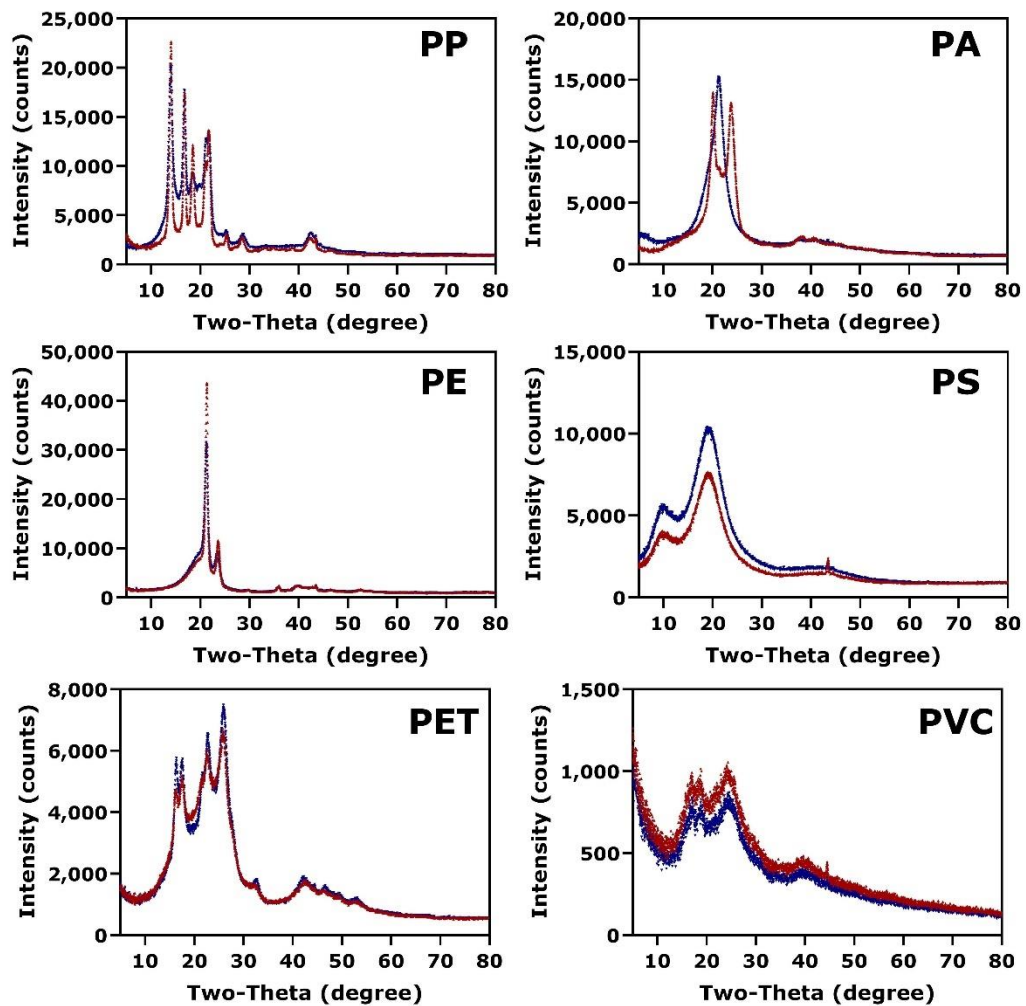


**Figure 2.15:** Crystallinity pattern of small and large microplastics as received from the supplier from x-ray diffraction (XRD) analysis. — = small particles and — = large particles. Sharp peaks represent crystalline regions.

Small PA (as received) was found to differ from large PA. The differing FT-IR spectra of the two PA sizes (Figure 2.6), the XRD patterns (Figure 2.15) and DSC analysis (Table 2.6; Figure 2.16) confirmed that the small and large PA particles were not made of the same material. The small PA, described by the supplier as having an average size of 18  $\mu\text{m}$ , was semi-crystalline (Table 2.6). On the other hand, the absence of a  $T_m$  peak indicated that large PA was amorphous. The  $T_m$  of small PA (221  $^{\circ}\text{C}$ ) matched polyamide-6 (PA6), also known as nylon 6 (Hamid, Akhbar and Halim 2013). Furthermore, small PA was rubbery ( $T_g < 0^{\circ}\text{C}$ ),



consistent with PA6 (Crawford and Quinn 2017; Guo, Chen and Wang 2019). The difference in the crystallinity between the two PA sizes can lead to erroneous data interpretation in an adsorption experiment using these microparticles (Moura Et. al. 2023). As expected, the combined material of small PA incorporated the thermal characteristics of both small PA and large PA as received. Two  $T_g$  (25.56 °C and 91.63 °C) and a  $T_m$  peak (221.10 °C) were detected in small PA (Figure 2.17; Table 2.6) as shown in large PA (as received; Figure 2.16; Table 2.6).

**Table 2.6:** Summary of differential scanning calorimetry (DSC) results of the microplastic types investigated, including the endotherm melting enthalpy change considering 100% crystallisation ( $\Delta H_{m100\%}^a$ ) of plastics, glass transition temperature ( $T_g$ ), melting temperature ( $T_m$ ), endotherm melting enthalpy change of microplastics ( $\Delta H_m$ ), and degree of crystallinity ( $X_c$ ).

Small particles							
Plastics	$\Delta H_{m100\%}^a$	$T_g$	$T_m$	$\Delta H_m$	$X_c$	Crystallinity	Glassiness
	(J g <sup>-1</sup> )	(°C)	(°C)	(J g <sup>-1</sup> )	(%)		
PP	207.1	< 0	145.37	65.486	32	Semi-crystalline	Rubbery
PE	293.6	< 0	102.95	44.169	15	Semi-crystalline	Rubbery
PET	140.1	81.44	250.37	32.882	23	Semi-crystalline	Glassy
PA <sup>b</sup> (as received)	230.1	< 0	221.64	51.938	23	Semi-crystalline	Rubbery
PA <sup>b</sup> (combined material)	230.1	25.56; 91.63	221.10	20.945	9	Semi-crystalline; Amorphous	Glassy
PS	n/a	95.32	n/a	n/a	0	Amorphous	Glassy
PVC	n/a	83.72	n/a	n/a	0	Amorphous	Glassy
Large particles							
Plastics	$\Delta H_{m100\%}^a$	$T_g$	$T_m$	$\Delta H_m$	$X_c$	Crystallinity	Glassiness
	(J g <sup>-1</sup> )	(°C)	(°C)	(J g <sup>-1</sup> )	(%)		
PP	207.1	< 0	160.94	96.643	47	Semi-crystalline	Rubbery
PE	293.6	< 0	104.67	49.473	17	Semi-crystalline	Rubbery
PET	140.1	80.87	247.12	26.325	19	Semi-crystalline	Glassy
PA	n/a	21.62; 93.62	n/a	n/a	0	Amorphous	Rubbery; Glassy
PS	n/a	96.21	n/a	n/a	0	Amorphous	Glassy
PVC	n/a	83.48	n/a	n/a	0	Amorphous	Glassy

<sup>a</sup> Values obtained from PerkinElmer Technical Bulletin (PerkinElmer application note, no date)

<sup>b</sup> Treated as nylon 6 (PA6)

Note: Large PA and both sizes of PS, and PVC were found to be amorphous polymers, thus the absence crystalline regions and melting peaks

The XRD pattern of PP revealed a difference between the small and large particles. The XRD showed that large PP has a lower degree of crystallinity compared to small PP (Figure 2.15) as indicated by its higher baseline. However, the DSC results showed that large PP has a higher degree of crystallinity (47%) than small PP (32%, Table 2.6). Lima et al., (2002) explain that the difference between XRD and DSC results can be due to the thermal history of the polymer. In the DSC analysis, the degree of crystallinity is calculated based on the melting enthalpy of the second heating run, which erases the thermal history of the polymer (equation 2.2). In the first heating run, small PP had a higher melting enthalpy peak compared to large PP (Figure 2.16), which aligns with the XRD results. Additionally, small PP had a lower  $T_m$  (145°C) than large PP (161°C). The difference in both  $X_c$  and  $T_m$  for small and large PP is also an indication of the presence of acrylic acid as a grafting agent in small PP particles. Mandal et al. (2017) have observed that the crystallinity of grafted PP films decreases with an increase in grafting as a result of the presence of the amorphous acrylic acid. According to Mandal et al. (2017), the  $T_m$  of the grafted PP decreased due to the grafting destroying the ordered structure of the PP crystals.

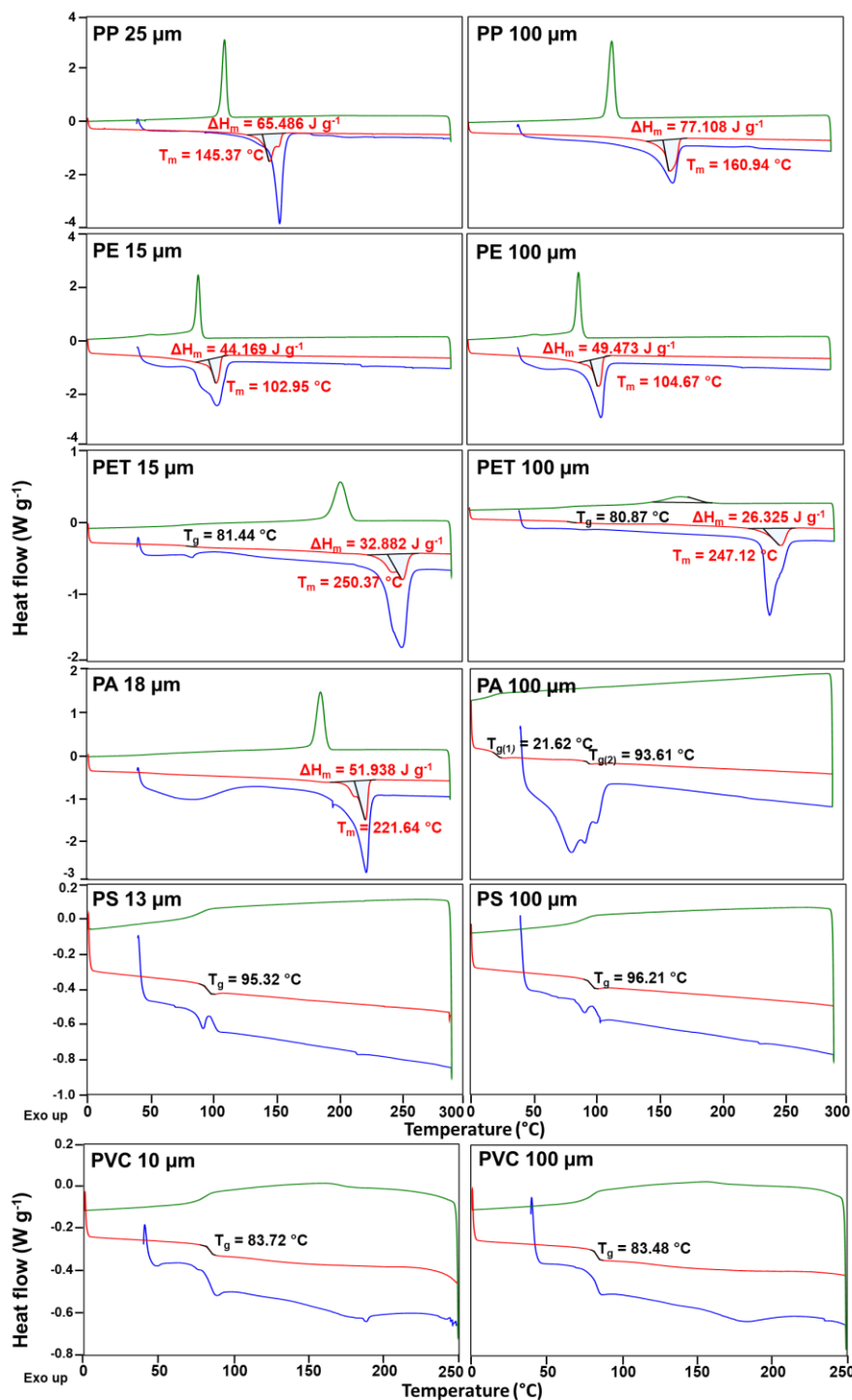


**Figure 2.16:** Thermodynamic properties the small and large microplastics received from the supplier from the differential scanning calorimetry (DSC) analysis. The sizes stated are as detailed by the supplier. For PP, PE, PET, PA, and PS, first heating run, 40-290 °C at 20 °C min<sup>-1</sup> (—), cooling run, 290-0 °C at 10 °C min<sup>-1</sup> (—), and second heating run 0-290 °C at 10 °C min<sup>-1</sup> (—). For PVC, first heating run, 40-250 °C at 20 °C min<sup>-1</sup> (—), cooling run, 250-0 °C at 10 °C min<sup>-1</sup> (—), and second heating run 0-250 °C at 10 °C min<sup>-1</sup> (—). N<sub>2</sub> was used as the purge gas. T<sub>g</sub> represents the glass transition temperature (°C), and ΔH<sub>m</sub> the endotherm melting enthalpy change of the microplastics (J g<sup>-1</sup>). Exo up means that peaks above the baseline refers to an exothermic peak, indicating that the sample is releasing heat as it undergoes a thermal transition.

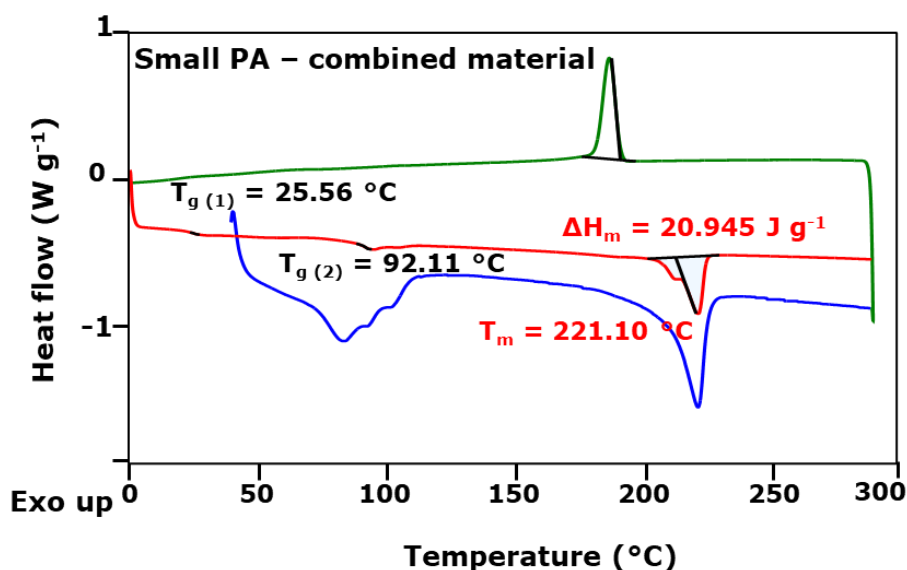


**Figure 2.17:** Thermodynamic properties of the size-standardised small from differential scanning calorimetry (DSC) analysis. First heating run, 40-290 °C at 20 °C min<sup>-1</sup> (—), cooling run, 290-0 °C at 10 °C min<sup>-1</sup> (—), and second heating run 0-290 °C at 10 °C min<sup>-1</sup> (—). N<sub>2</sub> was used as the purge gas. T<sub>g</sub> represents the glass transition temperature (°C), and ΔH<sub>m</sub> the endotherm melting enthalpy change of the microplastics (J g<sup>-1</sup>). Exo up means that peaks above the baseline refers to an exothermic peak, indicating that the sample is releasing heat as it undergoes a thermal transition.

### 2.3.5 Characterisation of virgin microplastics: evaluation of the surface charge and oxidation of the particles

The adsorption of organic compounds on microplastics is significantly influenced by electrostatic interactions (Atugoda et al. 2021). The zeta potential measurements demonstrated that the microplastic surface is negatively charged (Table 2.7). The surface charge of the microplastics varied from -10 mV for large PVC to -67 mV for small PVC. The increased surface charge of small PVC (with median sizes of D<sub>50</sub> 0.11 μm and D<sub>50</sub> 1.3 μm) might be due to its extremely small size. In general, the smaller particles displayed a higher surface charge compared to the larger particles (Table 2.7). A study has shown a clear correlation between the size of the particles and the zeta potential measurement (Nakatuka et al. 2015). According to Nakatuka et al. (2015), particles of smaller diameter are more easily affected by the random movement of fluid flow and

other particles when compared to larger particles. Therefore, the absolute value of effective zeta-potential of smaller particles is greater than larger particles.

**Table 2.7:** Zeta potential ( $\zeta$ ) measurement, and carboxyl index (CI) calculated using equation 2.1 of the size-standardised microplastics at both sizes (small and large).

Plastics	Small particles		Large particles	
	$\zeta$	CI	$\zeta$	CI
	(mV)		(mV)	
PP	-36	1.38	-12	0.05
PE	-18	0.02	-16	0.02
PET	-36	11.87	-25	10.78
PA	-36	0.74	-19	0.68
PS	-42	0.12	-16	0.06
PVC	-64	0.06	-10	0.15

The carboxyl index (CI) is used to specifically monitor the absorption band of the carbonyl species formed during thermo-oxidation processes. Carboxyl describes a chemical group that consists of a carbonyl and a hydroxyl bonded to each other. Meanwhile, carbonyl describes a chemical group that consists of one atom of carbon double bonded to one atom of oxygen. The CI was calculated by measuring the ratio of the carbonyl peak ( $1,850-1,650\text{ cm}^{-1}$ ), relative to a reference peak (Almond et al. 2020). For the current study, the C-H bend was chosen as a reference peak ( $1,500-1,420\text{ cm}^{-1}$ ) since it is typically not affected by oxidation processes. For virgin particles of PP, PE, PS, and PVC no carbonyl functional group should be detected in the FT-IR spectra (Figure 2.6), therefore a CI close to zero is expected (Table 2.7). However, the greater carboxyl index of small PP (CI 1.38) is a result of the presence of the carbonyl functional group on small PP samples (Figure 2.6). The increased CI measured in small PET (CI 11.87) and large PET (CI 10.78) is appropriate. The strong and sharp carbonyl peak detected on virgin particles of PET is typical due to the presence of a ketone carbonyl intensive peak at  $1,712\text{ cm}^{-1}$  (Table 2.7).

### **2.3.6 Characterisation of artificially aged microplastics: visual inspection of aged microplastics**

The weathering of microplastics can have a significant impact on the adsorption of organic compounds. Size-standardised virgin microplastics were subjected to artificial aging through exposure to ultraviolet (UV) and visible light from a xenon arc lamp. After 72 hours of irradiation, a change in colour for both sizes of PS, PA, and PVC was noticed. PS and PA showed yellowing while PVC, particularly the large particles, had a brown-reddish colour (Figure 2.18). The change in colour of plastics is a characteristic sign of polymer aging. The yellowing of PS is believed to be due to the build-up of conjugated bond sequences in the polymer backbone (Yousif and Haddad 2013). The yellowing of PA, on the other hand, was probably caused by thermal oxidation, which can lead to the formation of pyrrole materials (He et al. 2014). When pyrrole is exposed to air, it oxidizes into highly coloured polymeric products, resulting in yellowing (Ji Ram et al. 2019). PVC discoloration from white to dark-brown or black is a typical sign of degradation that occurs when the vinyl chloride polymers are exposed to light at 250–350 nm (Yousif and Hasan 2015). Photo and thermal degradation of PVC releases hydrochloric gas (dehydrochlorination), which leads to the formation of conjugate polyene sequences ( $-\text{CH}=\text{CH}$ ) in the polymer chains, giving PVC its reddish-brown colour (Hollande and Laurent 1997; De Campos and Martins Franchetti 2005). Extensive conjugation leads to colour. The longer the length of the conjugated segment, the greater the wavelength of the light that can be absorbed, eventually incorporating the wavelength range for visible light (380-700 nm, Seidlitz et al. 2001).

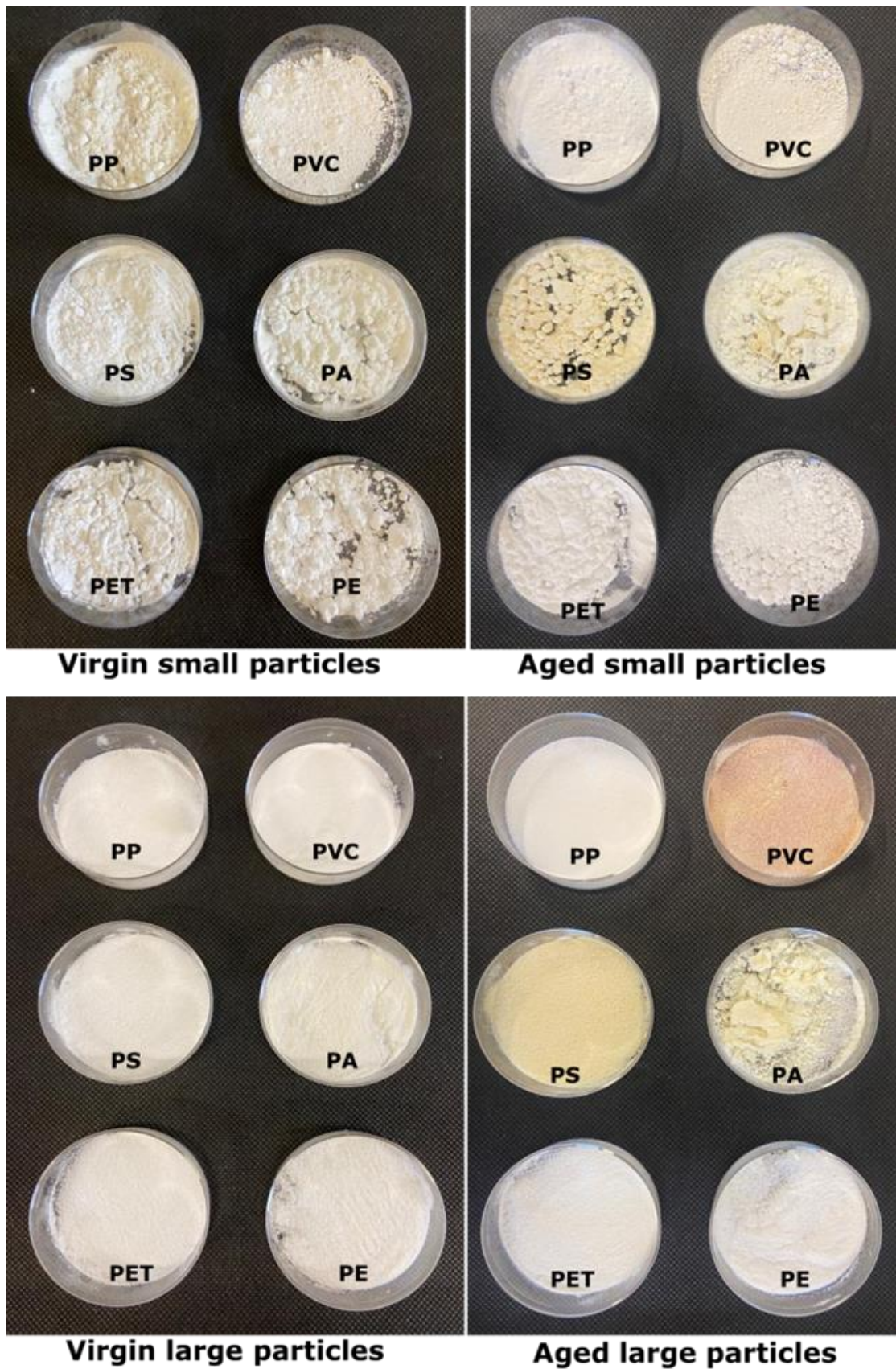


**Figure 2.18:** Effect of accelerated artificial weathering on small and large microplastics before (left) and after (right) 72 h exposure in weathering testing unit equipped with a 1,700 W xenon arc lamp operated at  $60 \text{ W m}^{-2}$  (300-400 nm) intensity.



### **2.3.7 Characterisation of artificially aged microplastics: evaluation of chemical structure of the aged microplastics**

The exposure of polymers to UV radiation causes photo-oxidative degradation which results in breakage of the polymer chains which, in turn, produces radicals (Yousif and Haddad 2013). FT-IR spectroscopy is one of the most common analytical techniques to monitor oxidation reactions (Almond et al. 2020). IR is particularly valuable for detecting polar functional groups, such as ketones and ester carbonyls (intense peaks at 1,715 and 1,735  $\text{cm}^{-1}$ , respectively), which are typical of oxidative degradation pathways (Chamas et al. 2020). A peak in the carbonyl function group IR absorption band (1,650-1,800  $\text{cm}^{-1}$ ) was detected in the samples of aged microplastics (Figure 2.19). However, the carbonyl peak formation cannot be observed on aged particles of PET due to the presence of a ketone carbonyl intensive peak at 1,712  $\text{cm}^{-1}$  typical of PET. The amide peak (C-N + C=O) in the PA samples at 1,635  $\text{cm}^{-1}$  can also make the detection and measurement of a carbonyl function groups peak in aged PA particles difficult. Overall, the FT-IR spectra of artificially aged microplastics compare well to microplastic occurring in environmental samples (Hendrickson, Minor and Schreiner 2018; Veerasingam et al. 2021).

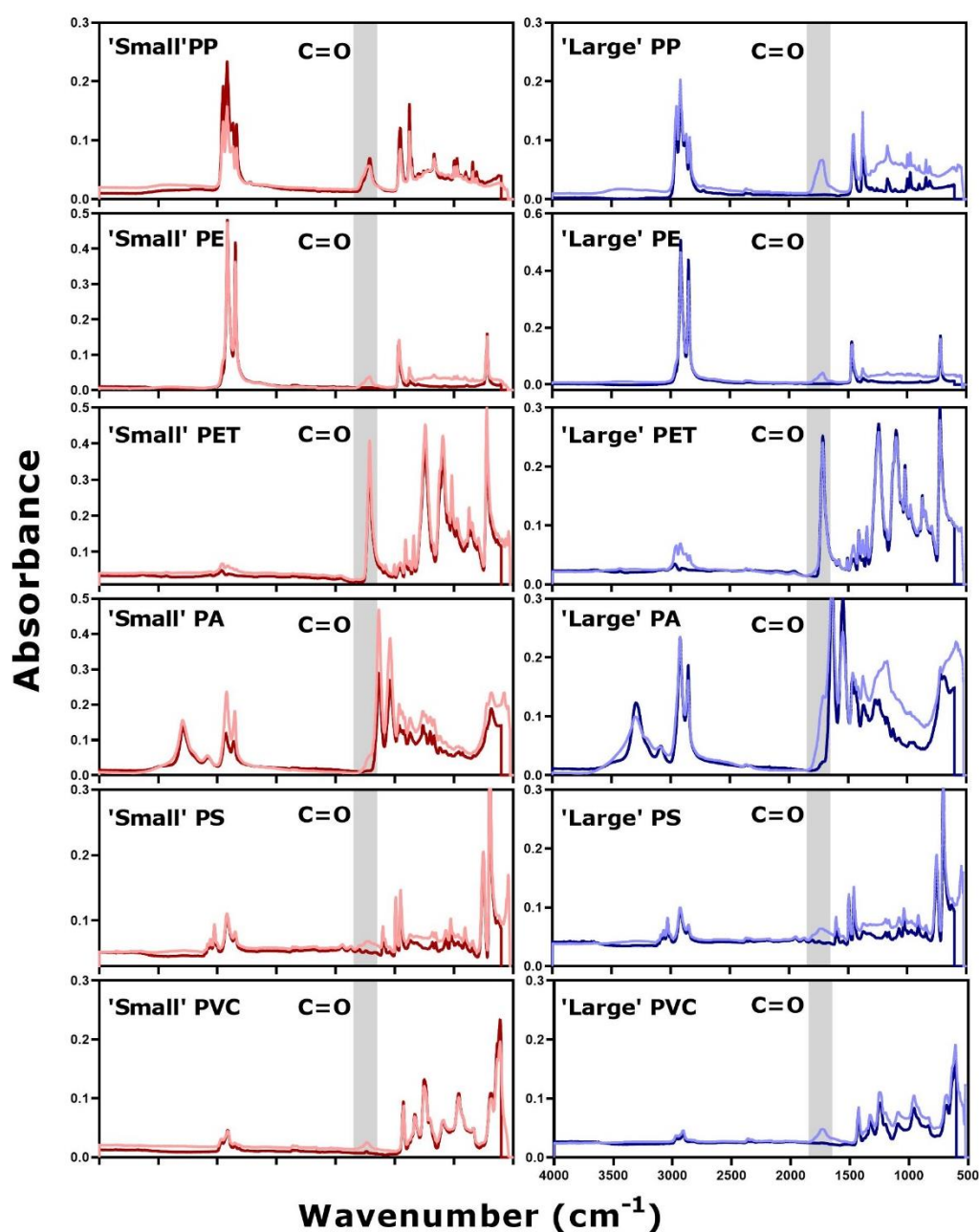


**Figure 2.19:** Evaluation of carbonyl functional groups formation in artificially aged microplastics using attenuated total reflectance Fourier transformer infrared (ATR FT-IR) analysis. The spectra of small (virgin —, aged —) and large (virgin —, aged —) microplastic are presented. Carbonyl functional group peak at 1,850-1,650  $\text{cm}^{-1}$  highlighted in grey (■).

The weathering mechanism of polymers mainly consists of degradation by thermal (high temperature), photo- (light) oxidation (oxygen), and hydrolysis (water, Chamas et al. 2020). During the development of this method, the

contact of the microplastics with water during the exposure to UV and visible light was considered. However, several tests were performed (data not shown) and no indication of hydrolysis was observed in the FT-IR spectra of the microplastics. The reason might be due to fast evaporation of the water when exposed to the intense simulated solar radiation. Furthermore, in the presence of water, the exposure to the light was different for each microplastic type, due to their different polarities, buoyancies, and densities (Table 2.2). To avoid interference with the light exposure due to buoyancy differences, spraying water on the microplastics in the aging chamber was considered. However, when water was sprayed on the microplastic samples, an aggregation of the microplastics was observed due to polarity differences, which also impacted the irradiation exposure of each microplastic type. Furthermore, because of the decreased amount of water used when sprayed, the contact time of the microplastics due to evaporation (~30 min) was found to be insufficient to cause hydrolysis. Therefore, no water was used for the aging of the particles.

During the aging process, the chamber temperature was set to 30 °C ( $29.3 \pm 3.4$  °C,  $n = 2788$ ). However, due the high intensity of the irradiation, the samples reached approximately 70 °C throughout the 72h exposure. Increasing temperatures, increases reaction rates and thermal degradation that accelerates the process of aging (Karlsson, Hassellöv and Jakubowicz 2018). Temperatures in some landfills and industrial composters have been reported to reach 80-100 °C, accelerating degradation rates provided sufficient oxygen for the thermal-oxidative degradation (Chamas et al. 2020).

### 2.3.8 Characterisation of artificially aged microplastics: evaluation of the particle size and surface area of the aged microplastics

Laser diffraction particle size analysis (PSA) of the aged microplastics was performed to evaluate whether the aging of the virgin microplastics caused fragmentation of the particles that could affect the adsorption of compounds. Aging had not caused fragmentation of the particles but instead led to their aggregation, especially for the smaller particles (Table 2.8; Figure 2.20).

**Table 2.8:** Summary of results of laser diffraction particle size analysis (PSA) range, PSA median of the particle size distribution ( $D_{50}$ ), simulated surface area ( $S_{PSA}$ ), and  $N_2$ -BET adsorption-desorption surface area ( $S_{BET}$ ) of artificially aged particles of small and large microplastics.

Small particles				
Aged plastic	PSA range	$D_{50}$	$S_{PSA}$	$S_{BET}$
	( $\mu\text{m}$ )	( $\mu\text{m}$ )	( $\text{m}^2 \text{g}^{-1}$ )	( $\text{m}^2 \text{g}^{-1}$ )
PP	52-976	22	0.31	49.29
PE	4-976	127	0.09	1.10
PET	10-59	30	0.21	0.38
PA	3-976	107	0.08	0.23
PS	2-976	42	0.17	0.69
PVC	1-163	7	1.11	2.89
Large particles				
Aged plastic	PSA range	$D_{50}$	$S_{PSA}$	$S_{BET}$
	( $\mu\text{m}$ )	( $\mu\text{m}$ )	( $\text{m}^2 \text{g}^{-1}$ )	( $\text{m}^2 \text{g}^{-1}$ )
PP	46-240	127	0.05	-0.03
PE	52-254	158	0.04	0.07
PET	10-272	103	0.07	0.10
PA	40-976	252	0.03	0.08
PS	46-186	108	0.06	0.23
PVC	52-976	119	0.05	0.07

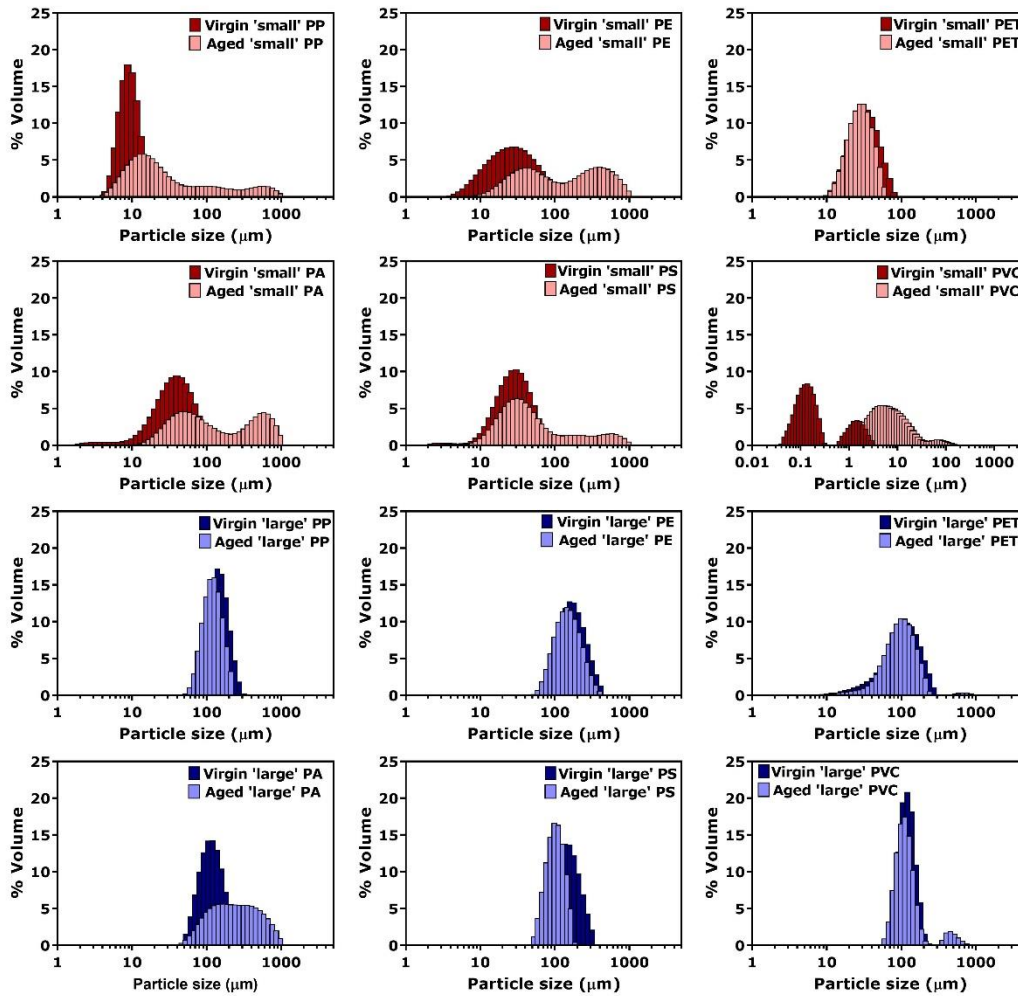


**Figure 2.20:** Particle size distribution of the virgin and artificially aged particles of small (■ = virgin particles, ■ = virgin particles) and large (■ = virgin particles, ■ = virgin particles) microplastics using a laser diffraction particle size analysis (PSA).

As a result, larger particles were recorded by the laser diffraction particle size analyser in the aged particles compared to the virgin particles. This resulted in the aged microplastics having a lower surface area ( $S_{BET}$ ) compared to the virgin microplastics (Table 2.8). Additionally, there were no noticeable differences in the surface morphology of the microplastics due to weathering (Figure 2.21).

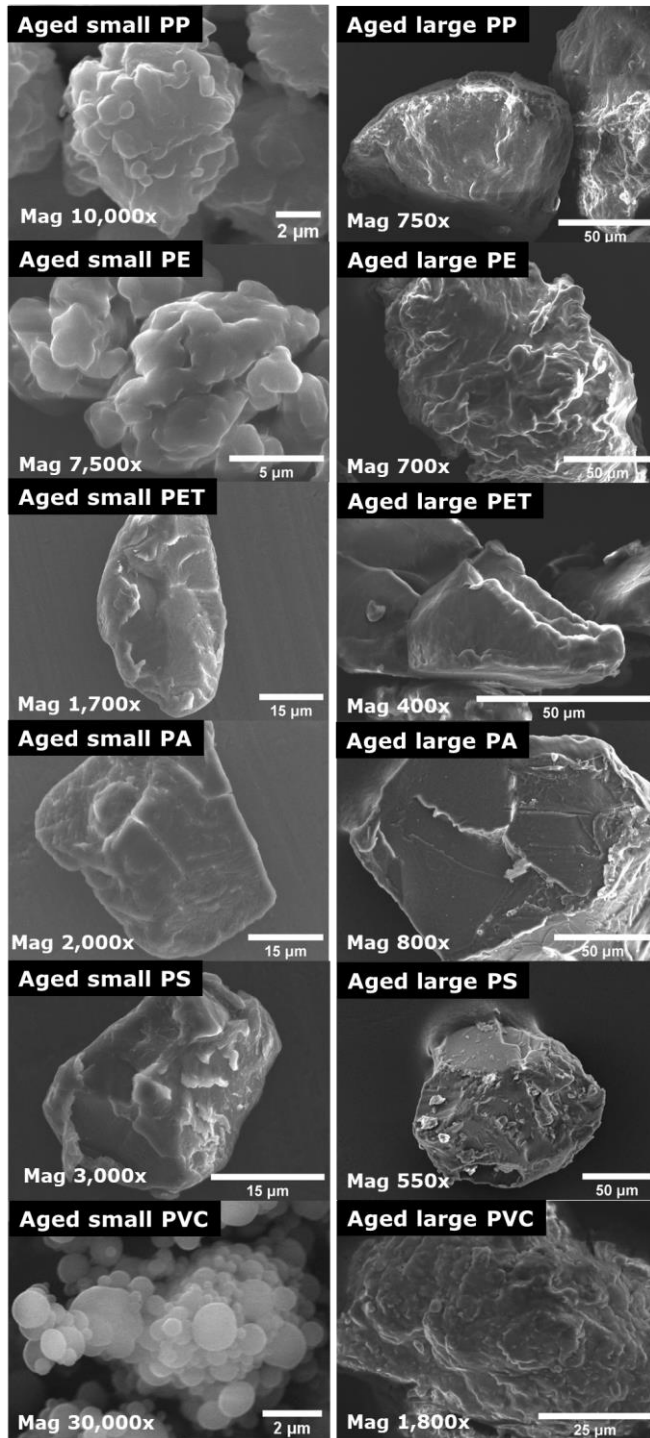


**Figure 2.21:** Surface morphology of artificially aged microplastics using scanning electron microscopy (SEM) images at sizes described as small and large. The magnification of the images ranged from 400x to 30,000x.

### **2.3.9 Characterisation of artificially aged microplastics: evaluation of the crystallinity and glassiness of the aged microplastics**

The aging of microplastics can impact the degree of crystallinity of microplastics (Prajapati, Narayan Vaidya and Kumar 2022). To evaluate this, x-ray diffraction (XRD) and differential scanning calorimetry (DSC) of the aged microplastics was performed. The XRD pattern did not show a difference when comparing the virgin and aged particles, except for small PA (Figure 2.22). The difference between the XRD pattern of virgin small PA can be attributed to the fact that XRD analysis of virgin microplastics was performed on the particles as received. On the other hand, the XRD analysis of aged microplastics consisted of the size-standardised microplastics. As mentioned, small PA used throughout this study was a composite material. The XRD pattern of aged small PA does not contain a sharp crystalline peak, which could lead to the erroneous conclusion that it is an amorphous structure (Figure 2.22). However, it is known that the small PA consist of a mixture of a semi-crystalline form (PA described by the supplier as having an average size of 18  $\mu\text{m}$ ) and an amorphous form of PA (PA described by the supplier as having an average size of 100  $\mu\text{m}$ ). Therefore, a melting temperature ( $T_m$ ) peak is detected on the DSC analysis of small, aged PA (Figure 2.23). This means that DSC analysis demonstrated to be more sensitive to the presence of semi-crystalline particles in the PA sample than XRD analysis.

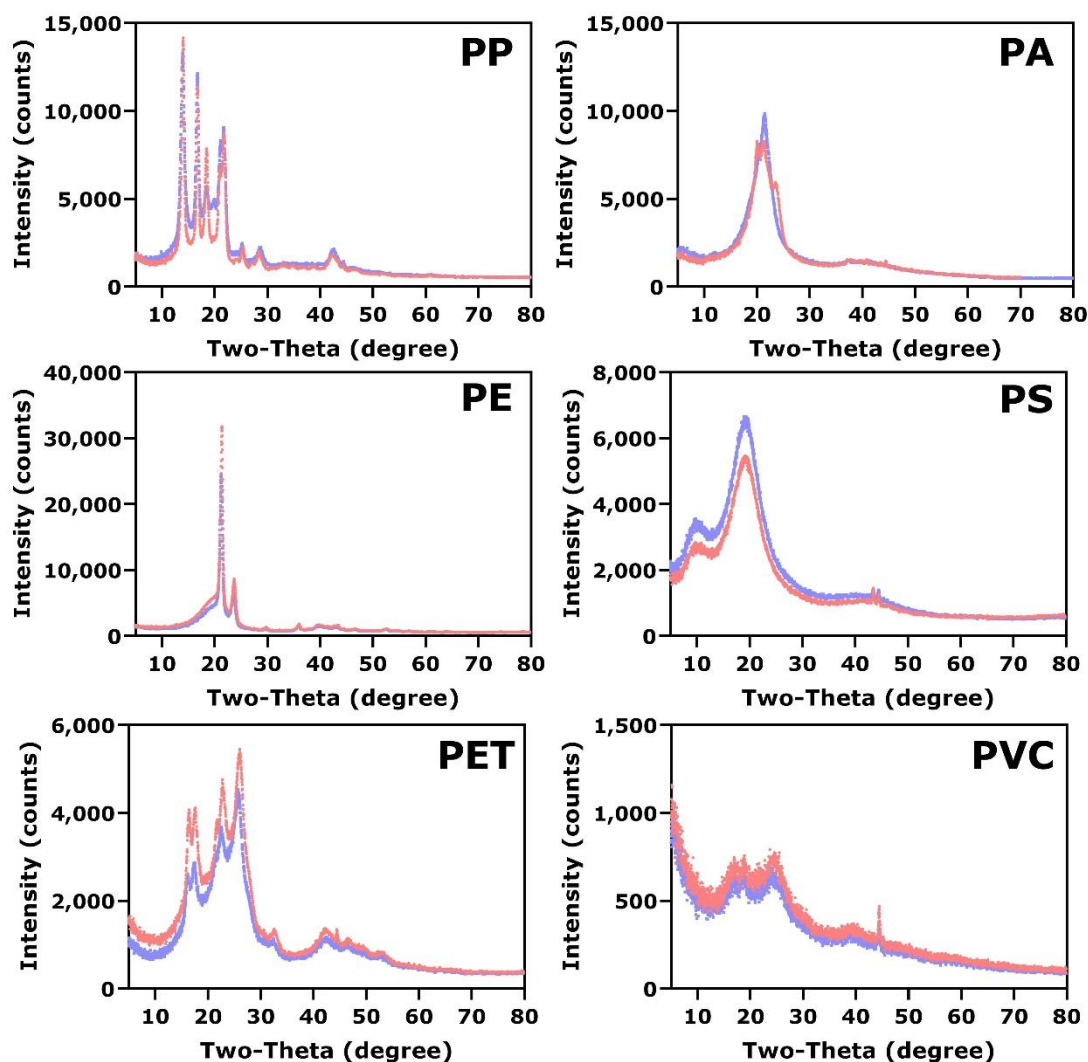


**Figure 2.22:** Crystallinity pattern of artificially aged microplastics using x-ray diffraction (XRD) of sizes small (—) and large (—) particles.

The DSC analysis of the aged microplastics showed no evident difference in the glass transition temperature ( $T_g$ ) between the virgin and aged particles (Table 2.9; Figure 2.23). No marked difference of the degree of crystallinity was found between the virgin and aged microplastics, with the exception of the large PP particles. Large PP showed a decrease in crystallinity from 47% to 30% (Table 2.9). Furthermore, the  $T_m$  of PP decreased when comparing virgin and aged particles of both sizes. A lower  $T_m$  of PP samples was also observed by Yakimets, Lai and Guigon (2004) over 7 weeks of exposure to UV radiation. On the other



hand, according to those authors, in oxygen diffusion-controlled processes, such as photo-oxidation, the crystallinity of PP increased with the rate of oxidation. Scission of macromolecules can lead to the formation of smaller, more mobile molecules that can pack together more efficiently, resulting in improved crystallization (Yakimets, Lai and Guigon 2004). In contrast, Blais et al. (1976) also found a decrease in  $T_m$  and  $X_C$  of PP after exposure to a xenon arc lamp for 240 h. Free radicals caused by photo-oxidation can react with other polymer chains, leading to the formation of chemical bonds between chains, known as crosslinking (Lomonaco et al. 2020). This process can restrict the movement of individual chains, making it more difficult for the chains to order themselves into a crystalline structure (Yousif and Haddad 2013). As a result, photo-oxidation can decrease the degree of crystallinity of polymers, such as PP, by reducing the amount of ordered, crystalline regions in the material.

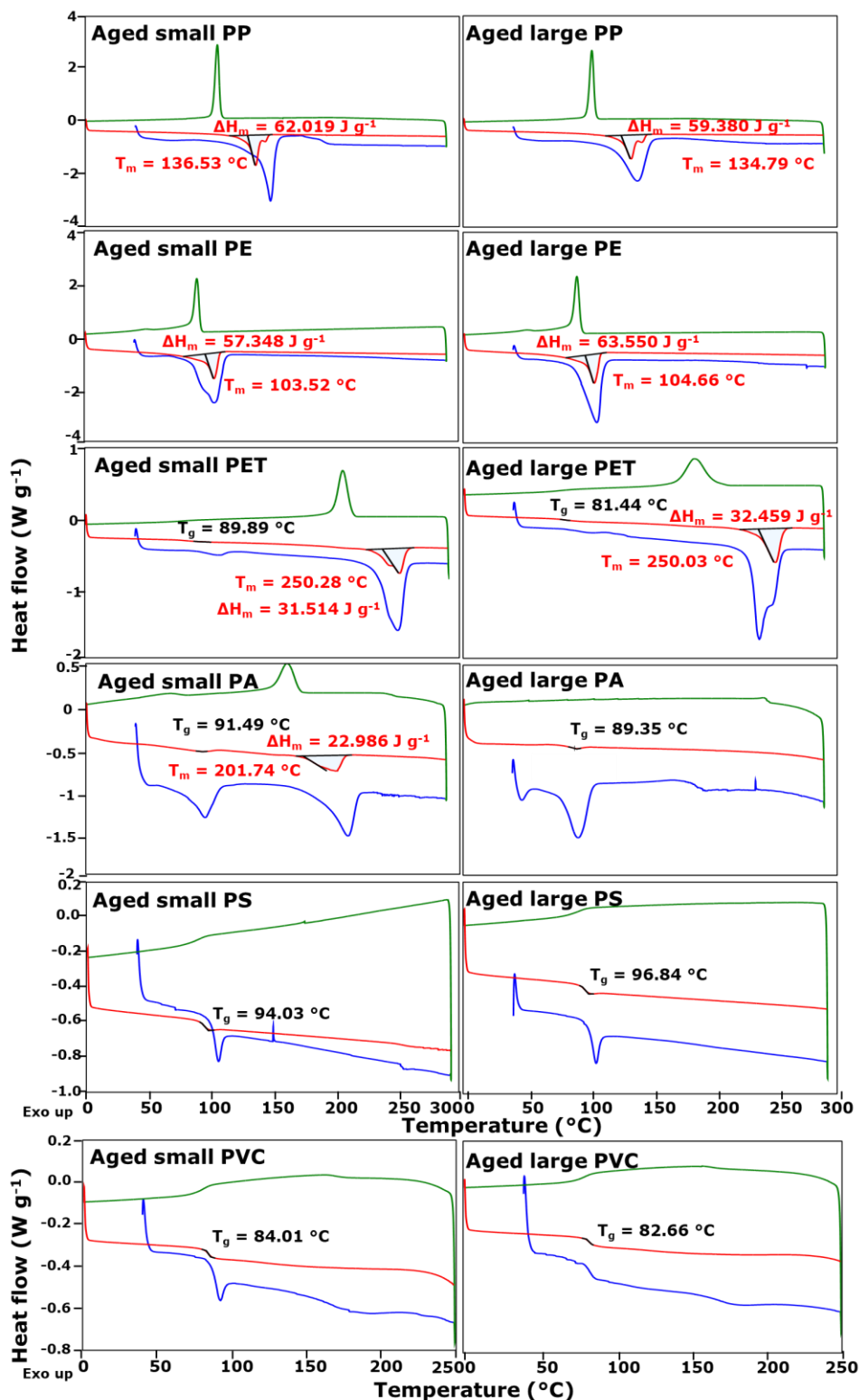


**Figure 2.23:** Thermodynamic properties of artificially aged microplastics. For PP, PE, PET, PA, and PS, first heating run, 40-290 °C at 20 °C min<sup>-1</sup> (—), cooling run, 290-0 °C at 10 °C min<sup>-1</sup> (—), and second heating run 0-290 °C at 10 °C min<sup>-1</sup> (—). For PVC, first heating run, 40-250 °C at 20 °C min<sup>-1</sup> (—), cooling run, 250-0 °C at 10 °C min<sup>-1</sup> (—), and second heating run 0-250 °C at 10 °C min<sup>-1</sup> (—). N<sub>2</sub> was used as the purge gas.  $T_g$  represents the glass transition temperature (°C), and  $\Delta H_m$  the endotherm melting enthalpy change of the microplastics (J g<sup>-1</sup>). Exo up means that peaks above the baseline refers to an exothermic peak, indicating that the sample is releasing heat as it undergoes a thermal transition.

**Table 2.9:** Differential scanning calorimetry (DSC) of the artificially aged microplastics, including the endotherm melting enthalpy change considering 100% crystallisation ( $\Delta H_{m100\%}^a$ ) of plastics, glass transition temperature ( $T_g$ ), melting temperature ( $T_m$ ), and endotherm melting enthalpy change of microplastics ( $\Delta H_m$ ).

<b>Small particles</b>					
<b>Aged plastic</b>	$\Delta H_{m100\%}^a$	$T_g$	$T_m$	$\Delta H_m$	$X_c$
	<b>(J g<sup>-1</sup>)</b>	<b>(°C)</b>	<b>(°C)</b>	<b>(J g<sup>-1</sup>)</b>	<b>(%)</b>
PP	207.1	<0	136.53	62.019	30
PE	293.6	<0	103.52	57.348	20
PET	140.1	89	250.28	31.514	22
PA <sup>b</sup>	230.1	91	201.74	23.149	10
PS	n/a	94	n/a	n/a	n/a
PVC	n/a	84	n/a	n/a	n/a
<b>Large particles</b>					
<b>Aged plastic</b>	$\Delta H_{m100\%}^a$	$T_g$	$T_m$	$\Delta H_m$	$X_c$
	<b>(J g<sup>-1</sup>)</b>	<b>(°C)</b>	<b>(°C)</b>	<b>(J g<sup>-1</sup>)</b>	<b>(%)</b>
PP	207.1	<0	134.79	59.380	29
PE	293.6	<0	104.66	63.550	22
PET	140.1	81	250.03	32.459	23
PA	n/a	89	n/a	n/a	n/a
PS	n/a	97	n/a	n/a	n/a
PVC	n/a	83	n/a	n/a	n/a

<sup>a</sup> Values obtained from Perkin Elmer Technical Bulletin (Perkin Elmer application note, no date)

<sup>b</sup> Treated as nylon 6 (PA6)

### **2.3.10 Characterisation of artificially aged microplastics: evaluation of the surface charge and oxidation of the aged microplastics**

Organic polymers can deteriorate when exposed to sunlight and oxygen, but there is a significant variability in their photo-oxidative susceptibility. Different microplastic types reacted differently to the same weathering conditions, with the differences being more pronounced in the large particles. PVC had the greatest susceptibility, followed by PP, while PE, PS, and PA had lower susceptibilities (Figure 2.24; Table 2.10). The degradation of polymers through UV light is primarily driven by the presence of UV-absorbing species (100-400 nm, chromophores) mixed in with the polymer (Tolinski 2015). PE, which is made up of only carbon-carbon single bonds, is less prone to photo-oxidative degradation due to the absence of UV-visible chromophores (Chamas et al. 2020). In a study

conducted by Gijsman et al. (1999), PP demonstrated a higher oxidation rate than polybutylene terephthalate and PA, while PE showed the lowest rate, according to oxygen uptake measurements. As anticipated, the comparison of aged and virgin microplastics showed that the aged particles had a higher CI value, resulting from the formation of carbonyl functional groups due to photo- and thermal-oxidation degradation (Figure 2.24).

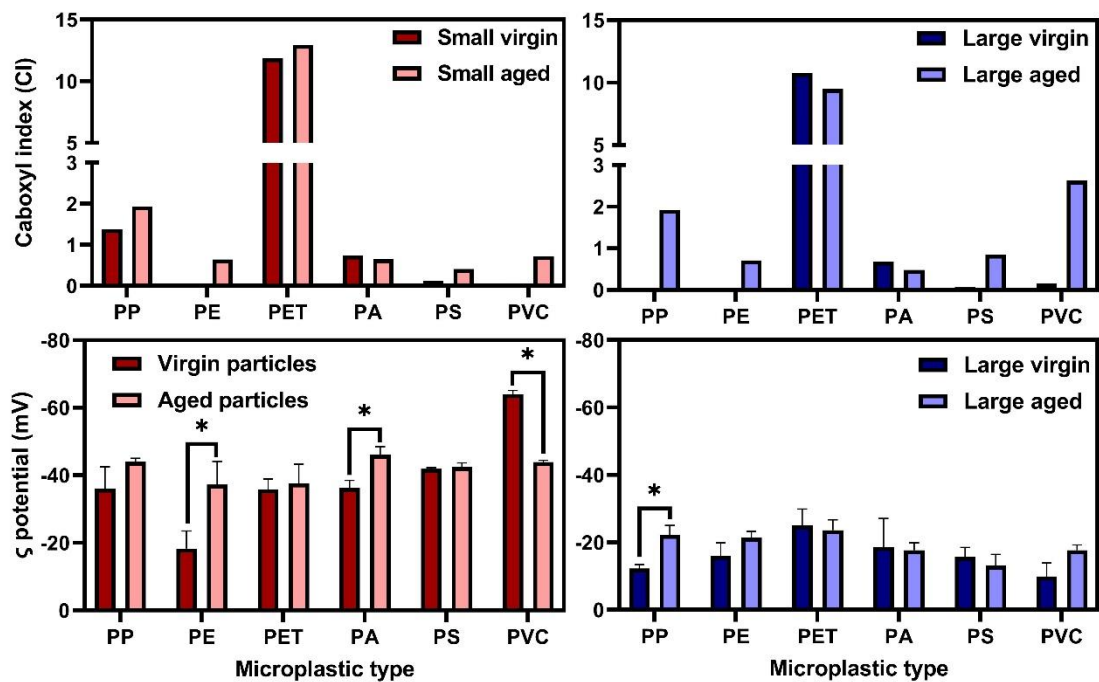


**Figure 2.24:** Carboxyl index (CI) and zeta potential measurement of virgin and aged of small (virgin ■, aged ■) and large (virgin ■, aged ■) particles. CI was calculated using equation 2.1. \*significant difference between the virgin and aged particles, t-test  $p < 0.05$ .

Additionally, large particles exhibited higher CI values than small particles. The size and shape of microplastics play a role in the amount and angle of radiation received by each particle, which in turn affects their degradation susceptibility. Individually, larger particles have a greater surface area than smaller particles, leading to greater surface contact for large microplastics. The carbonyl peak formation cannot be observed for aged PET particles due to the presence of an

intensive ester carbonyl peak at  $1,712\text{ cm}^{-1}$  which is typical of PET. The amide peak (C-N + C=O) in the PA samples at  $1,635\text{ cm}^{-1}$  can also make the detection and measurement of a carbonyl function group peak in aged particles of PA difficult. Overall, the FT-IR spectra of artificially aged microplastics compare favourably to microplastic from environmental samples (Hendrickson, Minor and Schreiner 2018; Veerasingam et al. 2021).

The zeta potential of the aged particles did not have a consistent trend compared to the virgin particles (Figure 2.24). Most microplastic types did not show a significant difference ( $p > 0.05$ ) when the zeta potential of virgin and aged particles was compared. The exception were the small particles of PE, PA, and PVC, and large PP, which had a more negative zeta potential in the aged particles. The surface charge of the microplastics ranged from  $-10\text{ mV}$  (virgin large PVC) to  $-64\text{ mV}$  (virgin small PVC), with small particles having a higher surface charge compared to large particles. Bhagat et al. (2022) observed that aging of microplastics resulted in a change of the zeta potential towards less negative values, as observed by small PVC in the current study. However, other studies have reported an enhanced negative surface charge of aged microplastics (Zhu et al. 2020).

**Table 2.10:** Summary of characterisation data of microplastics used in all experiments. Laser diffraction particle size analysis (PSA) range, median particle size ( $D_{50}$ ), simulated surface area ( $S_{PSA}$ ),  $N_2$  adsorption-desorption surface area ( $S_{BET}$ ), glass transition temperature ( $T_g$ ) measured by the differential scanning calorimetry (DSC) analysis, degree of crystallinity ( $X_c$ ), zeta potential ( $\zeta$ ) measurement, and carboxyl index (CI) of the virgin and artificially aged small and large microplastics.

Small particles								
Virgin plastic	PSA range	$D_{50}$	$S_{PSA}$	$S_{BET}$	$T_g$	$X_c$	$\zeta$	CI
	( $\mu\text{m}$ )	( $\mu\text{m}$ )	( $\text{m}^2 \text{g}^{-1}$ )	( $\text{m}^2 \text{g}^{-1}$ )	( $^{\circ}\text{C}$ )	(%)	(mV)	
PP	4-23	8	0.72	52.2	<0	32	-36	1.38
PE	3-209	24	0.31	1.5	<0	15	-18	0.02
PET	10-91	29	0.22	0.8	81	23	-36	11.87
PA	1-105	33	0.27	0.6	91	9	-36	0.74
PS	2-91	26	0.30	1.6	95	n/a	-42	0.12
PVC (1)	0.04-0.3	0.11	43.50	4.3	84	n/a	-64	0.06
PVC (2)	0.5-4	1.3						
Aged plastic	PSA range	$D_{50}$	$S_{PSA}$	$S_{BET}$	$T_g$	$X_c$	$\zeta$	CI
	( $\mu\text{m}$ )	( $\mu\text{m}$ )	( $\text{m}^2 \text{g}^{-1}$ )	( $\text{m}^2 \text{g}^{-1}$ )	( $^{\circ}\text{C}$ )	(%)	(mV)	
PP	52-976	22	0.31	49.29	<0	30	-44	1.94
PE	4-976	127	0.09	1.10	<0	20	-37	0.64
PET	10-59	30	0.21	0.38	89	22	-38	12.94
PA	3-976	107	0.08	0.23	91	10	-46	0.65
PS	2-976	42	0.17	0.69	94	n/a	-42	0.41
PVC	1-163	7	1.11	2.89	84	n/a	-44	0.72
Large particles								
Virgin plastic	PSA range	$D_{50}$	$S_{PSA}$	$S_{BET}$	$T_g$	$X_c$	$\zeta$	CI
	( $\mu\text{m}$ )	( $\mu\text{m}$ )	( $\text{m}^2 \text{g}^{-1}$ )	( $\text{m}^2 \text{g}^{-1}$ )	( $^{\circ}\text{C}$ )	(%)	(mV)	
PP	60-216	134	0.05	0.01	<0	47	-12	0.05
PE	60-478	157	0.04	0.28	<0	17	-16	0.02
PET	3-216	95	0.09	0.28	81	19	-25	10.78
PA	46-240	105	0.06	0.92	94	n/a	-19	0.68
PS	60-263	134	0.05	0.39	96	n/a	-16	0.06
PVC	52-240	107	0.053	0.41	83	n/a	-10	0.15
Aged plastic	PSA range	$D_{50}$	$S_{PSA}$	$S_{BET}$	$T_g$	$X_c$	$\zeta$	CI
	( $\mu\text{m}$ )	( $\mu\text{m}$ )	( $\text{m}^2 \text{g}^{-1}$ )	( $\text{m}^2 \text{g}^{-1}$ )	( $^{\circ}\text{C}$ )	(%)	(mV)	
PP	46-240	127	0.05	-0.03	<0	29	-22	1.92
PE	52-254	158	0.04	0.07	<0	22	-21	0.71
PET	10-272	103	0.07	0.10	81	23	-24	6.52
PA	40-976	252	0.03	0.08	89	n/a	-18	0.48
PS	46-186	108	0.06	0.23	97	n/a	-13	0.85
PVC	52-976	119	0.05	0.07	83	n/a	-18	2.63

## **2.4 Conclusion and recommendation for the pre-experimental characterisation of microplastic particles**

The aim was to select the type (polymer-based) and size of the microplastics representative of the microplastics found in freshwater environments. Six microplastic types in two sizes were selected and commercially acquired. A detailed characterisation was performed on the microplastics received. Results demonstrated inconsistencies in the purity, particle size, and degree of crystallinity of some of the microplastic received which highlighted the importance of not relying on the manufacturer information. It is important to highlight that the data from one supplier does not necessarily represent the situation with respect to other microplastic manufactures. However, the current study highlights that any commercially acquired microplastics should be characterised prior to any experimentation to ensure reliable interpretation of data. Further, the challenge of acquiring a uniform particle size for microplastic samples has been demonstrated. Particle separation techniques such as sieving might aid in obtaining a narrow size distribution of microplastics, however they represent a time-consuming process, in addition to the hazard of microplastic inhalation and unintentional spills. Furthermore, sieving microplastics does not remove the need for a detailed characterisation in order to achieve reliable information about the size distribution of the particles. As discussed by Moura et. al. (2023), among the analyses performed in this study to characterise the microplastics acquired commercially, Fourier Transform infrared (FT-IR) spectroscopy, particle size analysis (PSA) and differential scanning calorimetry (DSC) were shown to be crucial regarding the verification of physico-chemical properties of the commercially acquired microplastics. SEM images of the particles has also been shown to be valuable for verifying the particle sizes and

to evaluate the surface morphology of the microparticles. Additional analyses such as zeta potential measurement can also bring insights to interpret the factors affecting the adsorption of compounds on microplastics.

Finally, the characterisation of the artificially aged microplastics exhibited clear signs of thermal- and photo-oxidation of the virgin particles, such as the change of colour and the detection of the carbonyl free radical in the chemical structure of the aged particles. This means that the method developed to artificially age the size-standardised microplastics caused degradation of the virgin microplastics in a short exposure time (72 h). This chapter summarises all characterisation data about the microplastic used in this thesis, including the microplastic as received from the supplier, the size-standardised microplastics, and the artificially aged particles.



# **Chapter 3**

## **Adsorption of cyanotoxin (microcystins) onto microplastics**

<b>3 ADSORPTION OF CYANOTOXIN (MICROCYSTINS) ONTO MICROPLASTICS .....</b>	<b>98</b>
<b>3.1 Introduction .....</b>	<b>100</b>
3.1.1 Cyanobacterial blooms.....	100
3.1.2 Presence of cyanotoxins in freshwater environments .....	102
3.1.3 Selection of the microcystin analogues .....	104
3.1.4 Chapter aim and objectives .....	107
<b>3.2 Materials and methods.....</b>	<b>108</b>
3.2.1 Microplastics .....	108
3.2.2 Chemicals.....	109
3.2.3 Adsorption of a mixture of eight microcystin analogues on microplastics 109	
3.2.4 Competition of analogues on microplastics and evaluation of the sampling protocol.....	111
3.2.5 Adsorption of a mixture of three microcystin analogues on virgin and artificially aged microplastics .....	112
3.2.6 Adsorption isotherm and kinetics of MC-LR on small PP .....	113
3.2.7 Quantification of microcystin analogues in solution using liquid chromatography .....	113
3.2.8 Statistical analysis .....	117
<b>3.3 Results and discussion.....</b>	<b>119</b>
3.3.1 Adsorption of a mixture of eight microcystin analogues on polypropylene and polyethylene terephthalate .....	119
3.3.2 Evaluation of the sampling protocol .....	127
3.3.3 Evaluation of the competition of MC-LR and -LF onto microplastics.....	128
3.3.4 Adsorption of a mixture of MC-LR, -LW, and -LF onto small particles of six size-standardised virgin and artificially aged microplastics .....	131
3.3.5 Adsorption isotherm and kinetics.....	135
<b>3.4 Conclusions and environmental implications .....</b>	<b>140</b>

## **3.1 Introduction**

### **3.1.1 Cyanobacterial blooms**

Nutrient enrichment in waterbodies can lead to harmful algal blooms caused by cyanobacteria, also known as blue-green algae (Anderson, Glibert and Burkholder 2002). Cyanobacteria include about 2000 species in 150 genera, with a wide range of shapes and sizes. Cyanobacteria have a variety of cell types, cellular structures, and physiological strategies. They are of special interest to water quality managers because many strains produce taste and odour compounds, several types of toxins, and harmful blooms (Vincent 2009).

Cyanobacteria have been part of natural ecosystems for approximately 2 billion years, dating back to the Precambrian era (Taylor and Taylor 1993). These microorganisms have likely been producing cyanotoxins for an equally long time. Although the first scientific report on toxic cyanobacteria was published in the late 19th century (Francis 1878), earlier historical records have been analysed and interpreted as similar incidents of poisoning by toxic cyanobacteria (WHO 2021). A cyanobacterial bloom can be often recognised by the typical green colour of the water body (Figure 3.1).



**Figure 3.1:** Cyanobacterial bloom in Angaston Lake, Australia (copyright C. Pestana, used with permission).

Cyanobacteria can thrive in extreme physical conditions including high and low temperatures, light, salinity, pH and desiccation, and nutritional availability (Anand, Thajuddin and Dadheech 2019). In a cyanobacterial bloom, a variety of cyanobacterial species, with different morphologies, can be present. Often, on the basis of the numbers and biomass, the main phytoplankton taxonomic group in a eutrophic freshwater system is cyanobacteria (Poniewozik and Lenard 2022). Cyanobacteria range from unicellular (*Microcystis sp.*) to filamentous (*Planktothrix sp.* and *Dolichospermum sp.*) and include colonial species (Figure 3.2). Colonies of cyanobacteria may form filaments, sheets, or even hollow spheres. The cyanobacterial community may be altered by various physical/chemical factors, including change in environmental conditions such as climate change (Boopathi and Ki 2014).

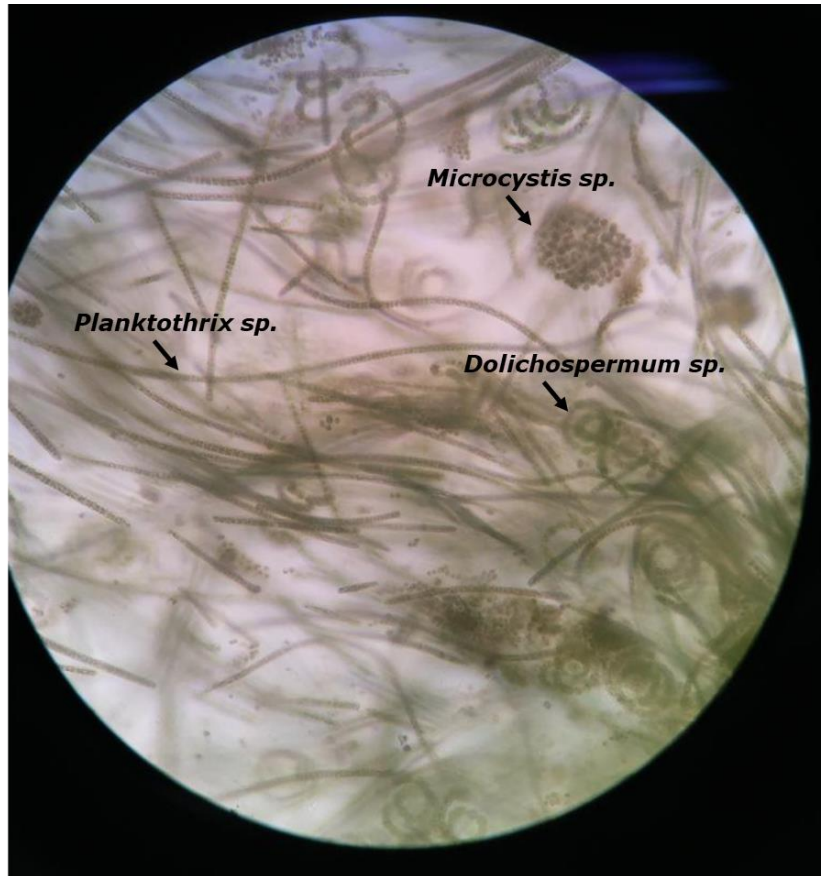


**Figure 3.2:** A range of cyanobacteria found in a freshwater reservoir in the North-Eastern part of Brazil.

### **3.1.2 Presence of cyanotoxins in freshwater environments**

Cyanobacteria can generate a vast range of secondary metabolites (cyanotoxins), some of which have known biosynthetic pathways for specific compounds or classes of compounds. While only a small fraction of these metabolites exhibit toxic properties, cyanotoxins have been linked to various cases of poisonings in both farm and wild animals. Such incidents demonstrate the harmful potential of these toxins. Furthermore, animal illnesses and deaths can be warning signs for potential human health risks (WHO 2021).

**Table 3.1:** Summary of widely reported cyanotoxins, their primary target organ in mammals, and their respective cyanobacteria producers. Information taken from O’Neil et al. (2012) and Martens (2017).

<b>Cyanotoxin</b>	<b>Primary target organ in mammals</b>	<b>Genera of cyanobacteria toxin producers</b>
Microcystins	Liver	<i>Microcystis, Dolichospermum, Nostoc, Planktothrix, Phormidium, Oscillatoria, Radiocystis, Gloeotrichia, Anabaenopsis, Rivularia, Tolypothrix, Hapalosiphon, Plectonema</i>
Nodularins	Liver	<i>Nodularia spumigena, Nostoc (symbiotic)</i>
Cylindrospermopsis	Liver	<i>Umezakia, Dolichospermum, Oscillatoria, Raphidiopsis, Aphanizomenon</i>
Anatoxin-a	Nerve synapse	<i>Dolichospermum, Phormidium, Aphanizomenon</i>
Anayoxin-a (S)	Nerve synapse	<i>Dolichospermum</i>
Saxitoxins	Nerve axons	<i>Aphanizomenon, Dolichospermum, Lyngbya, Planktothrix</i>
Lyngbyatoxins, Aplysiatoxins	Skin, gastrointestinal tract	<i>Lyngbya, Oscillatoria, Schizothrix</i>
BMAA <sup>a</sup> , DAB <sup>b</sup>	Nerve synapse	Many strains
Lipopolysaccharides	Irritant, affects exposed tissue	All strains

<sup>a</sup>  $\beta$ -Methylamino-L-alanine

<sup>b</sup> 2,4-diaminobutyric acid

Several incidents caused by cyanobacterial blooms have been reported around the world. In 1979, 138 children and 10 adults of Aboriginal/Islander descent from Palm Island, northern Queensland, Australia, were afflicted with an illness, which was named ‘Palm Island mystery disease’. The mystery disease was a result of the consumption of water contaminated with the toxic cyanobacterium *Cylindrospermopsis raciborskii* (Griffiths and Saker 2003). Another extreme example was the death of 52 haemodialysis patients in 1996 in Caruaru, Brazil. In a clinic in Brazil, 116 (89%) of 131 patients experienced visual disturbances, nausea, vomiting, and muscle weakness, following routine haemodialysis treatment, which led to 100 patients developing acute liver failure. Examination

of previous years' phytoplankton counts showed that cyanobacteria were dominant in the water supply reservoir since 1990. The tragedy was attributed to an intravenous exposure to cyanotoxin (microcystins), specifically microcystin (MC)-YR, -LR and -AR (Azevedo et al. 2002). In 2020 in Southern Africa, (Botswana), a total of 330 elephants were found dead. Many of the dead elephants were near watering holes. Following investigations Botswana's Department of Wildlife and National Parks found that the elephants probably died from ingesting cyanotoxin contaminated water (BBC 2020). In the United Kingdom (UK), during summer of 2022, two dogs died after contact with a green coloured water body in Aberdeenshire. The Scottish environment protection agency suspected that the pets were poisoned by cyanotoxins (AberdeenLive 2022).

### **3.1.3 Selection of the microcystin analogues**

The most common cyanobacterial group of toxins reported in the freshwater environment are the microcystins (Svirčev et al. 2019). Microcystins, are produced by a range of freshwater cyanobacteria, such as strains from the genera *Anabaena*, *Aphanizomenon*, *Dolichospermum*, *Limnothrix*, *Microcystis*, *Nostoc*, *Phormidium*, and *Planktothrix* (Table 3.1, Martens 2017). Microcystins are potent hepatotoxin widely reported in the freshwater environment (Su et al. 2018) with nearly 300 different analogues (Martens 2017). The microcystin family shares a common peptide structure containing non-standard amino acids and two variable amino acid moieties (Figure 3.3, Lawton et al. 2003).

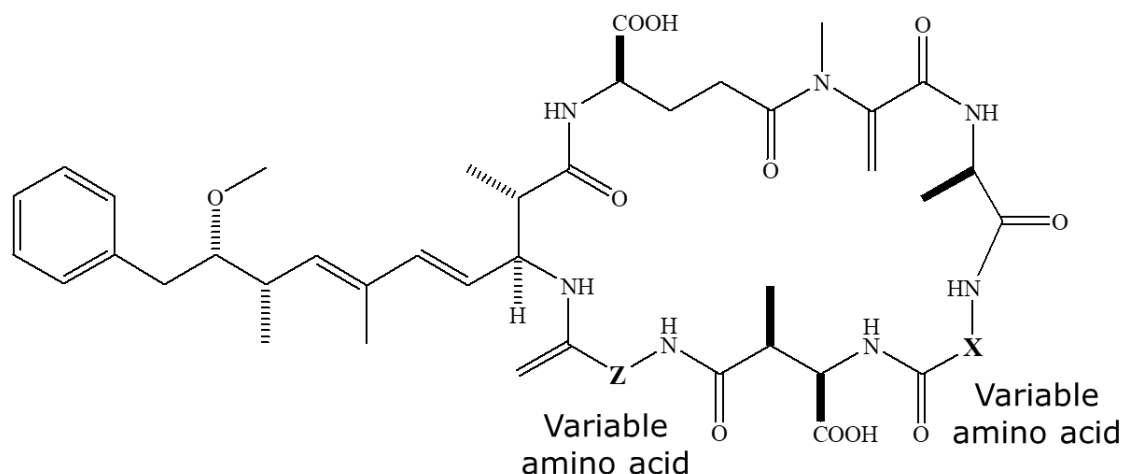


**Figure 3.3:** General chemical structure of microcystin where the letters X and Z represent the locations of the variable amino acids.

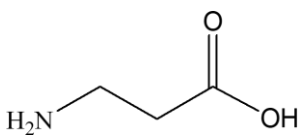
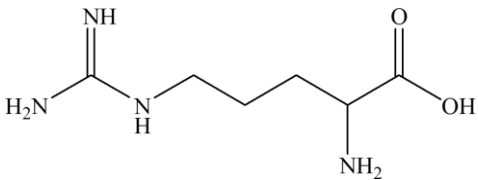
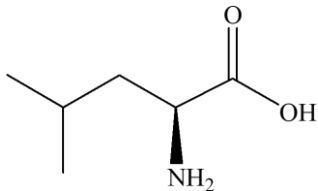
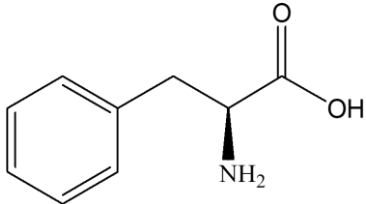
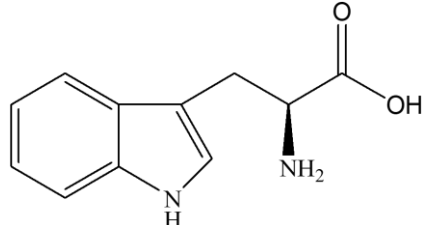
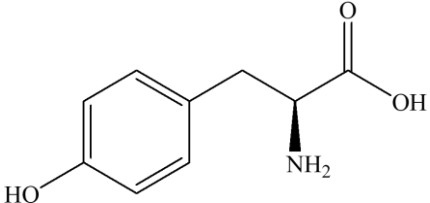
The two variable amino acids are each represented by their single letter amino acid code. For instance, in the case of microcystin-LR, the most commonly reported microcystin analogue, the letters L and R identify the amino acids, leucine and arginine, respectively (Table 3.2, Dawson 1998). The nature of the variable amino acids can substantially influence the overall hydrophobicity and the toxicity of the peptide (De Maagd et al. 1999; McCord et al. 2018). It is reported that the hydrophobicity of an organic compound affects its interaction behaviour with other contaminants sharing the same environment (Table 3.3, Velez et al. 2018). The hydrophobic nature of compounds can increase the adsorption onto microplastics through hydrophobic interactions.

**Table 3.2:** Variable amino acids that are incorporated into each microcystin analogue investigated in this thesis. See Figure 3.3 for the positions of X and Z in the structure.

Microcystin analogue	Variable amino acid - X	Variable amino acid - Z
MC-RR	Arginine (R)	Arginine (R)
MC-YR	Tyrosine (Y)	Arginine (R)
MC-LR	Leucine (L)	Arginine (R)
MC-WR	Tryptophan (W)	Arginine (R)
MC-LA	Leucine (L)	Alanine (A)
MC-LY	Leucine (L)	Tyrosine (Y)
MC-LW	Leucine (L)	Tryptophan (W)
MC-LF	Leucine (L)	Phenylalanine (F)



**Table 3.3:** Chemical structure, polarity and hydrophathy index of the variable amino acids of the microcystin analogues investigated in this thesis.

Variable amino acid	Chemical structure	Polarity	Hydrophathy index <sup>a</sup>
Alanine (A)		Nonpolar	1.8
Arginine (R)		Polar	-4.5
Leucine (L)		Nonpolar	3.8
Phenylalanine (F)		Nonpolar	2.8
Tryptophan (W)		Nonpolar	-0.9 <sup>b</sup>
Tyrosine (Y)		Polar	-1.3

<sup>a</sup> Hydrophathy index is a variable representing the hydrophobic or hydrophilic properties of the side chain of an amino acid (Kyte and Doolittle 1982). A negative value represents hydrophilicity, while a positive value represents hydrophobicity of the amino acid.

<sup>b</sup> Tryptophan (W), despite its value of -0.9 in the Kyte-Doolittle scale, has been classified in the international ImMunoGeneTics information system as a hydrophobic class, as it participates to the hydrophobic core of the structural domains (François, Ehrenmann Ouaray and Lefranc 2021).

In the proof of principle study conducted by the author prior to commencing the research reported in this thesis, the hydrophobicity of the microcystin analogue played an important role in the adsorption of microcystins onto microplastics (Pestana et al. 2021). MC-LF, the most hydrophobic analogue of the MC analogues investigated, when placed in contact with microplastics, demonstrated greater adsorption on microplastics when compared to MC-LR, which is a more hydrophilic analogue. In this thesis, in order to evaluate how the hydrophobicity affects the adsorption of each of the microcystin analogues, eight analogues were selected (Table 3.2). In contrast with the proof of principle study, a mixture of analogues (MC-RR, -YR, -LR, -WR, -LA, -LY, -LW, and -LF) was selected to evaluate the interaction with two microplastic types over two sizes (Moura et al. 2022). In this chapter, different solutions containing selected microcystin analogues are investigated either in a mixture or individually to fully understand whether analogues compete for binding sites on microplastics based on the hydrophobicity of the individual analogue.

### **3.1.4 Chapter aim and objectives**

Cyanotoxins are a natural water contaminant that can often co-exist with other pollutants, such as microplastics. Therefore, the aim of this chapter is to evaluate how a variety of microcystin analogues, with different hydrophobicities, interact with a range of microplastic types, sizes, and weathering states when co-occurring. This was achieved as follows:

- 1) Selection of the microcystin analogues
- 2) Evaluation of the interaction of microcystins of different hydrophobicities with up to six different microplastics (polypropylene, polyethylene,

polyethylene terephthalate, polyamide, polystyrene and polyvinyl chloride)  
in two sizes, individually or in a mixture

- 3) Evaluation of the competition between the analogues MC-LR and MC-LF for binding sites when in contact with microplastics
- 4) Investigation of the impact of the polymer composition of the microplastics on the adsorption of a mixture of analogues (MC-LR, -LW, and -LF) in contact with the six microplastic types
- 5) Investigation of how microplastic weathering can affect the interaction of a mixture of analogues (MC-LR, -LW, and -LF) in contact with six artificially aged microplastic types

## **3.2 Materials and methods**

### **3.2.1 Microplastics**

The two sizes (small and large) of the commercially acquired particles of polypropylene (PP) and polyethylene terephthalate (PET) were used as received in the experiments where the interaction of microplastics with eight microcystin analogues (section 3.2.3) and adsorption competition of MC-LR or MC-LF for binding sites (section 3.2.4) were evaluated. Later, the virgin and artificially aged particles of the six size-standardised microplastic types were used for experimentation. The small particles of the virgin and artificially aged microparticles of PP, PET, polyethylene (PE), polyamide (PA), polystyrene (PS), and polyvinyl chloride (PVC) were used for investigation of the interaction of three microcystin analogues (MC-LR, -LW, and -LR, section 3.2.5). Finally, small PP was used to evaluate the adsorption kinetics and isotherms of MC-LR in contact with its virgin particles (section 3.2.6). To avoid repetition, from this

point forward, the microplastic types (polymer-based) will be represented by their polymer composition abbreviation and described size (small and large).

### **3.2.2 Chemicals**

Artificial freshwater (AFW) was used as the experimental medium throughout the adsorption experiments. AFW was prepared with ultrapure water (18.2 M $\Omega$ ) and the addition of CaCl<sub>2</sub>·2H<sub>2</sub>O (58.5 mg L<sup>-1</sup>), MgSO<sub>4</sub>·7H<sub>2</sub>O (24.7 mg L<sup>-1</sup>), NaHCO<sub>3</sub> (12.0 mg L<sup>-1</sup>), and KCl (1.2 mg L<sup>-1</sup>) according to Akkanen and Kukkonen, (2003). For the experiments that evaluated the interaction of the virgin and artificially aged microparticles of small PP, PE, PET, PA, PS, and PVC with MC-LR, -LW, and -LF (section 3.2.5) and the adsorption kinetics and isotherms of small PP in contact with MC-LR (section 3.2.6), the media composition was modified to avoid degradation of the organic compounds during the experiment. Sodium azide (0.02% (w/v): NaN<sub>3</sub>) was added as a microbial inhibitor to AFW. The pH was adjusted to 7 either with HNO<sub>3</sub> or NaOH. Chemicals used were acquired from Fisher Scientific UK Ltd (UK) at analytical grade. Microcystin analogues were acquired as per Enzo Life Sciences, >95% purity. Microcystin-RR, -YR, -LR, -WR, -LA, -LY, -LW, and -LF, from the least to the most hydrophobic analogue, were selected due to their different hydrophobicities.

### **3.2.3 Adsorption of a mixture of eight microcystin analogues on microplastics**

For all adsorption experiments, samples were continuously horizontally agitated on a MaxQ 6000 orbital shaker (Thermo Scientific, UK) at 200 rpm and 25 °C in the dark for 48 h. The agitation and temperature used were selected according to

published adsorption experiments to have comparable data with the literature (Xu et al. 2018b; Guo and Wang 2019; Guo, Chen and Wang 2019; Elizalde-Velázquez et al. 2020). These parameters were also fixed throughout all adsorption experiments since both can interfere in the adsorption onto microplastics. A solution containing a mixture of eight microcystin analogues (MC-RR, -YR, -LR, -WR, -LA, -LY, -LW and -LF each at 5  $\mu\text{M}$  ( $4.93 \pm 0.40 \mu\text{M}$ ,  $n=24$ , Table 3.4) in AFW was prepared. MC solutions (2.5 mL) were combined with plastic particles (25 mg equivalent to 10 g L<sup>-1</sup>) in glass vials (4 mL). The mixture of the eight microcystin analogues was tested with PET and PP at each of the two particle sizes. Samples were taken at 2, 4, 6, 8, 12, 24, and 48 h. Samples (200  $\mu\text{L}$ ) were removed and filtered using a microcentrifuge tube filter (2 mL spin-X tubes made of PP, cellulose acetate filter, 0.22  $\mu\text{m}$  pore size, Corning USA). Samples (100  $\mu\text{L}$ ) were then analysed by HPLC-PDA. All samples (prior to filtration and filtered samples) were removed using a microlitre glass syringe (250  $\mu\text{L}$ ) with a stainless-steel needle (Hamilton, UK) to avoid contact of the toxin solution with laboratory plastics. A control containing the same concentration of microcystins was prepared without microplastic and analysed at each sampling point. All experiments and controls were conducted in triplicate. Throughout the investigation, contact with laboratory plastics was eliminated except for the filtration device which could not be avoided. Controls indicated that the loss through this step was between  $4 \pm 1\%$  (MC-LR) to  $11 \pm 1\%$  (MC-LW). The adsorption was calculated by the difference on the concentration of each microcystin analogue in the samples with microplastics, and in the control.

**Table 3.4:** Molecular weight and each analogue concentration (for a molar concentration of 5  $\mu\text{M}$ ) of the eight microcystin analogues investigated.

Microcystin analogue	Molecular weight	Concentration
	( $\text{g mol}^{-1}$ )	( $\mu\text{g mL}^{-1}$ )
MC-RR	1,038.2	5.2
MC-YR	1,045.2	5.2
MC-LR	995.2	5.0
MC-WR	1,068.2	5.3
MC-LA	910.0	4.6
MC-LY	1,002.2	5.0
MC-LW	1,025.2	5.1
MC-LF	986.2	4.9

### 3.2.4 Competition of analogues on microplastics and evaluation of the sampling protocol

Solutions containing either MC-LR ( $4.80 \pm 0.02 \mu\text{M}$ ,  $n=3$ ) or MC-LF ( $4.46 \pm 0.04 \mu\text{M}$ ,  $n=3$ ) were placed in contact individually with the small particles of PP or PET (as received, section 3.2.3) to investigate the impact on the amount of microcystin adsorbed on microplastics when the compounds are present individually. In the experiment described in the session 3.2.3, 1.4 mL out of 2.5 mL of the initial solution were removed after 7 sampling times over 48 h (2, 4, 6, 8, 12, 24, and 48 h). For this reason, the sampling protocol was evaluated by comparing the amount of MC-LR or -LF adsorbed at 48 h contact when samples (2, 4, 6, 8, 12, 24, and 48 h) were removed throughout 48 h (as section 3.2.3) compared with when a single sample was removed only after 48 h of contact with the microplastics. A comparison was then made with the data when multiple analogues were present to determine if there is competition for binding sites.

### **3.2.5 Adsorption of a mixture of three microcystin analogues on virgin and artificially aged microplastics**

In a mixture of eight analogues, the greatest amounts adsorbed onto small particles of PP and PET were the hydrophobic microcystins, including MC-LW and MC-LF (Moura et al. 2022, section 3.3.1). For this reason, further evaluation of the adsorption of microcystins on small particles of six microplastic types was performed. The impact of microplastic weathering on the adsorption was also evaluated. A solution containing a mixture of three microcystin analogues (MC-LR, -LW and -LF) each at 1  $\mu\text{M}$  ( $1.03 \pm 0.10 \mu\text{g mL}^{-1}$ ,  $n=9$ ) was prepared in AFW that included 0.02% (w/v)  $\text{NaN}_3$ . Virgin and artificially aged small microparticles of six size-standardised microplastic types (detailed in chapter 2 sections 2.3.6 to 2.6.10) were placed in contact with a mixture of three microcystin analogues.

To reduce the impact of sampling on the adsorption, the total volume of microcystin solution was increased from 2.5 mL to 25 mL. In addition, the concentration of microplastics was reduced (from  $10 \text{ g L}^{-1}$  to  $2 \text{ g L}^{-1}$ ; section 3.2.3), in order to be comparable to that cited in the scientific literature (Hüffer and Hofmann 2016; Guo and Wang 2019; Petrie et al. 2023). The mixture of the three microcystin analogues was tested with the small particles of virgin and artificially aged PP, PE, PET, PA, PS, and PVC. Samples (200  $\mu\text{L}$ ) were removed at 0.5, 1, 2, 4, 6, 10, 24, and 48 h.

### **3.2.6 Adsorption isotherm and kinetics of MC-LR on small PP**

The adsorption isotherms were conducted to investigate the intermolecular interaction of MC-LR in contact with the virgin particles of small PP. The concentration points of the isotherm were 1.0, 2.5, 5.0, 7.0 and 10.0  $\mu\text{M}$ . These were prepared in AFW + 0.02% (w/v)  $\text{NaN}_3$ . Microcystin solutions (2.5 mL) were combined with plastics particles (25 mg equivalent to  $10 \text{ g L}^{-1}$ ) in 4 mL vials. For the kinetics evaluation, shorter sampling intervals were used together with a greater number of sampling times. The samples intervals were adjusted to improve adsorption profile visualisation, since in the adsorption experiments conducted using this protocol, most of the adsorption occurred before the first sampling time (2 hours; Moura et. al. 2022). Also, the sampling method used sacrificial samples, i.e. repeated samples were not removed from the same vial. Sacrificial samples consisted of independent samples for each sample time (0.25, 0.50, 0.75, 1, 2, 4, 6, 12, 24, and 48 h) with microplastic and controls (without microplastic).

### **3.2.7 Quantification of microcystin analogues in solution using liquid chromatography**

In the current study, two different methods (method 1 and method 2) to detect microcystin analogues were applied. Both methods developed were able to separate eight microcystin analogues, MC-RR, -YR, -LR, -WR, -LA, -LY, -LW, and -LF simultaneously. Analysis of the microcystins was performed using high performance liquid chromatography (HPLC; Waters Corporation, UK). The equipment included a solvent delivery system (Alliance 2695) with detection by photodiode array (PDA, Alliance 2996). The PDA scanning wavelength was set from 200 to 400 nm. Separation of microcystin analogues was achieved using a



Symmetry dC18 column (2.1 mm internal diameter x 150 mm; 5 µm particles size) which was maintained at 40 °C. The mobile phases were ultra-pure water (18.2 MΩ) (A) and acetonitrile (B) each containing 0.05% (v/v) trifluoroacetic acid (TFA; Fisher Scientific UK Ltd, UK). TFA was used as an ion-pair agent to avoid microcystin ionisation and improve the chromatogram. The flow rate was 0.3 mL min<sup>-1</sup>. A linear gradient was used for the separation of the microcystin analogues.

Initially, the method developed consisted of gradient method of 15 minutes run time (Table 3.5). This method was applied for the evaluation the interaction of the mixture of eight microcystins analogues with microplastics (section 3.2.3) and for investigation of the sampling protocol and competition of MC-LR or MC-LF for binding sites (3.2.4). All microcystin analogues were measured according to UV absorption wavelength of microcystins (238 nm, Figure 3.4). The limit of quantification of microcystin analogues using this method was 0.05 µM (determined by a signal-to-noise ratio of 10:1).

**Table 3.5:** Solvent system used in the HPLC analysis of microcystin analogues for method 1. Solvent A: ultra-pure water (18.2 MΩ) + 0.05% (v/v) TFA; Solvent B: acetonitrile + 0.05% (v/v) TFA.

Time (min)	% Solvent A	% Solvent B	Gradient elution profile
0	70	30	-
11	40	60	Linear gradient
12	0	100	Step gradient
13	70	30	Step gradient
15	70	30	Step gradient

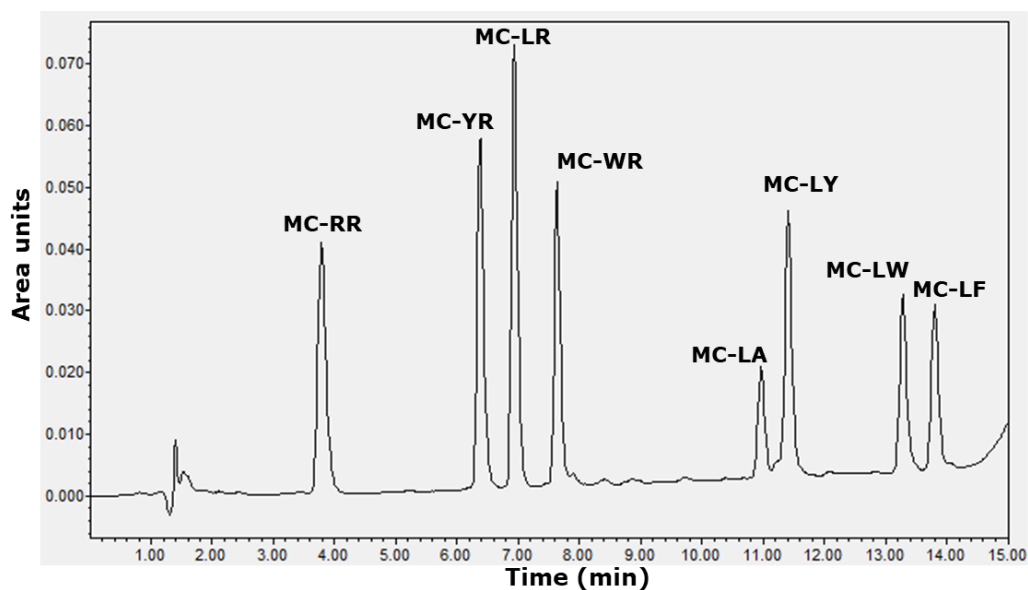


**Figure 3.4:** HPLC chromatogram of a mixture containing eight microcystin analogues (MC-RR, -YR, -LR, -WR, -LA, -LY, -LW, and -LF) eluted using method 1 (method used in the experiments described in the sections 3.2.3 and 3.2.4, Table 3.5). Wavelength set at 238 nm.

The method to detect and quantify the microcystin analogues in the solution was adjusted, to improve the chromatogram with a gradient method of 40 min (Table 3.6 and Figure 3.5). This method was used for the evaluation of the interaction of the mixture of three microcystins analogues with microplastics (section 3.2.5) and for the investigation of the adsorption kinetics and isotherms of MC-LR in contact with small PP (section 3.2.6). The hydrophobicity order of the analogues was determined according to the liquid chromatographic separation of the microcystins (Figure 3.5). The limit of quantification of the microcystin analogues using this method was 0.01  $\mu\text{M}$  (determined by a signal-to-noise ratio of 10:1).

**Table 3.6:** Solvent gradient used in the HPLC analysis of microcystin analogues 40 minutes run time (method 2). Solvent A: ultra-pure water (18.2 M $\Omega$ ) + 0.05% (v/v) TFA; Solvent B: acetonitrile + 0.05% (v/v) TFA.

Time (min)	% Solvent A	% Solvent B	Gradient elution profile
0	80	20	-
25	30	70	Linear gradient
27	0	100	Linear gradient
29	0	100	Step gradient
35	80	20	Step gradient
40	80	20	Step gradient

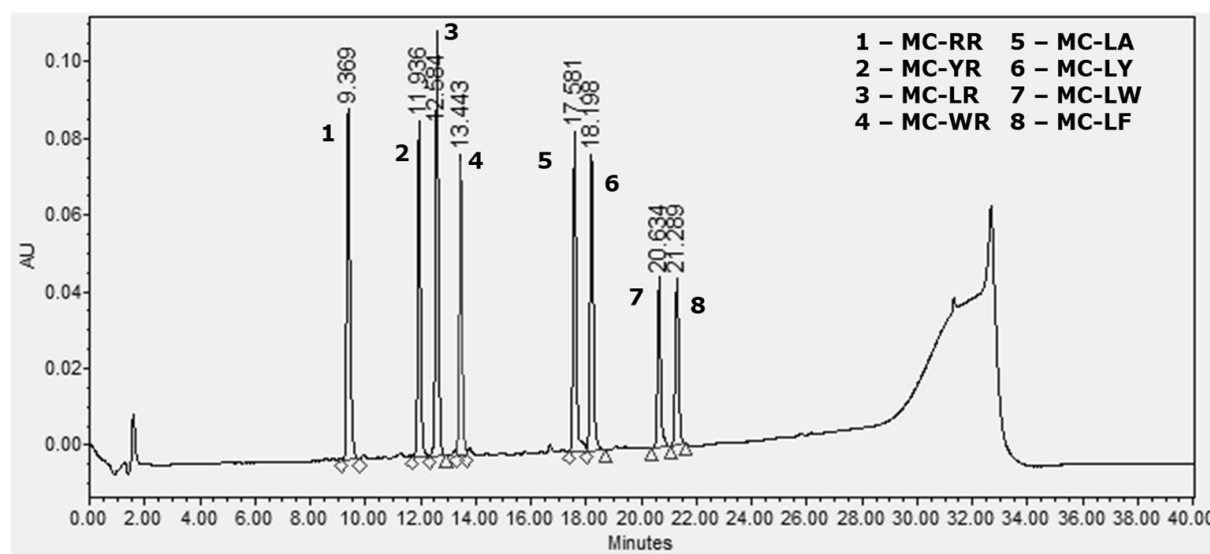


**Figure 3.5:** HPLC chromatogram of a mixture containing eight microcystin analogues (MC-RR, -YR, -LR, -WR, -LA, -LY, -LW, and -LF) eluted using method used 2 (method used in the experiments described in the sections 3.2.5 and 3.2.6, Table 3.6). Wavelength set at 238 nm. The large peak observed between 28 and 34 minutes is attributed to the column cleaning step, specifically employing pure acetonitrile, which exhibits strong absorption of UV light.

For both methods, the separation of MC-RR, -YR, -LR, -WR, -LA, -LY, -LW, and -LF followed this order, which is directly related to their hydrophobicity (Figure 3.4 and Figure 3.5).

### 3.2.8 Data analysis

The amount of organic compound adsorbed per unit mass of microplastics ( $\mu\text{mol kg}^{-1}$ ), was estimated using equation 3.1:

$$q_{(t)} = (C_{ctrl(t)} - C_{(t)})V/m \quad (3.1)$$

where,

- $q_{(t)}$  is the amount of organic compound adsorbed on microplastics ( $\mu\text{mol kg}^{-1}$ ) at sampling time  $t$
- $C_{ctrl(t)}$  is the control solution concentration of organic compound ( $\mu\text{M}$ ) at sampling time  $t$  as determined by HPLC-PDA
- $C_{(t)}$  is the sample solution concentration of organic compound ( $\mu\text{M}$ ) at sampling time  $t$  as determined by HPLC-PDA
- $m$  is the mass of plastic added to the vial (kg)
- $V$  is the total volume of solution (L) in the vial

The amount (as a percentage) of organic compound adsorbed onto the microplastic was calculated using equation 3.2:

$$\%Adsorbed_{(t)} = ((C_{ctrl(t)} - C_{(t)}) \times 100) / C_{ctrl(t)} \quad (3.2)$$

where,

- $\%Adsorbed_{(t)}$  is the percent of organic compound adsorbed onto the microplastics at sampling time  $t$

The amount of compound adsorbed per mass of adsorbent at equilibrium ( $\mu\text{mol kg}^{-1}$ ) was calculated using equation 3.3:

$$q_e = (C_{ctrl(e)} - C_e)V/m \quad (3.3)$$

where,

- $q_e$  is the amount of compound adsorbed per mass of adsorbent at equilibrium ( $\mu\text{mol kg}^{-1}$ )
- $C_{ctrl(e)}$  is the adsorbate concentration adsorbed per mass of adsorbent in the control at equilibrium ( $\mu\text{M}$ ) determined by HPLC-PDA
- $C_e$  is the residual adsorbate concentration in the solution at equilibrium ( $\mu\text{M}$ ) determined by HPLC-PDA
- $m$  is the mass of plastic added to the vial (kg) determined by HPLC-PDA
- $V$  is the total volume of solution (L) in the vial

Adsorption isotherm models applied to the experimental data of MC-LR with the virgin particles of small PP are presented in the Table 3.7.

**Table 3.7:** Adsorption isotherm models applied to the experimental data of small PP in contact with five different concentrations of MC-LR (range: 1-10  $\mu\text{M}$ ).

Adsorption isotherm	Equation	Linear form	Plot
Freundlich model	$q_e = K_F C_e^n ; n = \frac{1}{n_F}$	$\log q_e = \log K_F + n \log C_e$	$\log q_e$ vs $\log C_e$
Langmuir model	$q_e = \frac{K_L C_e}{1 + \alpha_L C_e} ; Q_0 = \frac{K_L}{\alpha_L}$	$\frac{C_e}{q_e} = \frac{\alpha_L}{K_L} C_e + \frac{1}{K_L}$	$\frac{C_e}{q_e}$ vs $C_e$
Linear model	$q_e = K_p C_e$	$q_e = K_p + C_e$	$q_e$ vs $C_e$

where,

- $q_e$  is the amount of compound adsorbed per mass of adsorbent at equilibrium ( $\mu\text{mol kg}^{-1}$ )
- $C_e$  is the residual adsorbate concentration in the solution at equilibrium ( $\mu\text{M}$ ) determined by HPLC-PDA
- $K_F$  and  $n_F$  are the Freundlich constant ( $\text{L kg}^{-1}$ ) and exponent, respectively
- $Q_0$  is the maximum adsorption capacity ( $\mu\text{mol kg}^{-1}$ )
- $\alpha_L$  is energy of adsorption ( $\text{L kg}^{-1}$ )
- $K_L$  is Langmuir constant ( $\text{L kg}^{-1}$ )
- $K_p$  is Partition constant ( $\text{L kg}^{-1}$ )

Further, the kinetics experiments were conducted with an initial microcystin-LR concentration of 5  $\mu\text{M}$ , the experimental data were fitted to two widely accepted kinetic models (Wang and Wang 2018a; Liu et al. 2019): the pseudo-first order and pseudo-second order models (Table 3.8).

**Table 3.8:** Kinetic models applied to the experimental data of MC-LR with virgin particles of small PP.

Kinetics model	Equation	Linear form	Plot
Pseudo first order	$\frac{dq_t}{dt} = K_1(q_e - q_t)$	$\log(q_e - q_t) = \log q_e - \frac{K_1}{2.303} t$	$\log(q_e - q_t)$ vs $t$
Pseudo second order	$\frac{dq_t}{dt} = K_1(q_e - q_t)^2$	$\frac{1}{q_t} = \frac{1}{K_2 q_e^2} + \frac{1}{q_e} t$	$\frac{t}{q_t}$ vs $t$

where,

- $q_e$  is the amount of compound adsorbed per mass of adsorbent at equilibrium ( $\mu\text{g g}^{-1}$ )
- $q_t$  is the amount of compound adsorbed per mass of adsorbent at time  $t$  ( $\mu\text{mol kg}^{-1}$ )
- $K_1$  and  $K_2$  are the first order ( $\text{L kg}^{-1}$ ) and second order constant ( $\text{L kg}^{-1}$ ), respectively

The Shapiro-Wilk normality test was applied to evaluate the distribution of the data. The test returned that normal distribution of the data cannot be assumed. Consequently, a Wilcoxon rank sum test was carried out to perform significance testing (RStudio Team, 2020; Table A3.1 to Table A3.5, Appendix). For all statistical tests, a significance level of 5% was set. A Pearson correlation matrix was performed to evaluate the correlation between variables of this study (Microsoft Excel; Table A3.6 and Table A3.7, Appendix). A correlation coefficient ( $r$ ) greater than 0.7 was considered a strong positive association, while  $r$  more negative than -0.7 was considered a strong negative association.

### **3.3 Results and discussion**

#### **3.3.1 Adsorption of a mixture of eight microcystin analogues on polypropylene and polyethylene terephthalate**

The interaction of eight different microcystin analogues was evaluated when in contact with PP and PET microplastics which are commonly found in freshwater environments (Koelmans et al. 2016). The interaction between the microplastics and microcystin analogues was influenced by the size of the microplastic, the type of microplastic, and the hydrophobicity of the microcystin analogues. Smaller particles showed a greater adsorption of the microcystin analogues, especially the small PP which adsorbed all the microcystin analogues in the mixture. Additionally, the hydrophobic analogues, such as MC-LW and -LF, adsorbed more onto the microplastics compared to the less hydrophobic analogues. After 4 hours of contact with small PP, five out of eight microcystin analogues were not detected in the solution. Given that all sources of possible

losses are accounted for this is indicative of an apparent 100% adsorption of MC-YR, -LR, -WR, -LW and -LF, which is equivalent to approximately 500  $\mu\text{mol kg}^{-1}$  of each microcystin analogue adsorbed per milligram of PP (Figure 3.6). On the other hand, MC-RR, -LA, and -LY had an adsorption rate of between 83% (MC-RR) and 94% (MC-LA and -LY) onto small PP within 4 hours of contact.

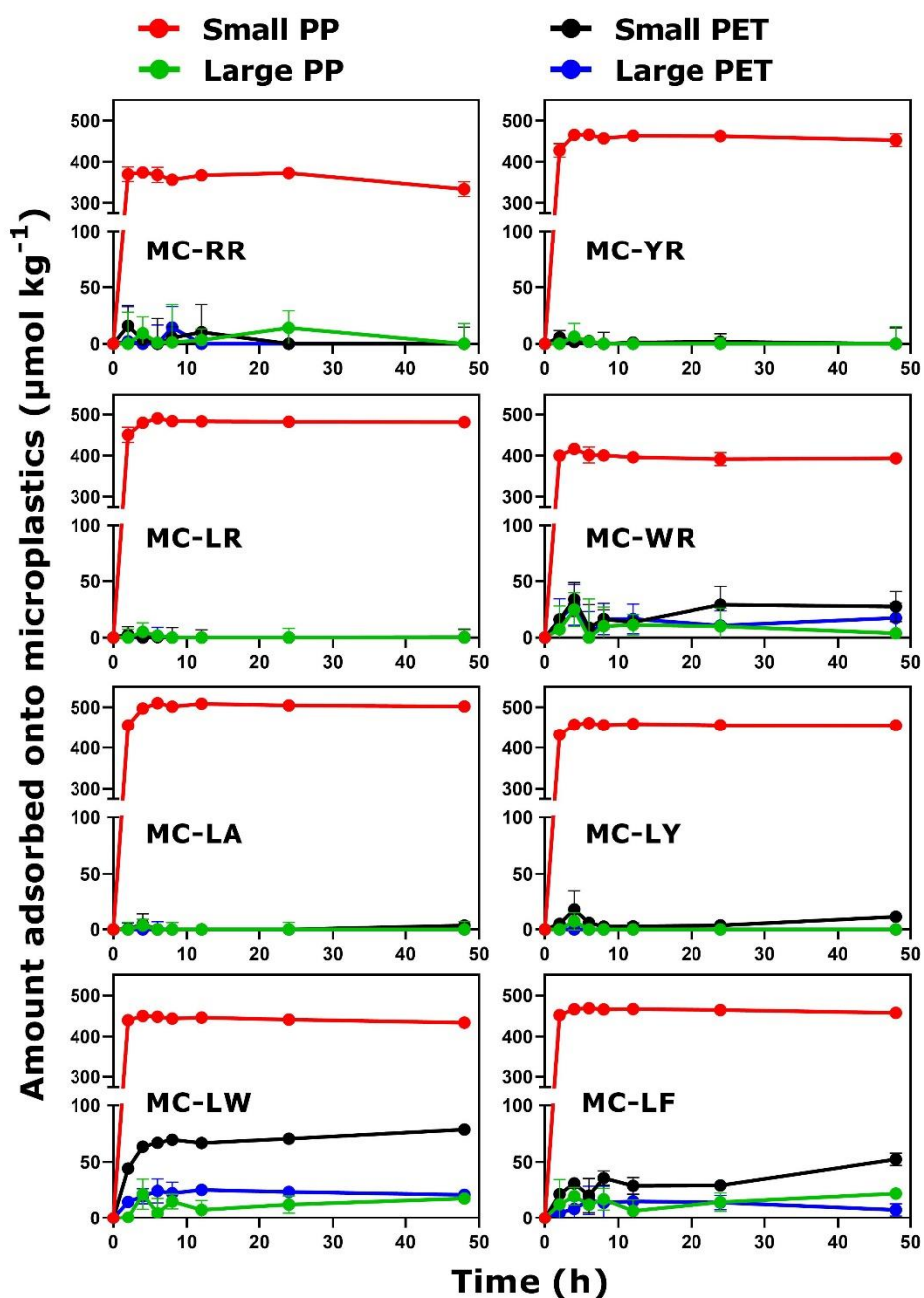


**Figure 3.6:** Amount of microcystin (MC) per analogue adsorbed ( $q_t$ ) on small ( $D_{50}$  8-28  $\mu\text{m}$ ) and large ( $D_{50}$  81-124  $\mu\text{m}$ ) PP and PET microplastic particles over 48 h in artificial freshwater with horizontal agitation in the dark.  $n=3$ , errors bars = 1 Standard deviation (SD).

In contrast to small PP, only the most hydrophobic microcystin analogues (MC-LW and MC-LF) were adsorbed by large PP, and the amount of adsorption was relatively low (approximately  $4 \pm 1\%$  for both MC-LW and -LF). The total amount of microcystin ( $\Sigma_{\text{MC}}$ ) adsorbed onto small PP was significantly higher ( $p < 0.05$ )



than that on large PP ( $\Sigma_{MC}$  3,511  $\mu\text{mol kg}^{-1}$  (small PP) vs  $\Sigma_{MC}$  52  $\mu\text{mol kg}^{-1}$  (large PP), Figure 3.7). The adsorption of small PP cannot be solely attributed to its size when compared to the larger particles of the same microplastic type. The presence of the carbonyl functional group (C=O) in the IR spectrum of small PP, which is not present in the large particles of PP (Figure 2.6, chapter 2), and its comparatively large surface area ( $S_{BET}$  52.2  $\text{m}^2 \text{g}^{-1}$ ) affect the adsorption potential of small PP. Despite unmodified PP being typically a non-polar polymer, the presence of the carbonyl functional group makes the virgin particles of small PP a more polar material. The large surface area of small PP suggests that pore filling, along with electrostatic and hydrophobic interactions, are the primary mechanisms of adsorption that occurred in the interaction of small PP with the microcystins, as also demonstrated by Moura et al. (2022). Furthermore, there was a strong positive correlation ( $r = 1.00$ ) between the  $\Sigma_{MC}$  and all microcystin analogues adsorbed onto microplastics and the surface area of the particles (Table A3.6).

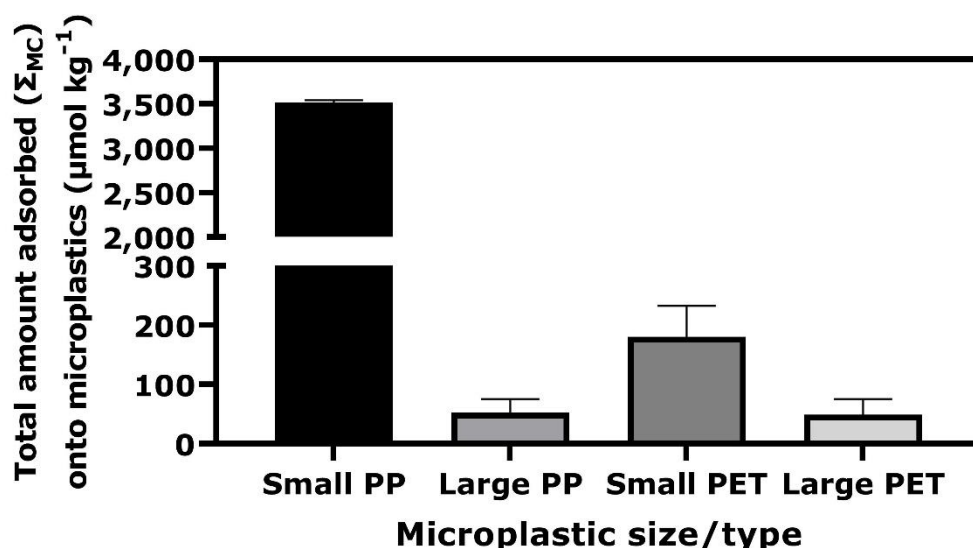


**Figure 3.7:** Total amount ( $\Sigma_{MC}$ ) of microcystin adsorbed onto small ( $D_{50}$  8-28  $\mu\text{m}$ ) and large ( $D_{50}$  81-124  $\mu\text{m}$ ) polypropylene (PP) and polyethylene terephthalate (PET) after 48 h in artificial freshwater with a mixture of the microcystins.  $n=3$ , errors bars = 1 SD.

For PET, the size of the particles played an important role regarding the adsorption of microcystin. Small PET adsorbed greater amounts ( $\Sigma_{MC}$  180  $\mu\text{mol kg}^{-1}$ ; Figure 3.7) compared to large PET ( $\Sigma_{MC}$  49  $\mu\text{mol kg}^{-1}$ ). In addition to the hydrophobic analogues (MC-LW and -LF), MC-WR also showed adsorption on small and large PET particles (Figure 3.8). As observed by the authors' previous study (Pestana et al., 2021), with particle size increase, the amount of microcystin adsorbed onto microplastics decreases. Furthermore, a strong negative correlation ( $r = -0.7$ ) between the  $\Sigma_{MC}$  adsorbed onto the microplastics and the particle size was observed (Table A3.6). That means that the smaller the particle size, the greater the adsorption onto microplastics. Zhan et al. (2016) and Wang et al. (2019) also demonstrated that the amount of a compound that is adsorbed is directly related to the adsorbent particle size. Zhan et al. (2016) found a threefold difference in adsorption of a 3,3',4,4'-tetrachlorobiphenyl (PCB77) on what was defined in their study as small PP particles (180-425  $\mu\text{m}$ ) in contrast to the larger particle size investigated (425-850, 850-2,000, and 2,000-5,000  $\mu\text{m}$ ) with similar observations made by Wang et al. (2019) investigating the adsorption of cadmium onto high-density polyethylene.

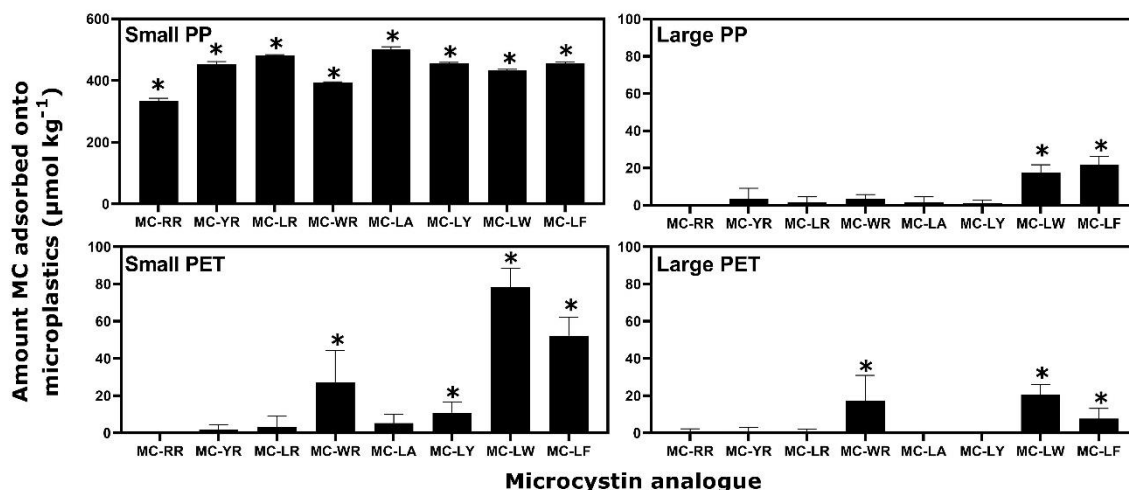


**Figure 3.8:** Amount of each microcystin analogue adsorbed onto small ( $D_{50}$  8-28  $\mu\text{m}$ ) and large ( $D_{50}$  81-124  $\mu\text{m}$ ) polypropylene (PP) and polyethylene terephthalate (PET) after 48 h in artificial freshwater with a mixture of the microcystins.  $n=3$ , errors bars = 1 SD. \* significant difference from the control,  $p < 0.05$ .

The adsorption of microcystin was found to be also affected by the type of polymer. Small PP showed a higher adsorption of microcystins ( $\Sigma_{\text{MC}}$  3,511  $\mu\text{mol kg}^{-1}$ ) when compared to small PET ( $\Sigma_{\text{MC}}$  181  $\mu\text{mol kg}^{-1}$ , Figure 3.7). Similarly, Kamp et al. (2016) demonstrated that containers made of PP had greater adsorption of microcystin analogues (MC-LR, -LA, and -LF) compared to other materials investigated (polyethylene terephthalate glycol, polystyrene, high density polyethylene, and polycarbonate), with approximately 40-80% adsorption observed after 48 h of contact.

Alimi et al. (2018) conducted a study comparing the adsorption capacities of a range of microplastic types. They found that PP demonstrated a greater adsorption capacity when compared to PET. This difference in adsorption behaviour can be attributed to their distinct properties such as glassiness, polarity, and crystallinity. As described in chapter 2, PP is a rubbery polymer with a glass transition temperature ( $T_g$ ) below 0  $^{\circ}\text{C}$ , while PET is a glassy polymer

with a  $T_g$  of 81 °C (Table 2.10, chapter 2). This means that PP is often soft and flexible plastics, allowing for greater diffusion of contaminants onto and into the polymer when compared to glassy polymers such as PET (Misumi 2011, Pascall et al. 2005). The polymer chains in the rubbery state have a higher mobility. This means that the individual polymer chains in PP can move more freely and easily, which allows for easier penetration of adsorbate (Grinsted, Clark and Koenig 1992).

The glassiness of the microplastics is not the only aspect affecting the adsorption of compounds. The antibiotics sulfamethazine ( $\log K_{ow}$  0.14) and sulfamethoxazole ( $\log K_{ow}$  0.89) showed greater adsorption on the glassy polymer, polyamide (PA,  $T_g$  47 °C), than on the rubbery polymer, polyethylene (PE,  $T_g$  -125 °C, Guo et al., 2019a, 2019b). The polarity of PA (polar) compared to PE (non-polar) was found to be the driving force for adsorption of the hydrophilic antibiotics. The crystallinity of the microplastics appeared to have a positive correlation ( $r > 0.7$ ) regarding the adsorption of all microcystin analogues by microplastics, while a negative correlation is expected (Table A3.6). Normally, the higher the degree of crystallinity, the lower the permeability of the polymer, which should decrease the adsorption potential of microplastics. The higher degree of crystallinity of PP ( $X_c$  32%) suggests that PP should have a lower adsorption potential than PET ( $X_c$  22%, Table 2.10, chapter 2). Li et al. (2018c) demonstrated no correlation between the crystallinity and the adsorption of antibiotics on microplastics, where the semi-crystalline polymer PA showed greater adsorption than amorphous polymers, such as PS, and PVC. These observations suggest that although the crystallinity of the microplastics can play a role in the adsorption by microplastics, it is not one of the main drivers of the

interaction. According to Guo et al. (2019b), the polarity of microplastics can influence the adsorption mechanisms, which was corroborated in the current study. The hydrophilic microcystin-WR adsorbed onto the polar PET (Seki et al., 2014) but not onto the non-polar large PP particles (Figure 3.8).

The overall hydrophobicity of microcystin molecules can be significantly influenced by the variable amino acids. For example, MC-LF is the most hydrophobic analogue among the microcystins analysed due to the presence of the non-polar amino acids leucine (L) and phenylalanine (F) in positions X and Z respectively (Table 3.3). On the other hand, MC-RR is the least hydrophobic microcystin in the current study due to the presence of the polar amino acid arginine (R) in both variable positions (X and Z). The hydrophobicity of the microcystin can also be influenced by the presence of aromatic rings and the size of the amino acid chain. Short-chain amino acids have stronger hydrophobic behaviour due to their smaller volume and larger surface-to-volume ratio. In the current study, the most hydrophilic analogues showed the lowest adsorption onto small-sized PP. Hüffer and Hofmann (2016) have shown a strong relationship between the sorption coefficients of the microplastics and the hydrophobicity of the sorbates, suggesting the hydrophobic interactions were a major force driving the sorption of microcystins on microplastics. Although most adsorption by microplastics is reported for hydrophobic contaminants (Velez et al. 2018; Yu et al. 2019), hydrophilic compounds have also been shown to interact with microplastics. This includes ciprofloxacin, a hydrophilic antibiotic, which was found to adsorb to PS and PVC microparticles (Liu et al. 2019).

### 3.3.2 Evaluation of the sampling protocol

MC-LR and -LF were placed individually in contact with small particles of PP and PET and two sampling methods were performed to evaluate whether the sampling method affected the adsorption of microcystin onto microplastics. In the method where samples were removed at 2, 4, 6, 8, 12, 24, and 48 h, MC-LF placed in contact with small PP was undetectable in the solution after 4 h, while, 99% of MC-LR adsorbed on small PP after 48 h exposure. For small PET, MC-LR adsorbed  $5 \pm 1\%$  on the particles, whereas MC-LF adsorbed  $28 \pm 1\%$  on small PET after 48 h. Evaluation of the sampling method showed there was no significant difference ( $p > 0.05$ ) between the adsorption results at 48 h when sampling seven times over the period of the experiment (2, 4, 6, 8, 12, 24, and 48 h) compared with sampling just once, at the end of the 48 h experiment (Figure 3.9). The reason is that the both MC-LR and -LF readily adsorb onto the microplastics. That means that the majority of the adsorption had occurred before the first sampling time (2 h). As a result, the sampling protocol did not affect the adsorption behaviour of the microcystin onto the microplastics.

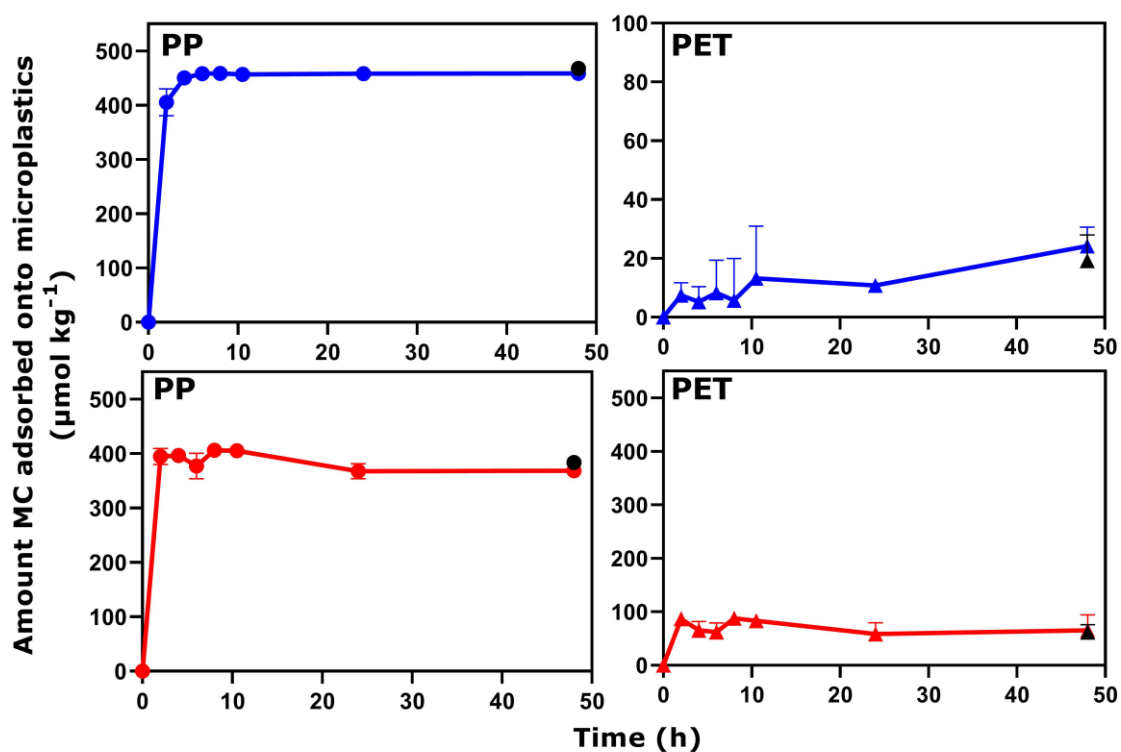


**Figure 3.9:** Individual adsorption of MC-LR and -LF on polypropylene (PP) and on polyethylene terephthalate (PET) sampling at 2, 4, 6, 8, 10, 24, and 48 h (blue = MC-LR, red = MC-LF), or sampling once after 48 h (black, ● = onto PP, ▲ = onto PET), both small ( $D_{50}$  8-28  $\mu\text{m}$ ) particle size.  $n=3$ , errors bars = 1 SD.

### 3.3.3 Evaluation of the competition of MC-LR and -LF onto microplastics

In cyanobacterial blooms, microcystins are frequently found as a combination of analogues. Many published studies on adsorption that in scientific literature have focused on examining how individual compounds interact with microplastics.

While it is important to comprehend the interaction between organic micropollutants and microplastics on an individual basis to elucidate the physico-chemical factors affecting adsorption, this method does not account for the possibility of intramolecular adsorption competition. The current study provides evidence of the existence of intramolecular competition. When MC-LR and -LF

were separately placed in contact with small PP and PET particles, they exhibited higher adsorption compared to when placed in the mixture (Figure 3.10).

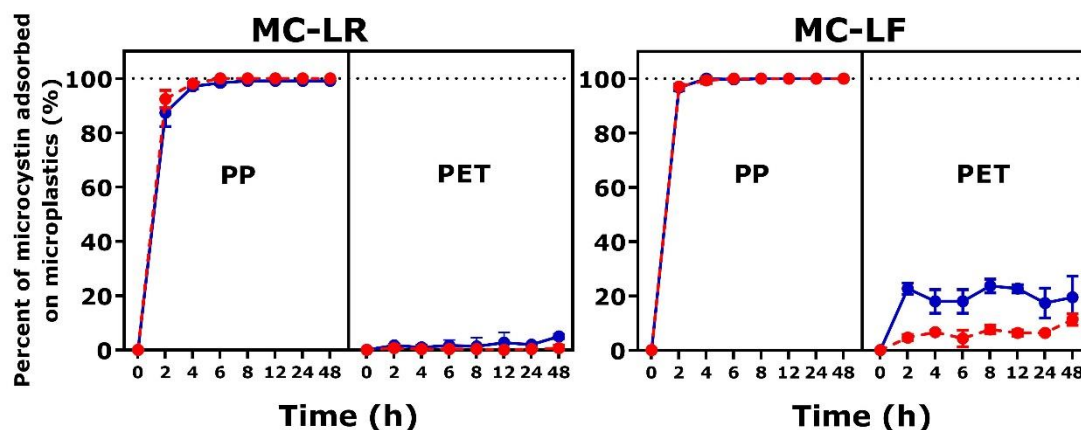


**Figure 3.10:** Competition evaluation for adsorption of MC-LR and -LF either as a mixture (●) or individually (●) on polypropylene (PP) and on polyethylene terephthalate (PET), both small ( $D_{50}$  8-28  $\mu\text{m}$ ) particle size.  $n=3$ , errors bars = 1 SD.

Small PP demonstrated the highest adsorption for all eight microcystin analogues, whether examined as a mixture or individually. MC-LF, when analysed as an individual compound, exhibited  $95 \pm 1\%$  adsorption onto 25 mg of small PP after a 2 h contact period, and was undetectable in the solution after 4 h of contact, which was comparable to its presence in a mixture. For MC-LR,  $87 \pm 3\%$  was adsorbed within 2 h of contact with 25 mg of small PP, with 99% of the initial concentration of MC-LR adsorbed by the end of the experiment (48 hours, Figure 3.10). In a mixture, MC-LR was not detectable after 4 h of contact with small PP (Figure 3.10). The rapid adsorption of both MC-LR and MC-LF onto small PP prevented the investigation of competition behaviour between them, since both were quickly and completely adsorbed both individually and as a mixture. In contrast, MC-LR did not exhibit adsorption in a mixture on small PET, but  $5 \pm 1\%$  adsorption ( $p < 0.05$ ) of MC-LR alone was observed. Similarly, a greater amount of MC-LF was adsorbed ( $19 \pm 1\%$ ) as an individual compound



compared to MC-LF in a mixture ( $11 \pm 2\%$ ) onto 25 mg of small PET (Figure 3.10).

The initial concentration of microcystins may have influenced its adsorption by microplastics. The total concentration of microcystins for all analogues was  $40 \mu\text{M}$ , whereas for each individual compound, MC-LR or MC-LF, it was  $5 \mu\text{M}$ . The concentration of the adsorbate, like pressure, can affect the adsorption process. At lower adsorbate concentrations, surface adsorption plays a more significant role, while at higher concentrations, partition (pore-filling) becomes dominant and can increase the amount of adsorption on microplastics. When a mixture of microcystins was used, small PET adsorbed  $\Sigma_{\text{MC}} 181 \mu\text{mol kg}^{-1}$  of the total microcystins (Figure 3.7), whereas MC-LR and MC-LF adsorbed approximately  $23 \mu\text{mol kg}^{-1}$  and  $61 \mu\text{mol kg}^{-1}$ , respectively, when examined individually. However, when considering each analogue individually, lower amounts of MC-LR ( $0.4 \mu\text{mol kg}^{-1}$ ) and MC-LF ( $52 \mu\text{mol kg}^{-1}$ ) adsorbed onto small PET in a mixture of microcystins. The decreased adsorption of MC-LF in a mixture suggested potential competition between the most hydrophobic microcystins tested.

In the microcystins mixture, MC-LW showed the greatest adsorption of the eight microcystin analogues onto small PET ( $18 \pm 2\%$  after 48 hours), followed by MC-LF ( $11 \pm 2\%$ ). Similarly, MC-LW adsorbed  $5 \pm 1\%$  after 48 hours, while MC-LF adsorbed  $2 \pm 1\%$  onto large PET. The results suggested that out of all microcystin analogues tested, MC-LW and -LF were the most likely analogues to adsorb onto small PET. Microcystin adsorption competition for binding sites on solid materials has been reported previously, with Wu et al., (2011) demonstrating a reduction of the amount of microcystin adsorbed onto

sediments when in a solution with an increased concentration of dissolved organic matter. Medium characteristics such as pH, salinity, ionic strength, and dissolved organic matter have all been reported to affect the adsorption of organic compounds onto microplastics (Guo, Chen and Wang 2019; Wagstaff, Lawton and Petrie 2021). Microplastic particle surfaces are negatively charged, therefore ions in the medium can bind electrostatically to the binding sites, disturbing the charge equilibrium of the surface (Atugoda et al. 2021).

### **3.3.4 Adsorption of a mixture of MC-LR, -LW, and -LF onto small particles of six size-standardised virgin and artificially aged microplastics**

A mixture containing the two most hydrophobic microcystin analogues (MC-LF and -LW) that also demonstrated adsorption onto PP and PET, and MC-LR were placed in contact with the small virgin and artificially aged particles of six microplastic types. The type of the microplastics, the microcystin analogue, and the weathering of the microplastics were determinant factors for the adsorption of microcystins onto microplastics. For both virgin and aged particles, the adsorption followed the same order: MC-LW > MC-LF > MC-LR. However, the aging of the microplastics significantly decreased from 15% (small PP) to 85% (small PE) the adsorption of microcystins by some microplastics. Results presented a positive correlation ( $r = 0.89$ ) between the microcystin adsorption and the surface area of the microplastics ( $S_{BET}$ , Table A3.7). For both virgin and aged particles, small PP ( $52.2 \text{ m}^2 \text{ g}^{-1}$ ) and small PVC ( $4.3 \text{ m}^2 \text{ g}^{-1}$ ) showed the greatest adsorption of the three microcystin analogues in the mixture (Figure 3.11). This suggests that the pore filling was the main adsorption mechanism taking place on the interaction of small PP and PVC with microcystin. No

adsorption was observed for PA, and only MC-LW adsorbed on virgin PET ( $15 \pm 1\%$ ), as also shown by this author in a proof-of-principle study (Pestana et al. 2021). Although lower amounts of microcystins were adsorbed on most of the artificially aged microplastics, the order of the microcystin adsorption remained unchanged (MC-LW > MC-LF > MC-LR).

Again, hydrophobic interactions played a role in the adsorption of microcystins by microplastics. The two most hydrophobic analogues (MC-LW and -LF) showed the greater adsorption onto microplastics, when compared to MC-LR. The three analogues in the mixture share leucine (L) at position X. They only differ in the Z-position amino acid (Table 3.2), those being arginine (R, MC-LR), phenylalanine (F, MC-LF), and tryptophan (W, MC-LW). The difference in adsorption between the MC-LW and -LF with similar chemical structures may be due to the differences in the chemical properties of the amino acids tryptophan and phenylalanine. Tryptophan has a larger size and contains an indole group ( $C_8H_7N$ ), which has a higher polarity compared to the benzyl group in phenylalanine (Table 3.3). An indole group consist of a six-membered benzene ring fused to a five-membered pyrrole ring. The higher polarity of tryptophan may allow for stronger interactions between the amino acid and the microplastic surface. Additionally, tryptophan has a more complex aromatic structure than phenylalanine, which could provide more surface area for interactions with the microplastics.

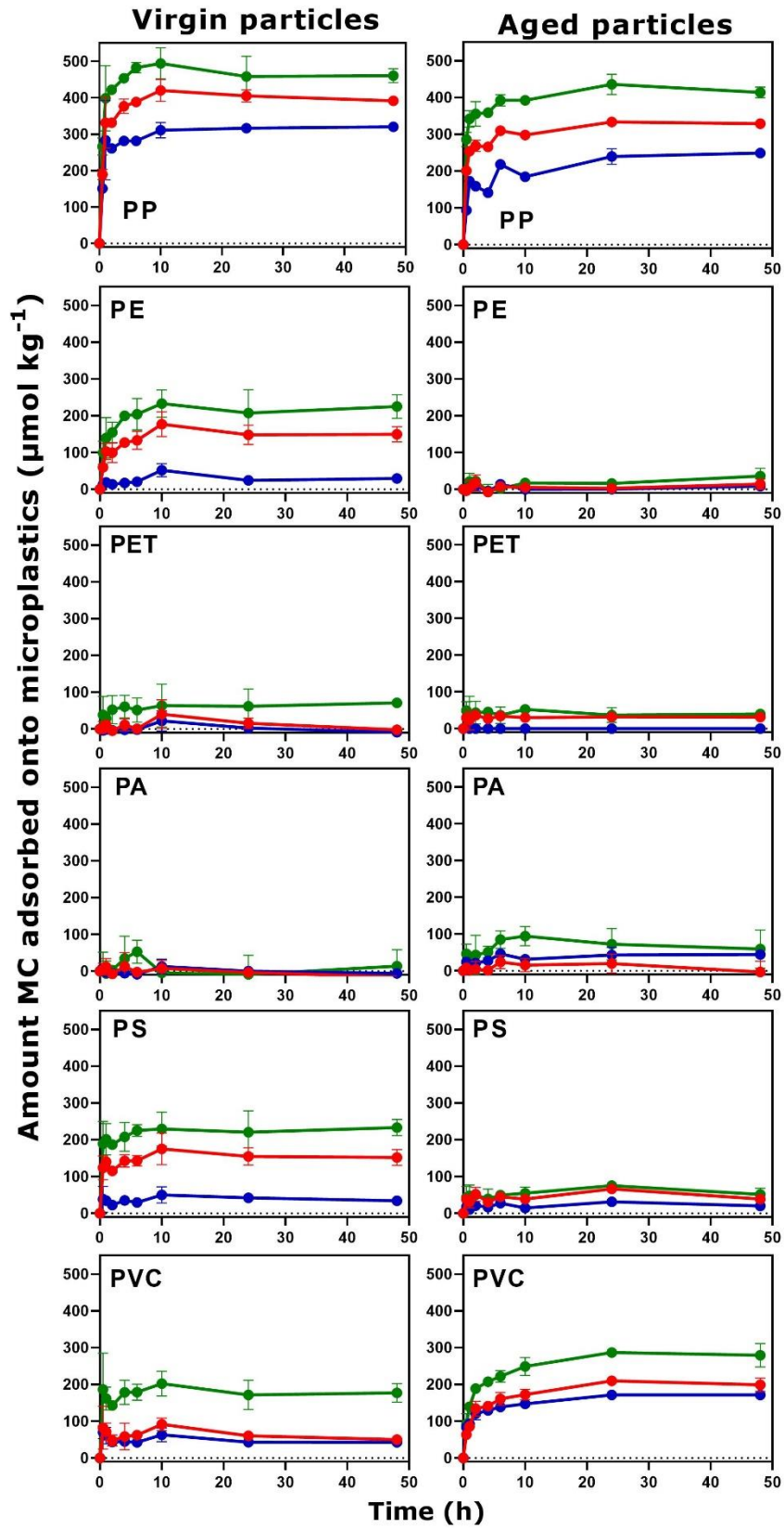


**Figure 3.11:** Amount of microcystin (MC) adsorbed ( $q_t$ ) onto the virgin and aged small particles of the six microplastic types investigated. MC-LR (●), MC-LW (●), and MC-LF (●) were in contact with microplastics over 48 h in artificial freshwater + 0.02% w/v  $\text{NaN}_3$  with horizontal agitation in the dark.  $n=3$ , errors bars = 1 SD.

Virgin PE and PS, considered non-polar polymers, showed greater adsorption when compared to polar polymers, such as PET and PA. As mentioned before, unmodified PP is typically a non-polar polymer, however, due to the presence of the carbonyl functional group (C=O), the virgin particles of small PP are actually a polar microplastic. Considering the total amount of microcystin adsorbed ( $\Sigma_{MC}$ ) on microplastics, PVC ( $\Sigma_{MC}$  269  $\mu\text{mol kg}^{-1}$  vs 649  $\mu\text{mol kg}^{-1}$ ) and PA ( $\Sigma_{MC}$  24  $\mu\text{mol kg}^{-1}$  vs 110  $\mu\text{mol kg}^{-1}$ ) showed a significant increase on the adsorption of microcystin onto the aged particles ( $p > 0.05$ ). Meanwhile, virgin PET (71  $\mu\text{mol kg}^{-1}$ ) and aged PET (68  $\mu\text{mol kg}^{-1}$ ) showed similar adsorption based on the total concentration following contact with the three microcystins in the solution. However, the adsorption onto virgin PET consisted exclusively of MC-LW adsorption, while onto aged PET, lower amounts of MC-LW (40  $\mu\text{mol kg}^{-1}$ ), and greater amounts of MC-LF (31  $\mu\text{mol kg}^{-1}$ ) were observed (Figure 3.12).

When considering the aged particles, the electrostatic interaction between microcystins and microplastics might be a reason for the decrease in the adsorption of small PP, PE, and PS. At pH 7, MC-LR is positively charged, while MC-LW and -LF are negatively charged (Lawton et al. 2003). Microplastics are typically negatively charged, as demonstrated by the zeta potential measurement (Figure 2.24, Table 2.10, chapter 2). The negative charge of microplastics can increase with the weathering of particles (Zhu et al. 2020). That means that with the increase of the negative surface charge of microplastics, an increase of the adsorption of MC-LR, and a decrease of the adsorption of MC-LF, and -LW is expected. However, in the current study, an increase of the negative surface charge of the microplastics was only observed

for aged small PE ( $\zeta$  -18 mV vs -37 mV), small PA ( $\zeta$  -36 mV vs -46 mV), and large PP ( $\zeta$  -12 mV vs -22 mV, Table 2.10, chapter 2). Furthermore, no association between the total microcystin amount ( $\Sigma_{MC}$ ) adsorbed onto microplastics and the zeta potential ( $\zeta$ ) of the microplastics was found ( $r = 0.02$ , Table A3.7).

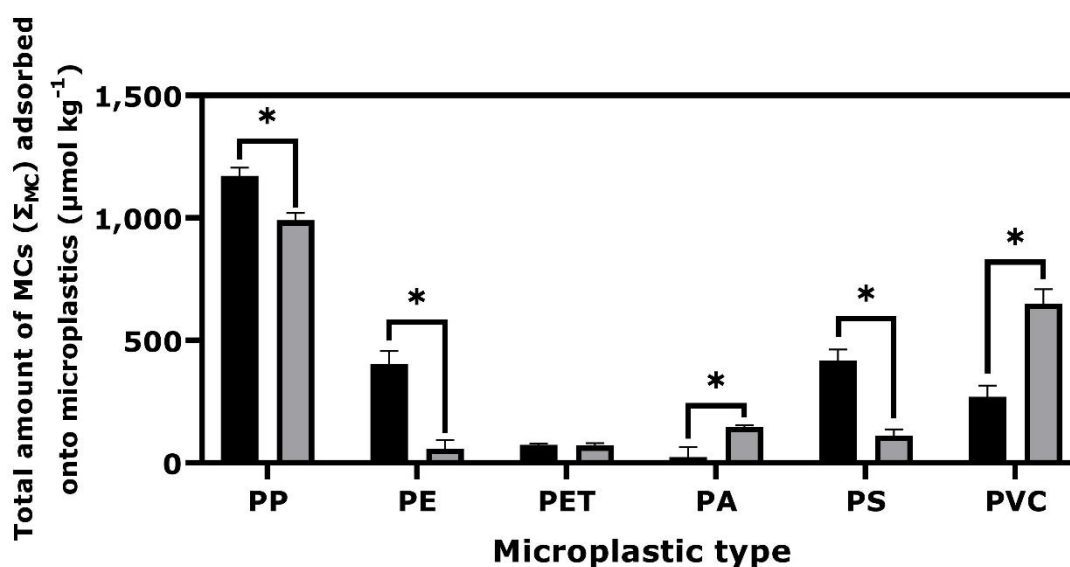


**Figure 3.12:** Total amount ( $\Sigma_{MC}$ ) of microcystin adsorbed onto small, virgin (■) and artificially aged (▨) microplastics after 48 h in a mixture of the microcystins (MC-LR, -LW, and -LF) in artificial freshwater + 0.02% (w/v) NaN<sub>3</sub>.  $n=3$ , errors bars = 1 SD. \*significant difference between the virgin and aged particles,  $p < 0.05$ .

### 3.3.5 Adsorption isotherm and kinetics

Adsorption can occur in various manners, the analyte can either interact strictly with the solid phase (microplastics), or also show interaction between the analyte molecules. An adsorption isotherm was performed to evaluate the interaction mechanism of small PP and MC-LR, a microcystin analogue widely reported in freshwater. The isotherm was conducted at the following concentrations: 1.0, 2.5, 5.0, 7.0 and 10.0  $\mu\text{M}$ . All initial concentration points achieved the equilibrium concentration ( $C_e$ ) by 24 hours of contact. However, due to the very

high surface area of small PP, the MC-LR concentrations selected were not able to completely saturate the microplastics to accurately fit an isotherm model. The most common models applied to evaluate the contact of microplastic with freshwater pollutants are the Freundlich, Langmuir and Linear models (Wu et al. 2016a; Li, Zhang and Zhang 2018; Wang and Wang 2018b; Wang et al. 2018b). The Freundlich and linear model were the best fit ( $R^2 = 0.9994$  each) to the experimental data when compared to the Langmuir model ( $R^2 = 0.5312$ , Table 3.9, Figure 3.13). For PP, that means that it is inconclusive whether the dominant interaction mechanism in place was either a sorption (Linear model) or mono and multilayer adsorption (Freundlich model). PP also fitted the Freundlich model when in contact with the pharmaceuticals, ciprofloxacin, and trimethoprim (Li, Zhang and Zhang 2018). On the other hand, adsorption experiments with PCB77 (3,3',4,4'-tetrachlorobiphenyl) and PP and the polycyclic aromatic hydrocarbon pyrene, which consists of 4 fused benzene rings, with PE, PS and PVC fitted the Langmuir model, therefore a homogeneous monolayer adsorption occurred under those studies conditions (Zhan et al. 2016; Wang and Wang 2018a).

Both the Freundlich and Langmuir models are non-linear models that consider the interaction of the solid phase and the analyte to be on the surface of the particle, a process called adsorption. The Freundlich model is based on the assumption that the adsorption process takes place on the heterogeneous surface of an adsorbent, and is applicable to both monolayer and multilayer adsorptions (Wang and Wang 2018a). The Langmuir model assumes monolayer coverage of the adsorbate over a homogenous adsorbent surface with no intermolecular interaction (Wu et al. 2020a). A homogeneous surface means that

all active sites of the solid phase, where the adsorption can take place, are energetically equivalent and homogeneously distributed over the surface of the adsorbent. On the other hand, a heterogeneous surface has active sites differently energised and distributed over the surface of the solid phase. The Linear model is applied when the Freundlich exponent is equal to one (Table 3.9) and implies that, in addition to the interaction on the surface of the solid phase with the adsorbate, an absorption behaviour (e.g., pore-filling) also takes place. Many studies show that the adsorption, either mono or multilayer, dominates the interaction of organic compounds with microplastics. For this reason, the term 'adsorption' has been adopted in this thesis.

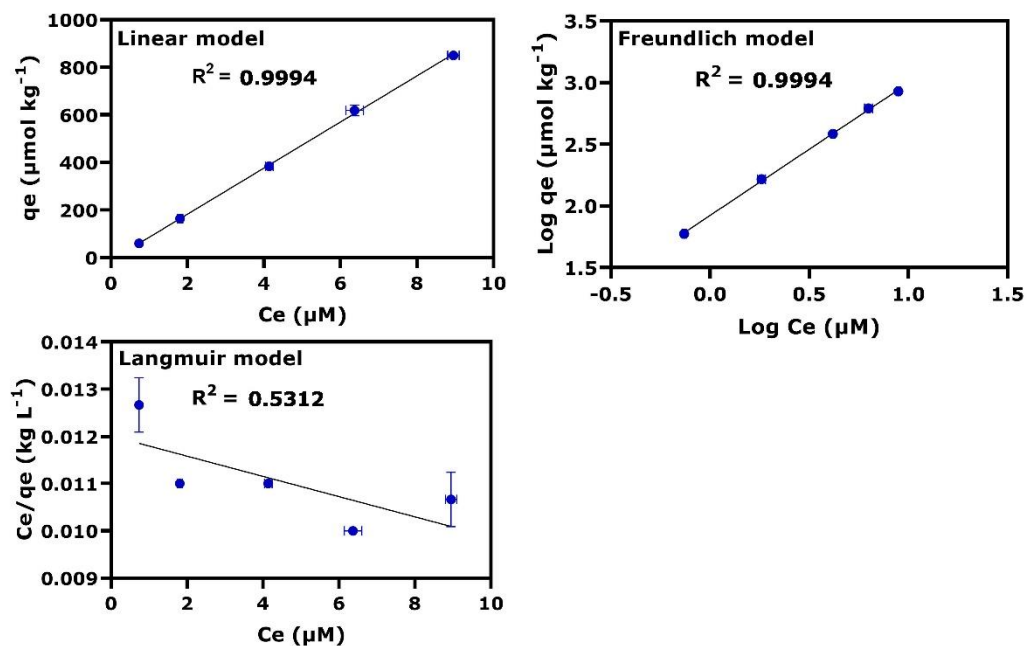


**Figure 3.13:** Application of the experimental data to the linear forms of the Linear model, Freundlich model, Langmuir model. The equilibrium concentration ( $C_e$ ) of MC-LR in contact with small PP in artificial freshwater + 0.02%  $\text{NaN}_3$  was taking as occurring after 24 h of contact for all initial concentrations. The equations are described in Table 3.7.



**Table 3.9:** Linear model, Freundlich model, and Langmuir model parameters, where  $K_F$  is the Freundlich model constant coefficient,  $K_L$  is the Langmuir constant coefficient, and the  $K_d$  is the Linear model constant coefficient.  $Q_0$  is the maximum adsorption calculated when the experimental data fits the Langmuir model.

<b>Isotherm model</b>	<b>Parameters</b>		
Freundlich	$K_F$ (L kg <sup>-1</sup> )	$n_F$ (1/n)	$R_2$
	85.57	0.59	0.9994
Langmuir	$K_L$ (L kg <sup>-1</sup> )	$Q_0$ (μmol kg <sup>-1</sup> )	$R_2$
	83.26	-4,669	0.5312
Linear	$K_d$ (L kg <sup>-1</sup> )		$R_2$
	96.93		0.9994

Adsorption kinetics is the measure of the adsorption uptake with respect to time at a constant pressure or concentration (Saha and Grappe 2017). The experimental data did not fit the pseudo first order model ( $R^2 = 0.4809$ ). However, it adjusted ( $R^2 = 0.9982$ ) to the linear form of the pseudo-second order model (Figure 3.14). In a study conducted with pyrene in contact with PET, PS and PVC, the data fitted well to the pseudo second order kinetic model (Wang and Wang 2018a).

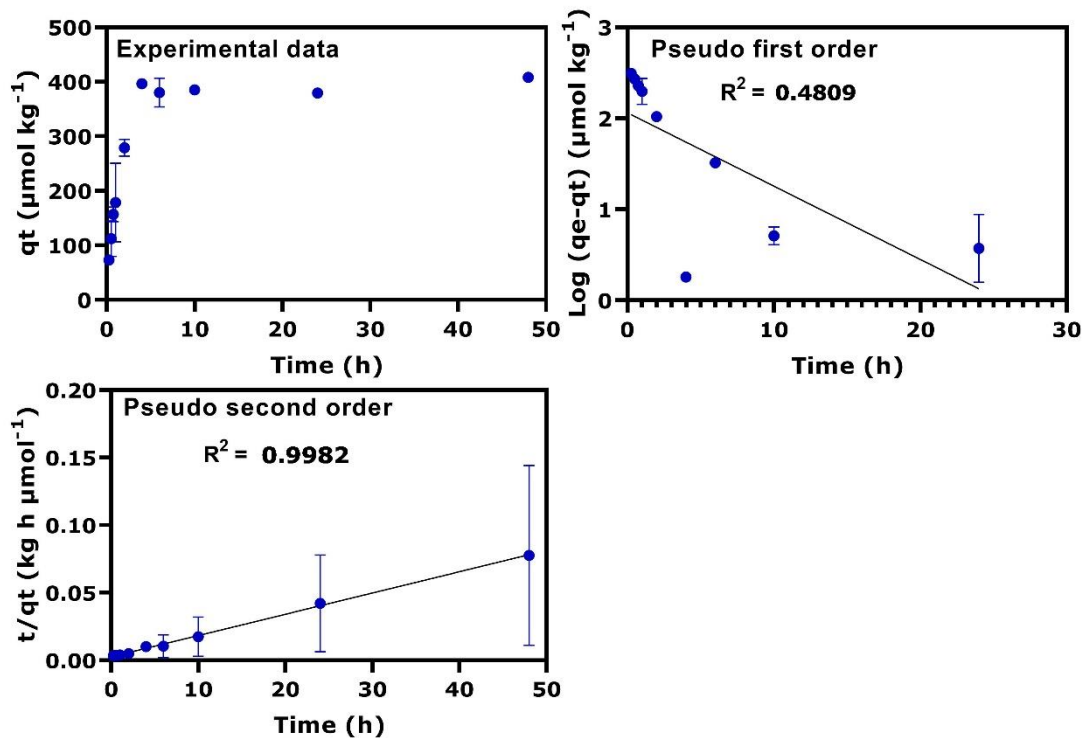


**Figure 3.14:** Kinetics of MC-LR placed in contact with small PP over 48 h (top left), linear form of pseudo first order model, and pseudo second order model. The kinetic models were calculated using the equations in the Table 3.8. The initial concentration of MC-LR in contact with small PP in artificial freshwater + 0.02% NaN<sub>3</sub> was 5 µM, and sacrificial samples were removed at 0.25, 0.50, 0.75, 1, 2, 4, 6, 24, and 48 h.

Adsorption kinetics also provides a valuable insight into the mechanisms involved in the transport of adsorbates within adsorbents (Wang and Wang 2018a) measuring diffusion of adsorbate in the pores. Adsorption experiments involving microplastics placed in contact with freshwater organic compounds often fit either pseudo first or second order models (Wu et al. 2016a; Li, Zhang and Zhang 2018; Wang and Wang 2018b; Wang et al. 2018b). A pseudo-order is usually applied when one of the reactants is either in excess or maintained at a constant concentration altering the reaction behaviour to a lower order. For instance, a pseudo first order reaction is a second order reaction by nature but has been altered to make it a first order reaction (Toppr 2021). A pseudo second order reaction refers to a reaction that appears to follow second-order kinetics,

while the actual reaction mechanism may be more complex. The pseudo second order model indicates that the adsorption process between microplastics and compounds involves a mechanism that facilitates a higher order of interaction or association compared to simple adsorption. This can occur due to factors such as chemical bonding, surface area availability, or cooperative effects that promote the adsorption of the compounds onto the microplastics.

### **3.4 Conclusions and environmental implications**

In this chapter, a range of microcystin analogues were placed in contact with virgin and artificially aged particles of six microplastic types. The effect of the hydrophobicity, the competition for binding sites, and the effect of the weathering of the microplastics for the adsorption of microcystins were evaluated. The findings presented in the current study have improved the understanding of the interaction of microplastics with natural pollutants in aqueous ecosystems.

The adsorption of microcystins onto microplastics was influenced by the hydrophobicity of microcystin analogues, polymeric material, and weathering of microplastics. The current study found that highly toxic hydrophobic microcystin analogues had a higher potential to be transported into the food chain by microplastics. Specifically, the hydrophobic analogues MC-LW and -LF adsorbed more onto all microplastic samples investigated, which is concerning as hydrophobicity has been linked to higher microcystin toxicity (Fischer et al. 2010a). Moreover, MC-LR, which is commonly used as a representative of microcystins in studies, is not the most toxic analogue, with MC-LF being 1.4 to 3.5 times more toxic than MC-LR (Ward and Codd, 1999). This is important

because other, more hydrophobic, microcystin analogues are more likely to adsorb onto microplastic particles compared to MC-LR, which raises concerns about microcystins becoming bioavailable through microplastic particles in the food web. Further compounding this problem is the fact that MC-LR is frequently used in studies as a representative of the entire group of microcystins, despite the fact that it is not the most toxic or most likely to adsorb microcystin analogue. It has clearly been demonstrated in the present chapter that other, more hydrophobic, microcystin analogues are more likely to adsorb onto microplastic particles when compared to MC-LR.

Another factor affecting the adsorption onto microplastics is the weathering of the particles. It has been demonstrated that the aging of the microplastics enhances the adsorption of compounds onto microplastics (Zhang et al. 2018; Liu et al. 2020). However, the weathering of microplastics only increased the adsorption onto aged PA and PVC. On the other hand, the virgin particles of small PP, PE, and PS showed greater adsorption of microcystin than the artificially aged particles. This highlights the complexity of the interaction of organic compounds with microplastics. The difference in the adsorption behaviour of microcystin onto aged microplastics according to the microplastic type demonstrate the challenge of predicting the interaction of organic compounds onto microplastics without experimental data.

The third factor affecting adsorption is the type of polymer. Plastic polymers present varied properties that can influence the adsorbance of aquatic contaminants. The adsorption of hydrophobic microcystin is enhanced when in contact with small particles of PP, PA, and PVC. Furthermore, particle properties

such as surface area had strong association with the adsorption of microcystin. Due to their high porosity, small PP and PVC (virgin and aged) microparticles can potentially also act as a vector for hydrophilic analogues.

The factors affecting the adsorption behaviour of microcystin onto microplastics are interwoven and complex. Hydrophobicity of the microcystin analogue, particle size, weathering of the microplastics and the polymer material all play roles to varying degrees. Based on the findings presented in this chapter, a worst-case scenario would be the co-occurrence of hydrophobic microcystin analogues (MC-LW and -LF), and small particulate PP in either its virgin or aged form.

# **Chapter 4**

## **Adsorption and desorption mechanism of pharmaceuticals onto and from microplastics**

<b>4 ADSORPTION AND DESORPTION MECHANISM OF PHARMACEUTICALS ONTO AND FROM MICROPLASTICS .....</b>	<b>143</b>
<b>4.1 Introduction.....</b>	<b>145</b>
4.1.1 Pharmaceuticals and personal care products .....	145
4.1.2 Pharmaceutical pollution in aquatic systems.....	147
4.1.3 Selection of pharmaceuticals .....	148
4.1.4 Chapter aim and objectives .....	152
<b>4.2 Materials and methods.....</b>	<b>153</b>
4.2.1 Microplastics .....	153
4.2.2 Chemicals.....	153
4.2.3 Adsorption of a mixture of five pharmaceuticals onto virgin and artificially aged microplastics .....	155
4.2.4 Adsorption/desorption isotherm and kinetics of fluoxetine on/from small polypropylene, polyamide, and polyvinyl chloride .....	157
4.2.5 Quantification of pharmaceuticals in the solution using liquid chromatography .....	159
4.2.6 Statistical analysis .....	161
<b>4.3 Results and discussions .....</b>	<b>164</b>
4.3.1 Differential adsorption of the five pharmaceuticals by the six microplastics.....	164
4.3.2 The effect of the physico-chemical characteristics of the six microplastic types onto the adsorption of pharmaceuticals.....	169
4.3.3 The effect of aging on the adsorption of five pharmaceuticals by six microplastic types.....	173
4.3.4 Adsorption/desorption kinetics of fluoxetine onto/from virgin and artificially aged small microplastics .....	176
4.3.5 Adsorption/desorption isotherm of fluoxetine onto/from virgin and artificially aged small microplastics .....	187
<b>4.4 Conclusion and environmental implications .....</b>	<b>198</b>

## 4.1 Introduction

### 4.1.1 Pharmaceuticals and personal care products

Pharmaceuticals and personal care products (PPCPs) are a diverse group of chemicals that include all drugs, including prescription, over-the-counter medications, and veterinary therapeutic drugs, and non-medicinal consumer chemicals (EPA 2013). PPCPs contain diverse groups of organic compounds. The pharmaceuticals include antibiotics, hormones, anti-inflammatory drugs, antiepileptic drugs, blood lipid regulators,  $\beta$ -blockers, contrast media, cytostatic drugs, and antidepressants for pharmaceuticals while personal care products cover antimicrobial agents, synthetic musks, insect repellents, preservatives, and sunscreen ultraviolet (UV) filters (Table 4.1).

**Table 4.1:** Classification of pharmaceuticals and personal care products (PPCPs) and examples of compounds for each subgroup. Information taken from Liu and Wong (2013) and Wang and Wang (2016).

Classification	Subgroups	Functions	Examples of compounds
Pharmaceuticals	Antibiotics	Kill bacteria	Clarithromycin
			Erythromycin
			Sulfamethoxazole
			Sulfadimethoxine
			Ciprofloxacin
			Norfloxacin
			Ofloxacin
	Hormones	Regulation of metabolism; control of sexual development; homeostasis	Chloramphenicol
			Estrone
			Estradiol
	Analgesics and anti-inflammatory drugs	Reduce pain and inflammation	Ethinylestradiol
			Diclofenac
			Ibuprofen
			Acetaminophen
	Antiepileptic drugs	Treat mood disorders	Acetylsalicylic acid
Carbamazepine			
Blood lipid regulators	Regulation of triglycerides and cholesterol in blood	Primidone	
		Clofibrate	
			Gemfibrozil



Classification	Subgroups	Functions	Examples of compounds	
	β-blockers	Inhibit the hormone adrenalin and the neurotransmitter noradrenalin	Metoprolol	
			Propranolol	
	Contrast media	Enhancement of vascular visibility during magnetic resonance imaging	Diatrizoate	
			Iopromide	
	Cytostatic drugs	Control or kill neoplastic cells	Ifosfamide	
			Cyclophosphamide	
	Antidepressants	Treat clinical depression and other conditions including generalised anxiety disorder	Fluoxetine	
			Venlafaxine	
	Personal Care Products	Antimicrobial agents/Disinfectants	Kill unwanted microorganisms and parasites	Triclosan
				Triclocarban
Synthetic musks/Fragrances		Create a pleasant odour	Galaxolide	
			Toxalide	
Insect repellents		<i>Prevent, repel, or mitigate pests</i>	N,N-diethyl-m-toluamide	
Preservatives		Prevent decomposition by microbial growth or by undesirable chemical changes	Parabens (alkyl-p-hydroxybenzoates)	
Sunscreen UV filters		Protect the skin from the sun's ultraviolet radiation, and reduces sunburn and other skin damage	2-ethyl-hexyl-4-trimethoxycinnamate	
	4-methyl-benzilidene-camphor			

Many PPCPs are highly bioactive, most are polar, many are optically active. When present in the environment, they usually occur at no more than trace concentrations. However, PPCPs are a class of emerging contaminants that have raised great concern in recent years. PPCPs have gained attention for various reason. These include:

(1) their continuous introduction into the environment via effluent from sewage treatment facilities and from septic systems;

(2) they are developed with the intention of causing a biological effect, this being especially the case for pharmaceuticals;

(3) PPCPs often have the same type of physico-chemical behaviour as other harmful xenobiotics (chemical substance found in an organism that is not naturally produced or expected to be present in the organism); and

(4) PPCPs are used in large quantities (i.e. similar to those of many pesticides, Barceló and Petrovic 2007).

#### **4.1.2 Pharmaceutical pollution in aquatic systems**

The widespread and intensive use of chemicals such as PPCPs has given rise to concern on their occurrence in, and impact on, aquatic ecosystems (Kandie et al. 2020). After consumption, most pharmaceuticals are excreted in urine and faeces as parent compounds or metabolites, which can end up in the sewage system. However, wastewater treatment plants (WWTPs) often do not remove pharmaceuticals, leading to their discharge into surface waters in WWTP effluents (Santos, Rodríguez-Mozaz and Barceló 2021). Data on the discharge of PPCPs from WWTP and on their concentrations in the environment exhibit great variability, leading to inconclusive results (Tarpani and Azapagic 2018). Although detected concentrations of individual pharmaceuticals in water bodies are typically in the ng to  $\mu\text{g L}^{-1}$  range (micropollutant range), ecotoxicological effects can still be observed (Jones, Voulvoulis and Lester 2002). Several pharmaceuticals are on priority pollutant lists developed by the European Union (EU) and the United States Environmental Protection Agency (USEPA). Priority lists identify a wide variety of chemicals present in wastewaters and storm water runoff that may pose a threat to receiving water bodies including surface water (Ebele, Abou-Elwafa Abdallah and Harrad 2017). The presence of

pharmaceuticals in the freshwater environment is widely reported (Petrie, Barden and Kasprzyk-Hordern 2015; Boxall and Kookana 2018; Fekadu et al. 2019).

Although not all PPCPs are persistent in the aquatic environment, their continuous use and release to the environment means that many have greater potential for environmental presence than other organic contaminants (Ebele, Abou-Elwafa Abdallah and Harrad 2017). This means that pharmaceuticals with high prescription rates and/or low biodegradability are more likely to be detected in the environment.

In a global-scale study conducted by Wilkinson et al. (2022), the pharmaceutical pollution in 258 freshwater bodies (rivers), which represented the environmental influence of 471.4 million people across 137 geographic regions, was investigated. Pharmaceuticals were detected in the river samples across all continents. The most contaminated sites were in low- to middle-income countries and were associated with areas with poor wastewater and waste management infrastructure and in areas with pharmaceutical manufacturing. The most frequently detected active pharmaceutical ingredients were carbamazepine, metformin, and caffeine, which were detected at over half of the sites monitored. Concentrations of at least one pharmaceutical at 25.7% of the sampling sites was greater than concentrations considered safe for aquatic organisms, or which are of concern in terms of selection for antimicrobial resistance.

#### **4.1.3 Selection of pharmaceuticals**

Environmental relevance was considered in the selection of pharmaceutical compounds investigated in respect to their interaction with microplastics. The chemical parameters that were evaluated to inform pharmaceutical selection

included toxicity to aquatic organisms, persistence in the freshwater environment, and hydrophobicity. The pharmaceuticals selected following this evaluation were: ibuprofen, carbamazepine, fluoxetine, ofloxacin, and venlafaxine (Table 4.2).

A review by Hughes, Kay and Brown (2013) analysed the presence of 203 pharmaceuticals in freshwater ecosystems across 41 countries. According to the authors, the painkiller ibuprofen was consistently within the top five identified compounds across all regions. In Asia, the antibiotic ofloxacin was evident in high concentrations (up to  $0.011 \mu\text{g mL}^{-1}$ ). The antidepressant fluoxetine is in the top 20 North American compounds found in freshwater systems, causing concern as it was found to induce mussel spawning (Wang et al. 2019b). The antidepressant venlafaxine has the highest concentration and is most frequently recorded in European aquatic environments, and more likely to be found in Europe when compared to Africa (Fekadu et al. 2019). Meanwhile, carbamazepine is the single most widely studied and detected compound in Europe and North America. Carbamazepine was the pharmaceutical most frequently detected in river samples in a study that investigated 1,052 sampling sites in 104 countries across all continents (Wilkinson et al. 2022). Venlafaxine and fluoxetine were also included in the list of pharmaceuticals most commonly detected in rivers across the world.

In 2011, the World Health Organisation (WHO) reported that fluoxetine and ibuprofen were observed at higher concentrations ranging from 200 to 3000  $\text{ng L}^{-1}$  (Wang et al., 2019b) among 16 pharmaceuticals evaluated in drinking waters in the UK. The antidepressant fluoxetine was found to bioaccumulate in lower

trophic animals, such as *Daphnia magna* (Nkoom et al. 2019). Ibuprofen is considered susceptible to biodegradation whereas carbamazepine appears relatively resistant to biological attack, suggesting that, amongst other factors, chemical structure controls susceptibility to biological degradation (Petrie et al. 2014).

**Table 4.2:** Pharmaceuticals selected on the basis of their environmental relevance and toxicity (Thomas and Hilton 2004; Hughes, Kay and Brown 2013; AstraZeneca 2015; Fekadu et al. 2019; NCCOS 2021).

Pharmaceutical	Subgroup	Detection	Max conc. reported in freshwater	EC <sub>50</sub> <i>Daphnia magna</i>
			(µg mL <sup>-1</sup> )	(µg mL <sup>-1</sup> )
Ibuprofen	Anti-inflammatory	Top 5 compound in Europe, North America, and Asia	0.031	9.06
Carbamazepine	Antiepileptic	Compound most reported in freshwater systems in Europe and North America	0.011	> 13.80
Fluoxetine	Antidepressant	Top 10 most reported compound in North America	5.7x10 <sup>-4</sup>	0.82
Ofloxacin	Antibiotic	Top 11 most reported compound in Asia	0.011	76.58
Venlafaxine	Antidepressant	Top 8 psychiatric treatment drug in Africa and Europe	0.3	141.28

According to the One Health Breakthrough Partnership tool launched by the Scottish Environment Protection Agency (SEPA), between 2013 and 2022 carbamazepine and ibuprofen have been widely detected in freshwater across Scotland. Carbamazepine was detected in 60 different locations with an average concentration of 318 ng L<sup>-1</sup> (0.5-137,000 ng L<sup>-1</sup>). Only two samples at locations downstream of WWTPs contained carbamazepine above the predicted no-effect concentration (PNEC) of carbamazepine (2,500 ng L<sup>-1</sup>). Ibuprofen has also been widely detected (58 locations) in surface waters across Scotland with an average concentration of 130 ng L<sup>-1</sup> (1-6,600 ng L<sup>-1</sup>). However, approximately half of the samples contained ibuprofen concentrations over the PNEC (220 ng L<sup>-1</sup>). The antidepressant fluoxetine (PNEC 47 ng L<sup>-1</sup>) and venlafaxine (PNEC 13 ng L<sup>-1</sup>) have the lowest PNEC values among the pharmaceuticals selected. This means that those pharmaceuticals have greater potential toxic effects to wildlife. Across Scotland, fluoxetine was detected in 22 locations at average concentration of 10 ng L<sup>-1</sup> (0.1-188 ng L<sup>-1</sup>), and approximately 20% of the samples contained fluoxetine at concentrations over its PNEC value. While venlafaxine was only detected in five locations at an average concentration of 69 ng L<sup>-1</sup> (2.6-176 ng L<sup>-1</sup>), in three locations, the concentration of venlafaxine detected was over its PNEC value. No data was available for ofloxacin. The fact that venlafaxine is detected in only a few locations and the absence of detection data for ofloxacin, does not mean that these pharmaceuticals are not present in the surface water samples. The absence of a specific pharmaceutical detection could be attributed to either the utilisation of a detection method that does not specifically target these particular pharmaceuticals or to the possibility that the concentration of these pharmaceuticals falls below the detection limit of the applied method.

#### 4.1.4 Chapter aim and objectives

The presence of pollutants such as microplastics and pharmaceuticals has been widely reported. There is an increasing recognition that microplastics can act as a vector for those micropollutants when in the same aquatic environment.

Therefore, the aim of this chapter is to evaluate how a variety of pharmaceuticals, with different hydrophobicities, interact with a range of microplastic types, sizes, and weathering states when co-occurring. This was achieved by the following steps:

- 1) Selection of pharmaceuticals
- 2) Evaluation of the interaction of five pharmaceuticals (ibuprofen, venlafaxine, carbamazepine, fluoxetine, and ofloxacin) in a mixture with six virgin microplastic types (polypropylene, polyethylene, polyethylene terephthalate, polyamide, polystyrene, and polyvinyl chloride) across two particle sizes
- 3) Investigation of how microplastic weathering can affect the interaction of the mixture of five pharmaceuticals in contact with six artificially aged microplastic types covering two particle sizes
- 4) Evaluation of the adsorption and desorption mechanisms of the pharmaceuticals that showed the greatest adsorption (fluoxetine) in contact with the virgin microplastic types that adsorbed the greatest amounts of pharmaceuticals (small polypropylene, polyamide, and polyvinyl chloride)
- 5) Investigation of how the weathering of the microplastics can affect the adsorption and desorption mechanism of fluoxetine onto and from artificially aged microparticles of small polypropylene, polyamide, and polyvinyl chloride

- 6) Evaluation of the kinetic model of fluoxetine adsorption and desorption onto and from virgin and artificially aged small polypropylene, polyamide, and polyvinyl chloride

## **4.2 Materials and methods**

### **4.2.1 Microplastics**

Virgin and artificially aged, size-standardised microparticles of polypropylene (PP), polyethylene (PE), polyethylene terephthalate (PET), polyamide (PA), polystyrene (PS), and polyvinyl chloride (PVC) in the two sizes (small and large, described in chapter 2) were used for the investigation of the interaction of five pharmaceuticals in a mixture in contact with microplastics (section 4.2.3). Due to the high microcystin and pharmaceutical adsorption of small PP, PA and PVC, the virgin and aged particles of these microplastics were used in the adsorption/desorption experiments (section 4.2.4). To avoid repetition, from this point forward, the microplastic types (polymer-based) will be represented by their polymer composition abbreviation and size (small and large).

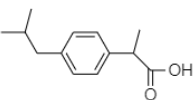
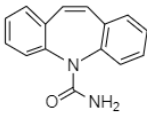
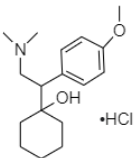
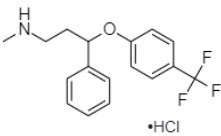
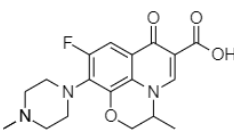
### **4.2.2 Chemicals**

Artificial freshwater (AFW) with 0.02% (w/v) sodium azide ( $\text{NaN}_3$ ) was used as the experimental medium in the adsorption experiments described in this chapter. AFW + 0.02% (w/v)  $\text{NaN}_3$  was prepared as described in section 3.2.2. The pH was adjusted to 7 either with  $\text{HNO}_3$  or  $\text{NaOH}$ . The pharmaceuticals ibuprofen (CAS RN 15687-27-1), carbamazepine (CAS 298-46-4), fluoxetine hydrochloride (CAS 56296-78-7), venlafaxine hydrochloride (CAS 99300-78-4), and ofloxacin (CAS 82419-36-1) were acquired from the Tokyo Chemical



Industry (UK) at HPLC grade > 97%. Stock solutions at concentrations of 10  $\mu\text{g mL}^{-1}$  (10 mg in 1,000 mL, carbamazepine), 20  $\mu\text{g mL}^{-1}$  (10 mg in 500 mL, ibuprofen), or 100  $\mu\text{g mL}^{-1}$  (10 mg in 100 mL, fluoxetine, venlafaxine, and ofloxacin) were prepared using AFW + 0.02%  $\text{NaN}_3$  depending on the pharmaceutical water solubility. No organic solvents were used to avoid cosolvent interference on the adsorption experiment. Prior to use, the stock solutions were stored in the fridge (4°C) in the dark. Due to the different molecular weight among the pharmaceuticals investigated in the current study, as in chapter 3, the initial concentration used was measured as moles per volume. The initial concentration of each pharmaceutical used was 16  $\mu\text{M}$  (16  $\mu\text{mol L}^{-1}$ ), which represents 5  $\mu\text{g mL}^{-1}$  of venlafaxine, chosen as a reference compound (Table 4.3).

**Table 4.3:** Chemical structure, molecular weight, octanol-water partition coefficient (log  $K_{OW}$ ), pH dependent octanol-water partition coefficient (Log  $D_{OW}$ ), acid dissociation constant ( $pK_a$ ), and charge of ibuprofen, carbamazepine, venlafaxine hydrochloride, fluoxetine hydrochloride, and ofloxacin. Initial concentration ( $C_0$ ) of each pharmaceutical that corresponds to 16  $\mu\text{M}$ .

Pharmaceutical	Structure	Molecular weight (g mol <sup>-1</sup> )	$C_0$ ( $\mu\text{g mL}^{-1}$ )	Log $K_{OW}^*$ / Log $D_{OW}^{**}$ (at pH 7)	$pK_a^{***}$ (charge at pH 7)
Ibuprofen		206.29	3.29	3.97 / 4.85	4.85 <sup>a</sup> (-) <sup>b</sup>
Carbamazepine		236.27	3.76	2.45 / 2.45	- <sup>c</sup> (neutral) <sup>c</sup>
Venlafaxine hydrochloride		313.87	5.00	0.43 / -1.97	9.4 <sup>d</sup> (+)
Fluoxetine hydrochloride		345.78	5.51	4.05 / 1.25	9.80 <sup>a</sup> (+) <sup>e</sup>
Ofloxacin		361.37	5.76	-0.39 / -0.40	5.35 <sup>a</sup> ; 6.72 <sup>a</sup> (-) <sup>f</sup>

\* Values taken from NCCOS, (2021).

\*\* Calculated as equation:  $\text{Log } D_{OW} = \text{Log } K_{OW} - \text{Log} (1 + 10^{(pK_a - \text{pH})})$ .

\*\*\* Note: Two  $pK_a$  values are shown when the pharmaceutical contains two different acidic functional groups, each of which can donate a proton to a solution.

Values taken from: <sup>a</sup> ChemAxon, (2023), <sup>b</sup> Oh et al. (2016), <sup>c</sup> Park et al. (2018), <sup>d</sup> Sharma and Jain (2009), <sup>e</sup> Wagstaff, Lawton and Petrie (2021a), and <sup>f</sup> Nurchi et al. (2019).

### 4.2.3 Adsorption of a mixture of five pharmaceuticals onto virgin and artificially aged microplastics

As described in chapter 3 in section 3.2.3, for all adsorption experiments, samples were continuously horizontally agitated on a MaxQ 6000 orbital shaker (Thermo Scientific, UK) at 200 rpm and 25 °C in the dark for 48 h. Samples (200  $\mu\text{L}$ ) were removed using a microlitre glass syringe and filtered using a

microcentrifuge tube filter (2 mL spin-X tubes made of PP, cellulose acetate filter, 0.22  $\mu\text{m}$  pore size, Corning USA). Samples (100  $\mu\text{L}$ ) were then analysed by HPLC-PDA. A microlitre glass syringe with a stainless-steel needle (Hamilton, UK) was used to avoid contact of the toxin solution with laboratory plastics unless unavoidable. A control containing the investigated pharmaceutical without microplastic particles was also prepared and analysed at each sampling point. All experiments and controls were conducted in triplicate. Throughout the investigation, contact with laboratory plastics was eliminated except for the microcentrifugation filtration device which could not be avoided. Controls indicated that the loss through this step was between  $1 \pm 0.5\%$  (venlafaxine) to  $11 \pm 4\%$  (fluoxetine). The adsorption was calculated by the difference on the concentration of the organic compound in the samples with microplastics, and in the control (without microplastics, but including the pharmaceuticals).

A solution containing a mixture of the five selected pharmaceuticals each at 16  $\mu\text{M}$  was placed in contact with size-standardised (small and large) virgin and artificially aged microplastic types (PP, PE, PET, PA, PS, and PVC).

Pharmaceutical solutions (50 mL) were combined with plastic particles (100 mg equivalent to  $2 \text{ g L}^{-1}$ ) in 100 mL Erlenmeyer flasks. The experiment was conducted as described in section 3.2.5, chapter 3, and samples were removed after 0.5, 1, 2, 4, 6, 10, 24, and 48 h contact.

#### **4.2.4 Adsorption/desorption isotherm and kinetics of fluoxetine on/from small polypropylene, polyamide, and polyvinyl chloride**

Adsorption/desorption kinetics and isotherm of fluoxetine onto/from virgin and aged particles of the small PP, PA, and PVC was performed, due to the marked observed adsorption by these materials (see results in section 4.3.1). Fluoxetine was adsorbed onto both virgin and aged particles of small PP, PA, and PVC, which enabled the evaluation of whether the weathering of the microplastics affected the adsorption mechanism of the particles. To avoid the inconclusive isotherm results obtained for adsorption of MC-LR onto small PP (section 3.3.5, chapter 3), tests were performed prior to the experiments to select the isotherm initial concentrations (Figure A4.1 and Figure A4.2) for each microplastic types. For the kinetics experiments, fluoxetine at  $145 \mu\text{M}$  ( $50 \mu\text{g mL}^{-1}$ ) was placed in contact with virgin and aged small PP. For virgin and aged small PA and PVC, on the other hand, the initial concentration of fluoxetine was  $14 \mu\text{M}$  ( $5 \mu\text{g mL}^{-1}$ ). Samples were removed at 0.5, 1, 2, 4, 6, 10, 24, and 48 h contact. For the isotherm experiments, fluoxetine at initial concentrations of 1, 2.5, 5, 10, and  $15 \mu\text{g mL}^{-1}$  was placed in contact with virgin and aged particles of small PA and PVC ( $2 \text{ g L}^{-1}$ ). Due to the adsorption potential of small PP, fluoxetine at initial concentrations 15, 25, 50, 75, and  $100 \mu\text{g mL}^{-1}$  was placed in contact with virgin and aged particles of small PP ( $2 \text{ g L}^{-1}$ ). The molar concentration was calculated using the molecular weight of fluoxetine hydrochloride ( $345.78 \text{ g mol}^{-1}$ , Table 4.4).

**Table 4.4:** Summary of the initial concentrations of fluoxetine hydrochloride (molecular weight: 345.78 g mol<sup>-1</sup>) and the respective molar concentrations used in the adsorption isotherm experiment followed by the desorption isotherm experiment performed at 25 °C.

<b>Concentration (<math>\mu\text{g mL}^{-1}</math>)</b>	<b>Molar concentration (<math>\mu\text{M}</math>)</b>
1.0	3
2.5	7
5.0	14
10	29
15	43
25	72
50	145
75	217
100	289

As previous adsorption experiments, adsorption/desorption samples were continuously horizontally agitated on a MaxQ 6000 orbital shaker (Thermo Scientific, UK) at 200 rpm and 25 °C in the dark for 24 h. A control without microplastics was performed at each concentration point. After 24 h, the solution containing microplastics was filtered using a GF/F filter (Fisher scientific, UK) to recover the fluoxetine-loaded microplastics.

To evaluate the adsorption/desorption mechanism of organic compounds in contact with microplastics, the equilibrium concentration at different initial concentrations of the compound must be investigated. Results and prior tests (Figure A4.1 and Figure A4.2) observed that the adsorption had reached the equilibrium after 24 h contact. Although the control did not contain any microplastics, the control solution with fluoxetine was also filtered to evaluate whether fluoxetine was adsorbed by the filter, potentially impacting the desorption results. The filter without (control) and with microplastics was placed into a 50 mL Erlenmeyer flask which was filled with 25 mL AFW + 0.02% NaN<sub>3</sub> (2 g L<sup>-1</sup>). The samples were continuously horizontally agitated on a MaxQ 6000

orbital shaker (Thermo Scientific, UK) at 200 rpm and 25 °C in the dark. After 24 h, the concentration of fluoxetine was evaluated in the samples. Prior tests (Figure A4.1 and Figure A4.2) demonstrated that the desorption equilibrium was also achieved after 24 h in AFW + 0.02% NaN<sub>3</sub>.

#### **4.2.5 Quantification of pharmaceuticals in the solution using liquid chromatography**

Analysis of the pharmaceuticals was performed using high performance liquid chromatography (HPLC; Waters Corporation, UK). The equipment included a solvent delivery system (Alliance 2695) with detection by photodiode array (PDA, Alliance 2996). The PDA scanning wavelength was set from 200 to 400 nm. Separation of pharmaceutical analogues was achieved using a Symmetry dC18 column (2.1 mm internal diameter x 150 mm; 5 µm particles size) which was maintained at 40 °C. The mobile phases were ultra-pure water (18.2 MΩ) (A) and acetonitrile (B) each containing 0.05% (v/v) trifluoroacetic acid (TFA; Fisher Scientific UK Ltd, UK). TFA was used as an ion-pair agent to avoid ionisation of the pharmaceuticals and improve the chromatogram. The flow rate was 0.3 mL min<sup>-1</sup>. A gradient for the separation of the pharmaceuticals of 35 minutes run time (Table 4.5), and an injection volume of 35 µL was applied. The peak for Ibuprofen (220 nm), carbamazepine (285 nm), venlafaxine (226 nm), fluoxetine (227 nm), and ofloxacin (294 nm) was measured according to each pharmaceutical UV absorption wavelength (Figure 4.2). The limit of detection and quantification of each individual pharmaceutical using this method was 0.01 µg mL<sup>-1</sup> (determined by a signal-to-noise ratio of 3.3:1) and 0.05 µg mL<sup>-1</sup> (determined by a signal-to-noise ratio of 10:1), respectively.

**Table 4.5:** Solvent gradient used in the HPLC analysis of ofloxacin, venlafaxine, carbamazepine, fluoxetine, and ibuprofen. Solvent A: ultra-pure water (18.2 M $\Omega$ ) + 0.05% (v/v) TFA; Solvent B: acetonitrile + 0.05% (v/v) TFA.

Time (min)	% Solvent A	% Solvent B	Gradient elution profile
0	90	10	-
21	20	80	Linear gradient
26	0	100	Step gradient
35	90	10	Step gradient

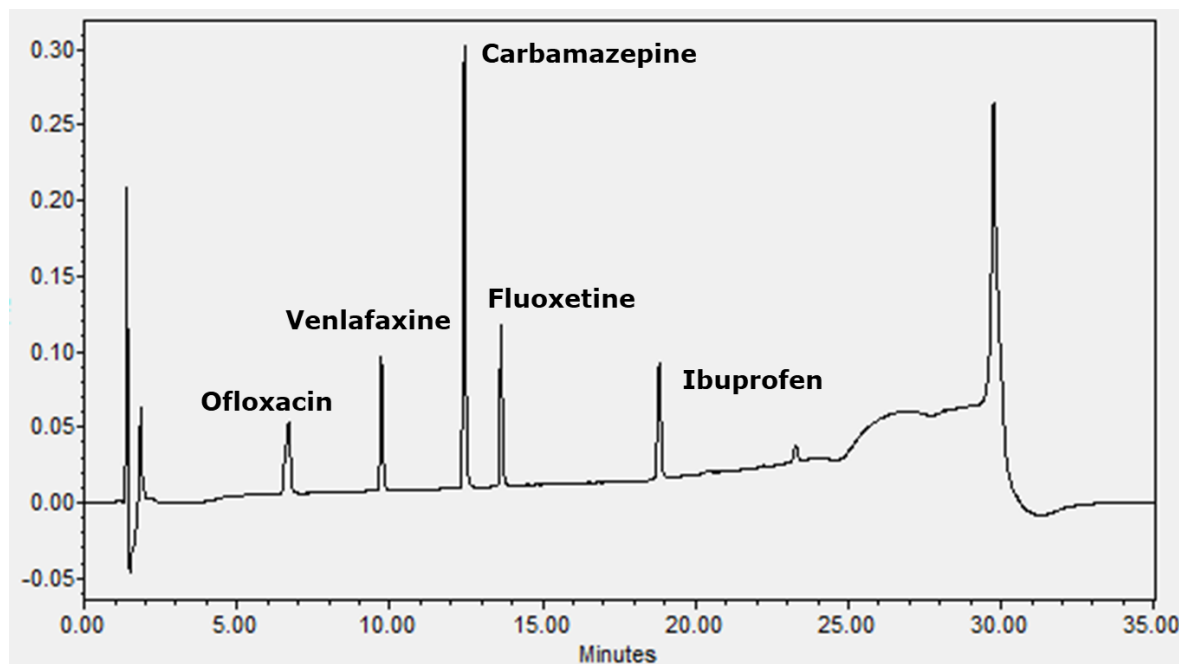


**Figure 4.1:** HPLC chromatogram of a mixture containing five pharmaceuticals (ofloxacin, venlafaxine, carbamazepine, fluoxetine, and ibuprofen) using the method detailed (Table 4.5). The detection wavelength was set in accordance with the maximum UV absorption determined for each compound (Figure 4.2). The large peak observed between 25 and 30 minutes is attributed to the column cleaning step, specifically employing pure acetonitrile, which exhibits strong absorption of UV light.

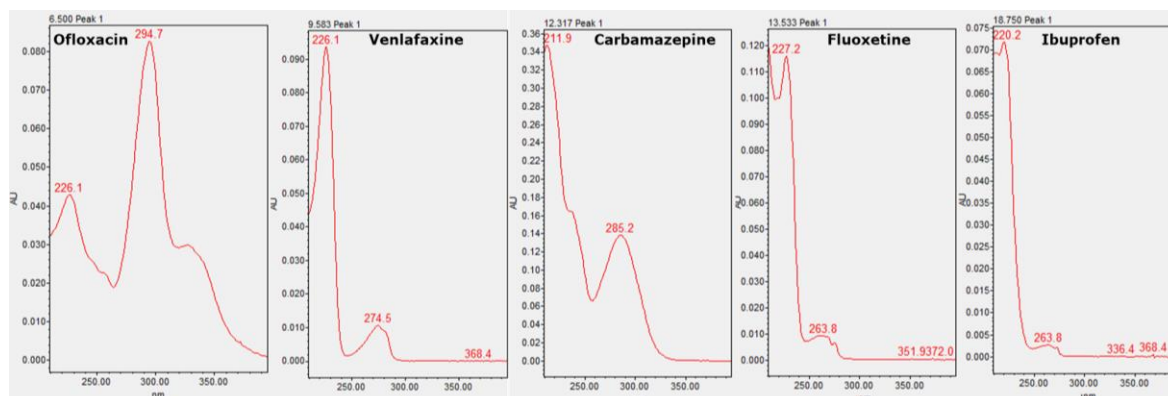


**Figure 4.2:** UV spectra of ofloxacin, venlafaxine, carbamazepine, fluoxetine, and ibuprofen.

#### 4.2.6 Data analysis

The amount of pharmaceutical adsorbed per unit mass of microplastic ( $\mu\text{mol g}^{-1}$ ), was estimated using equation 4.1:

$$q_{(t)} = (C_{ctrl(t)} - C_{(t)})V/m \quad (4.1)$$

The amount of pharmaceutical desorbed per unit mass of microplastic ( $\mu\text{mol g}^{-1}$ ), was estimated using equation 4.2:

$$q_t^* = (C_{(t)} - C_{ctrl(t)})V/m \quad (4.2)$$

where,

- $q_{(t)}$  is the amount of pharmaceutical adsorbed onto the microplastic ( $\mu\text{mol g}^{-1}$ ) at sampling time  $t$
- $C_{ctrl(t)}$  is the control solution concentration of the pharmaceutical ( $\mu\text{M}$ ) at the sampling time  $t$  as determined by HPLC-PDA
- $C_{(t)}$  is the sample solution concentration of the pharmaceutical ( $\mu\text{M}$ ) at the sampling time  $t$  as determined by HPLC-PDA
- $m$  is the mass of plastic added to the Erlenmeyer flask (g)
- $V$  is the total volume of solution (L) in the Erlenmeyer flask

Note: \* Negative values were assigned a zero value.

The percentage of pharmaceutical adsorbed at a specific sample time point ( $t$ ) onto the microplastic was calculated using equation 4.3:

$$\%Adsorbed_{(t)} = ((C_{ctrl(t)} - C_{(t)}) \times 100) / C_{ctrl(t)} \quad (4.3)$$

where,

- $\%Adsorbed_{(t)}$  is the percent of pharmaceutical adsorbed onto the microplastic at sampling time  $t$

The total amount of all pharmaceuticals adsorbed after 48 h per unit mass of microplastic ( $\mu\text{mol g}^{-1}$ ) was calculated using equation 4.4:

$$\sum_{PHA} = q_{Ibuprofen(48h)}^* + q_{Carbamazepine(48h)}^* + q_{Venlafaxine(48h)}^* + q_{Fluoxetine(48h)}^* + q_{Ofloxacin(48h)}^* \quad (4.4)$$

where,



- $\Sigma_{\text{PHA}}$  is the amount of all pharmaceuticals in the mixture adsorbed per unit mass of microplastic after 48 h ( $\mu\text{mol g}^{-1}$ )
- $q_{[\text{Pharmaceutical}]} (48 \text{ h})$  is the amount adsorbed per unit mass of microplastic after 48 h ( $\mu\text{mol g}^{-1}$ ) of each pharmaceutical in the mixture calculated using equation 4.1.

Note: \* The amount adsorbed onto microplastics that was not statistically different from the control ( $p > 0.05$ ) was assigned a zero value.

The amount of pharmaceutical adsorbed and desorbed per unit mass of microplastic ( $\mu\text{mol g}^{-1}$ ) at equilibrium, was estimated using equation 4.5:

$$q_e = (C_{\text{ctrl}(24 \text{ h})} - C_e)V/m \quad (4.5)$$

where,

- $q_e$  is the amount of pharmaceutical adsorbed / desorbed onto / from the microplastic ( $\mu\text{mol g}^{-1}$ ) at sampling time 24 h
- $C_{\text{ctrl}(24 \text{ h})}$  is the control solution concentration of the pharmaceutical ( $\mu\text{M}$ ) at the sampling time 24 h as determined by HPLC-PDA
- $C_e$  is the sample solution concentration of the pharmaceutical ( $\mu\text{M}$ ) at equilibrium which consisted of the sampling time 24 h as determined by HPLC-PDA
- $m$  is the mass of plastic added to the Erlenmeyer flask (g)
- $V$  is the total volume of solution (L) in the Erlenmeyer flask

Adsorption/desorption isotherm models applied to the experimental data of fluoxetine with the virgin and artificially aged particles of small PP, PA, and PVC are presented in the Table 4.6.

**Table 4.6:** Adsorption isotherm models applied to the experimental data of small PP in contact with five different concentrations of MC-LR (1-10  $\mu\text{M}$ ).

Adsorption isotherm	Equation	Linear form	Plot
Freundlich model	$q_e = K_F C_e^n ; n = \frac{1}{n_F}$	$\log q_e = \log K_F + n \log C_e$	$\log q_e \text{ vs } \log C_e$
Langmuir model	$q_e = \frac{K_L C_e}{1 + \alpha_L C_e} ; Q_0 = \frac{K_L}{\alpha_L}$	$\frac{C_e}{q_e} = \frac{\alpha_L}{K_L} C_e + \frac{1}{K_L}$	$\frac{C_e}{q_e} \text{ vs } C_e$
Linear model	$q_e = K_p C_e$	$q_e = K_p + C_e$	$q_e \text{ vs } C_e$

where,

- $q_e$  is the amount of compound adsorbed per mass of adsorbent at equilibrium ( $\mu\text{mol g}^{-1}$ )
- $C_e$  is the residual adsorbate concentration in the solution at equilibrium ( $\mu\text{M}$ ) determined by HPLC-PDA
- $K_F$  and  $n_F$  are the Freundlich constant ( $\text{L g}^{-1}$ ) and exponent, respectively
- $Q_0$  is the maximum adsorption capacity ( $\mu\text{mol g}^{-1}$ )
- $\alpha_L$  is energy of adsorption ( $\text{L g}^{-1}$ )
- $K_L$  is Langmuir constant ( $\text{L g}^{-1}$ )

- $K_p$  is Partition constant ( $L g^{-1}$ )

Further, the kinetics experiments were conducted with an initial fluoxetine concentration of  $5 \mu g mL^{-1}$  ( $14 \mu M$ ), the experimental data were fitted to two widely accepted kinetic models: the pseudo-first order and pseudo-second order models (Wang and Wang 2018; Liu et al. 2019, Table 4.7).

**Table 4.7:** Kinetic models applied to the experimental data of fluoxetine with virgin and artificially aged particles of small PP, PA, and PVC.

Kinetics model	Equation	Linear form	Plot
Pseudo first order	$\frac{dq_t}{dt} = K_1(q_e - q_t)$	$\log(q_e - q_t) = \log q_e - \frac{K_1}{2.303} t$	$\log(q_e - q_t) vs t$
Pseudo second order	$\frac{dq_t}{dt} = K_2(q_e - q_t)^2$	$\frac{1}{q_t} = \frac{1}{K_2 q_e^2} + \frac{1}{q_e} t$	$\frac{t}{q_t} vs t$
Interparticle diffusion	$qt = K_i t^{1/2} + C$	-	$q_t vs t^{0.5}$

where,

- $q_e$  is the amount of compound adsorbed per mass of adsorbent at equilibrium ( $\mu mol g^{-1}$ )
- $q_t$  is the amount of compound adsorbed per mass of adsorbent at time  $t$  ( $\mu mol g^{-1}$ )
- $K_1$ ,  $K_2$ , and  $K_i$  are the first order ( $L g^{-1}$ ), second order ( $L g^{-1}$ ), and intraparticle diffusion ( $\mu mol g^{-1} h^{-1/2}$ ) constant, respectively

Student's t-test was carried out to perform significance testing (Microsoft Excel).

For all statistical tests, a significance level of 5% was set. A Pearson correlation matrix was performed to evaluate a correlation between variables of this study (Microsoft Excel; Table A4.1). A correlation coefficient ( $r$ ) greater than 0.7 was considered a strong positive correlation, while a  $r$  lower than -0.7 was considered a strong negative correlation.

## **4.3 Results and discussions**

### **4.3.1 Differential adsorption of the five pharmaceuticals by the six microplastics**

The interaction of pharmaceuticals with microplastics is multifactorial in nature. In the current study, the properties of the pharmaceutical, the weathering, and the type of microplastics were all key factors affecting this interaction. Results demonstrated that fluoxetine was the pharmaceutical that was most readily adsorbed onto the microplastics (Figure 4.3), with aging generally increasing the adsorption by the microplastics. Among the microplastic types investigated, PET showed minimal adsorption, even after aging of the particles (Figure 4.3). In the mixture of the five pharmaceuticals, fluoxetine was the only compound to be adsorbed by virgin particles of small PA ( $56 \pm 4\%$  adsorption after 48 h) and large PA ( $45 \pm 4\%$  adsorption after 48 h). Furthermore, fluoxetine was adsorbed in greater amounts onto small, virgin PVC ( $71 \pm 3\%$  adsorption) and small virgin PE ( $8 \pm 2\%$  adsorption) relative to some of the other pharmaceuticals such as venlafaxine ( $8 \pm 1\%$  adsorption on small, virgin PVC) and ibuprofen ( $4 \pm 1\%$  adsorption on small, virgin PE, Figure 4.3). Although ofloxacin appeared initially to adsorb  $8 \pm 8\%$  on small, virgin PVC, no significant difference was observed when compared to the control after 48 h contact ( $p = 0.24$ ). Furthermore, while all pharmaceuticals investigated adsorbed onto virgin particles of small PP, fluoxetine showed the greatest adsorption (97%), while ibuprofen and carbamazepine demonstrated the lowest adsorption (16%). Interestingly, there was a difference in the adsorption of venlafaxine by virgin and aged small PP. After 48 h, the adsorption of fluoxetine and venlafaxine was similar for the virgin particles (approximately  $6 \mu\text{mol g}^{-1}$  adsorption each), but quite different for the

aged particles. Fluoxetine adsorbed similar amounts onto aged PP ( $5.87 \pm 0.11 \mu\text{mol g}^{-1}$ ), while venlafaxine adsorbed in lower amounts ( $3.19 \pm 0.16 \mu\text{mol g}^{-1}$ ).

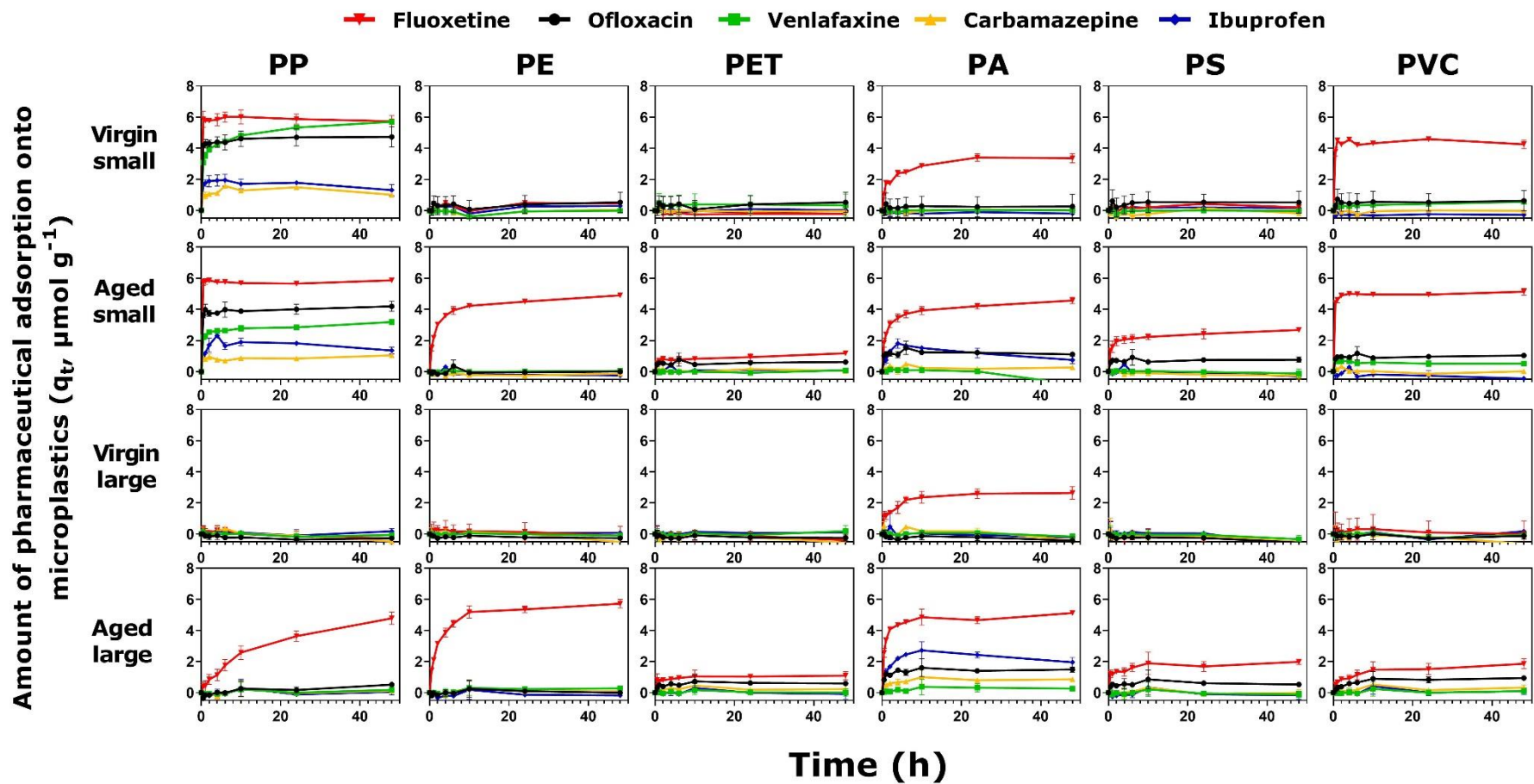


**Figure 4.3:** Amount of pharmaceutical adsorbed onto small ( $D_{50} < 35 \mu\text{m}$ ) and large ( $D_{50} 95\text{-}157 \mu\text{m}$ ) particles of the six microplastics investigated over 48 h in artificial freshwater with 0.2% (w/v)  $\text{NaN}_3$  in contact with a mixture of five pharmaceuticals. The data is presented on the basis of size (small or large) and the nature of the microplastics (virgin or aged).  $n=3$ , errors bars = 1 SD.

Studies have shown that the hydrophobicity of organic compounds plays an important role regarding the adsorption of compounds onto microplastics (Prajapati, Narayan Vaidya and Kumar 2022). For the five pharmaceuticals studied, fluoxetine has the greatest  $\log K_{OW}$  (4.05), while ofloxacin has the lowest (-0.39, Table 4.3) based on the literature data (NCOSS, 2021). However, the pH of the test or environmental system is important because, as the pH changes, the state of ionisation changes and this will have an impact on adsorption. Most pharmaceuticals are ionisable, with the extent of their ionisation varying with the pH of the media (Wagstaff, Lawton and Petrie 2021). This needs to be taken into account when considering the environmental fate of such compounds. This is achieved using the pH dependent octanol-water partition coefficient ( $\log D_{OW}$ ). The pH of the experimental media was pH 7. The consequence of this for the hydrophobicity of fluoxetine is that it decreases markedly ( $\log D_{OW}$  1.25). At pH 7, ibuprofen is the most hydrophobic ( $\log D_{OW}$  4.85) and venlafaxine is least hydrophobic compound in the mixture ( $\log D_{OW}$  - 1.97).

Although the virgin particles of small PE ( $r = 0.83$ ) showed a strong positive correlation with  $\log K_{OW}$  (Table A4.1, Figure 4.4), small amounts of fluoxetine ( $0.45 \pm 0.1 \mu\text{mol g}^{-1}$ ) and ibuprofen ( $0.29 \pm 0.08 \mu\text{mol g}^{-1}$ ) adsorbed onto small, virgin PE. A strong correlation of virgin small PS with pH dependent coefficient ( $\log D_{OW}$  0.77) for the five pharmaceuticals was also observed. Virgin small PP, on the other hand, presented a strong, negative correlation ( $r = -0.81$ ) when compared with the  $\log D_{OW}$  of the pharmaceuticals investigated. Apart from these, no correlation was observed when comparing the adsorption of each pharmaceutical with their respective  $\log K_{OW}$  and  $\log D_{OW}$  (Table A4.1). This

means that the hydrophobicity of the pharmaceuticals may not be the major driving factor regarding their interaction with microplastics. Other adsorption mechanisms, such as electrostatic interactions, may be more important for some pharmaceuticals.

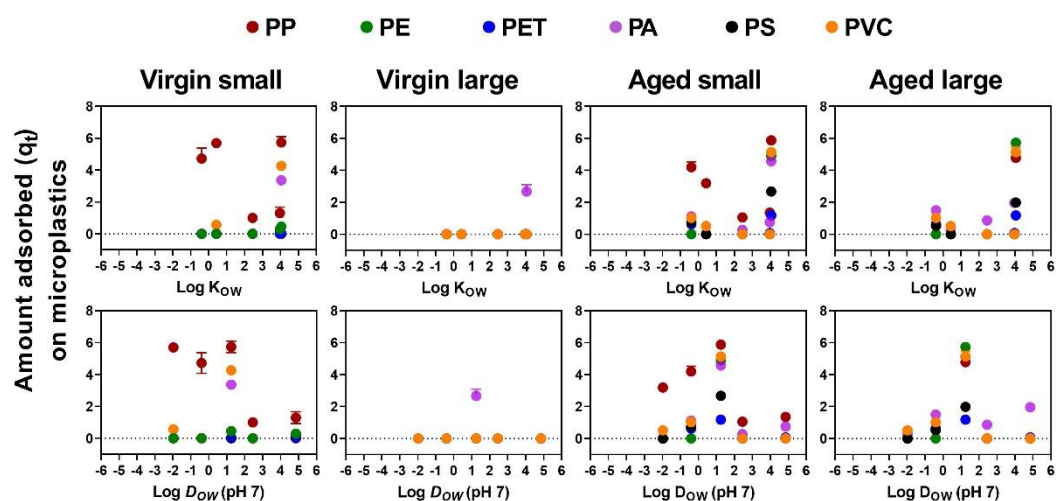


**Figure 4.4:** Comparison of the amount of pharmaceutical adsorbed onto microplastics after 48 h with the octanol-water partition coefficient ( $\log K_{ow}$ , Table 1) and the pH dependent octanol-water partition coefficient ( $\log D_{ow}$  at pH 7, Table 4.3).  $n=3$ , error bars = 1 SD.

Electrostatic and hydrophobic attractions play a significant role in the marked uptake of fluoxetine on microplastics (Atugoda et al. 2021). At pH 7, fluoxetine and venlafaxine are positively charged, ibuprofen and ofloxacin are negatively charged, and carbamazepine is uncharged (Table 4.3). The positive charge of fluoxetine at pH 7, and the negatively charged surface of microplastics makes electrostatic interaction favourable. Although venlafaxine is also positively charged at the pH of the experimental media, its hydrophilicity can have a negative impact on the adsorption onto microplastics, especially when co-occurring with highly hydrophobic and also cationic compounds such as fluoxetine. Moura et al., (2022) have demonstrated that hydrophobic compounds can compete for binding sites and be adsorbed in greater amounts when placed

in a mixture with more hydrophilic compounds. Fluoxetine has been reported to be adsorbed in greater amounts onto PA microparticles when compared to the cationic (i.e., positively charged) pharmaceuticals atenolol, pseudoephedrine, metoprolol, tramadol, propranolol, and amitriptyline (Wagstaff, Lawton and Petrie 2021).

### 4.3.2 The effect of the physico-chemical characteristics of the six microplastic types onto the adsorption of pharmaceuticals

The type of microplastic can affect the adsorption behaviour of pharmaceuticals by microparticles. In the current study, the total amount of the pharmaceuticals adsorbed by the microplastics varied according to the polymeric material (Figure 4.5).

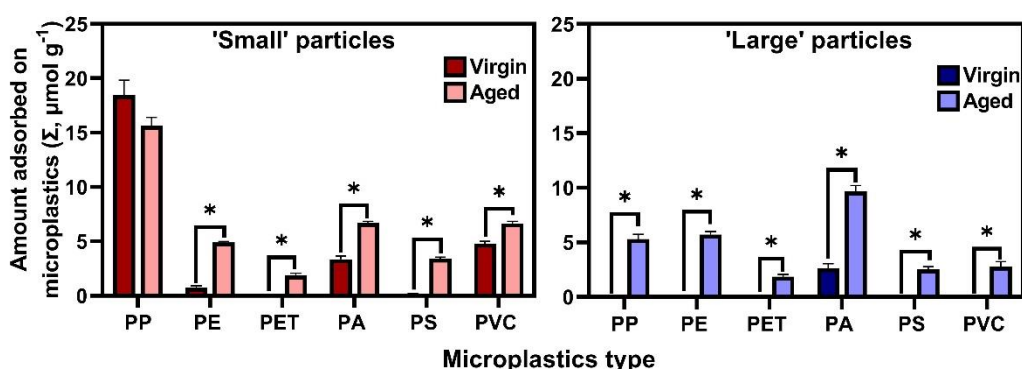


**Figure 4.5:** Total amount of pharmaceuticals adsorbed onto small ( $D_{50} < 35 \mu\text{m}$ ) and large ( $D_{50} 95\text{-}157 \mu\text{m}$ ) microplastics after 48 h in artificial freshwater with 0.02% (w/v)  $\text{NaN}_3$  in contact with a mixture of pharmaceuticals.  $n=3$ , errors bars = 1 SD. \*significant difference between the virgin and aged particles,  $p < 0.05$ .

Additionally, the adsorption behaviour for each pharmaceutical depended on the type of microplastics. Small PP showed the greatest adsorption among the microplastics investigated, followed by PA. In the mixture, the virgin particles of small PP adsorbed from 16% (ibuprofen and carbamazepine) to 97%



(fluoxetine). A similar adsorption capacity is observed for the aged particles of small PP. For the virgin microplastics, the size of the particles affected the amount adsorbed on the microplastics. For the small virgin particles, only PP, PA, and PVC showed a marked adsorption of fluoxetine with varying amounts of the other pharmaceuticals being adsorbed. Meanwhile, no significant adsorption ( $p > 0.05$ ) was observed onto small PET after 48 h contact. For small PS, a small amount of ibuprofen ( $2 \pm 1\%$  adsorption) demonstrated a significant difference ( $p = 0.02$ ) from the control after 48 h contact. Discrete adsorption was also observed by small PE, where fluoxetine and ibuprofen adsorbed  $8 \pm 2\%$  ( $p = 0.02$ ) and  $4 \pm 1\%$  ( $p = 0.02$ ) onto small PE, respectively. There is a marked increase in adsorption of the pharmaceuticals by the small particles following aging. When considering the combined amount ( $\Sigma_{\text{PHA}}$ ) of all pharmaceuticals in the mixture, except for PP and PVC, the small particles demonstrated a significantly greater ( $p < 0.05$ ) adsorption when compared to the amount of pharmaceuticals adsorbed onto the virgin microplastics (Figure 4.5).

Considering the virgin microplastics, the size of the particles affected the amount adsorbed on the microplastics. Overall, the virgin microplastics described as small showed greater adsorption of the pharmaceuticals when compared to the large particles. Minimal adsorption of pharmaceuticals was observed by the large virgin particles, except for large PA that stands out for its adsorption of fluoxetine (45% adsorption). Large PA is an amorphous form of PA, like PS and PVC that are typically amorphous. Amorphous polymers, in which crystalline regions are absent, are expected to show greater adsorption when compared to more crystalline polymers (Seo et al. 2022). Furthermore, large PA has the greatest  $S_{\text{BET}}$  ( $0.92 \text{ m}^2 \text{ g}^{-1}$ ) when compared to the other large microplastics

(0.01-0.41 m<sup>2</sup> g<sup>-1</sup>). The combination of the polar nature, greater surface area, and amorphous properties of large PA might explain why fluoxetine showed a marked adsorption onto the large PA particles.

For PP and PVC, the size of the particles is not the only factor affecting the adsorption when compared to the larger particles of the same microplastic type. For small PP, the presence of the carbonyl functional group (C=O) in the IR spectrum that is not present in the large particles of PP and its comparatively large surface area ( $S_{BET}$  52.2 m<sup>2</sup> g<sup>-1</sup>) affected the adsorption of small PP.

Although unmodified PP is typically a non-polar polymer, due to the presence of the carbonyl functional group (C=O), the virgin particles of small PP behaved more like a polar microplastic which will have an impact on adsorption. Polar polymers usually contain polar functional groups, such as hydroxyl (-OH), carboxyl (-COOH), or amino (-NH<sub>2</sub>) groups, which create regions of partial positive and negative charges within the polymer structure. These charged or polar regions can interact with hydrophilic compounds through intermolecular forces such as hydrogen bonding,  $\pi$ - $\pi$  interactions, or ion- $\pi$  interactions. As a result, organic compounds can more easily adsorb onto the surface of polar polymers due to these attractive forces. Furthermore, the greater the surface area, the greater the adsorption expected (Chen, Sawyer and Regan 2013). The large surface area of small PP suggests that along with electrostatic and hydrophobic interactions, pore filling was the main mechanism of adsorption taking place in the interaction of small PP with the pharmaceuticals, as also demonstrated by Moura et al., (2022). Likewise, for small PVC, small particles size and the spongy surface morphology identified for the particles might have additional effects on the interaction with the pharmaceuticals when compared to

the smooth surface morphology which was a characteristic of the large PVC determined during detailed assessment of the material. Moreover, the polar surface and increased  $S_{BET}$  of small PP and PVC ( $S_{BET}$  4.3 m<sup>2</sup> g<sup>-1</sup>) affect the dispersion of the particles through the water column, which might be the reason that the adsorption of pharmaceuticals onto the virgin and aged PP and PVC rapidly attains a plateau when compared to non-polar and less porous microplastics, such as large PP and PE (Figure 4.3). The  $S_{BET}$  showed a stronger positive correlation when comparing the total amount of pharmaceuticals adsorbed onto virgin ( $r=0.97$ ) and aged ( $r=0.83$ ) microplastics (Table A4.1). That means that other interaction mechanisms such as electrostatic interactions are in place along with  $S_{BET}$  when pharmaceuticals are placed in contact with aged microplastics.

In addition to the density of the microplastics also plays an important role regarding the buoyancy of the particles in the water column. Less dense microplastics such as PP, PE, and PS tend to float when in contact with water, which can decrease the surface area in contact with organic compounds dissolved in the liquid phase. The decreased surface contact can lower the adsorption potential of the hydrophobic microplastic. Polarity might be the main reason that the polymers investigated in the current study (e.g., small PP, PA, and PVC) showed the greatest adsorption of pharmaceuticals onto the virgin particles when compared to non-polar polymers (PP, PE, and PS).

### 4.3.3 The effect of aging on the adsorption of five pharmaceuticals by six microplastic types

The weathering of microplastics had clear consequences for the adsorption of pharmaceuticals by microplastics. In the current study, artificially aged microplastics showed greater adsorption when compared to the virgin particles for both microplastic sizes (Figure 4.3 and Figure 4.5). The aging of the small particles increased adsorption up to 3.5-fold (small PE) of all pharmaceuticals combined. While for the large particles, the amount of all pharmaceuticals adsorbed on aged PP ( $\Sigma_{\text{PHA}} 5.70 \pm 0.68 \mu\text{mol g}^{-1}$ ) was approximately 30-fold greater when compared to virgin PP ( $\Sigma_{\text{PHA}} 0.18 \pm 0.18 \mu\text{mol g}^{-1}$ , Figure 4.5). The large particles of all microplastic types showed significantly greater adsorption ( $p < 0.05$ ) by the aged particles compared to the virgin particles. For example, the large particles of PA demonstrated a significant increase ( $p = 0.0001$ ) in the adsorption of pharmaceuticals between the virgin ( $\Sigma_{\text{PHA}} 2.65 \pm 0.42 \mu\text{mol g}^{-1}$ ) and aged ( $\Sigma_{\text{PHA}} 9.68 \pm 0.53 \mu\text{mol g}^{-1}$ ) material. In this case the increased adsorption was due to changes in the adsorption of all five pharmaceuticals ( $p < 0.05$ ). This contrasts with PE which, although it showed a significant increase in adsorption, the change was almost entirely due to an increase in the adsorption of fluoxetine (Figure 4.3).

As highlighted, fluoxetine consistently was the pharmaceutical that was most readily adsorbed by the microplastics, the adsorption being enhanced by aging. Only fluoxetine adsorbed ( $78 \pm 3\%$ ) on large, aged PP, while virgin particles of large PP did not adsorb any of the pharmaceuticals in the mixture (Figure 4.3). Ibuprofen and ofloxacin were adsorbed by aged particles of both sizes of PA (Figure 4.3). Aging also enhanced the adsorption of ofloxacin by PS and PET

relative to the virgin particles. Ofloxacin showed the second highest absolute adsorption after fluoxetine. However, lower amounts of fluoxetine and ofloxacin adsorbed onto aged PET when compared to aged PS. In general, aging increases the adsorption of less hydrophobic and hydrophilic organic compounds by microplastics (Prajapati, Narayan Vaidya and Kumar 2022). Liu et al. (2019) have also reported an increase in the adsorption of the hydrophilic antibiotic ciprofloxacin ( $\log K_{ow}$  0.4) onto PS and PVC microparticles (size  $\sim 70 \mu\text{m}$ ). The authors suggested the adsorption on microplastics is not limited to hydrophobic organic compounds, especially due to the increasing number of oxygen-containing functional groups present in aged particles (Liu et al. 2019). Carbonyl functional groups contain a carbon which has a partial positive charge, while the oxygen has a partial negative charge. The positive charge of the carbonyl carbon might favour the electrostatic interaction of anionic (negatively charged) pharmaceuticals such as ibuprofen and ofloxacin.

Aging clearly changes the adsorption potential for the large particles, especially in respect of fluoxetine. The results indicated that the size of the microplastics was a secondary factor affecting the adsorption when compared to the weathering of the particles. Considering the combined amount ( $\Sigma_{\text{PHA}}$ ) of all the pharmaceuticals adsorbed, the aged particles of small PA ( $\Sigma_{\text{PHA}} 6.75 \pm 0.20 \mu\text{mol g}^{-1}$ ) adsorbed in significantly lower amounts ( $p = 0.01$ ) when compared with large, aged PA ( $\Sigma_{\text{PHA}} 9.68 \pm 0.53 \mu\text{mol g}^{-1}$ ). Likewise, large, aged PE ( $\Sigma_{\text{PHA}} 6.13 \pm 0.47 \mu\text{mol g}^{-1}$ ) showed significant greater adsorption ( $p = 0.02$ ) of pharmaceuticals in comparison to aged particles of small PE ( $\Sigma_{\text{PHA}} 5.00 \pm 0.14 \mu\text{mol g}^{-1}$ , Figure 4.5). Along with the size of the particles, properties such as glassiness, crystallinity and the polarity of microplastics have shown to impact

the adsorption behaviour of organic compounds (Liu et al. 2019). In the current study, the polarity of both virgin and aged microplastics had a considerable impact on the adsorption of the pharmaceuticals. For instance, small PP, PA, and PVC, considered polar polymers (the small PP because of the presence of a compound with a carbonyl group), were the virgin microplastic types that showed greatest adsorption of the pharmaceuticals investigated (Figure 4.3 and Figure 4.5). Furthermore, due to photo-oxidation and weathering, microplastics, including originally non-polar polymers (e.g., large PP, PE, and PS), develop polar oxygen-containing groups that can favour hydrogen bond interaction (Prajapati, Narayan Vaidya and Kumar 2022) along with electrostatic and hydrophobic interactions. The absence of oxygen-containing groups that favour those interactions might be the reason that, for both sizes of virgin PE, there was no adsorption of the pharmaceuticals, while fluoxetine was adsorbed onto small (82%) and large (93%) particles of aged PE. According to Li et al., (2018), the formation of hydrogen bonds (H-bond) was the key mechanism underlying the high adsorption of the hydrophilic antibiotics amoxicillin, tetracycline, and ciprofloxacin on PA. However, H-bond interactions are weaker compared to hydrophobic and electrostatic interactions (Prajapati, Narayan Vaidya and Kumar 2022). Aliphatic polymers, such as PE and PVC, normally undergo Van der Waals interactions, while for aromatic polymers, such as PS, adsorption is usually attributed to  $\pi$ - $\pi$  interactions (Tourinho et al. 2019).

Several studies have observed an increase in the adsorption of organic compounds on aged microplastics when compared to virgin microplastics (Hüffer, Weniger and Hofmann 2018b; Zhang et al. 2018; Liu et al. 2020b; Bhagat et al. 2022). The increase in the adsorption capacity of the aged particles can be

explained by the change in the hydrophobicity and the surface charge caused by thermal- and photo-oxidation processes. According to Atugoda et al. (2021), the aging of microplastics decreases the hydrophobicity and increases the electrostatic interactions between the aged microplastics and pharmaceutical compounds, resulting in their retention on the polymer. The addition of polar, oxygen-containing functional groups to the surface results in a trend towards higher hydrophilicity and surface free energy of microplastics (Bhagat et al. 2022).

#### **4.3.4 Adsorption/desorption kinetics of fluoxetine onto/from virgin and artificially aged small microplastics**

Fluoxetine was placed individually in contact with virgin and aged small PP, PA, and PVC, and its adsorption kinetics when co-occurring with those microplastics was evaluated. As when in a mixture, the artificially aged particles of small PA and PVC adsorbed greater amounts of fluoxetine when comparing to the virgin PA and PVC, and similar adsorption was observed by virgin and aged small PP (Figure 4.6).

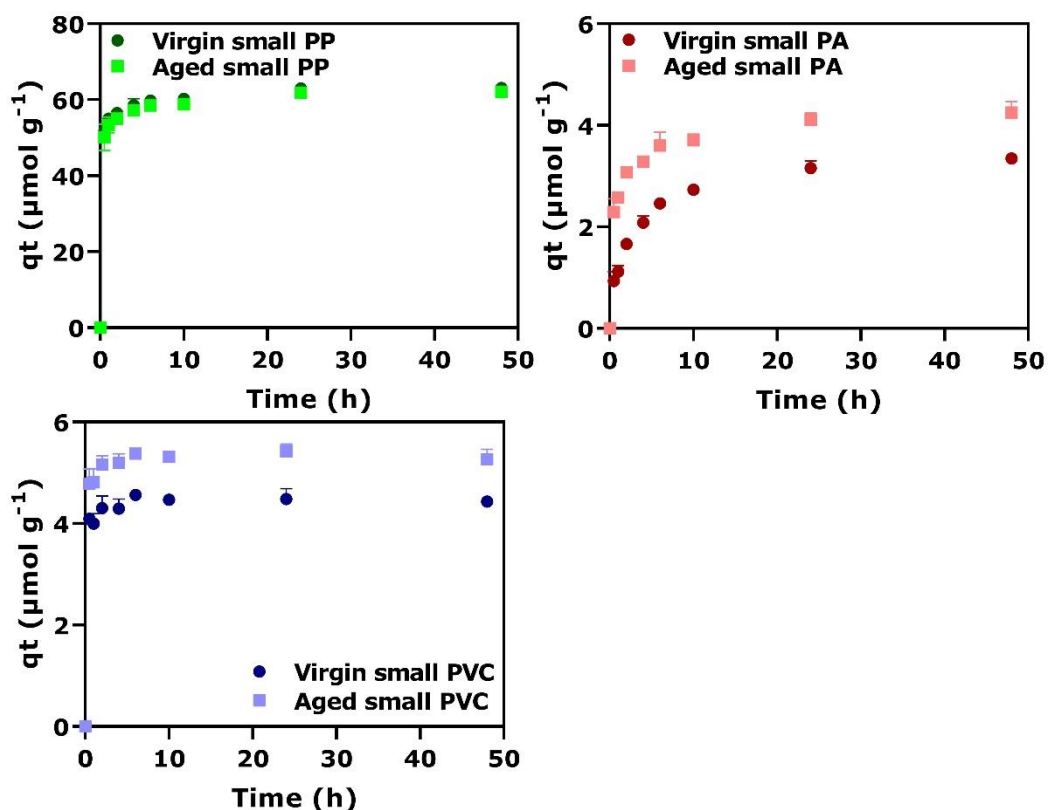


**Figure 4.6:** Amount of fluoxetine ( $q_t$ ) adsorbed onto microplastics over 48 h contact in artificial freshwater + 0.02% (w/v)  $\text{NaN}_3$  at initial fluoxetine concentration of 145  $\mu\text{M}$  (50  $\mu\text{g mL}^{-1}$ ) for small PP, and 14  $\mu\text{M}$  (5  $\mu\text{g mL}^{-1}$ ) for small PA and PVC. The total amount desorbed from microplastics was calculated using the equation 4.2.

Small PP ( $S_{\text{BET}}$  52.2  $\text{m}^2 \text{g}^{-1}$ ) and PVC ( $S_{\text{BET}}$  4.3  $\text{m}^2 \text{g}^{-1}$ ), the two microplastic types with the greatest surface area, readily adsorbed fluoxetine, as also observed when in contact with a mixture of pharmaceuticals (Figure 4.6). The majority of the amount of fluoxetine adsorbed onto virgin small PP ( $83 \pm 2\%$  at 30 min) and PVC ( $69 \pm 2\%$  at 30 min) occurred after 30 min contact. Likewise, within 30 min contact, the aged particles of small PP and PVC adsorbed approximately 80% onto the weathered particles. While for small PA, the adsorption onto the microplastics was slower when compared to PP and PVC. After 30 min, fluoxetine adsorbed  $16 \pm 3\%$  onto small virgin particles of PP and PVC and  $39 \pm 4\%$  onto small aged PA.



For all three microplastic types investigated (PP, PA, and PVC), the adsorption experiment data fitted the pseudo second order model (Figure 4.7 to Figure 4.9, Table 4.8). The experimental data fitting the pseudo second order kinetics suggests a chemical adsorption over a physical process (e.g., Van der Waals forces) dominates the interactions between the fluoxetine and the microplastics investigated (Wagstaff, Lawton and Petrie 2021). In a study conducted by Wang and Wang (2018), the adsorption of the organic compound, pyrene, onto PE, PS, and PVC also fitted the pseudo second order model. The same was observed when the antibiotic ofloxacin was placed in contact with PVC microparticles (Yu et al. 2020). Small PA was the only microplastic type where the intraparticle diffusion model appears to fit (Figure 4.8), since there are two adsorption segments when plotting  $q_t$  vs  $\text{time}^{1/2}$ . The intraparticle diffusion model emphasises that adsorption is a multi-step process involving transport of the adsorbate from bulk solution to external surface and then into the interior pores of the sorbent (Wang and Wang 2018a).

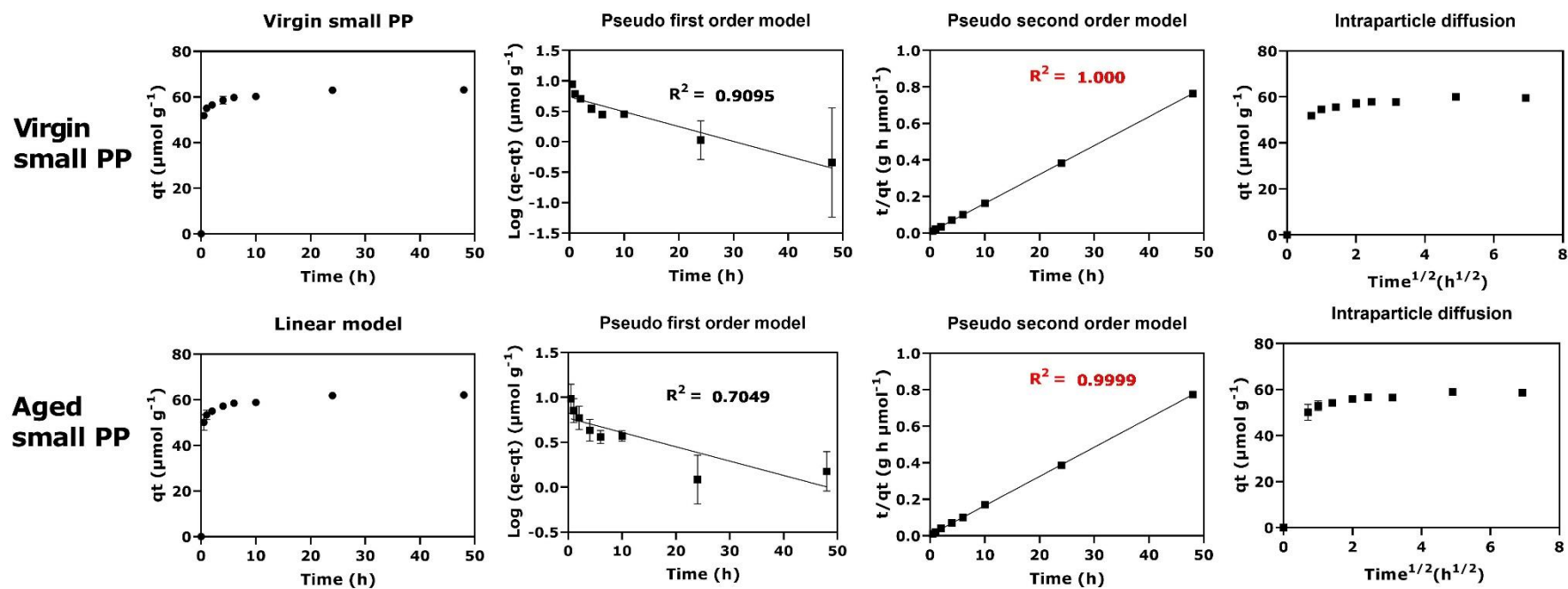


**Figure 4.7:** Application of the experimental adsorption data of virgin and artificially aged small PP in contact with fluoxetine ( $43\text{-}289\ \mu\text{M}$ ;  $15\text{-}100\ \mu\text{g mL}^{-1}$ ) to the linear forms of the linear, pseudo first order, pseudo second order, and intraparticle diffusion models. Highlighted in red are the  $R^2$  of the isotherm model that showed the best fit to the experimental data. The equations are described in Table 4.7.

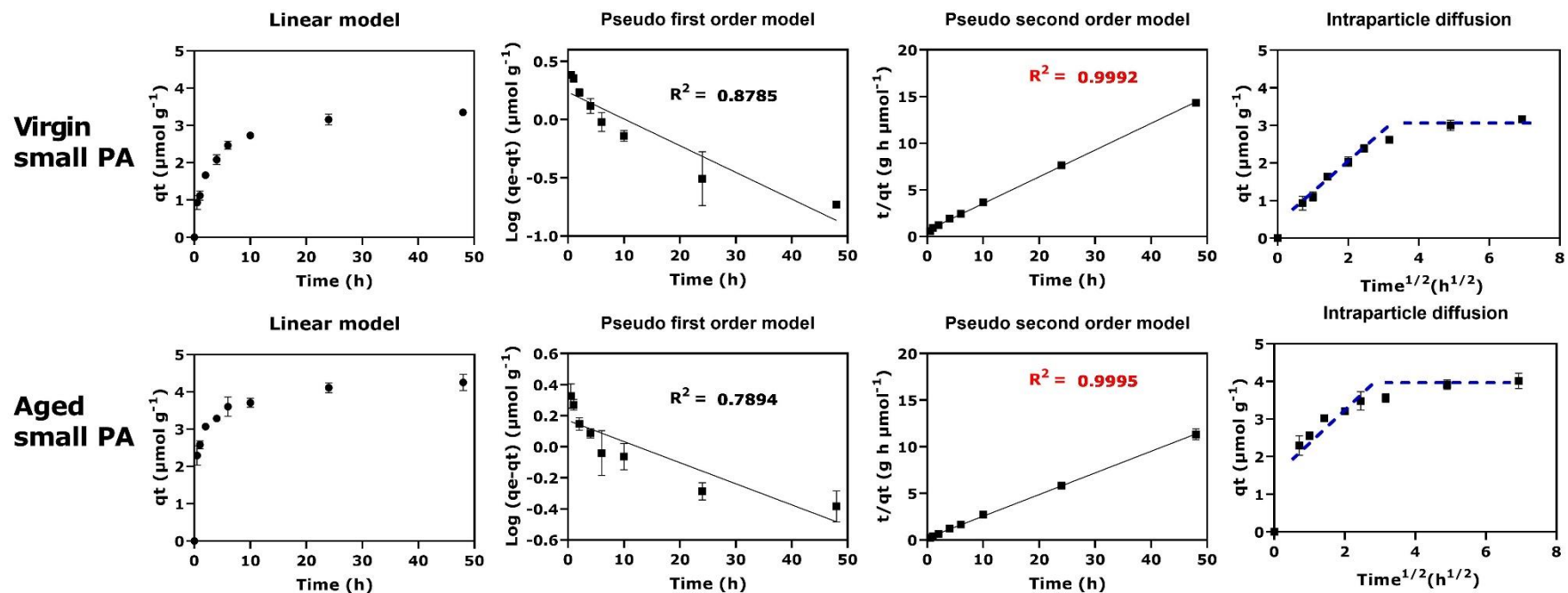


**Figure 4.8:** Application of the experimental adsorption data of virgin and artificially aged small PA in contact with fluoxetine ( $43\text{-}289 \mu\text{M}; 15\text{-}100 \mu\text{g mL}^{-1}$ ) to the linear forms of the linear, Pseudo first order, Pseudo second order, and intraparticle diffusion models. The dashed in blue line (□□) represents the intraparticle diffusion segments. Highlighted in red are the  $R^2$  of the isotherm model that showed the best fit to the experimental data. The equations are described in Table 4.7.

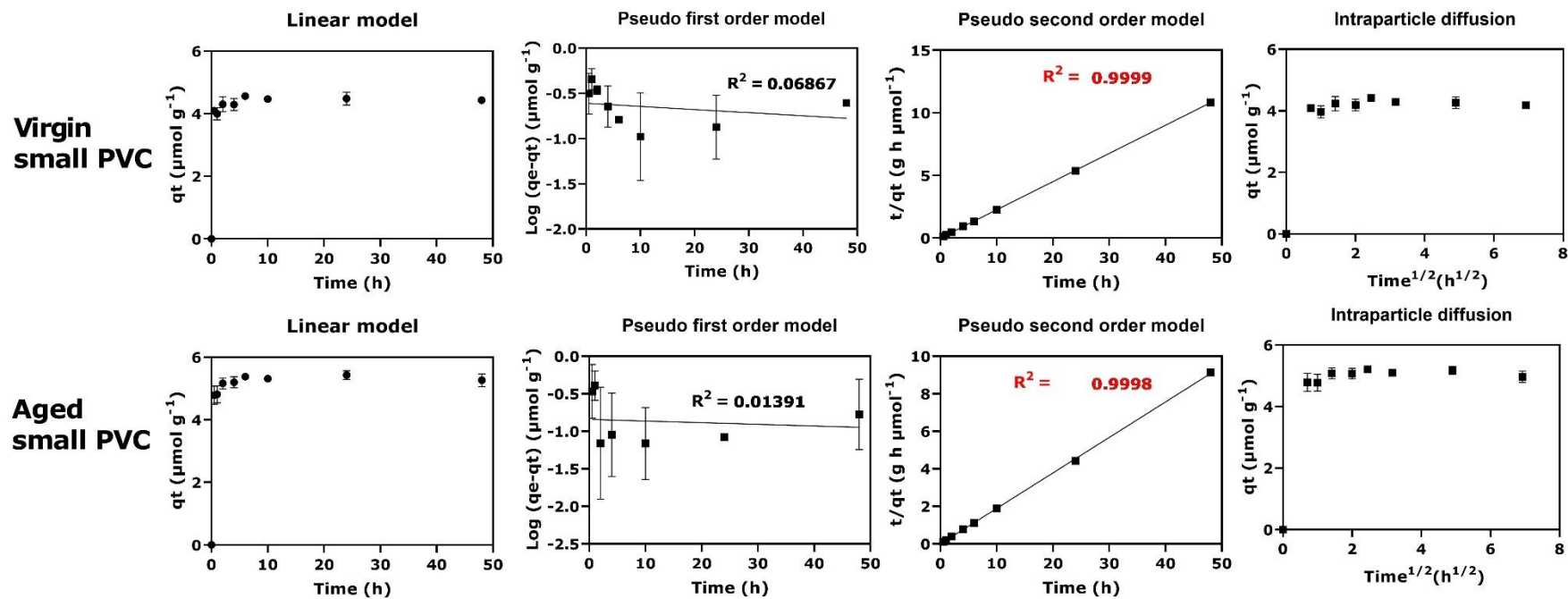


**Figure 4.9:** Application of the experimental adsorption data of virgin and artificially aged small PVC in contact with fluoxetine ( $43\text{-}289 \mu\text{M}; 15\text{-}100 \mu\text{g mL}^{-1}$ ) to the linear forms of the linear, pseudo first order, pseudo second order, and intraparticle diffusion models. Highlighted in red are the  $R^2$  of the isotherm model that showed the best fit to the experimental data. The equations are described in Table 4.7.

The kinetics of fluoxetine desorption from microplastics was evaluated by placing the filtered fluoxetine pre-exposed microplastics into fresh media. The maximum fluoxetine desorption was observed from virgin, small PVC ( $1.50 \pm 0.04 \mu\text{M}$ ) followed by virgin, small PA ( $1.42 \pm 0.04 \mu\text{M}$ ). The microplastic type and the weathering of the microplastics were the key factors affecting the desorption of fluoxetine from microplastics. Among the microplastic types investigated (PP, PA, and PVC), fluoxetine did not appear to desorb from the small PP microparticles (Figure 4.10). The negative desorption values of virgin small PP are attributed to the higher concentration of fluoxetine detected in the control samples (47-86% after 48 h) when compared to the samples contained the filtered particles of small PP. The desorption control samples consisted of the filtered adsorption control (samples without microplastics) that was placed in contact with fresh media. This procedure was performed to prevent a potential influence of dissolved fluoxetine adsorbed on the GF/F filter on the desorption results, since fluoxetine might be transferred from the solution to the filter. Therefore, in the experimental design applied, if the concentration of fluoxetine in the control solution was greater or similar to the concentration of fluoxetine in solution with the filtered microplastics, the desorption of fluoxetine from the microplastics cannot be assumed.

Greater desorption amounts ( $q_t$ ) were observed from aged small PP ( $-0.60 \mu\text{mol g}^{-1}$  after 48 h) when compared to virgin PP ( $-1.08 \mu\text{mol g}^{-1}$  after 48 h). However, desorption cannot be assumed, since greater concentration of fluoxetine was detected in the control when compared to the samples with microplastics (virgin and aged). For this reason, the experimental data for small PP could not be fitted

to the kinetic models selected (pseudo first order, pseudo second order, and intraparticle diffusion models).

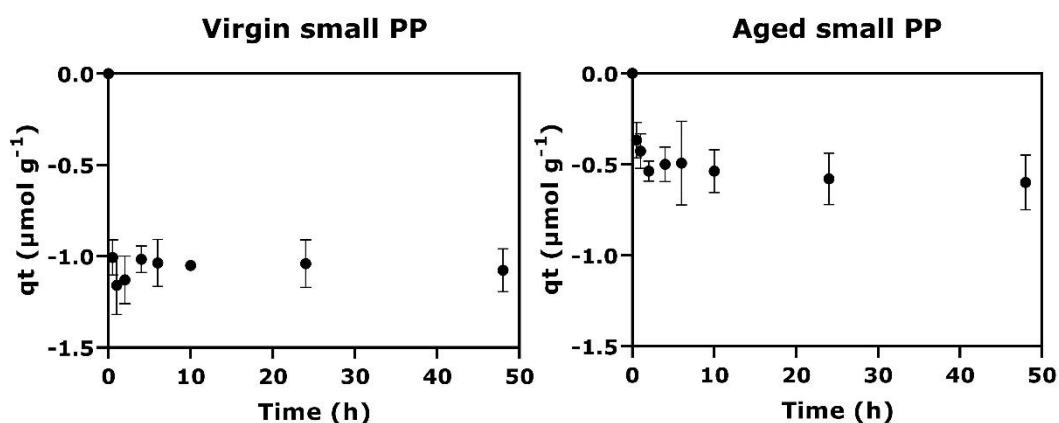


**Figure 4.10:** Amount of fluoxetine desorbed from virgin and artificially aged particles of small PP pre exposed to fluoxetine ( $145 \mu\text{M}$ ,  $50 \mu\text{g mL}^{-1}$ ) over 48 h in artificial freshwater + 0.02% (w/v)  $\text{NaN}_3$  at  $25^\circ\text{C}$  in the dark ( $2 \text{ g L}^{-1}$  plastics). The total amount desorbed from microplastics was calculated using the equation 4.2.

The experimental data of fluoxetine desorbed from PA and PVC also fitted the second order model ( $R^2 > 0.99$ ) as observed in the adsorption of fluoxetine onto microplastics (Table 4.8). For both virgin and aged small PA and PVC, the desorption equilibrium was achieved after 6 h in fresh media (Figure 4.11 and Figure 4.12), however the majority of the desorption occurred after 30 min. The virgin particles of PA ( $q_e 0.50 \mu\text{mol g}^{-1}$ ) and PVC ( $q_e 0.53 \mu\text{mol g}^{-1}$ ) desorbed in greater amounts of fluoxetine when compared to artificially aged particles of PA ( $q_e 0.22 \mu\text{mol g}^{-1}$ ) and PVC ( $q_e 0.28 \mu\text{mol g}^{-1}$ , Table 4.8).

Fluoxetine has been shown to fit the second order model when desorbing from PET microparticles (maximum  $300 \mu\text{m}$ , Wagstaff and Petrie 2022) in river water at  $20^\circ\text{C}$ . Furthermore, Wagstaff and Petrie (2022) have also demonstrated that greater desorption of fluoxetine can occur in gastric fluid simulated media when compared to intestinal fluid and river water. As observed in the current study, Liu

et al. (2020b) has demonstrated that the aging process of PS microparticles (~50  $\mu\text{m}$ ) suppressed the desorption of pharmaceuticals. According to Liu et al. (2020b), the reason is that the aging of the microplastics decreases the hydrophobic and  $\pi$ - $\pi$  interactions, but at the same time, increases the electrostatic interaction between aged microplastics and pharmaceuticals, which became less affected by the media components (gastrointestinal).

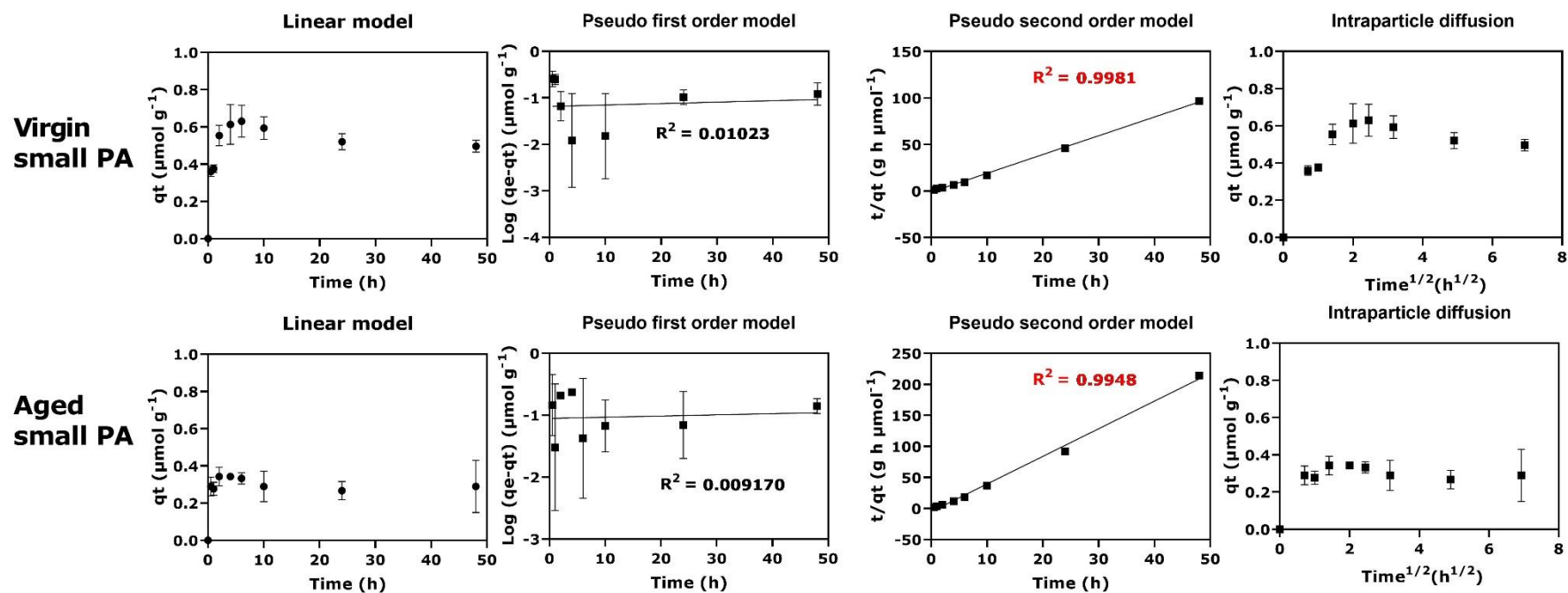


**Figure 4.11:** Application of the experimental desorption data of virgin and artificially aged small PA in contact with fluoxetine ( $14 \mu\text{M}; 5 \mu\text{g mL}^{-1}$ ) to the linear forms of the linear, pseudo first order, pseudo second order, and intraparticle diffusion models. Highlighted in red are the  $R^2$  of the isotherm model that showed the best fit to the experimental data. The equations are described in Table 4.7.



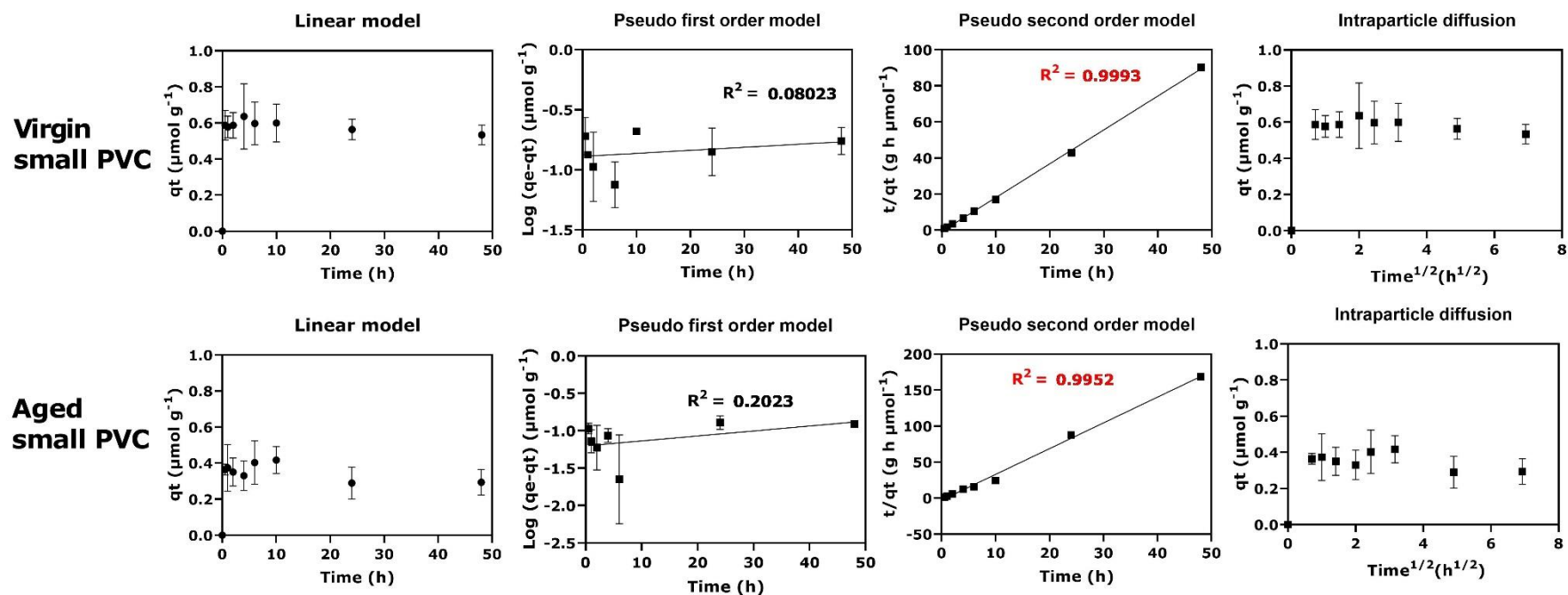


**Figure 4.12:** Application of the experimental desorption data of virgin and artificially aged small PVC in contact with fluoxetine ( $14 \mu\text{M}; 5 \mu\text{g mL}^{-1}$ ) to the linear forms of the linear, pseudo first order, pseudo second order, and intraparticle diffusion models. Highlighted in red are the  $R^2$  of the isotherm model that showed the best fit to the experimental data. The equations are described in Table 4.7.

**Table 4.8:** Summary of the adsorption and desorption parameters of the pseudo first order and second order models. Data was not obtained for PP as explained in the text.

<b>Adsorption</b>				
<b>Kinetics model</b>	<b>Plastic</b>	<b>Parameters</b>		
<b>Pseudo first order</b>		<b><math>k_1</math> (<math>\text{h}^{-1}</math>)</b>	<b><math>q_e</math> (<math>\mu\text{mol g}^{-1}</math>)</b>	<b><math>R^2</math></b>
	PP <sub>VIRGIN</sub>	0.0561	5.45	0.9095
	PP <sub>AGED</sub>	0.0367	5.87	0.7049
	PA <sub>VIRGIN</sub>	0.0529	1.72	0.8785
	PA <sub>AGED</sub>	0.0313	1.48	0.7894
	PVC <sub>VIRGIN</sub>	0.0080	0.25	0.06867
	PVC <sub>AGED</sub>	0.0051	0.14	0.01391
<b>Pseudo second order</b>		<b><math>k_2</math> (<math>\text{g } \mu\text{mol}^{-1} \text{h}^{-1}</math>)</b>	<b><math>q_e</math> (<math>\mu\text{mol g}^{-1}</math>)</b>	<b><math>R^2</math></b>
	PP <sub>VIRGIN</sub>	0.0623	63.21	1.000
	PP <sub>AGED</sub>	0.0480	62.54	0.9999
	PA <sub>VIRGIN</sub>	0.1249	3.49	0.9992
	PA <sub>AGED</sub>	0.2358	4.31	0.9995
	PVC <sub>VIRGIN</sub>	19.1787	4.44	0.9999
	PVC <sub>AGED</sub>	-6.0335	5.29	0.9998
<b>Desorption</b>				
<b>Kinetics model</b>	<b>Plastic</b>	<b>Parameters</b>		
<b>Pseudo first order</b>		<b><math>k_1</math> (<math>\text{h}^{-1}</math>)</b>	<b><math>q_e</math> (<math>\mu\text{mol g}^{-1}</math>)</b>	<b><math>R^2</math></b>
	PA <sub>VIRGIN</sub>	-0.0071	0.07	0.01023
	PA <sub>AGED</sub>	-0.0044	0.09	0.00917
	PVC <sub>VIRGIN</sub>	-0.0058	0.13	0.08023
	PVC <sub>AGED</sub>	-0.0153	0.06	0.2023
<b>Pseudo second order</b>		<b><math>k_2</math> (<math>\text{g } \mu\text{mol}^{-1} \text{h}^{-1}</math>)</b>	<b><math>q_e</math> (<math>\mu\text{mol g}^{-1}</math>)</b>	<b><math>R^2</math></b>
	PA <sub>VIRGIN</sub>	-3.7424	0.50	0.9981
	PA <sub>AGED</sub>	-3.8593	0.22	0.9948
	PVC <sub>VIRGIN</sub>	-4.6788	0.53	0.9993
	PVC <sub>AGED</sub>	-4.5571	0.28	0.9952

#### 4.3.5 Adsorption/desorption isotherm of fluoxetine onto/from virgin and artificially aged small microplastics

Adsorption/desorption isotherms were performed to evaluate the adsorption/desorption mechanisms of fluoxetine in contact with highly adsorbent microplastics. Fluoxetine, a highly hydrophobic pharmaceutical that showed the greatest adsorption onto microplastics, was placed in contact with small particles

of virgin and artificially aged PP, PA, and PVC. The adsorption isotherm experiment demonstrated that the isotherm model depends on the type and the weathering of the microplastics. For the three microplastic types tested, the virgin and the artificially aged particles showed different fits to the isotherm models investigated. For all microplastics evaluated, none of the isotherms fitted the linear model. That means that 'adsorption' was the key mechanism regarding the interaction of fluoxetine with microplastics, and no 'absorption' was observed.

For small PP, the Langmuir model showed the best fit to the experimental data for both the virgin and the aged particles of small PP (Figure 4.13). That means that the aging of the particles did not alter the monolayer adsorption behaviour of fluoxetine onto small PP. As result, a maximum adsorption capacity ( $Q_0$ ) could be calculated. Virgin PP ( $Q_0$  112  $\mu\text{mol g}^{-1}$ ) and aged PP ( $Q_0$  115  $\mu\text{mol g}^{-1}$ ) presented similar adsorption capacity (Table 4.9). Like PP, the aging of small PA did not modify the adsorption mechanism of fluoxetine in contact with small PA. However, multilayer adsorption with intramolecular interaction of fluoxetine (Freundlich model) was the adsorption mechanism of small PA (Figure 4.14). In contrast, the virgin particles of small PVC demonstrated multilayer adsorption with intramolecular interaction of fluoxetine (Freundlich model,  $R^2$  0.9830, Figure 4.15), while a monolayer adsorption observed for the aged PVC (Langmuir model,  $R^2$  0.9741, Table 4.9). The aged particles of small PVC showed an adsorption capacity of 9.69  $\mu\text{mol g}^{-1}$  (Table 4.9).

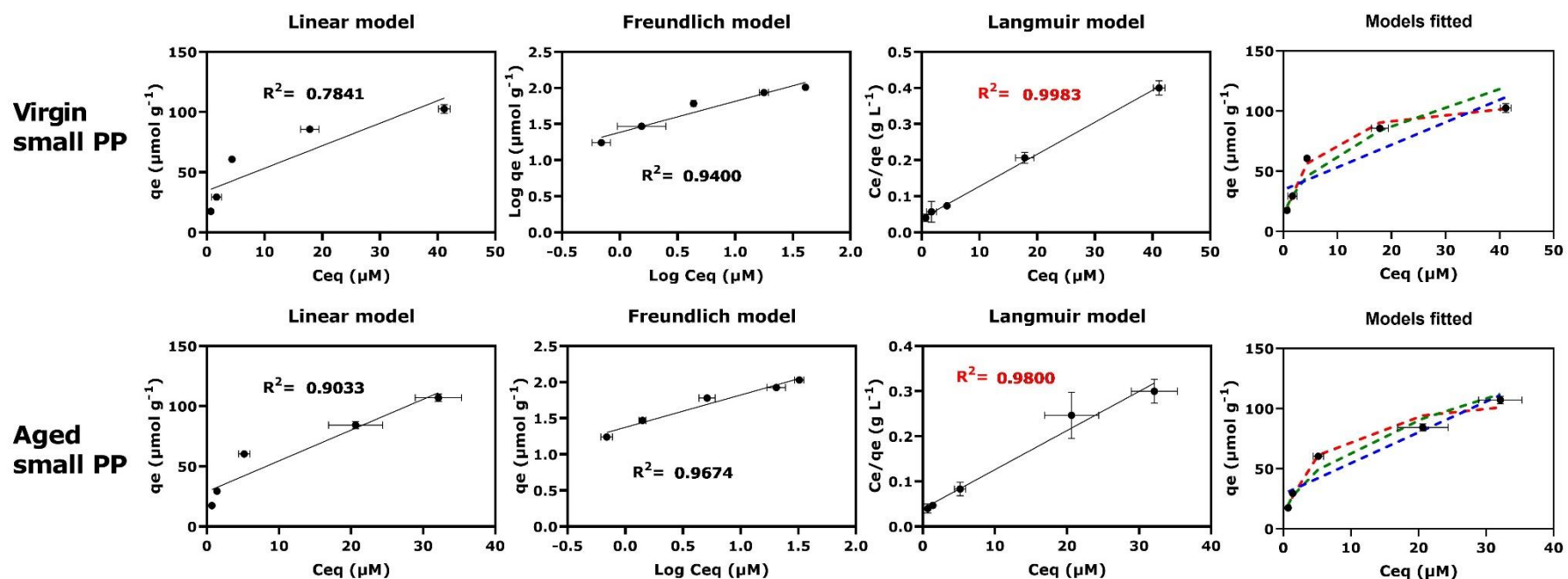


**Figure 4.13:** Application of the experimental adsorption data of virgin and artificially aged small PP in contact with fluoxetine ( $43\text{-}289\ \mu\text{M}; 15\text{-}100\ \mu\text{g mL}^{-1}$ ) to the linear forms of the linear, Freundlich, and Langmuir models. Experimental data (●) compared to the fitted curves of linear (---), Freundlich (---), and Langmuir (---) models of adsorption equilibria of fluoxetine in solution from virgin and artificially aged PP. The equilibrium concentration ( $C_e$ ) of fluoxetine loaded on small PP in artificial freshwater + 0.02% (w/v)  $\text{NaN}_3$  was considered at 24 h contact time for all initial concentrations. Highlighted in red are the correlation coefficient ( $R^2$ ) of the isotherm model that showed the best fit to the experimental data. The equations are described in Table 4.6.

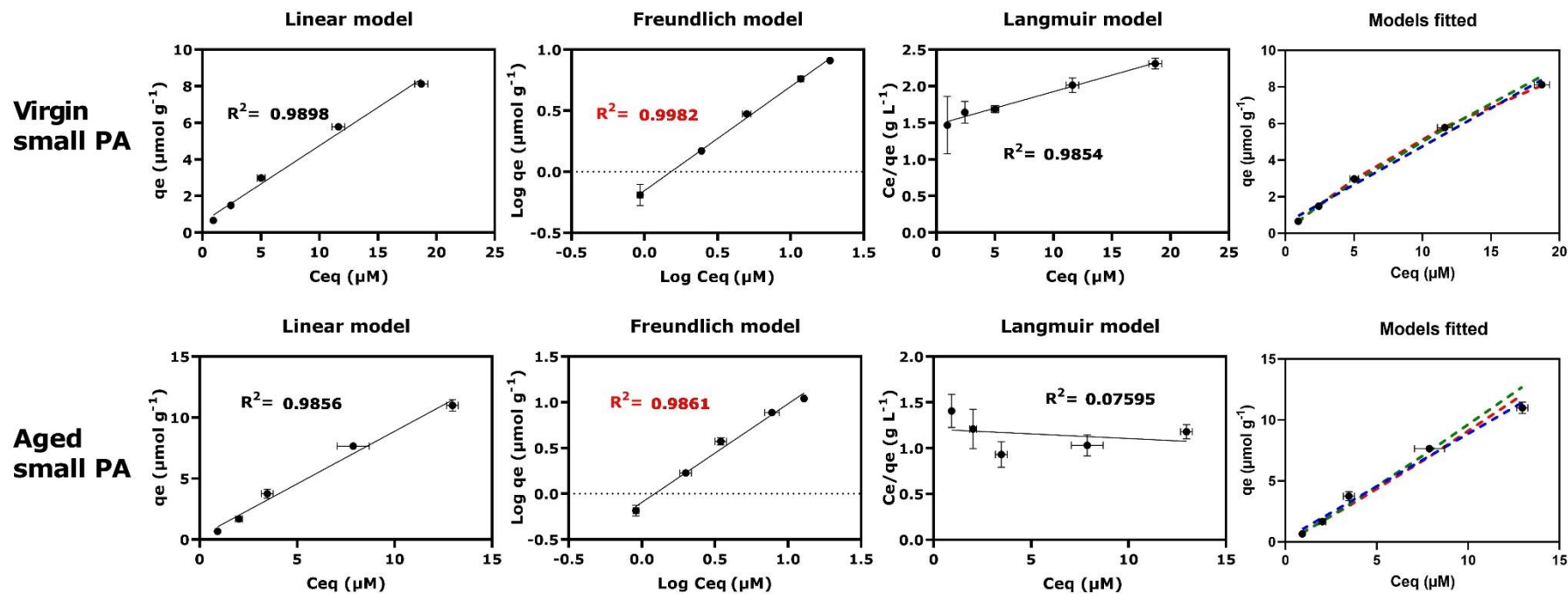


**Figure 4.14:** Application of the experimental adsorption data of virgin and artificially aged small PA in contact with fluoxetine (3-43  $\mu\text{M}$ ; 0-15  $\mu\text{g mL}^{-1}$ ) to the linear forms of the linear, Freundlich, and Langmuir models. Experimental data ( $\bullet$ ) compared to the fitted curves of linear (---), Freundlich (---), and Langmuir (---) models of adsorption equilibria of fluoxetine in solution from virgin and artificially aged PA. The equilibrium concentration ( $C_e$ ) of fluoxetine loaded on small PA in artificial freshwater + 0.02% (w/v)  $\text{NaN}_3$  was considered at 24 h contact time for all initial concentrations. Highlighted in red are the correlation coefficient ( $R^2$ ) of the isotherm model that showed the best fit to the experimental data. The equations are described in Table 4.6.

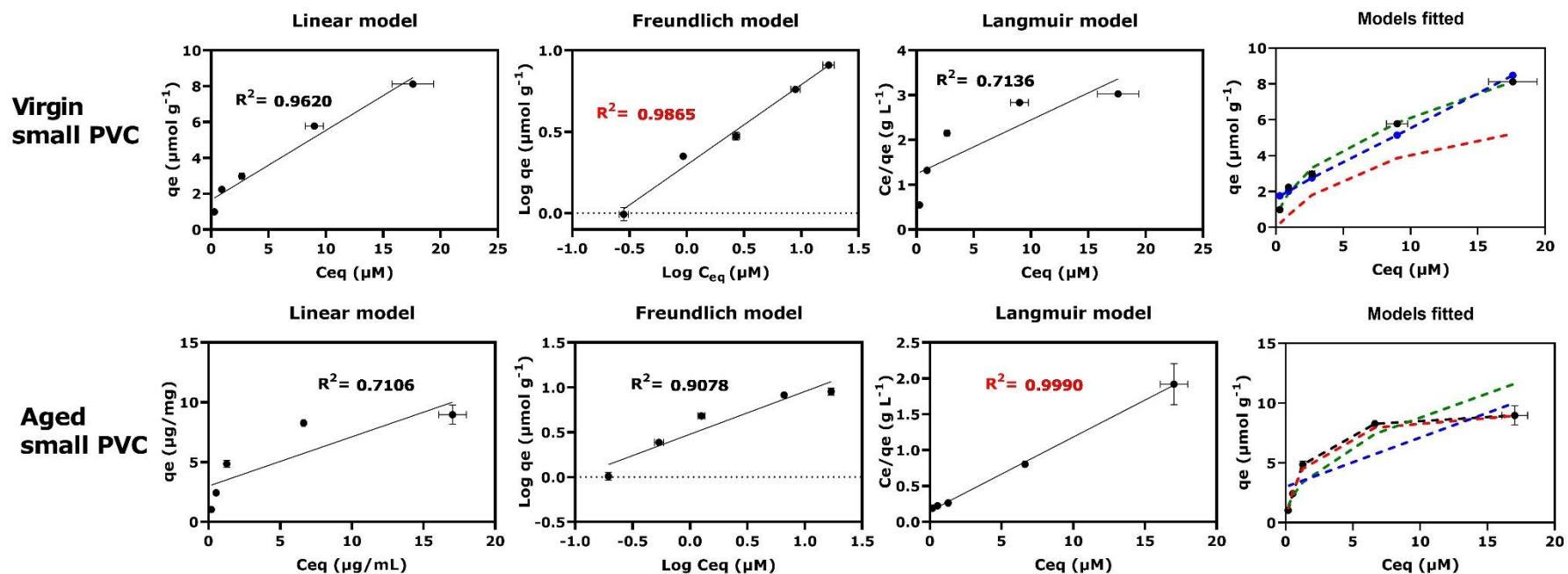


**Figure 4.15:** Application of the experimental adsorption data of virgin and artificially aged small PVC in contact with fluoxetine (3-43  $\mu\text{M}$ ; 0-15  $\mu\text{g mL}^{-1}$ ) to the linear forms of the linear, Freundlich, and Langmuir models. Experimental data ( $\bullet$ ) compared to the fitted curves of linear ( $\square$ ), Freundlich ( $\square$ ), and Langmuir ( $\square$ ) models of adsorption equilibria of fluoxetine in solution from virgin and artificially aged PVC. The equilibrium concentration ( $C_e$ ) of fluoxetine loaded on small PVC in artificial freshwater + 0.02% (w/v)  $\text{NaN}_3$  was considered at 24 h contact time for all initial concentrations. Highlighted in red are the correlation coefficient ( $R^2$ ) of the isotherm model that showed the best fit to the experimental data. The equations are described in Table 4.6.

After 24 h contact with the different concentrations of fluoxetine, the solution containing microplastics was filtered and the filter containing the retained microplastics was placed in contact with fresh media (AFW + 0.2% w/v  $\text{NaN}_3$ ) to evaluate the desorption mechanisms of fluoxetine from microplastics. Again, the desorption of fluoxetine from the microplastics varied according to the type and the weathering of the microplastics. Generally, the desorption of fluoxetine fits the linear model. Since no desorption was observed from virgin small PP, the experimental data could not be fitted to any isotherm model. Especially, the experimental data could not be fitted to the linear form of the Freundlich model, since the logarithm of negative numbers cannot be obtained. On the other hand, for the aged particles, desorption was only observed from the small PP pre exposed to higher fluoxetine concentrations such as 217 and 289  $\mu\text{M}$ , which fitted the linear model ( $R^2$  0.9643, Figure 4.16). Likewise, the experimental data fitted the linear model for both virgin and aged particles of PA (Figure 4.17). For small PA, however, fluoxetine desorbed from the microplastics spiked at all initial concentrations of fluoxetine tested (3-43  $\mu\text{M}$ ). For small PVC two different desorption mechanisms were observed when comparing virgin and aged particles. The experimental desorption data of small virgin PVC fitted to the Freundlich model ( $R^2$  0.9881), while the aged particles fit the linear model ( $R^2$  0.9958, Figure 4.18).

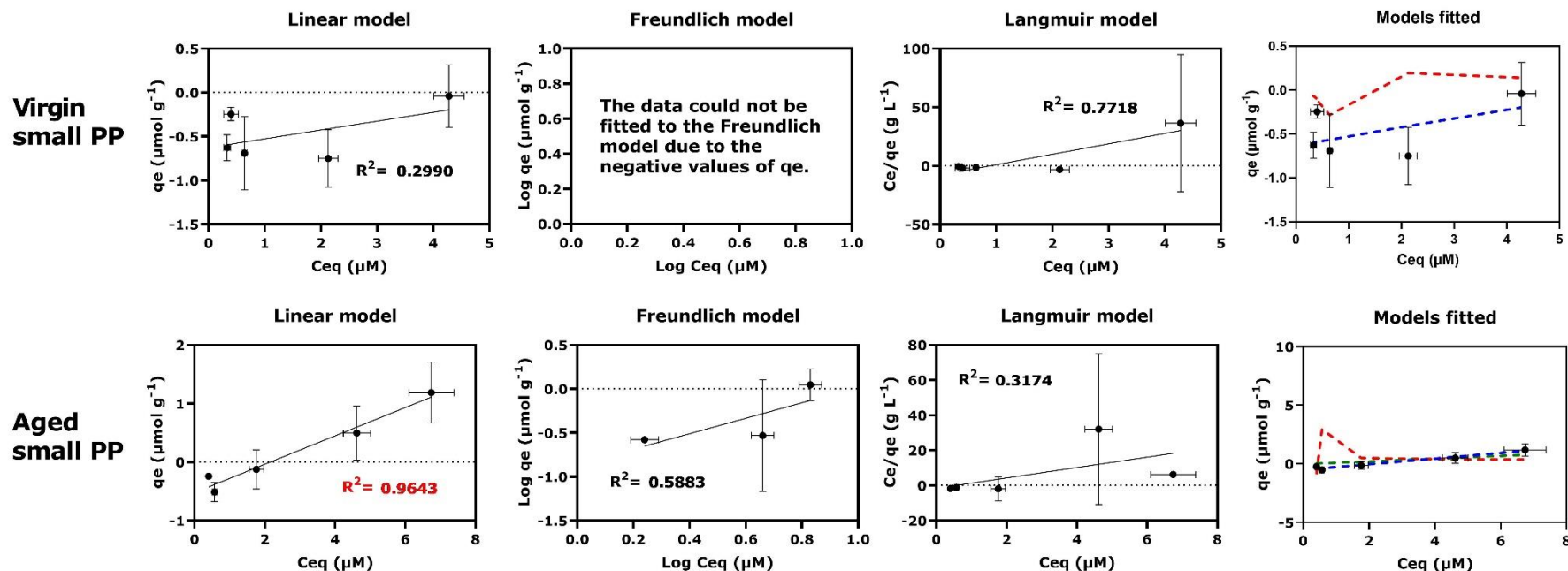


**Figure 4.16:** Application of the experimental desorption data of virgin and artificially aged small PP pre exposed to fluoxetine ( $43\text{-}289\ \mu\text{M}; 15\text{-}100\ \mu\text{g mL}^{-1}$ ) to the linear forms of the linear, Freundlich, and Langmuir models. Experimental data (●) compared to the fitted curves of linear (□□), Freundlich (□□□), and Langmuir (□□□) models of desorption equilibria of fluoxetine in solution from virgin and artificially aged PP. The equilibrium concentration ( $C_e$ ) of fluoxetine loaded on small PP in artificial freshwater + 0.02% (w/v)  $\text{NaN}_3$  was considered at 24 h contact time for all initial concentrations. Highlighted in red are the correlation coefficient ( $R^2$ ) of the isotherm model that showed the best fit to the experimental data. The equations are described in Table 4.6.



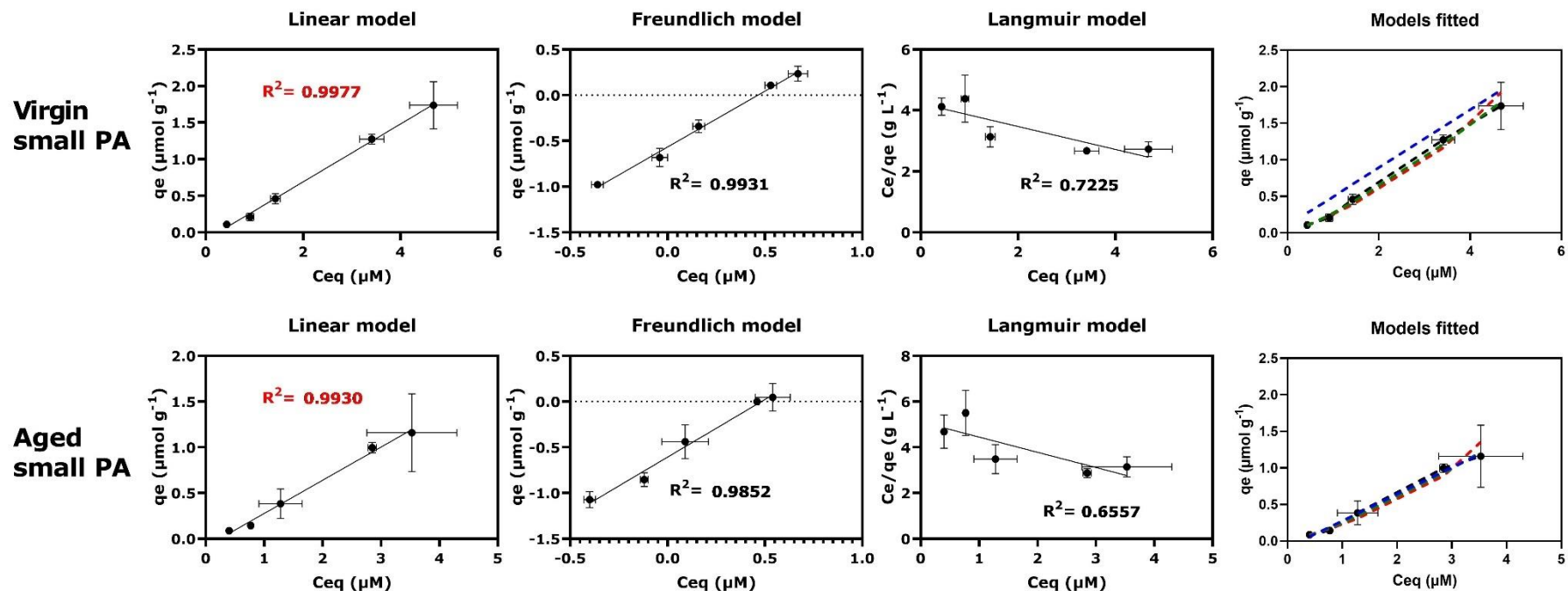


**Figure 4.17:** Application of the experimental desorption data of virgin and artificially aged small PA pre exposed to fluoxetine (3-43  $\mu\text{M}$ ; 1-15  $\mu\text{g mL}^{-1}$ ) to the linear forms of the linear, Freundlich, and Langmuir models. Experimental data (●) compared to the fitted curves of linear (---), Freundlich (---), and Langmuir (---) models of desorption equilibria of fluoxetine in solution from virgin and artificially aged PA. The equilibrium concentration ( $C_e$ ) of fluoxetine loaded on small PA in artificial freshwater + 0.02% (w/v)  $\text{NaN}_3$  was considered at 24 h contact time for all initial concentrations. Highlighted in red are the correlation coefficient ( $R^2$ ) of the isotherm model that showed the best fit to the experimental data. The equations are described in Table 4.6.

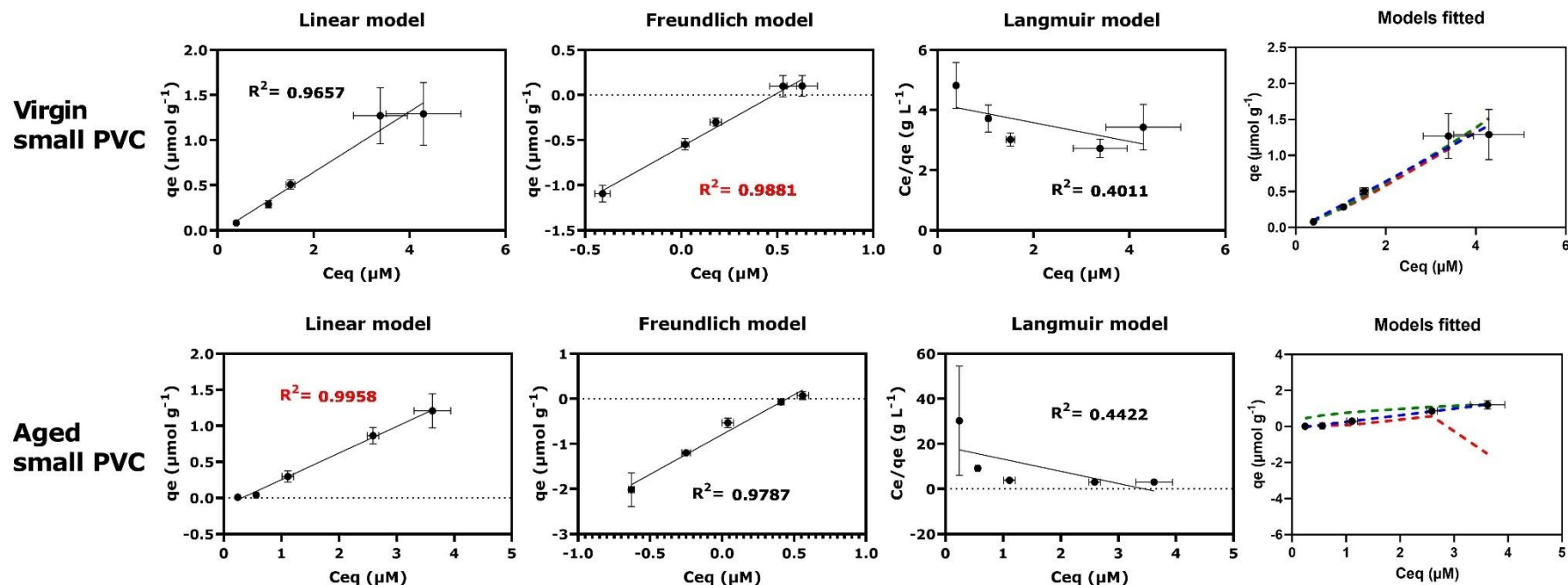


**Figure 4.18:** Application of the experimental desorption data of virgin and artificially aged small PA pre exposed to fluoxetine (3-43  $\mu\text{M}$ ; 1-15  $\mu\text{g mL}^{-1}$ ) to the linear forms of the linear, Freundlich, and Langmuir models. Experimental data (●) compared to the fitted curves of linear (---), Freundlich (---), and Langmuir (---) models of desorption equilibria of fluoxetine in solution from virgin and artificially aged PA. The equilibrium concentration ( $C_e$ ) of fluoxetine loaded on small PA in artificial freshwater + 0.02%  $\text{NaN}_3$  (w/v) was considered at 24 h contact time for all initial concentrations. Highlighted in red are the correlation coefficient ( $R^2$ ) of the isotherm model that showed the best fit to the experimental data. The equations are described in Table 4.6.

**Table 4.9:** Summary of the adsorption and desorption parameters of the linear, Freundlich, and Langmuir models. The parameters include the partition coefficient ( $K_p$ ), Freundlich coefficient ( $K_F$ ), Freundlich exponent ( $1/n$ ), Langmuir coefficient ( $K_L$ ), energy of adsorption ( $\alpha_L$ ), maximum adsorption capacity ( $Q_0$ ), and the correlation coefficient ( $R^2$ ).

Isotherm model	Plastic	Adsorption Parameters				Desorption Parameters			
		$K_p$ ( $L g^{-1}$ )			$R^2$	$K_p$ ( $L g^{-1}$ )			$R^2$
Linear	PP <sub>VIRGIN</sub>	34.51			0.7841	-0.63			0.299
	PP <sub>AGED</sub>	28.96			0.9033	-0.52			0.9643
	PA <sub>VIRGIN</sub>	0.57			0.9898	-0.1			0.9977
	PA <sub>AGED</sub>	0.25			0.9856	-0.09			0.993
	PVC <sub>VIRGIN</sub>	1.65			0.962	-0.03			0.9657
	PVC <sub>AGED</sub>	2.99			0.7106	-0.12			0.9958
Freundlich		$K_F$ ( $L g^{-1}$ )	$n$		$R^2$	$K_F$ ( $L g^{-1}$ )	$n$		$R^2$
	PP <sub>VIRGIN</sub>	24.27			0.94	-	-		-
	PP <sub>AGED</sub>	23.66	0.449		0.9674	0.09	1.121		0.5883
	PA <sub>VIRGIN</sub>	0.71	0.853		0.9982	0.27	1.222		0.9931
	PA <sub>AGED</sub>	0.8	1.077		0.9861	0.25	1.26		0.9852
	PVC <sub>VIRGIN</sub>	1.98	0.493		0.9865	0.27	1.187		0.9881
PVC <sub>AGED</sub>	3.01	0.477		0.9078	0.77	0.369		0.9787	
Langmuir		$K_L$ ( $L g^{-1}$ )	$\alpha_L$ ( $L g^{-1}$ )	$Q_0$ ( $\mu mol g^{-1}$ )	$R^2$	$K_L$ ( $L g^{-1}$ )	$\alpha_L$ ( $L g^{-1}$ )	$Q_0$ ( $\mu mol g^{-1}$ )	$R^2$
	PP <sub>VIRGIN</sub>	25.83	0.229	112.71	0.9983	-0.13	-1.122	0.11	0.7718
	PP <sub>AGED</sub>	25.51	0.221	115.27	0.98	-0.6	-1.765	0.34	0.3174
	PA <sub>VIRGIN</sub>	0.68	0.031	22.22	0.9854	0.24	-0.089	-2.66	0.7225
	PA <sub>AGED</sub>	0.83	-0.008	-98.81	0.0759	0.2	-0.13	-1.5	0.6557
	PVC <sub>VIRGIN</sub>	0.81	0.097	8.29	0.7136	0.24	-0.074	-3.21	0.4011
PVC <sub>AGED</sub>	6.66	0.687	9.69	0.999	0.06	-0.283	-0.21	0.4422	

The adsorption of fluoxetine onto the microplastics investigated followed the following order: PP > PA > PVC. For all initial concentrations, fluoxetine presented similar adsorption amounts onto virgin and aged small PP (Figure 4.19). In general, the greater the amount adsorbed onto the microplastics, the greater the amount desorbed from the microplastics.

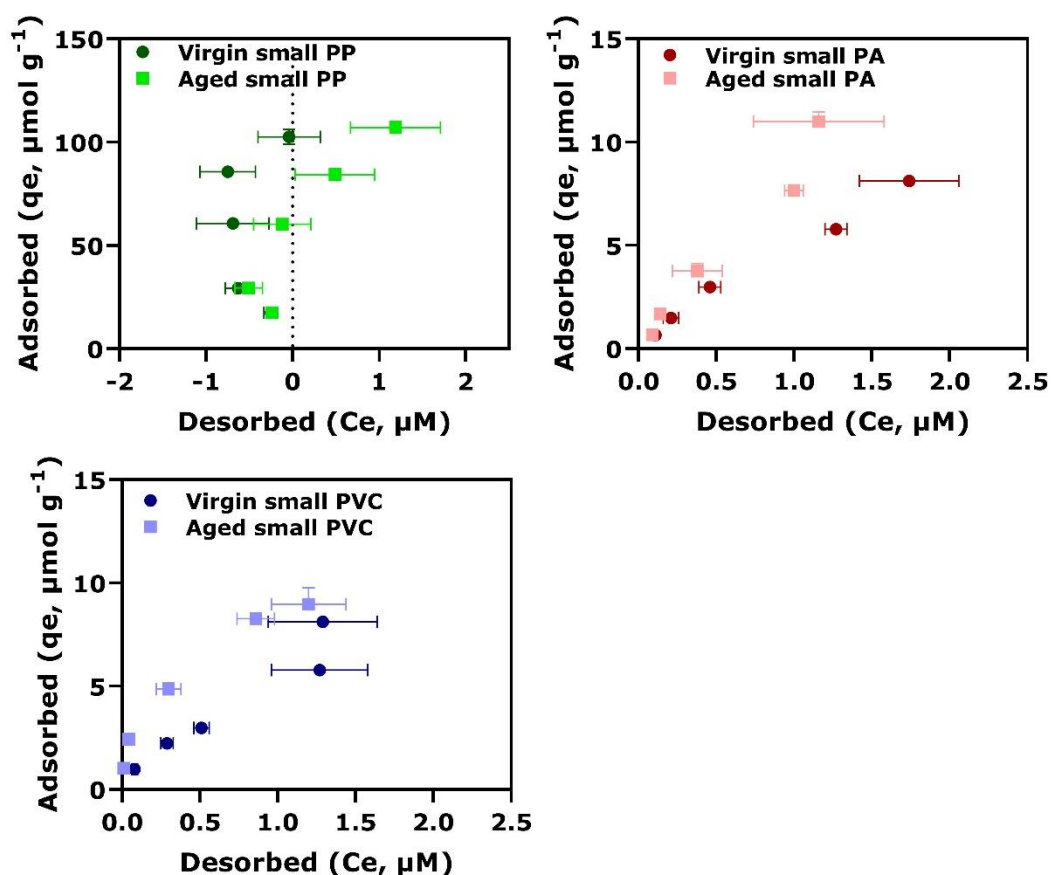


**Figure 4.19:** Comparison between the amount adsorbed onto microplastics and the amount desorbed from the microplastics at the five different fluoxetine initial concentrations (PP: 43-269  $\mu\text{M}$ , 15-100  $\mu\text{g mL}^{-1}$ ; PA and PVC: 3-43  $\mu\text{M}$ , 1-15  $\mu\text{g mL}^{-1}$ ).

Proportionally, a larger percentage of the amount adsorbed onto microplastics desorbed from the virgin particles (Figure 4.20). For the aged particles of small PVC, there is a clear correlation between the initial concentration (3-43  $\mu\text{M}$ ) of fluoxetine pre-exposed to small PVC microplastics and the percentage desorption from microplastics (1-13%). There is a similar amount of desorption from small,

aged PP compared to PA and PVC at higher fluoxetine initial concentrations (Figure 4.19). However, proportionally, the amount desorbed from small, aged PP is approximately 1% of the amount adsorbed onto the particles.

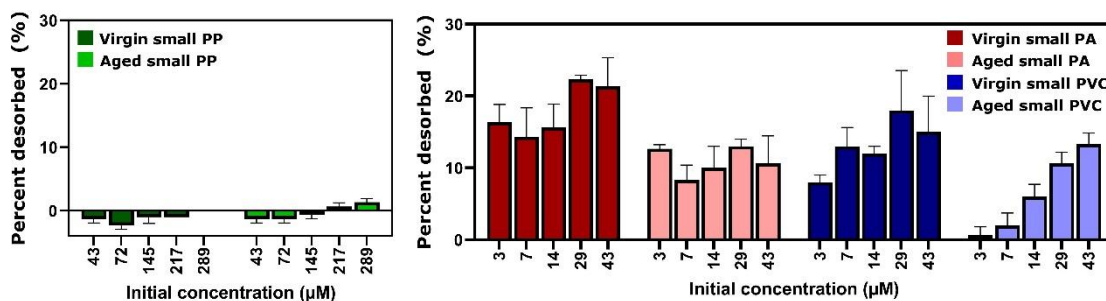


**Figure 4.20:** Percentage of the amount adsorbed onto virgin and artificially small, aged particles of PA, PVC, and PP that desorbed from the particles per initial concentration of fluoxetine. To calculate the percentage desorption the concentration of fluoxetine desorbed from the particles was divided by the concentration adsorbed onto the microplastics. Note: The negatives values of virgin small PP are due to the greater concentration of fluoxetine in the control solution (filter without microplastics) compared to the concentration of fluoxetine in the solution with filtered microplastics. For the aged PP, fluoxetine was only detected in greater concentrations in the solutions containing aged PP pre exposed to fluoxetine at concentrations of 217 μM (75 μg mL<sup>-1</sup>) and 289 μM (100 μg mL<sup>-1</sup>) comparing to the control solutions.

#### 4.4 Conclusion and environmental implications

The interaction of a mixture of pharmaceuticals in contact with virgin and aged particles of six microplastic types was investigated. The adsorption and desorption mechanisms involving three microplastic types was also evaluated. The weathering of the microplastics, the polymer composition of the microplastics, and the pharmaceutical properties were the key factors affecting the adsorption of pharmaceuticals onto microplastics. The results have clearly demonstrated the considerable potential of microplastics to adsorb micropollutants and potentially act as a vector in aquatic environments, especially oxidised microplastics following UV and visible light exposure. This is especially pertinent given that fluoxetine adsorbed onto the particles was bioavailable when desorbed from small PA and PVC. Furthermore, small particles

of PP, a plastic type most widely used for single-use purposes and the microplastic type most commonly reported in the environment, adsorbed all the pharmaceuticals investigated in both its virgin and aged state, notwithstanding the fact that the small, virgin PP contained a component which possessed a carbonyl functional group which influenced the adsorption. The fact that fluoxetine did not desorb from the particles of PP in artificial freshwater at 25°C, shows that in the environment, small PP particles can be fully loaded with fluoxetine when ingested by wildlife, which might increase the fluoxetine-loaded PP potential toxic effect to aquatic organisms within the time frame studied. Furthermore, hydrophobic and positively charged compounds such as fluoxetine displayed greater adsorption by microplastics when compared to hydrophilic and negatively charged compounds. Concerningly, among the pharmaceuticals investigated, fluoxetine has also been reported to have the greatest ecotoxicological effects on aquatic organisms, such as the water quality indicator organism *Daphnia magna*.

Most studies on the adsorption of aquatic pollutants onto microplastics have used virgin microplastics. However, microplastics acquired commercially might not be representative of what is encountered in the environment, especially when using perfect spherically shaped microplastics which only represent 14% of the microplastic type reported in the freshwater environment (Koelmans et al. 2019). In the current study, a wide range of microplastic types with different sizes and shapes were evaluated to achieve a better representation of the microplastic found in the aquatic environment. However, simulating the type of physico-chemical and biological processes particles undergo when in the environment is a challenge. Artificially aging microplastics is a multifactorial process. The degree

of weathering of polymers depends on the type and the intensity of light sources, the presence/absence of water and the ambient temperature. Particles have been aged in the laboratory using a variety of light sources, radiation intensities, and exposure times. The most commonly used types of light sources to age microplastics, to date, are UV-based (UV-A, -B, and -C, 100-400 nm, Almond et al., 2020; Fan et al., 2021; Liu et al., 2019; Mylläri et al., 2015; J. Wu et al., 2020). However, in sunlight, UV light only accounts for a small portion (~10%) when compared to the high amount of visible light (Liu et al. 2021). For these reasons, a combination of UV and visible light sources such as xenon arc lamps with appropriate filters might be a better representation of microplastics exposure to sunlight.

The pharmaceuticals investigated in this study have high prescription rates globally and low biodegradability in the environment. They are also widely reported in the freshwater environment (Fekadu et al. 2019). Micropollutants such as pharmaceuticals are often detected as a mixture in freshwater systems (Ebele, Abou-Elwafa Abdallah and Harrad 2017). The majority of adsorption studies to date only evaluated individual compounds in contact with microplastics. Although it is important to understand how organic micropollutants interact individually with microplastics, this approach does not consider potential intramolecular adsorption competition as observed by Moura et al. (2022). Hydrophobic organic compounds, such as fluoxetine, are readily adsorbed onto microplastics when in a mixture of less hydrophobic compounds, as confirmed by the current study. Although environmentally representative concentrations were not used in this particular study, this is still worrisome as a positive correlation between hydrophobicity and an organic compounds toxicity has been reported

(Fischer et al. 2010b). Among the pharmaceuticals evaluated, fluoxetine has been shown to be the most toxic to *Daphnia magna*. Fluoxetine at concentration as low as 0.82  $\mu\text{g mL}^{-1}$  has resulted in toxic effects on *D. magna* (Brooks et al. 2003). However, there is a knowledge gap on how microplastics pre-exposed to organic compounds affect aquatic organisms such as *D. magna*. Moreover, how different microplastic types and weathering of the microplastics would affect the ecotoxicity of these particles.



# **Chapter 5**

## **Ecotoxicity of microplastic particles and pollutant-loaded microplastic particles to *Daphnia magna***

<b>5 ECOTOXICITY OF MICROPLASTIC PARTICLES AND POLLUTANT-LOADED MICROPLASTIC PARTICLES TO DAPHNIA MAGNA .....</b>	<b>202</b>
<b>5.1 Introduction .....</b>	<b>204</b>
5.1.1 Ingestion of microplastics.....	204
5.1.2 Ecotoxic evaluation .....	205
5.1.3 Selection of test parameters of the ecotoxicity test.....	206
5.1.4 Chapter aim and objectives .....	209
<b>5.2 Materials and methods.....</b>	<b>210</b>
5.2.1 Microplastics .....	210
5.2.2 Test organisms and test parameters .....	211
5.2.3 Experimental set-up .....	215
5.2.4 Visualisation of the neonates and capture of images .....	218
5.2.5 Quantification of fluoxetine in the solution .....	219
5.2.6 Statistical analysis .....	220
<b>5.3 Results and discussion.....</b>	<b>221</b>
5.3.1 Effect of the protocol and fluoxetine controls on the survival of <i>D. magna</i> neonates .....	221
5.3.2 Evaluation of the effects of ingestion of microplastics by <i>D. magna</i> neonates .....	224
5.3.3 Effect of fluoxetine-loaded microplastics on the survival of <i>D. magna</i> neonates .....	229
<b>5.4 Conclusions and environmental impact.....</b>	<b>233</b>

## **5.1 Introduction**

### **5.1.1 Ingestion of microplastics**

Microplastics are widely detected in the environment. The ingestion of plastic particles by wildlife is expected when they are present in prey species or co-occur in the environment. A variety of animals from all trophic levels in the food web have been reported to ingest microplastics. For instance, five groups of zooplankton, copepods, chaetognaths, jellyfish, shrimp, and fish larvae, collected from the northern South China Sea were found to have ingested microplastics, mainly polyester (Sun et al. 2017). Microplastics were found in the gastrointestinal tract of three fish species (317 individuals) from the South-Eastern Black Sea coast of Turkey (Eryaşar, Gedik and Mutlu 2022). Fibres (49%) and fragments (42%) were the most common microplastic shapes in these fish. Furthermore, PP (35%), PE (23%), PET (15%), and PA (12%) were the microplastic types most commonly detected by the study (Eryaşar, Gedik and Mutlu 2022). The most recent assessment of plastic particles in fulmar (seabird) stomachs, published in 2022, shows that currently 51% of beached North Sea fulmars have more than 0.1 g of plastics in their stomachs, exceeding the Fulmar Threshold Value of 10% (OSPAR commission 2023). Microplastics were also found in the stomach and intestines of stranded, bycaught, or mercy-killed seals found at the coast of the federal state of Schleswig-Holstein in Germany (Philipp, Unger and Siebert 2022). Microplastics have also been detected in human organs (Horvatits et al. 2022) and placenta (Ragusa et al. 2021). In March of 2022, for the first time, microplastics were detected in the blood of four volunteers in a study of 22 adults conducted in the Netherlands (Leslie et al. 2022).

### 5.1.2 Ecotoxic evaluation

Although the ingestion of microplastics is a reality, the impact of the ingestion of microplastics on wildlife and human health is undetermined. Studies have investigated how the ingestion of microplastic can have an effect on food uptake, mobility, and survival of various organisms (Aiguo et al. 2022; Gong et al. 2022). However, the study of vertebrates for scientific purposes poses difficulties, including ethical issues. For this reason, the zooplankton *Daphnia sp.* (crustacea) has been widely used in the research field to evaluate how compounds can impact wildlife (Horton et al. 2018; Nkoom et al. 2019; Lee et al. 2021). *Daphnia sp.*, more specifically *D. magna*, is the most commonly used organism in the study and control of water quality, and is also a sensitive freshwater organism, i.e., a water quality indicator organism (Villegas-Navarro et al. 1999). *D. magna* was found to be a sensitive and useful parameter for detecting water quality changes and how these alter the function of keystone organisms (Jeong and Simpson 2019).

Many toxicity studies detail analyses of *D. magna* behavioural and physiological properties especially and its sensitivity to toxicants. Its ease of culture and handling make this species the most preferred model daphnid used in ecotoxicological investigations (Tkaczyk et al. 2021). However, there is no standardised procedure to evaluate the toxic effect of microplastics on *D. magna*. The Organisation for Economic Co-operation and Development (OECD) guideline for testing of chemicals, '*Daphnia sp.*, acute immobilisation test' (OECD 202), '*D. magna* reproduction test' (OECD 211), and the International Standard ISO 6341:2012, 'Determination of the inhibition of the mobility of *Daphnia magna* Straus (Cladocera, Crustacea) — Acute toxicity test' are widely used as reference

guidelines for the investigation of chemicals when in contact with *Daphnia sp.*, especially, *D. magna*. However, these guidelines have been adapted to permit the investigation of the consequences of the exposure of *D. magna* to other water pollutants such as microplastics. In general, the test conditions recommended by the three guidelines overlap. The three guidelines recommend *D. magna* neonates (less than 24 h old) as the test organism. The guidelines also state that the use of first brood should be avoided due to potential bias introduced by previous unknown culture conditions.

The culture of *D. magna* should be performed at 18-22 °C with a 16:8 h light: dark photoperiod. The media containing *D. magna* should not be aerated, since the neonates can get trapped in the water bubbles. The diet of the parent animals should preferably be living algal cells between 0.1 and 0.2 mg carbon *Daphnia*<sup>-1</sup> day<sup>-1</sup>.

### **5.1.3 Selection of test parameters of the ecotoxicity test**

A variety of parameters must be considered when investigating the interaction of *Daphnia sp.* with microplastics. The microplastic type, the particle size, the degree of weathering of the microplastics, the particle shape, and the microplastic concentration are the main variables when considering the properties of the microplastic exposed to *D. magna*. Moreover, which species of the *Daphnia sp.*, the type of food, the dietary regime, the age of the organism, the culture medium, and the exposure time to microplastics are key variables when evaluating the toxic effect of microplastics to daphnids. For all guidelines (OCDE 202, 211 and ISO 6341:2012), the recommendation is to use the neonates, which are less than 24 h old organisms. However, daphnids from

neonates to 18 day old *D. magna* have been used as test organisms (Table 5.1). The use of adult organisms is understandable since adult *D. magna* can represent the organisms found in the aquatic environment. Furthermore, adult *D. magna* are more likely to ingest larger microplastics. As discussed in chapter 2, commercially acquiring microplastics of a particle size that can be ingested by neonates can be a challenge.

Seven toxicity studies using *D. magna* exposed to microplastics published in the past five years (2018 and end 2022) and that are highly cited (over 200 citations, Table 5.1) were selected to assess their study parameters and support the selections in the current study. In the selected scientific literature, the exposure time of *D. magna* to microplastics can vary from 12 min (Ogonowski et al. 2016) to 21 days (OECD 211 recommendation, Zimmermann et al. 2020; Schwarzer et al. 2022). The organisms can be fed either prior to the experiment (Xiang et al. 2022) or during the experiment (especially when *D. magna* are exposed to microplastics for longer periods of time). *Chlorella vulgaris*, a unicellular green microalga, is widely used to feed these organisms on a daily basis (Table 5.1). However, yeast and spirulina cells can also be used as a food source (Canniff and Hoang 2018). *D. magna* can be obtained from different sources, from natural ponds (Aljaibachi et al. 2019), commercially acquired organisms to be cultured and reproduced in laboratory (Zimmermann et al. 2020) to dormant eggs (Nielsen and Roslev 2018).

**Table 5.1:** Selection of studies that exposed *D. magna* to microplastics. The microplastic type, the particle size (as stated by the authors), the food source, diet regime, the *D. magna* age, the exposure time, and the microplastics concentration studied were evaluated.

Plastic	Size	Diet	Daphnia age	Exposure	Microplastic concentration	Reference
PE beads	63-75 µm	Fed daily <i>Raphidocelis subcapitata</i> (green algae) and yeast	7 days old	5 days	100 mg L <sup>-1</sup>	Canniff and Hoang (2018)
PE beads fragments	Beads: ~39.54 µm Fragments: ~34.43 µm & ~17.23 µm	Fed daily <i>Chlorella vulgaris</i> (green algae)	4 days old	21 days	5 mg L <sup>-1</sup>	An et al. (2021)
PE beads fragments	Spherical: ~4.1 µm Fragments: ~2.6 µm	Fed every other day <i>Raphidocelis subcapitata</i> (green algae)	Neonates (< 24 h old)	12 min to 21 days	100 – 10,000 particles mL <sup>-1</sup>	Ogonowski et al. (2016)
PS bead	2 µm	Fed every other day yeast and <i>Chlorella vulgaris</i> (green algae)	18 days old	21 days	100 – 800 particles mL <sup>-1</sup>	Aljaibachi and Callaghan (2018)
PS	Spheres: 6 and 20 µm Fragments: 5.7 and 18 µm Fibres: length: D <sub>90</sub> : 75 µm	Fed daily <i>Scenedesmus obliquus</i> (green algae)	Adult (1 <sup>st</sup> and 2 <sup>nd</sup> brood removed)	21 days	500 and 5,000 particles mL <sup>-1</sup>	Schwarzer et al. (2022)
PS beads	1 µm	Fed prior to experimentation <i>Chlorella pyrenoidosa</i> (green algae)	Neonates (< 24 h old)	10 h	5 mg L <sup>-1</sup>	Xiang et al. (2022)
Polyurethane (PUR), PVC, and polylactic acid (PLA) fragments	PVC: ~20 µm PUR and PLA: ~40 µm	Fed daily <i>Desmodesmus subspicatus</i> (green algae)	Neonates (< 24 h old)	21 days	10, 50, 100 and 500 mg L <sup>-1</sup>	Zimmermann et al. (2020)
Virgin and aged: PP PA PVC	PP: 4-23 µm (D <sub>50</sub> 8 µm) PA: 1-105 µm (D <sub>50</sub> 33 µm) PVC: (1) 0.04-0.3 µm (D <sub>50</sub> 0.11 µm) (2) 0.5-4 µm (D <sub>50</sub> 1.3 µm)	Fed 2 h prior to experimentation <i>Spirulina</i> (biomass from cyanobacteria)	Neonates (< 24 h old)	48 h	50 and 100 mg L <sup>-1</sup>	This study

For the experiments described in this chapter, *D. magna* neonates were selected as test organisms. Neonates of *D. magna* are the test organisms recommended by all guidelines for toxicity tests with *D. magna*, therefore it makes it easier to compare the results with that in the literature. Further, neonates are generally more sensitive to environmental stressors and toxic substances than adults (Wagner, Simpson and Simpson 2017), due to their smaller size and less-developed physiological systems, which make them more susceptible to chemical exposure. Finally, neonates are relatively uniform in terms of age, size, and physiological condition. This uniformity allows for greater control and reproducibility in experimental setups.

In the current study, the neonates were fed once prior to experimentation to avoid death of the organisms due to starvation. Aljaibachi and Callaghan (2018) demonstrated a negative impact on the uptake of PS beads by 18 day old *D. magna* when co-occurring with algae (food source). However, to evaluate the impact of microplastic loaded with micropollutants on *D. magna* neonate mobility and survival, the ingestion of the microplastics by the neonates is essential. Thus, *D. magna* neonates were not fed during the exposure (48 h) to encourage uptake of microplastic particles. The size of the particles selected in this thesis are similar or smaller than the reported size ingested by *D. magna* neonates.

#### **5.1.4 Chapter aim and objectives**

The ingestion of microplastics by wildlife has been widely reported, as well as the adsorption of co-occurring micropollutants in freshwater onto microplastics. The aim of this chapter is to investigate whether microplastics can act as a vector for micropollutants when co-existing in the environment, and subsequently have a



toxic effect on aquatic wildlife (Figure 5.1). This was achieved through the following objectives:

- 1) Determine the optimal test organism and test parameters
- 2) Evaluate whether the exposure of different microplastic types and microplastic weathering have an impact on the mobility and survival of *Daphnia magna* when exposed to these particles for 24 h and 48 h.
- 3) Evaluate the effect of the pharmaceutical fluoxetine on *D. magna*, both in solution and loaded onto different microplastic types and microplastic weathering in different microplastic concentrations for 24 h and 48 h.

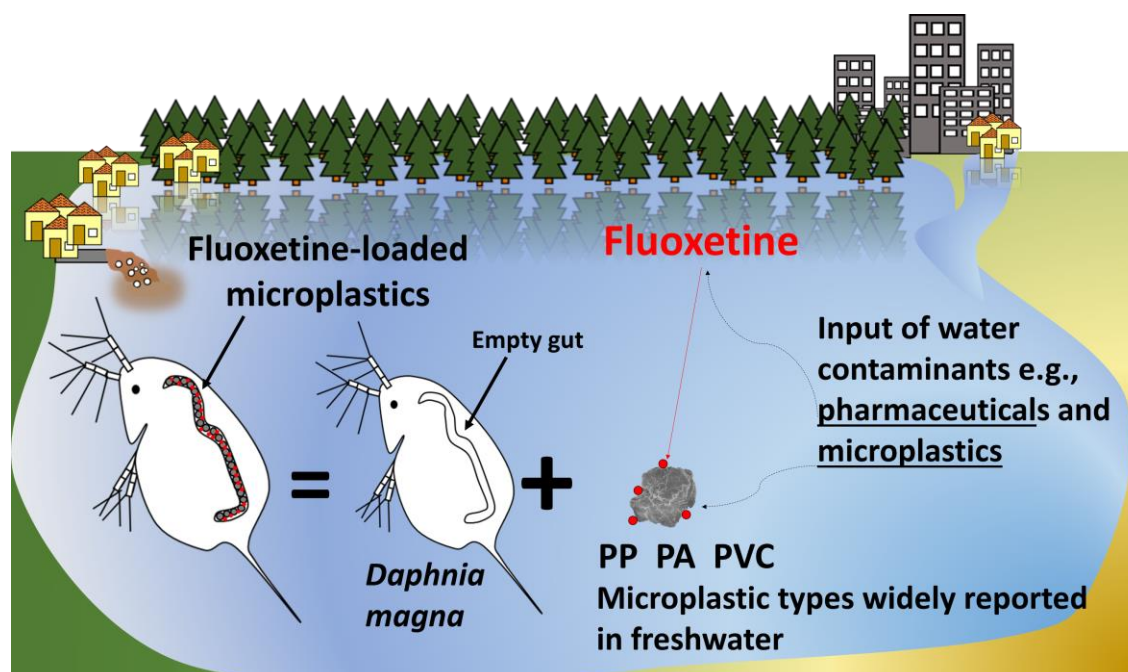


**Figure 5.1:** Interaction of the antidepressant fluoxetine with microplastic types widely detected in freshwater, and which can potentially enter the food web when loaded onto microplastics ingested by wildlife.

## 5.2 Materials and methods

### 5.2.1 Microplastics

Fluoxetine-loaded small, virgin PP ( $D_{50}$  8  $\mu\text{m}$ ) was selected to perform a proof of principle ecotoxicity test. Later, a second experiment was performed to

investigate the ecotoxicity of aged particles of PP and the virgin and aged particles of small PA ( $D_{50}$  33  $\mu\text{m}$ ) and small PVC ( $D_{50 (1)}$  0.11  $\mu\text{m}$ ,  $D_{50 (2)}$  1.3  $\mu\text{m}$ ) pre exposed to fluoxetine to *D. magna*. These microplastic types were selected due to their adsorption capacity in both their virgin and aged state as demonstrated in previous chapters. Furthermore, *D. magna* neonates have been reported to ingest microplastics at a similar or greater size than the particle size of small PP, PA, and PVC reported above (Zimmermann et al. 2020, Table 5.1).

### **5.2.2 Test organisms and test parameters**

To evaluate whether fluoxetine-loaded microplastics can act as a vector for fluoxetine into the food web, an ecotoxicity experiment with *Daphnia magna* neonates was performed using a Daphtoxkit F (Microbiotest, BE). The operational procedure of the Daphtoxkit F magna assay is identical to the test methodology described by the guidelines, ISO 6341 (2012) and OCDE 202 (2004), for acute testing with this crustacean test species, with the exception that the test organisms are obtained by hatching of dormant eggs, instead of being taken from laboratory stock cultures. Cryptobiotic eggs are produced by *D. magna* in nature and occasionally also occur in laboratory cultures under specific environmental conditions. These eggs, resulting from sexual reproduction, are encapsulated in a protective carapace called an ephippium, and can remain 'dormant' (and viable) for many years. Only when triggered by specific stimuli does the embryonic development resume and culminate in the hatching of neonates (Persoone et al. 2009).

The experimental media consisted of artificial freshwater (AFW), which was prepared with ultrapure water (18.2 M $\Omega$ ) and the addition of CaCl<sub>2</sub>·2H<sub>2</sub>O (294 mg L<sup>-1</sup>), MgSO<sub>4</sub>·7H<sub>2</sub>O (123.25 mg L<sup>-1</sup>), NaHCO<sub>3</sub> (64.75 mg L<sup>-1</sup>), and KCl (5.75 mg L<sup>-1</sup>) according to the kit manual. The pH of the media was determined as 8. The media was constantly sparged with sterile air for 15 min before use for both hatching the dormant eggs and to prepare the solutions used in this experiment. The ephippia were poured into a microsieve, rinsed with tap water, and transferred to a petri dish with 15 mL pre-aerated AFW. The covered petri dish was incubated for 72 h at 20 °C under continuous illumination of approximately 6,000 lux (Figure 5.2). To assure the light intensity, the cool white fluorescence lamp irradiation was measured using a StellarNet spectrometer (BLACK-Comet C-RS-50 model, USA, Figure 5.3).

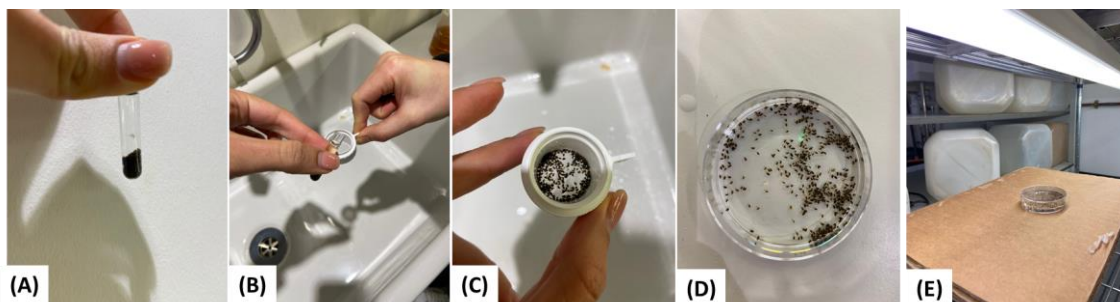


**Figure 5.2:** Hatching procedure for the Daphtoxkit (A) vial containing ephippia, (B) pouring ephippia into the microsieve, (C) rinsing the ephippia with tap water, (D) ephippia in 15 mL pre-aerated artificial freshwater pH 8, (E) hatching the ephippia for 72 h at 20 °C under 6,000 lux.

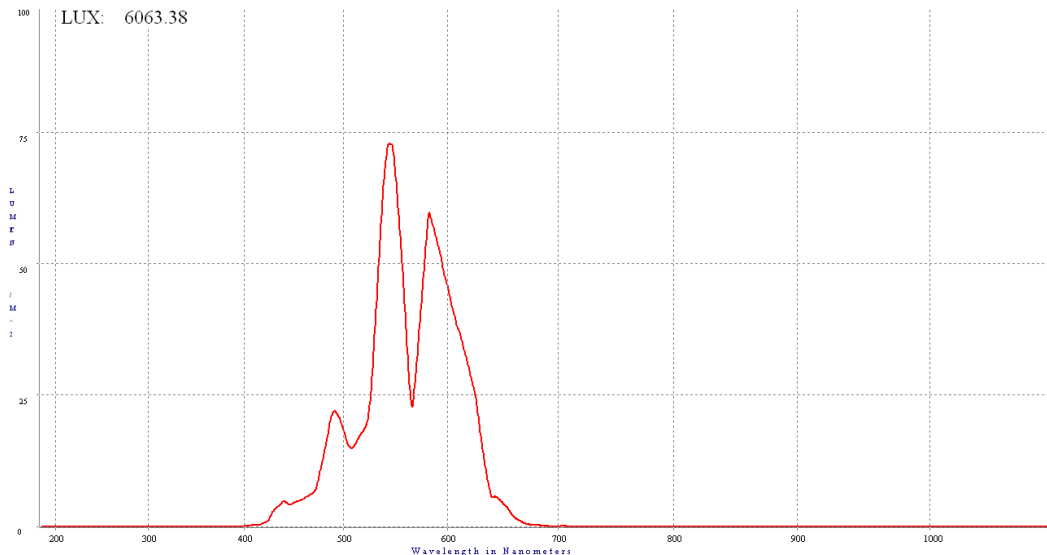


**Figure 5.3:** Light spectrum and intensity of the light measured by the StellarNet which the *D. magna* ehippia were exposed to for 72 h at 20 °C during the hatching process.

Two hours prior to collecting the neonates for the experiment, a suspension of spirulina was poured into the hatching petri dish (Figure 5.4 and Figure 5.5). This food uptake provides the neonates with an energetic reserve and precludes mortality by starvation (which would bias the test results) during the subsequent 48 h test exposure during which the organisms are not fed.



**Figure 5.4:** Pre-feeding of the *D. magna* neonates, which consisted of a vial containing spirulina powder provided by Daphtoxkit that was dissolved in the media and poured into the hatching dish two hours prior to collecting the neonates.

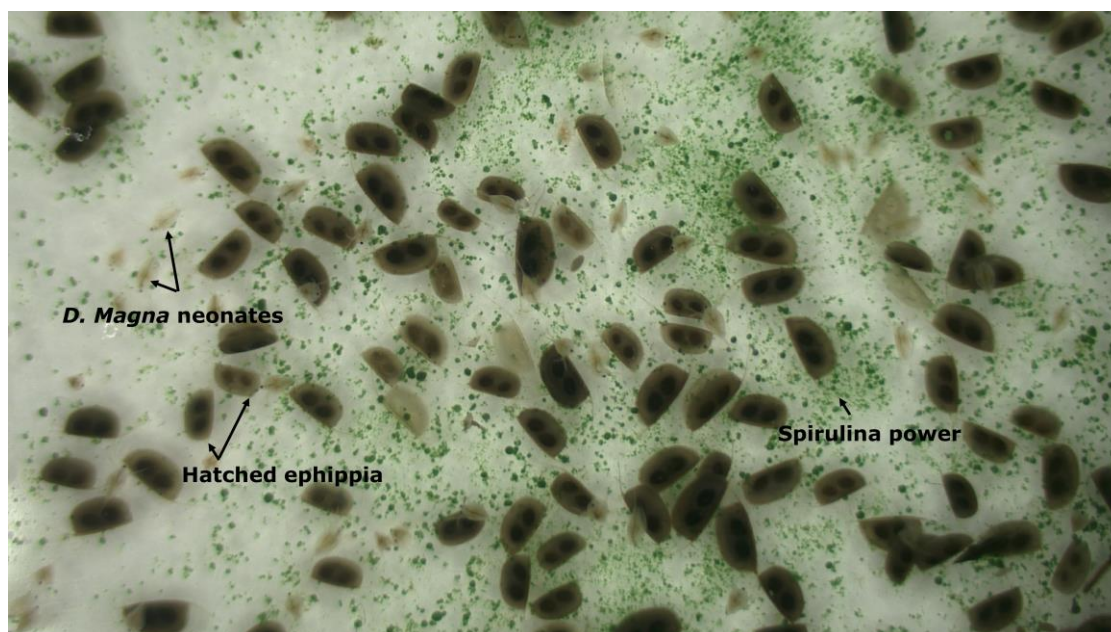


**Figure 5.5:** Hatched petri dish after 2 h pre-feeding with spirulina power. The arrows point to the neonates, the hatched ephippia, and the spirulina power (green). The blurriness of neonates was caused by the motility of the organisms.

A polystyrene (PS) multiwell plate was provided by the supplier as a neonate incubator. However, as demonstrated by this study, fluoxetine can adsorb onto the surface of plastics, which can interfere with the fluoxetine concentrations throughout the experiment. For each treatment, instead of using a PS multiwell plate, the experimental incubator consisted of four 20 mL glass vials, grouped in a 400 mL beaker covered with a PS petri dish lid to avoid cross contamination of potential volatile compounds during the experiment (Figure 5.6) and to limit evaporation.

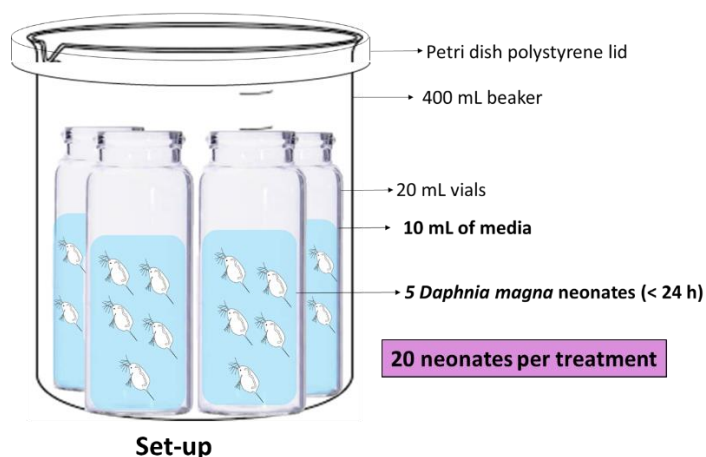


**Figure 5.6:** Adapted incubator used for each treatment consisting of four 20 mL vials grouped in a 400 mL beaker covered with a polystyrene petri dish.

### 5.2.3 Experimental set-up

Five different treatments each containing a total of 20 neonates (5 neonates in each vial) were evaluated. The transfer of the daphnids to the vials was accomplished in two steps under a dissection microscope at low magnification (e.g., 10x) using a micropipette (Figure 5.8). Firstly, at least 20 neonates were transferred from the hatching petri dish into the rinsing vials. Each rinsing vial contained 10 mL of the experimental media of each treatment. Secondly, exactly 5 neonates from the rinsing vials were transferred to the 4 test vials. Each test vial contained 10 mL of the experimental medium.

The treatments consisted of a protocol control (media only), fluoxetine control (3  $\mu\text{M}$ , 1  $\mu\text{g mL}^{-1}$ ), virgin microplastic control (100  $\mu\text{g mL}^{-1}$  plastic), fluoxetine-loaded microplastics (50  $\mu\text{g mL}^{-1}$  plastic, Experiment 1 Figure 5.8) and fluoxetine-loaded microplastics (100  $\mu\text{g mL}^{-1}$  plastic, Experiment 2, Figure 5.7).

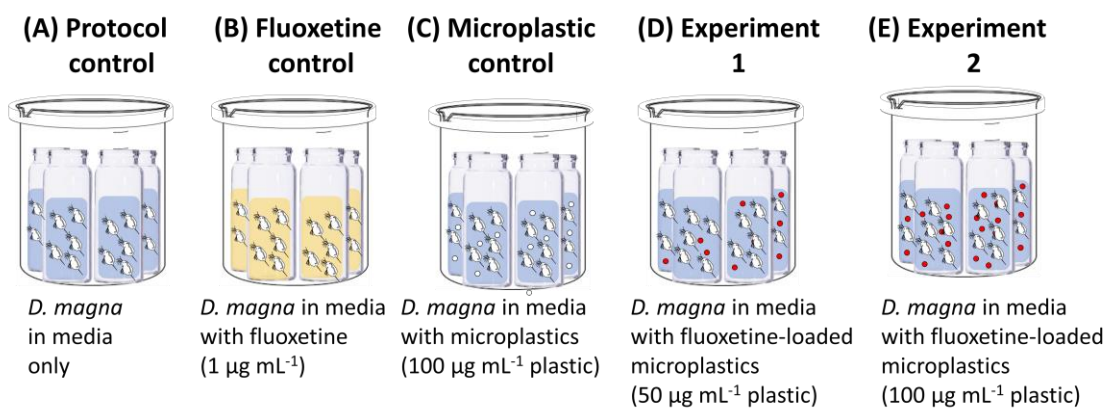


**Figure 5.7:** Five different treatments were evaluated. a) protocol control (media only), b) fluoxetine control (fluoxetine,  $1 \mu\text{g mL}^{-1}$ ), microplastic control ( $100 \mu\text{g mL}^{-1}$  plastic), fluoxetine-loaded microplastics ( $50 \mu\text{g mL}^{-1}$  plastic, Experiment 1, red dots) and fluoxetine-loaded microplastics ( $100 \mu\text{g mL}^{-1}$  plastic, Experiment 2, red dots). For experiments 1 and 2, fluoxetine was loaded onto virgin PP ( $231 \mu\text{M}$  adsorbed), aged PP ( $196 \mu\text{M}$  adsorbed), virgin PA ( $20 \mu\text{M}$  adsorbed), aged PA ( $26 \mu\text{M}$  adsorbed), virgin PVC ( $18 \mu\text{M}$  adsorbed), and aged PVC ( $23 \mu\text{M}$  adsorbed).

The concentration of the fluoxetine control was chosen according to the reported  $\text{EC}_{50}$  of fluoxetine ( $0.82 \mu\text{g mL}^{-1}$ ) to *D. magna* (Brooks et al. 2003).

The plastic concentrations were chosen based on previously published concentrations. The ingestion of microplastics by *D. magna* has been reported at microplastic concentrations of  $50$  and  $100 \mu\text{g mL}^{-1}$  (Frydkjær, Iversen and Roslev 2017). Further, the concentration of fluoxetine used to load the microplastics was selected based on the adsorption capacity of the each microplastic type. The concentration of fluoxetine loaded onto microplastics was chosen based on the results of the adsorption isotherms for each microplastic type investigated as described in chapter 4. This approach was chosen to ensure the saturation of the particles with fluoxetine. As discussed in chapter 4, small particles of PP showed greater adsorption capacity of fluoxetine when compared to small PA and PVC. Therefore, a greater concentration of fluoxetine was needed to saturate the particles of PP compared to PA and PVC. Fluoxetine-loaded PP microparticles were prepared by adding them ( $2 \text{ g L}^{-1}$  plastic) to a solution of medium containing  $289 \mu\text{M}$  ( $100 \mu\text{g mL}^{-1}$ ) of fluoxetine in the AFW described in section

5.2.2. For virgin and aged PA and PVC, the particles were pre exposed to 43  $\mu\text{M}$  ( $15 \mu\text{g mL}^{-1}$ ) of fluoxetine ( $2 \text{ g L}^{-1}$  plastic) based on isotherm results discussed previously. As performed in the adsorption studies (chapter 3 and 4), the fluoxetine-loading of the microplastics and the control were horizontally shaken at 200 rpm and  $25^\circ\text{C}$  using a MaxQ 6000 (Thermofisher scientific, UK) for 24 h. After 24 h, the microplastics were filtered using a GF/F filter (Fisher scientific, UK). In order to avoid potential degradation of fluoxetine adsorbed onto microplastics during the drying process of the fluoxetine-loaded microplastics, the microplastics were used wet to prepare the experimental solutions. Prior tests (data not shown) demonstrated the dried weight of microplastics corresponds to between 60 to 100% of the wet weight of microplastics depending on the microplastic type and aging, therefore the microplastics weight was adjusted to prepare the experimental solutions. For the  $100 \mu\text{g mL}^{-1}$  plastic treatment, 20 mg (dry weight) fluoxetine-loaded microplastics was dispersed in 200 mL of fresh media, while for the  $50 \mu\text{g mL}^{-1}$  plastic treatment, 10 mg (dry weight) fluoxetine-loaded microplastics was dispersed in 200 mL of fresh media. The microplastic control was treated exactly as the  $100 \mu\text{g mL}^{-1}$  plastic fluoxetine-loaded microplastic treatment. That means that the 200 mg of the microplastic used in the microplastic control were shaken in 100 mL medium (without fluoxetine,  $2 \text{ g L}^{-1}$  plastics) for 24 h at  $25^\circ\text{C}$ , filtered and 20 mg (dry weight) of unloaded microplastics was collected and placed in 200 mL fresh media ( $100 \mu\text{g mL}^{-1}$  plastic) to prepare the microplastic control samples. The vials were placed in an incubator (MaxQ 6000, Thermofisher scientific, UK) at  $20^\circ\text{C}$  in the dark for 48 h without agitation.



#### 5.2.4 Visualisation of the neonates and capture of images

A dissecting microscope (HWF 15x, Vickers instruments, UK) was used to facilitate:

- (1) transfer the neonates from the hatching petri dish to the rinse vial;
- (2) transfer the neonates from the rinse vial to the four experimental vials; and
- (3) counting the number of dead neonates after 24 h and 48 h exposure to the treatments (Figure 5.8).

The neonates which were not able to swim after gentle agitation of the liquid for 15 seconds were considered immobilized, even if they could still move their antennae. To avoid repetition and extended phrases, both immobilised and dead neonates will be considered 'dead' in this chapter.

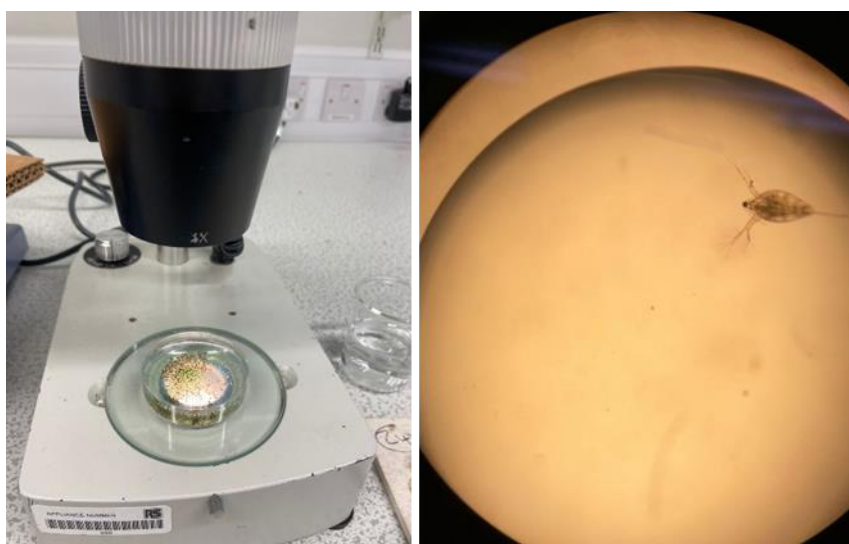


**Figure 5.8:** Transfer of *D. magna* neonates to rinsing vials using a dissection microscope (left) and an image of a neonate at magnification 15x (right).

After assessing the toxic response of the *D. magna* neonates after 48 h exposure, at least three organisms from different vials were collected using a Pasteur pipette and placed in a well plate (Thermofisher scientific, UK) to take

the photographs (Figure 5.9). After placing the neonate in the well plate, the maximum possible amount of water was removed to immobilise the individual neonate prior to taking the photograph. From the three individuals, one was randomly selected as a representative for each of the treatments. The pictures of the *D. magna* neonates were taken using a stereo microscope (S1503 model, Sunny Instruments, Singapore) with a coupled camera (YenCam 16, Yenmay, China).

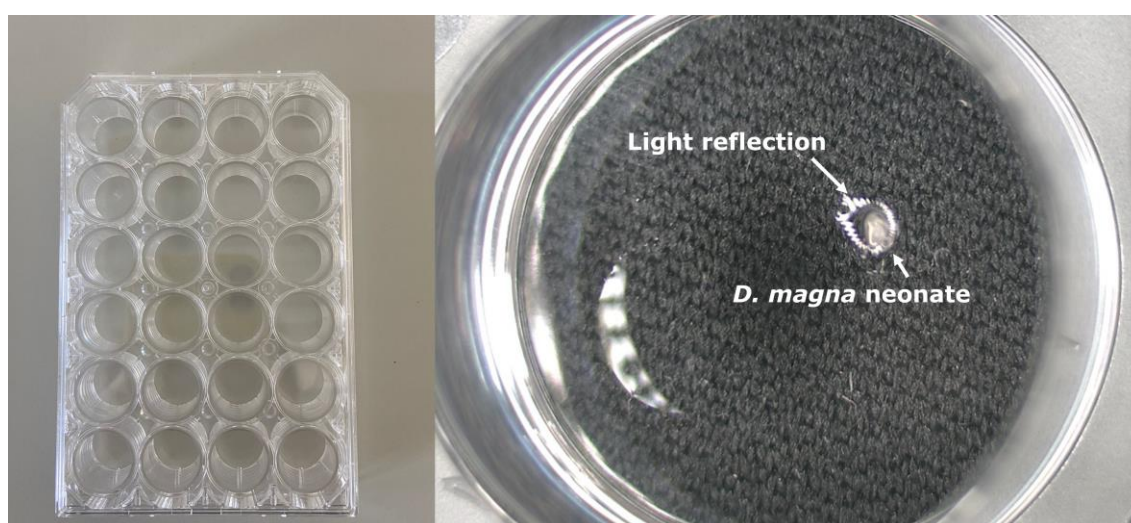


**Figure 5.9:** Well plate (left) used to take the micrograph of the neonates after 48 h exposure to the experimental treatments. A single individual was placed in each well to take the micrograph (right). A black background was used for improved contrast with the white/clear microplastics ingested by the neonates. Magnification 10x (right).

The software ImageJ (National Institutes of Health, US) was used to measure the neonates and to add a reference scale in the pictures.

### 5.2.5 Quantification of fluoxetine in the solution

The concentration of fluoxetine was measured:

(1) in the fluoxetine solution prepared to load microplastics and in the solution containing fluoxetine placed in contact with microplastics ( $2 \text{ g L}^{-1}$  plastics) after

24 h contact to evaluate the concentration of fluoxetine adsorbed onto microplastics;

(2) in the solution of fluoxetine control prior to experimentation and at the end of the experiment to evaluate potential fluoxetine degradation during the experiment; and

(3) in the vials containing fluoxetine-loaded microplastics (50 and 100  $\mu\text{g mL}^{-1}$ ) at the end of the experiment (48 h) to evaluate the concentration of fluoxetine desorbed from the fluoxetine-loaded microplastics.

The fluoxetine in solution was quantified using the HPLC-PDA method described in section 4.2.5. All samples that contained microplastics were filtered prior to injection for liquid chromatography.

### **5.2.6 Statistical analysis**

Student's t-test was carried out to perform significance testing (Microsoft Excel). For all statistical tests, a significance level of 5% was set. A Pearson correlation matrix was performed to evaluate a correlation between variables of this study (Microsoft Excel; Table A5.1). A correlation coefficient ( $r$ ) greater than 0.7 was considered a strong positive association, while a  $r$  lower than -0.7 was considered a strong negative association.

## 5.3 Results and discussion

### 5.3.1 Effect of the protocol and fluoxetine controls on the survival of *D. magna* neonates

A protocol control and a fluoxetine control were performed along with each of the two experimental tests. For this reason, two fluoxetine control results are shown (Figure 5.10). For the first experiment (virgin PP), 5 of 20 *D. magna* neonates were dead when exposed to fluoxetine in solution ( $3 \mu\text{M}$ ,  $1 \mu\text{g mL}^{-1}$ ), while 13 neonates were dead in the second experiment (aged PP; virgin and aged PA and PVC), both after 24 h. On the other hand, the protocol control demonstrated the same results for the two batches of experiments, where only a single organism (1 out of 20) died in the first 24 h.

Brooks et al. (2003) reported  $0.82 \mu\text{g mL}^{-1}$  as half maximal effective concentration ( $\text{EC}_{50}$ ) of fluoxetine on *D. magna*, which is consistent with the mortality of *the D. magna* neonates in the fluoxetine control in the second experiment (65% mortality). The  $\text{EC}_{50}$  is the concentration of a substance in an environmental medium expected to produce a certain effect in 50% of test organisms in a given population under a defined set of conditions. However, the reported  $\text{EC}_{50}$  values of *D. magna* neonates exposed to fluoxetine in solution varies in the literature. For instance, another study showed an acute toxic effect (48 h) of fluoxetine to *D. magna* neonates at approximately 10-fold greater fluoxetine concentrations when compared to Brooks et al. (2003). Varano, Fabbri and Pasteris (2017) observed an acute toxic effect of fluoxetine to *D. magna* neonates between  $6.4$  and  $9.1 \mu\text{g mL}^{-1}$  and demonstrated a chronic effect (21 days) at a concentration of  $0.23 \mu\text{g mL}^{-1}$ . The different  $\text{EC}_{50}$  values reported in the literature and the different mortality observed between the two experiments

when *D. magna* neonates were exposed to identical fluoxetine concentration, under the identical conditions, highlight the complexity of studying living organisms.

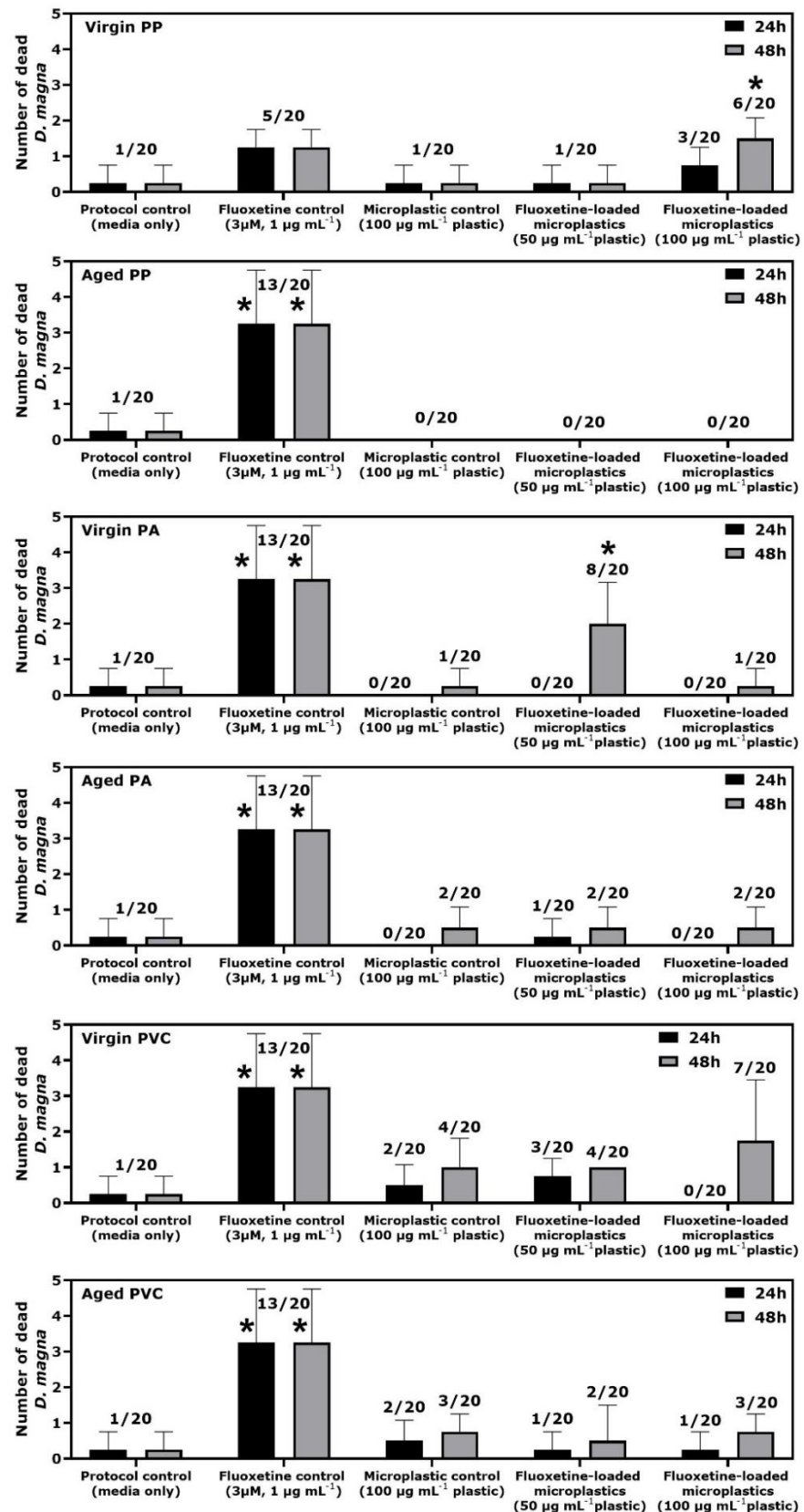


**Figure 5.10:** Summary of the average number of dead *D. magna* neonates across the 4 vials (5 neonates in each vial, totalising 20 neonates) after 24 h and 48 h. Total number of dead organisms out of twenty is represented on the top of the bars. \*significant difference between the treatment and the control, t-test  $p < 0.05$ .  $n=4$ , errors bars = 1 SD.

Fluoxetine has been found to have a behavioural and reproductive effect, moulting and growth inhibition, oxidative stress and an immune response, and endocrine disruption on organisms (Yamindago et al. 2021). Yamindago et al. (2021) observed neurotransmission-based behavioural changes and probably endocrine disruption in fluoxetine-exposed fish. They further suggested that the decreased swimming activities in the fish *Oryzias javanicus* could affect the fitness, population size, and migration of aquatic organisms. Further, according to Ding et al. (2017), fluoxetine could easily enter *D. magna* filtering chamber through the feeding current, therefore the uptake would occur via respiratory gas exchange at the inner wall of the carapace. In a study conducted by Nielsen and Roslev (2018), fluoxetine accelerated the death by starvation of *D. magna*. According to the authors, fluoxetine exposure can increase respiratory metabolism and decrease energy reserves in *D. magna*, which may be a contributing factor to the decreased tolerance to starvation of *D. magna* in the presence of neuroactive pharmaceuticals (Nielsen and Roslev 2018).

### **5.3.2 Evaluation of the effects of ingestion of microplastics by *D. magna* neonates**

As expected, neither microplastics nor any particles were observed in the guts of the control organisms in media solution only and in the fluoxetine control (Figure 5.11). Furthermore, after 48 h of experiment, there was no remnants of spirulina in the gut of the neonates.

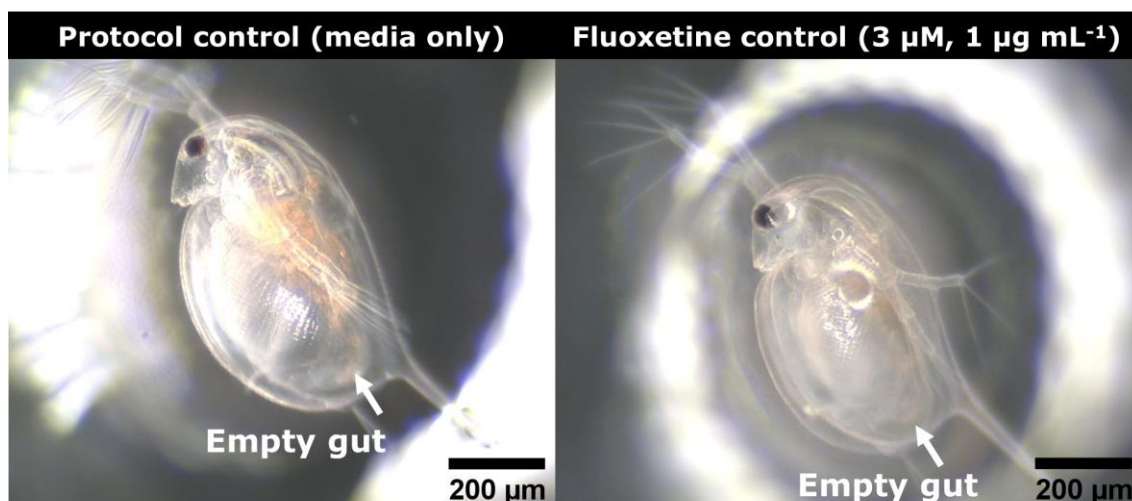


**Figure 5.11:** *D. magna* neonates after 48 h in media only (left) and in a solution containing fluoxetine at 3  $\mu\text{M}$  ( $1 \mu\text{g mL}^{-1}$ , right). The arrows point to the empty gut of the neonates. Magnification 45x.

The ingestion of microplastics was observed in all treatments where microplastics were included (Figure 5.11 to Figure 5.14), which includes the microplastic control ( $100 \mu\text{g mL}^{-1}$  plastics) and the fluoxetine-loaded microplastics at two plastic concentrations ( $50 \mu\text{g mL}^{-1}$  and  $100 \mu\text{g mL}^{-1}$  plastics). No correlation ( $-0.7 < r < 0.7$ ) was observed regarding the amount ingested by *D. magna* neonates and the concentration of microplastics in the solution ( $50$  and  $100 \mu\text{g mL}^{-1}$  plastics, Table A5.1). Likewise, after visual inspection, no clear association was observed between the size of the particles (PVC < PP < PA size) and the amount ingested by the neonates. However, the *D. magna* neonates appear to ingest the lowest amounts when exposed to the lower plastic concentration of fluoxetine-loaded aged PA ( $50 \mu\text{g mL}^{-1}$  plastics, Figure 5.14). The decreased ingestion might be due to great aggregation of aged PA after the aging process, which led to settling of the particles and large PA agglomerates that could not be ingested by *D. magna* neonates.

Furthermore, no correlation was observed between the density of the microplastics and both the ingestion of the microplastics and the mortality of the



neonates (Table A5.1). According to visual analysis of microplastic buoyancy, PP tended to both float on the top of and disperse in the water column, while virgin PA was completely dispersed in the water column. The aggregated particles of PA, however, sank to the bottom of experimental vials. Likewise, PVC particles seemed to both sink and disperse in the water column. Among the microplastics analysed, the neonates exposed to both virgin (four out of 20, 48 h) and aged particles (three out of 20, 48 h) of PVC showed greatest mortality. However, the microplastic itself did not show significant ( $p > 0.05$ ) toxic effects on the neonates. Previous experimental studies have shown that microplastics within the size range 0.020–5  $\mu\text{m}$  are commonly ingested by *D. magna*, as they represent a similar size range to their common algal food sources (Horton et al. 2018).

In a study conducted by An et al. (2021), polyethylene (PE) fragments (approximately 17  $\mu\text{m}$  and 35  $\mu\text{m}$ ) exhibited chronic toxicity to *Daphnia magna* after 21 days exposure. While, Canniff and Hoang (2018) showed that despite the fact that *D. magna* were able to ingest PE microbeads at a size of 63–75  $\mu\text{m}$ , results did not show an effect on survival and reproduction after 5 days.

Schwarzer et al. (2022) have concluded that the observed changes such as food uptake, mobility, and survival, were induced by microplastics ingestion and not merely by food depletion. The leachate of chemicals from microplastics can be a factor regarding the effect of the microplastics on *D. magna* (Zimmermann et al. 2020). However, the effect of leachate from the particles is probably not pertinent for this experiment. The microplastic controls and fluoxetine-loaded microplastics were shaken in medium, without and with fluoxetine, respectively, for 24 h prior to experimentation. This process is expected to desorb any readily

available chemicals present onto the commercial microplastics such as plasticisers and grafting agents, that could be potentially toxic to *D. magna*.

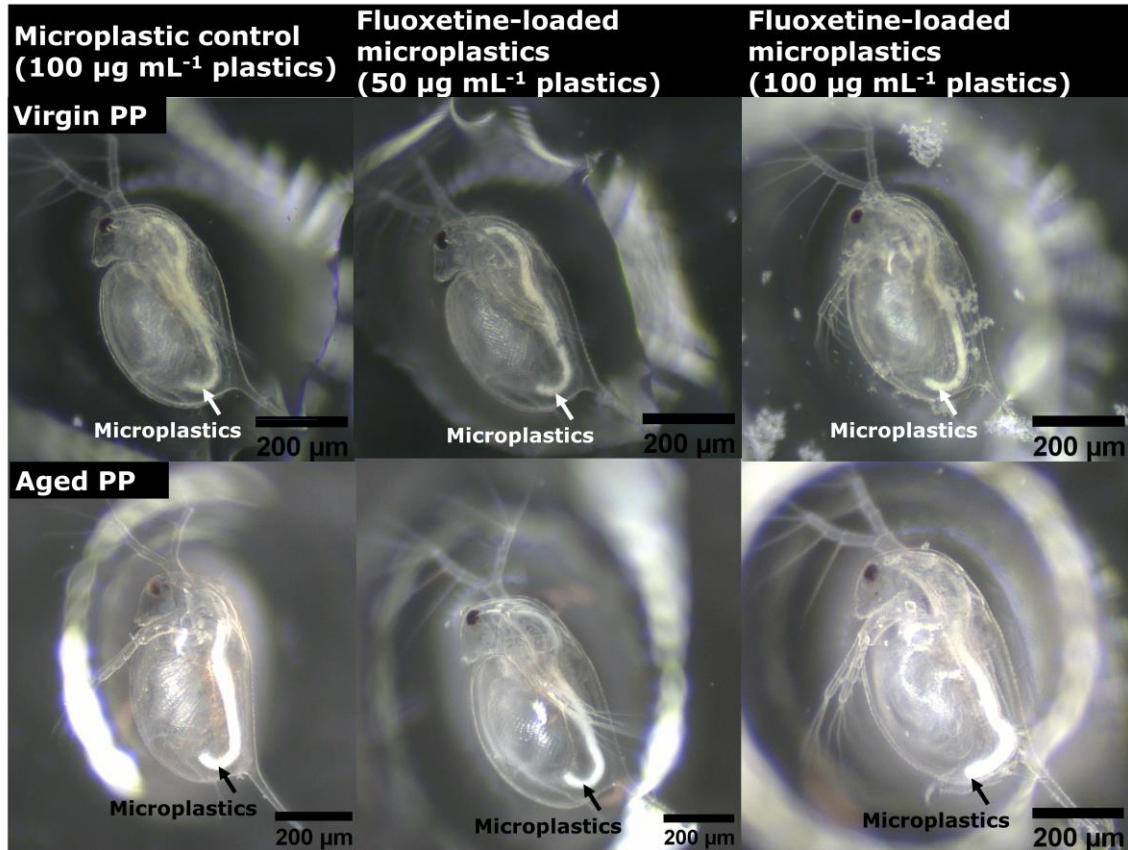


**Figure 5.12:** *D. magna* neonates after 48 h exposure to: microplastic control (100 µg mL<sup>-1</sup> plastics, left), fluoxetine-loaded microplastics (50 µg mL<sup>-1</sup>, middle), and fluoxetine-loaded microplastics (100 µg mL<sup>-1</sup>, right). The microplastics tested were virgin PP (top) and aged PP (bottom). The arrows point to microplastics in the gut of the neonates. Magnification 45x.

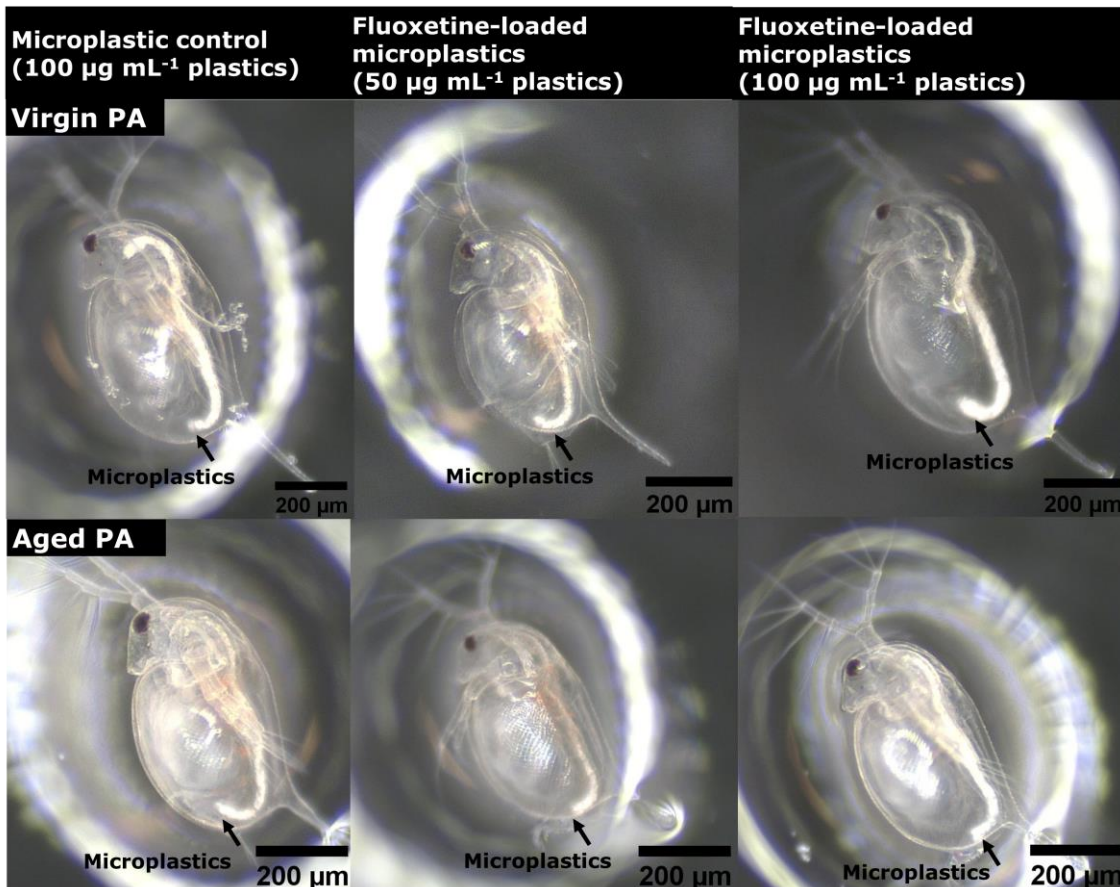


**Figure 5.13:** *D. magna* neonates after 48 h exposed to: microplastic control (100  $\mu\text{g mL}^{-1}$  plastics, left), fluoxetine-loaded microplastics (50  $\mu\text{g mL}^{-1}$ , middle), and fluoxetine-loaded microplastics (100  $\mu\text{g mL}^{-1}$ , right). The microplastic tested were virgin PA (top) and aged PA (bottom). The arrows point to microplastics in the gut of the neonates. Magnification 45x.

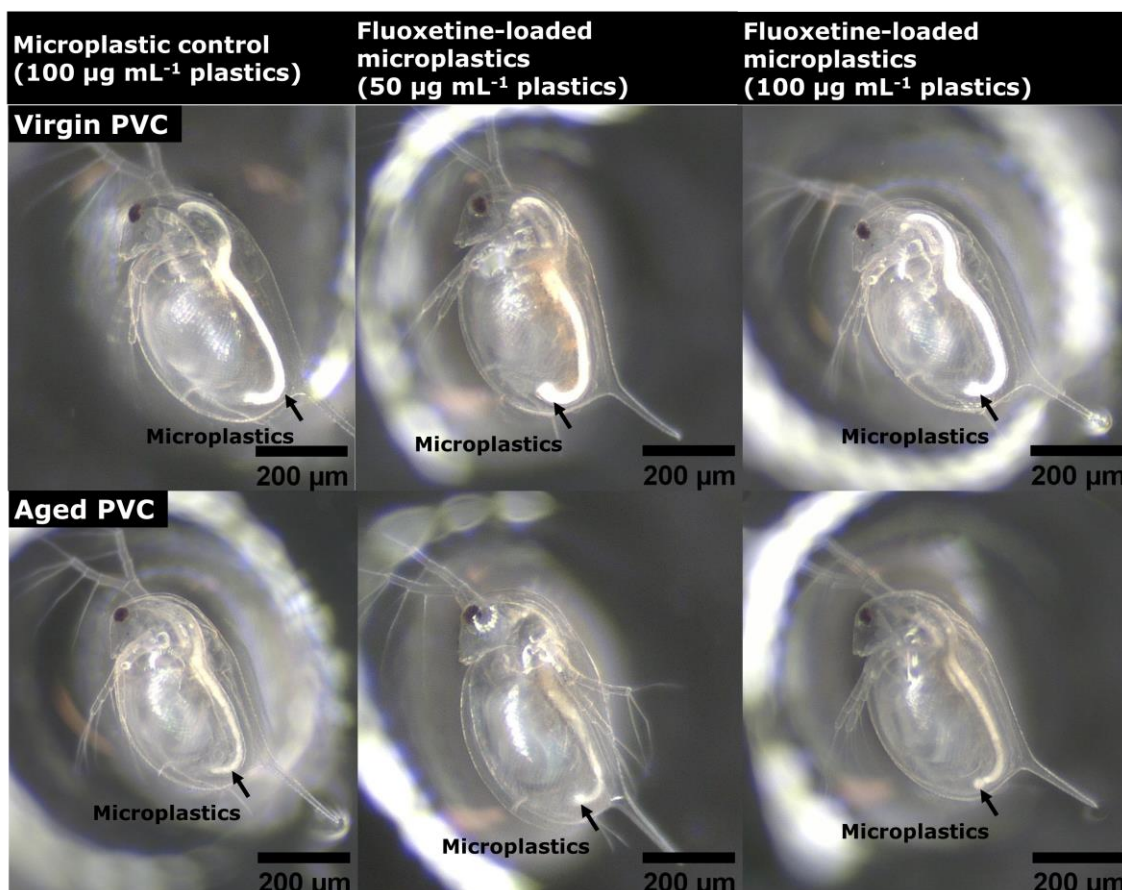


**Figure 5.14:** *D. magna* neonates after 48 h exposed to: microplastic control (100  $\mu\text{g mL}^{-1}$  plastics, left), fluoxetine-loaded microplastics (50  $\mu\text{g mL}^{-1}$ , middle), and fluoxetine-loaded microplastics (100  $\mu\text{g mL}^{-1}$ , right). The microplastic tested were virgin PVC (top) and aged PVC (bottom). The arrows point to microplastics in the gut of the neonates. Magnification 45x.

### 5.3.3 Effect of fluoxetine-loaded microplastics on the survival of *D. magna* neonates

The mortality of the neonates exposed to fluoxetine-loaded microplastics varied throughout the experiment. However, no correlation was observed when comparing the mortality of the neonates after 24 h and 48 h exposure with parameters such as the microplastic concentration, the concentration of fluoxetine adsorbed onto the microplastics, and the concentration of fluoxetine desorbed from the microplastics (Table A5.1).

As expected, greater concentrations of fluoxetine were detected in the treatments at the higher concentration of microplastics. The greatest desorption was observed with virgin particles of PP ( $1.19 \pm 0.05 \mu\text{M}$ ) in the treatment with the higher microplastic concentration ( $100 \mu\text{g mL}^{-1}$  plastics), while the lowest desorption of fluoxetine from the particles was observed for aged PVC ( $0.16 \pm 0.02 \mu\text{M}$ ) in the treatment with the lower microplastic concentration ( $50 \mu\text{g mL}^{-1}$  plastics). However, the concentration of fluoxetine detected in the two treatments containing fluoxetine-loaded microplastics was not directly proportional to the microplastic concentration in the treatment. The concentrations of fluoxetine desorbed from the fluoxetine-loaded microplastics at the lower concentration ( $50 \mu\text{g mL}^{-1}$  plastics) were similar to the fluoxetine desorbed from the experiment at the higher plastic concentration ( $100 \mu\text{g mL}^{-1}$  plastics, Table 5.2). This highlights the complexity of the bioavailability of micropollutants adsorbed onto the microplastics. In this thesis, bioavailability refers to the availability of the micropollutants adsorbed to the microplastics when exposed to wildlife either by contact or ingestion. There are several factors that can influence the observed concentration of fluoxetine in the media, even if the microplastic concentrations are different. Some of these factors are the aggregation, floating and settling of the microplastics that can influence the surface contact with water, thus allowing for more or less desorption to occur. For all treatments containing fluoxetine-loaded microplastics, the concentration of fluoxetine desorbed from the microplastics was lower when compared to the fluoxetine control concentration ( $3 \mu\text{M}$ ). Microplastics were detected in the gut of the *D. magna* neonates in the treatments containing fluoxetine-loaded microplastics. That means that the presence of fluoxetine in the solution did not stop the organism from ingesting the microplastics loaded with fluoxetine.

**Table 5.2:** Summary of the adsorption and desorption onto and from microplastics according to the microplastic type, microplastic weathering, and the plastic concentration tested.

Weathering	Plastic	Initial fluoxetine concentration ( $\mu\text{M}$ )	Concentration adsorbed onto microplastics ( $\mu\text{M}$ )	Plastic concentration ( $\text{g L}^{-1}$ )	Concentration desorbed from microplastics ( $\mu\text{M}$ )	Reported fluoxetine $\text{EC}_{50}^{\text{a}}$ ( $\mu\text{M}$ )
Virgin	PP	289	$231.58 \pm 28.4$	50	$0.99 \pm 0.05$	2.46
				100	$1.19 \pm 0.05$	
Aged	PP		$196.5 \pm 7.41$	50	$0.63 \pm 0.07$	
				100	$0.97 \pm 0.03$	
Virgin	PA	43	$20.01 \pm 1.24$	50	$0.37 \pm 0.03$	
				100	$0.56 \pm 0.03$	
Aged	PA		$26.2 \pm 1.63$	50	$0.31 \pm 0.02$	
				100	$0.44 \pm 0.02$	
Virgin	PVC		$18.95 \pm 1.12$	50	$0.21 \pm 0.02$	
				100	$0.24 \pm 0.003$	
Aged	PVC		$23.14 \pm 1.08$	50	$0.16 \pm 0.02$	
				100	$0.21 \pm 0.03$	

<sup>a</sup> Information taken from Brooks et al. (2003).

The presence of fluoxetine in the solution had an effect on neonate survival. For both fluoxetine controls, the same number of *D. magna* neonates were dead after 24 h and 48 h exposure to fluoxetine (Figure 5.10). Meanwhile, for the fluoxetine loaded onto microplastics treatments, a greater mortality was observed after 48 h compared to 24 h exposure to the loaded particles. Virgin loaded particles showed greater effects on the organisms compared to the artificially aged and loaded particles. Virgin fluoxetine-loaded PP particles (6 out of 20 in the 100  $\mu\text{g mL}^{-1}$  plastics samples) and PA (8 out of 20 in the 50  $\mu\text{g mL}^{-1}$  plastics samples) showed a significant ( $p < 0.05$ ) toxic effect to *D. magna* (Figure 5.10) when compared to the control. That means that for virgin PA, the lower concentrations of microplastics were more toxic to *D. magna* than the higher concentrations. Microscopic analysis of the neonates after 48 h exposure showed that the lower concentration of microplastics did not correspond to a lower ingestion of the microplastics by the organism (Figure 5.12), therefore excluding a feed-load effect on *D. magna*. Since both microplastic concentrations (50 and 100  $\mu\text{g mL}^{-1}$ ) had the same amount of fluoxetine adsorbed onto the particles, the microplastic concentration investigated was not a factor regarding the toxicity of fluoxetine-loaded PA. A marked mortality (7 out of 20 neonates) was observed after 48 h exposure to virgin PVC loaded with fluoxetine, however the number of dead organisms was not significantly different from the control ( $p = 0.24$ ).

Greater amounts of fluoxetine were adsorbed onto virgin PP (251  $\mu\text{mol g}^{-1}$ ) when compared to virgin PA (20  $\mu\text{mol g}^{-1}$ ) and virgin PVC (19  $\mu\text{mol g}^{-1}$ ). This is expected since, due to small PP significant adsorption capacity shown in chapters 3 and 4, small PP was exposed to a greater fluoxetine concentration (289  $\mu\text{M}$ ,

100  $\mu\text{g mL}^{-1}$ ) than small PA and PVC (43  $\mu\text{M}$ , 15  $\mu\text{g mL}^{-1}$ ). That means that fluoxetine might be more bioavailable when adsorbed onto the glassy polymers like PA and PVC, than onto the rubbery polymers like PP. In the current experiment, as detected in the desorption experiments described in chapter 4, similar fluoxetine desorption was observed from virgin and aged particles for all three microplastics investigated. This, allied to the fact the three aged microplastic types showed greater aggregation of the particles, might indicate that fluoxetine adsorbed onto the particles is less bioavailable when compared to the virgin particles. A study carried out by Wagstaff and Petrie (2022) observed a similar exposure risk of fluoxetine desorption from PET microplastics (maximum size 300  $\mu\text{m}$ ) with temperatures corresponding to the internal temperatures of warm-blooded organisms (37 °C) over that of cold-blooded organisms such as *D. magna*. (20 °C). However, at the same time, greater fluoxetine desorption was observed in gastric fluid media compared to river water. The gut temperature of *D. magna* tends to closely match the surrounding water temperature and the pH of *D. magna* guts varies between 6 and 7.2 (Ebert 2005).

#### **5.4 Conclusions and environmental impact**

The acute effect of fluoxetine loaded onto microplastics on *D. magna* neonate motility and survival was investigated. Virgin and aged particles of three microplastic types widely reported in freshwater (PP, PA, and PVC) loaded with fluoxetine were exposed to *D. magna* for 48 h. Results indicate that different microplastic types with different buoyancies can be ingested by *D. magna* neonates after short periods of exposure such as 48 h. The ingestion of microplastic itself is worrisome since microplastic can accumulate in the food



web. Additionally, pollutant-free microplastics can cause harm. PVC particles have demonstrated a marked effect on the survival of *D. magna*. Allied to this, microplastic loaded with the antidepressant fluoxetine exhibited acute toxicity to *D. magna* neonates. Fluoxetine is commonly detected in freshwater environments across the globe, it is in the top 20 North American pharmaceutical residue found in freshwater systems. Fluoxetine has widely been found in freshwater bodies across Scotland. Microplastics and fluoxetine can co-exist in the environment, and fluoxetine can accumulate onto microplastics, thus entering the food web. Demonstrating that microplastics can act as a vector for at least one pharmaceutical.

As observed in previous chapters, the toxicity of fluoxetine-loaded microplastics depends on the microplastic type and weathering of the microplastics. For instance, results demonstrated that virgin particles are more likely to pose an acute toxic effect to *D. magna* when compared to aged particles. On the other hand, that does not mean that the aged particles are not harmful to wildlife. Aged microplastics have been demonstrated to adsorb greater amounts of micropollutants than virgin particles when co-occurring. Further, aged particles were also shown to adsorb hydrophilic compounds along with hydrophobic compounds, which might be more readily available in water.

Fluoxetine, when in solution, has also been demonstrated to display acute toxic effects on *D. magna* neonates. Fluoxetine loaded onto virgin PP and virgin PA was shown to be as toxic to *D. magna* as fluoxetine in solution. It has been clearly demonstrated that the ingestion of microplastics loaded with micropollutants can be a route for micropollutants into the food web with

potentially lethal effects to wildlife. Although both the loaded concentration and the microplastic concentration used in this study were not environmentally relevant, this is particularly worrisome considering the comparatively short period of time demonstrated for toxic effects to occur compared to the average reported life span of *D. magna* of 10 to 30 days (or even up to 100 days in a predator-free environment). Furthermore, *D. magna* is at a low trophic level in the food web, and studies (Sun et al. 2017; Nelms et al. 2018) have found that microplastics can transfer through the food web. Therefore, the toxic effects of fluoxetine loaded onto microplastics could potentially be transferred through the food web to higher trophic levels and impact a whole ecosystem.

# **Chapter 6**

## **Conclusions and Future work**

## 6.1 Conclusions

The aim of this thesis was to elucidate the potential role of environmentally relevant microplastics as a vector for natural and anthropogenic contaminants, both as individual compounds and as mixtures, and to assess the bioavailability and the potential toxicity of the compounds adsorbed to the particles should they desorb in the digestive track of biota.

More specifically, thesis proposed to select, artificially aged, and fully characterise microplastic types widely reported in freshwater environments (objective 1). The characterisation of these microplastics led to a publication that highlights the importance of a detailed characterisation of commercial microplastics for reliable interpretation of experimental data (Moura et al. 2023). The analytical findings uncovered inconsistencies in purity of small polypropylene (PP) and size of small polyamide (PA) and polyvinyl chloride (PVC) that had implications for the adsorption of the organic compounds investigated (chapter 2). An extreme example was the pronounced adsorption of all microcystins analogues (80-100%) and pharmaceuticals (16-97%) investigated by small PP. The characterisation of the particles detected the presence of a possible grafting agent (that contained a C=O group) in the virgin particles of small PP (which was not present in the large PP particles), and comparatively large surface area was measured. The oxygen-containing functional group and the great surface area impacted the adsorption of the compounds investigated onto the small PP particles. Without a detailed characterisation of the particles, the great adsorption of small PP could have been mistakenly attributed to the size alone.

The findings demonstrated that published studies that did not verify polymer material and particle size must be viewed with caution. Results also demonstrated that sieving microplastics is not an effective approach to ensure specific particle size distribution. In future, it is hoped that certified microplastics become widely available thus increasing confidence in the findings and comparison between different studies.

Another objective of this thesis was to evaluate the interaction of micropollutants with microplastics (objective 2). Overall, the microplastic type, weathering of the microplastics, the size of the particles, and the properties of the compound were all key factors affecting the adsorption onto microplastics. Results demonstrated that use of virgin particles in research might lead to an underestimation of the potential of microplastics to adsorb micropollutants in aquatic environments. However, the statement that the aging of microplastics enhances the adsorption of organic compounds must be used carefully. The aging of the microplastics decreased up to 85% (small PE) the adsorption of negatively charged (at pH 7) compounds, such as MC-LW and -LF (chapter 3), while it increased the adsorption (up to 30-fold on large PP) of positively charged pharmaceuticals, such as fluoxetine and venlafaxine (chapter 4). The findings presented in this thesis demonstrated that the hydrophobicity of the pharmaceuticals may not be the major driving factor in their interaction with microplastics, and other adsorption mechanisms, such as electrostatic interactions, may be more important. More worryingly, for all compounds investigated, the most toxic compounds in the mixtures of microcystins (MC-LW and -LF) and pharmaceuticals (fluoxetine) adsorbed in the greatest amounts onto the microplastics (among all compounds investigated).

The desorption of fluoxetine from the microplastic under conditions similar to freshwater environments and to *Daphnia magna* gut conditions (artificial freshwater, pH 7 at 25 °C) also varied according to the microplastic type. Chemical adsorption and desorption (when it occurred) took place when fluoxetine was placed in contact with selected microplastics (small PP, PA, PVC). The aging of the microplastic did not seem to affect the desorption of fluoxetine from the microplastics. Similar concentration of fluoxetine desorbed from the virgin microplastics when compared to the aged microplastics. This means the increase in the adsorption of fluoxetine onto the aged microplastics was due to strong, almost irreversible, interactions such as electrostatic interactions. The fluoxetine adsorbed onto small PA and PVC showed greater bioavailability (approximately 1.5 µM desorption each) when compared to small PP (no desorption). The findings demonstrated that the amount adsorbed onto microplastics can be an indication of potential toxicity of the loaded particles, however, it does not mean that the adsorbed compound is bioavailable. For this reason, toxicity tests are crucial for further evaluation of how the pollutant-loaded microplastics can affect the wildlife.

Finally, this thesis aimed to investigate the toxic effects of micropollutant-loaded microplastics on *Daphnia magna* (objective 3). The results presented in this thesis have demonstrated that the ingestion of microplastics loaded with micropollutants can be a route for micropollutants into the food web with potentially hazardous effects to wildlife. Again, the type and the weathering of microplastic played an important role regarding the toxicity of both the unloaded microplastic and the fluoxetine-loaded microplastics. The ecotoxicity experiments demonstrated that, *Daphnia magna* neonates can ingest microplastics at the two

plastic concentrations analysed within 48 h exposure. Furthermore, results demonstrated that fluoxetine-loaded small, virgin PP (six out of 20 neonates dead after 48 h) can be as toxic as fluoxetine in solution (five out of 20 neonates dead after 48 h). Therefore, the absence of desorption of fluoxetine from the virgin small PP particles did not mean absence of toxicity of the particles. The ingestion of the microplastic itself also appeared to have toxic effects on the *D. magna* neonates, which was the case for small, virgin PVC (four out of 20 neonates dead after 48 h). When it comes to toxicity effects, where the leachate of chemicals is not taken into consideration, the size of the particles and the buoyancy of the particles are probably the driving factors for the toxicity of micropollutant-loaded microplastics on *D. magna*. That is why the virgin particles were more toxic to *D. magna* neonates comparing to the aged particles, which aggregated more and sank on the bottom of the experimental vials, i.e., lower availability in the water column and the aggregated particles were too big to be ingested by *D. magna* neonates.

More importantly, all three microplastic types investigated when loaded with fluoxetine had a negative impact on the *D. magna* neonate survival. In this thesis, the results extensively demonstrated that one microplastic type should not be used as a proxy representative of microplastics. Microplastics are present as a non-homogeneous mixture in the environment with further heterogeneity introduced by grafting and colouring agents, as well as plasticisers within a given polymer type. The findings highlight the complexity of the implications of plastic pollution to aquatic environments.

## 6.2 Future work

This thesis has demonstrated that microplastics can act as a vector and have toxic effects in wildlife for at least one pharmaceutical. However, further investigation is required to fully understand how the ingestion of pollutant-loaded microplastics can affect wildlife. For instance, the evaluation of environmentally relevant micropollutant ( $\mu\text{g L}^{-1}$  range) and microplastics ( $\text{mg L}^{-1}$  range) concentrations along with a more complex matrix such as natural freshwater. Natural freshwater contains natural organic matter that can compete for binding sites and decrease the adsorption of micropollutants by microplastics. Furthermore, the evaluation of microplastics loaded with a mixture of contaminants would be more environmentally relevant since a range of micropollutants can co-exist in the environment. Likewise, the investigation of a mixture of microplastic types loaded with micropollutants and whether this affects their toxicity on *D. magna*. Moreover, it would be highly relevant to extend the investigation from the current bench scale to a mesocosm scale.

Ideally, a mesocosm containing a range of freshwater organisms with spiked micropollutants and microplastics under environmental conditions to evaluate whether the co-occurrence of micropollutants and microplastics can have chronic effects on the organisms. Experiments performed in natural freshwater will also enable the investigation of how water elements such as organic matter can impact the adsorption of micropollutants onto microplastics.

Another aspect of concern when microplastics can adsorb micropollutants when co-occurring is the potential for the underestimation of micropollutant concentrations in water samples. Many published water sampling protocols require environmental samples to be filtered prior to micropollutant analysis,



removing any suspended particles to determine dissolved concentrations. This practice might lead to an underestimation of the micropollutant load knowing that the pollutants adsorbed to the surface of microplastic particles can be biologically available as demonstrated by this thesis. For future research, current water sampling protocols should be assessed to evaluate whether the presence of microplastics in the water leads to a decrease in the detected concentration of micropollutants. If this is the case, an amended sampling protocol that avoids micropollutant underestimation in environmental samples must be developed.

It can be concluded from the results presented throughout this thesis that microplastics have a clear potential to act as a vector for micropollutants in the aquatic environment and have toxic effects to wildlife. Further research is essential to comprehensively understand the implications of the toxic aspects of pollutant-loaded microplastics on ecosystems and potential impacts on human health, particularly if the toxic effects of pollutant-loaded microplastics can transfer into and through the food web. Furthermore, the findings presented in this thesis can have an impact on all microplastic-related research. The promising results published from the detailed microplastic characterisation highlight the urge for certified microplastics to become commercially available to enhance confidence in the findings and to enable comparisons between different studies.

# References

ABBASI, N.A. et al., 2022. Ecotoxicological risk assessment of environmental micropollutants. In: *Environmental Micropollutants: A Volume in Advances in Pollution Research*. Elsevier. pp. 331–337.

ABERDEENLIVE, 2022. *Aberdeenshire pet owners warned after dogs die in suspected blue-green algae poisonings*. [online]. Available from: <https://www.aberdeenlive.news/news/health/aberdeenshire-pet-owners-warned-after-7465571>

AIGUO, Z. et al., 2022. Characteristics and differences of microplastics ingestion for farmed fish with different water depths, feeding habits and diets. *Journal of Environmental Chemical Engineering*, 10(2), 107189.

AKKANEN, J. and KUKKONEN, J.V.K., 2003. Biotransformation and bioconcentration of pyrene in *Daphnia magna*. *Aquatic Toxicology*, 64, pp. 53–61.

ALFONSO, M.B. et al., 2020. First evidence of microplastics in nine lakes across Patagonia (South America). *Science of the Total Environment*, 733, 139385.

ALIMI, O.S., HERNANDEZ, L.M. and TUFENKJI, N., 2018. Microplastics and Nanoplastics in Aquatic Environments : Aggregation , Deposition , and Enhanced Contaminant Transport. *Environmental Science and Technology*, 52, pp. 1704–1724.

ALJAIBACHI, R. et al., 2020. Impacts of polystyrene microplastics on *Daphnia magna*: A laboratory and a mesocosm study. *Science of The Total Environment*, 705, 135800.

ALJAIBACHI, R. and CALLAGHAN, A., 2018. Impact of polystyrene microplastics on *Daphnia magna* mortality and reproduction in relation to food availability.

*PeerJ*, 6: e4601.

ALMOND, J. et al., 2020. Determination of the carbonyl index of polyethylene and polypropylene using specified area under band methodology with ATR-FTIR spectroscopy. *E-Polymers*, 20(1), pp. 369–381.

AMBROSINI, R. et al., 2019. First evidence of microplastic contamination in the supraglacial debris of an alpine glacier. *Environmental Pollution*, 253, pp. 297–301.

AN, D. et al., 2021. Size-dependent chronic toxicity of fragmented polyethylene microplastics to *Daphnia magna*. *Chemosphere*, 271, 129591.

ANAND, N., THAJUDDIN, N. and DADHEECH, P.K., 2019. Cyanobacterial Taxonomy: Morphometry to Molecular Studies. *Cyanobacteria: From Basic Science to Applications*, pp. 43–64.

ANDERSON, D.M., GLIBERT, P.M. and BURKHOLDER, J.M., 2002. Harmful algal blooms and eutrophication: Nutrient sources, composition, and consequences. *Estuaries*, 25(4), pp. 704–726.

ANDRADY, A.L., 2017. The plastic in microplastics: A review. *Marine Pollution Bulletin*, 119(1), pp. 12–22.

ARTIOLI, Y., 2008. Adsorption. *Encyclopedia of Ecology, Five-Volume Set*, pp. 60–65.

ASTRAZENECA, 2015. *Environmental Risk Assessment Data of Tamoxifen*.

ATUGODA, T. et al., 2020. Adsorptive interaction of antibiotic ciprofloxacin on polyethylene microplastics: Implications for vector transport in water. *Environmental Technology & Innovation*, 19, 100971.

- ATUGODA, T. et al., 2021. Interactions between microplastics, pharmaceuticals and personal care products: Implications for vector transport. *Environment International*.
- AZEVEDO, S.M.F.O. et al., 2002. Human intoxication by microcystins during renal dialysis treatment in Caruaru—Brazil. *Toxicology*, 181–182, pp. 441–446.
- BAEKELAND, L.H., 1909. Method of making insoluble products of phenol and formaldehyde. *United States Patent Office*, 3.
- BAHAMONDE, P.A., MUNKITTRICK, K.R. and MARTYNIUK, C.J., 2013. Intersex in teleost fish: Are we distinguishing endocrine disruption from natural phenomena? *General and Comparative Endocrinology*, 192, pp. 25–35.
- BALDWIN, A.K., CORSI, S.R. and MASON, S.A., 2016. Plastic Debris in 29 Great Lakes Tributaries: Relations to Watershed Attributes and Hydrology. *Environmental Science and Technology*, 50(19), pp. 10377–10385.
- BARCELÓ, D. and PETROVIC, M., 2007. Pharmaceuticals and personal care products (PPCPs) in the environment. *Analytical and Bioanalytical Chemistry*, 387(4), pp. 1141–1142.
- BBC, 2020. *Botswana: Mystery elephant deaths caused by cyanobacteria*. [online]. Available from: <https://www.bbc.co.uk/news/world-africa-54234396>
- BERTOLDI, C. et al., 2021. First evidence of microplastic contamination in the freshwater of Lake Guaíba, Porto Alegre, Brazil. *Science of the Total Environment*, 759, 143503.
- BHAGAT, K. et al., 2022. Aging of microplastics increases their adsorption affinity towards organic contaminants. *Chemosphere*, 298, 134238.

- BLÁHA, L., BABICA, P. and MARŠÁLEK, B., 2009. Toxins produced in cyanobacterial water blooms - toxicity and risks. *Interdisciplinary Toxicology*, 2(2), pp. 36–41.
- BLAIR, R.M. et al., 2019. Microscopy and elemental analysis characterisation of microplastics in sediment of a freshwater urban river in Scotland, UK. *Environmental Science and Pollution Research*, 26(12), pp. 12491–12504.
- BLAIS, P. et al., 1976. The Photo-Oxidation of Polypropylene Monofilaments: Part II: Physical Changes and Microstructure. *Textile Research Journal*, 46(9), pp. 641–648.
- BOOPATHI, T. and KI, J.S., 2014. Impact of environmental factors on the regulation of cyanotoxin production. *Toxins*, 6(7), pp. 1951–1978.
- BOULARD, L. et al., 2020. Spatial distribution and temporal trends of pharmaceuticals sorbed to suspended particulate matter of German rivers. *Water Research*, 171, 115366.
- BOXALL, A.B.A. and KOOKANA, R., 2018. Pharmaceuticals in the Environment and Human Health. In: A.B.A. BOXALL and R.S. KOOKANA, eds. *Health Care and Environmental Contamination*. Heslington: Elsevier. pp. 123–136.
- BOYD, C.E., 2016. *Water Quality: An Introduction*. 3rd ed. Auburn: Springer.
- BRANDAU, O., 2012. Material Basics. In: *Stretch Blow Molding*. Ontario: William Andrew Publishing. pp. 5–25.
- BRODIN, T. et al., 2013. Dilute Concentrations of a Psychiatric Drug Alter Behavior of Fish from Natural Populations. *Science*, 339(6121), pp. 814–815.
- BROOKS, B.W. et al., 2003. Waterborne and sediment toxicity of fluoxetine to

select organisms. *Chemosphere*, 52(1), pp. 135–142.

BROWN, D., 2014. Acrylic Acid. *Encyclopedia of Toxicology: Third Edition*, pp. 74–75.

CAI, C. et al., 2008. Grafting acrylic acid onto polypropylene by reactive extrusion with pre-irradiated PP as initiator. *Radiation Physics and Chemistry*, 77(3), pp. 370–372.

DE CAMPOS, A. and MARTINS FRANCHETTI, S.M., 2005. Biotreatment effects in films and blends of PVC/PCL previously treated with heat. *Brazilian Archives of Biology and Technology*, 48(2), pp. 235–243.

CANNIFF, P.M. and HOANG, T.C., 2018. Microplastic ingestion by *Daphnia magna* and its enhancement on algal growth. *Science of the Total Environment*, 633, pp. 500–507.

CERA, A. et al., 2022. Occurrence of Microplastics in Freshwater, pp. 201–226.

CHAMAS, A. et al., 2020. Degradation Rates of Plastics in the Environment. *ACS Sustainable Chemistry & Engineering*, 8(9), pp. 3494–3511.

CHAWLA, K.K., 2012. *Composite Materials: Science and Engineering*. 3rd ed. New York: Springer Verlag.

CHEMAXON, 2023. *Calculator Plugins Were Used for Structure Property Prediction and Calculation, Marvin 20.16.0*. [online]. Available from: <https://chemaxon.com/>

CHEN, J., SAWYER, N. and REGAN, L., 2013. Protein–protein interactions: General trends in the relationship between binding affinity and interfacial buried surface area. *Protein Science : A Publication of the Protein Society*, 22(4), 510.

- CHEN, X. et al., 2021. Comparison of adsorption and desorption of triclosan between microplastics and soil particles. *Chemosphere*, 263, 127947.
- COLE-PARMER, 2023. *Chemical Compatibility Database*. [online]. Available from: <https://www.coleparmer.com/chemical-resistance>.
- COLE, M., 2016. A novel method for preparing microplastic fibers. *Scientific Reports*, 6, pp. 1–7.
- COWIE, J.M.G. and ARRIGHI, V., 2007. *Polymers: Chemistry and Physics of modern Materials*. Third edit. CRC Press.
- CRAWFORD, C.B. and QUINN, B., 2017. *Microplastic Pollutants*. Amsterdam: Elsevier Ltd.
- CUMMING, H. and RÜCKER, C., 2017. Octanol-Water Partition Coefficient Measurement by a Simple H NMR Method. *ACS Omega*, 2(9), pp. 6244–6249.
- DAWSON, R., 1998. the toxicology of microcystins. *Toxicon*, 36(7), pp. 953–962.
- DI, M. and WANG, J., 2018. Microplastics in surface waters and sediments of the Three Gorges Reservoir, China. *Science of the Total Environment*, 616–617, pp. 1620–1627.
- DING, J. et al., 2017. Bioconcentration of the antidepressant fluoxetine and its effects on the physiological and biochemical status in *Daphnia magna*. *Ecotoxicology and Environmental Safety*, 142, pp. 102–109.
- DOKULIL, M.T. and TEUBNER, K., 2011. Eutrophication and Climate Change: Present Situation and Future Scenarios. In: A.A. ANSARI et al., eds. *Eutrophication: Causes, Consequences and Control*. Springer. pp. 1–16.



- DRIS, R. et al., 2015. Beyond the ocean : contamination of freshwater ecosystems with (micro-) plastic particles. *Csiro*, 12, pp. 539–550.
- EBELE, A.J., ABOU-ELWAFI ABDALLAH, M. and HARRAD, S., 2017. Pharmaceuticals and personal care products (PPCPs) in the freshwater aquatic environment. *Emerging Contaminants*, 3, pp. 1–16.
- EBERT, D., 2005. Introduction to Daphnia biology. In: *Ecology, Epidemiology, and Evolution of Parasitism in Daphnia*. National Center for Biotechnology Information (US). pp. 1–21.
- EERKES-MEDRANO, D., THOMPSON, R.C. and ALDRIDGE, D.C., 2015. Microplastics in freshwater systems : A review of the emerging threats , identification of knowledge gaps and prioritisation of research needs. *Water Research*, 75, pp. 63–82.
- ELIZALDE-VELÁZQUEZ, A. et al., 2020. Sorption of three common nonsteroidal anti-inflammatory drugs (NSAIDs) to microplastics. *Science of the Total Environment*, 715, 136974.
- ELIZALDE-VELÁZQUEZ, A. et al., 2020. Sorption of three common nonsteroidal anti-inflammatory drugs (NSAIDs) to microplastics. *Science of The Total Environment*, 715, 136974.
- VAN EMMERIK, T. et al., 2019. Seasonality of riverine macroplastic transport. *Scientific Reports*, 9(1), pp. 1–9.
- EPA, 2013. *Contaminants of Emerging Concern (CECs ) in Fish: Pharmaceuticals and Personal Care Products (PPCPs)*.
- ERIKSEN, M. et al., 2013. Microplastic pollution in the surface waters of the Laurentian Great Lakes. *Marine Pollution Bulletin*, 77(1–2), pp. 177–182.

- ERYAŞAR, A.R., GEDIK, K. and MUTLU, T., 2022. Ingestion of microplastics by commercial fish species from the southern Black Sea coast. *Marine Pollution Bulletin*, 177, pp. 1–8.
- FAN, X. et al., 2021. Investigation on the adsorption and desorption behaviors of antibiotics by degradable MPs with or without UV ageing process. *Journal of Hazardous Materials*, 401, 123363.
- FEKADU, S. et al., 2019. Pharmaceuticals in freshwater aquatic environments: A comparison of the African and European challenge. *Science of The Total Environment*, 654, pp. 324–337.
- FELDMAN, D., 2002. Polymer weathering: Photo-oxidation. *Journal of Polymers and the Environment*, 10(4), pp. 163–173.
- FISCHER, A. et al., 2010a. The role of organic anion transporting polypeptides (OATPs/SLCOs) in the toxicity of different microcystin congeners in vitro: A comparison of primary human hepatocytes and OATP-transfected HEK293 cells. *Toxicology and Applied Pharmacology*, 245(1), pp. 9–20.
- FISCHER, A. et al., 2010b. The role of organic anion transporting polypeptides (OATPs/SLCOs) in the toxicity of different microcystin congeners in vitro: A comparison of primary human hepatocytes and OATP-transfected HEK293 cells. *Toxicology and Applied Pharmacology*, 245(1), pp. 9–20.
- FRANCIS, G., 1878. Poisonous Australian lake. *Nature*, 18, pp. 11–12.
- FRANÇOIS, EHRENMANN OUARAY, Z. and LEFRANC, M.-P., 2021. *Amino acids*. [online]. IMGT.
- FRYDKJÆR, C.K., IVERSEN, N. and ROSLEV, P., 2017. Ingestion and Egestion of Microplastics by the Cladoceran *Daphnia magna*: Effects of Regular and Irregular

- Shaped Plastic and Sorbed Phenanthrene. *Bulletin of Environmental Contamination and Toxicology*, 99(6), pp. 655–661.
- GARCIA-PICHEL, F., 2009. Cyanobacteria. *Encyclopedia of Microbiology*, pp. 107–124.
- GARCIA-PICHEL, F. et al., 2020. What's in a name? The case of cyanobacteria. *Journal of Phycology*, 56(1), pp. 1–5.
- GEIL, P.H., 2017. Polymer characterization. *Modern Textile Characterization Methods*.
- GEYER, R., JAMBECK, J.R. and LAW, K.L., 2017. Production, use, and fate of all plastics ever made. *Science Advances*, 3(7), e1700782.
- GIGAULT, J. et al., 2018. Current opinion: What is a nanoplastic? *Environmental Pollution*, 235, pp. 1030–1034.
- GIJSMAN, P., MEIJERS, G. and VITARELLI, G., 1999. Comparison of the UV-degradation chemistry of polypropylene, polyethylene, polyamide 6 and polybutylene terephthalate. *Polymer Degradation and Stability*, 65(3), pp. 433–441.
- GILFILLAN, L.R., 2009. *Occurrence of plastic micro-debris in the southern California Current system*. CalCOFI Reports.
- GOLDSTEIN, M.C., ROSENBERG, M. and CHENG, L., 2012. Increased oceanic microplastic debris enhances oviposition in an endemic pelagic insect. *Biology Letters*, 8, pp. 817–820.
- GONG, X. et al., 2022. Effects of microplastics of different sizes on the *Chlorella vulgaris* - *Ganoderma lucidum* co-pellets formation processes. *Science of The*

*Total Environment*, 820, 153266.

GOOGLE TRENDS, 2023. *Google Trends*. [online]. Available from:  
<https://trends.google.com/>

GORITO, A.M. et al., 2018. Constructed wetland microcosms for the removal of organic micropollutants from freshwater aquaculture effluents. *Science of the Total Environment*, 644, pp. 1171–1180.

GREENPEACE, 2019. *Upstream: Microplastics in UK rivers*.

GRIFFITHS, D.J. and SAKER, M.L., 2003. The Palm Island mystery disease 20 years on: A review of research on the cyanotoxin cylindrospermopsin. *Environmental Toxicology*, 18(2), pp. 78–93.

GRIGORESCU, R.M. et al., 2019. Waste Electrical and Electronic Equipment: A Review on the Identification Methods for Polymeric Materials. *Recycling 2019*, Vol. 4, Page 32, 4(3), 32.

GRINSTED, R.A., CLARK, L. and KOENIG, J.L., 1992. Study of Cyclic Sorption–Desorption into Poly(methyl methacrylate) Rods Using NMR Imaging. *Macromolecules*, 25(4), pp. 1235–1241.

GUO, X., CHEN, C. and WANG, J., 2019. Sorption of sulfamethoxazole onto six types of microplastics. *Chemosphere*, 228, pp. 300–308.

GUO, X., LIU, Y. and WANG, J., 2019. Sorption of sulfamethazine onto different types of microplastics : A combined experimental and molecular dynamics simulation study. *Marine Pollution Bulletin*, 145, pp. 547–554.

GUO, X. and WANG, J., 2019. Sorption of antibiotics onto aged microplastics in freshwater and seawater. *Marine Pollution Bulletin*, 149, 110511.

- GUO, X. et al., 2018. Sorption properties of tylosin on four different microplastics. *Chemosphere*, 209, pp. 240–245.
- HAMID, F., AKHBAR, S. and HALIM, K.H.K., 2013. Mechanical and thermal properties of polyamide 6/HDPE-g-MAH/high density polyethylene. *Procedia Engineering*, 68, pp. 418–424.
- HANKE, G. et al., 2013. *Guidance on Monitoring of Marine Litter in European Seas*. Luxembourg: Publications Office of the European Union.
- HE, Y. et al., 2014. Thermal stability and yellowing of polyamide finished with a compound anti-thermal-yellowing agent. *The Journal of The Textile Institute*, 106(12), pp. 1263–1269.
- HENDRICKSON, E., MINOR, E.C. and SCHREINER, K., 2018. Microplastic Abundance and Composition in Western Lake Superior As Determined via Microscopy, Pyr-GC/MS, and FTIR. *Environmental Science and Technology*, 52(4), pp. 1787–1796.
- HERNÁNDEZ-PRIETO, M.A., SEMENIUK, T.A. and FUTSCHIK, M.E., 2014. Toward a systems-level understanding of gene regulatory, protein interaction, and metabolic networks in cyanobacteria. *Frontiers in Genetics*, 5, pp. 1–18.
- HOLLANDE, S. and LAURENT, J.L., 1997. Study of discolouring change in PVC, plasticizer and plasticized PVC films. *Polymer Degradation and Stability*, 55(2), pp. 141–145.
- HORTON, A.A. et al., 2017. Large microplastic particles in sediments of tributaries of the River Thames, UK – Abundance, sources and methods for effective quantification. *Marine Pollution Bulletin*, 114(1), pp. 218–226.
- HORTON, A.A. et al., 2018. Acute toxicity of organic pesticides to *Daphnia magna*

is unchanged by co-exposure to polystyrene microplastics. *Ecotoxicology and Environmental Safety*, 166, pp. 26–34.

HORVATITS, T. et al., 2022. Microplastics detected in cirrhotic liver tissue. *EBioMedicine*, 82, 104147.

HÜFFER, T. and HOFMANN, T., 2016. Sorption of non-polar organic compounds by micro-sized plastic particles in aqueous solution. *Environmental Pollution*, 214, pp. 194–201.

HÜFFER, T., WENIGER, A.K. and HOFMANN, T., 2018a. Sorption of organic compounds by aged polystyrene microplastic particles. *Environmental Pollution*, 236, pp. 218–225.

HÜFFER, T., WENIGER, A.K. and HOFMANN, T., 2018b. Sorption of organic compounds by aged polystyrene microplastic particles. *Environmental Pollution*, 236, pp. 218–225.

HUGHES, S.R., KAY, P. and BROWN, L.E., 2013. Global synthesis and critical evaluation of pharmaceutical data sets collected from river systems. *Environmental Science and Technology*, 47(2), pp. 661–677.

HUI, J. et al., 2021. Graphitic-C<sub>3</sub>N<sub>4</sub> coated floating glass beads for photocatalytic destruction of synthetic and natural organic compounds in water under UV light. *Journal of Photochemistry and Photobiology A: Chemistry*, 405, 112935.

HURLEY, R. et al., 2020. Plastic waste in the terrestrial environment. In: *Plastic Waste and Recycling*. Elsevier. pp. 163–193.

HUSSAIN, M. et al., 2010. Synthesis, characterization, and photocatalytic application of novel TiO<sub>2</sub> nanoparticles. *Chemical Engineering Journal*, 157(1), pp. 45–51.

JEONG, T.Y. and SIMPSON, M.J., 2019. *Daphnia magna* metabolic profiling as a promising water quality parameter for the biological early warning system. *Water Research*, 166, 115033.

JI RAM, V. et al., 2019. Five-Membered Heterocycles. *The Chemistry of Heterocycles*, pp. 149–478.

JOHNSON, G.W. et al., 1964. Polychlorinated Biphenyls. In: *Environmental Forensics*. Academic Press. pp. 187–225.

JONES, O.A.H., VOULVOULIS, N. and LESTER, J.N., 2002. Aquatic environmental assessment of the top 25 English prescription pharmaceuticals. *Water Research*, 36(20), pp. 5013–5022.

JOO, S.H. et al., 2021. Microplastics with adsorbed contaminants: Mechanisms and Treatment. *Environmental Challenges*, 3, 100042.

KANDIE, F.J. et al., 2020. Occurrence and risk assessment of organic micropollutants in freshwater systems within the Lake Victoria South Basin, Kenya. *Science of the Total Environment*, 714, 136748.

KARLSSON, T.M., HASSELLÖV, M. and JAKUBOWICZ, I., 2018. Influence of thermooxidative degradation on the in situ fate of polyethylene in temperate coastal waters. *Marine Pollution Bulletin*, 135, pp. 187–194.

KASPRZYK-HORDERN, B., DINSDALE, R.M. and GUWY, A.J., 2009. The removal of pharmaceuticals, personal care products, endocrine disruptors and illicit drugs during wastewater treatment and its impact on the quality of receiving waters. *Water Research*, 43, pp. 363–380.

KAUSAR, A., 2017. Physical properties of hybrid polymer/clay composites. *Hybrid Polymer Composite Materials: Properties and Characterisation*, pp. 115–132.

- KOELMANS, A.A. et al., 2016. Microplastic as a Vector for Chemicals in the Aquatic Environment: Critical Review and Model-Supported Reinterpretation of Empirical Studies. *Environmental Science and Technology*, 50, pp. 3315–3326.
- KOELMANS, A.A. et al., 2019. Microplastics in freshwaters and drinking water: Critical review and assessment of data quality. *Water Research*, 155, pp. 410–422.
- KYE, H. et al., 2023. Microplastics in water systems: A review of their impacts on the environment and their potential hazards. *Heliyon*, 9(3), e14359.
- KYOUNG SONG, Y. et al., 2017. Combined Effects of UV Exposure Duration and Mechanical Abrasion on Microplastic Fragmentation by Polymer Type. *Environmental Science & Technology*, 51, pp. 4368–4376.
- KYTE, J. and DOOLITTLE, R.F., 1982. A simple method for displaying the hydrophobic character of a protein. *Journal of Molecular Biology*, 157, pp. 105–132.
- LAHENS, L. et al., 2018. Macroplastic and microplastic contamination assessment of a tropical river (Saigon River, Vietnam) transversed by a developing megacity. *Environmental Pollution*, 236, pp. 661–671.
- LAWTON, L.A. et al., 2003. Processes influencing surface interaction and photocatalytic destruction of microcystins on titanium dioxide photocatalysts. *Journal of Catalysis*, 213(1), pp. 109–113.
- LEE, Y. et al., 2021. Combined exposure to microplastics and zinc produces sex-specific responses in the water flea *Daphnia magna*. *Journal of Hazardous Materials*, 420, 126652.
- LEO, A., HANSCH, C. and ELKINS, D., 1971. Partition coefficients and their uses.



*Chemical Reviews*, 71(6), pp. 525–616.

LESLIE, H.A. et al., 2022. Discovery and quantification of plastic particle pollution in human blood. *Environment International*, 163.

LI, C., BUSQUETS, R. and CAMPOS, L.C., 2020. Assessment of microplastics in freshwater systems: A review. *Science of The Total Environment*, 707, 135578.

LI, J., ZHANG, K. and ZHANG, H., 2018. Adsorption of antibiotics on microplastics. *Environmental Pollution*, 237, pp. 460–467.

LI, J., LIU, H. and CHEN, J.P., 2018. Microplastics in freshwater systems: A review on occurrence, environmental effects, and methods for microplastics detection. *Water Research*, 137, pp. 362–374.

LI, Y. et al., 2019. Effects of particle size and solution chemistry on Triclosan sorption on polystyrene microplastic. *Chemosphere*, 231, pp. 308–314.

LIMA, M.F.S., VASCONCELLOS, M.A.Z. and SAMIOS, D., 2002. Crystallinity changes in plastically deformed isotactic polypropylene evaluated by x-ray diffraction and differential scanning calorimetry methods. *Journal of Polymer Science Part B: Polymer Physics*, 40(9), pp. 896–903.

LIU, G. et al., 2019a. Sorption behavior and mechanism of hydrophilic organic chemicals to virgin and aged microplastics in freshwater and seawater. *Environmental Pollution*, 246, pp. 26–33.

LIU, G. et al., 2019b. Sorption behavior and mechanism of hydrophilic organic chemicals to virgin and aged microplastics in freshwater and seawater. *Environmental Pollution*, 246, pp. 26–33.

LIU, J.L. and WONG, M.H., 2013. Pharmaceuticals and personal care products

(PPCPs): A review on environmental contamination in China. *Environment International*, 59, pp. 208–224.

LIU, P. et al., 2020a. Effect of aging on adsorption behavior of polystyrene microplastics for pharmaceuticals: Adsorption mechanism and role of aging intermediates. *Journal of Hazardous Materials*, 384, 121193.

LIU, P. et al., 2020b. Effect of aging on adsorption behavior of polystyrene microplastics for pharmaceuticals: Adsorption mechanism and role of aging intermediates. *Journal of Hazardous Materials*, 384, 121193.

LIU, P. et al., 2020c. Desorption of pharmaceuticals from pristine and aged polystyrene microplastics under simulated gastrointestinal conditions. *Journal of Hazardous Materials*, 392, 122346.

LIU, P. et al., 2021. Review of the artificially-accelerated aging technology and ecological risk of microplastics. *Science of The Total Environment*, 768, 144969.

LLORCA, M. et al., 2018. Adsorption of perfluoroalkyl substances on microplastics under environmental conditions. *Environmental Pollution*, 235, pp. 680–691.

LOMONACO, T. et al., 2020. Release of harmful volatile organic compounds (VOCs) from photo-degraded plastic debris: A neglected source of environmental pollution. *Journal of Hazardous Materials*, 394, 122596.

LUO, Y. et al., 2014. A review on the occurrence of micropollutants in the aquatic environment and their fate and removal during wastewater treatment. *Science of the Total Environment*, 473–474, pp. 619–641.

MA, J. et al., 2019. Effect of microplastic size on the adsorption behavior and mechanism of triclosan on polyvinyl chloride. *Environmental Pollution*, 254, 113104.

DE MAAGD, P.G. et al., 1999. pH-dependent hydrophobicity of the cyanobacteria toxin microcystin-LR. *Water Research*, 33(3), pp. 677–680.

MACKAY, D. et al., 1980. Relationships between aqueous solubility and octanol-water partition coefficients. *Chemosphere*, 9(11), pp. 701–711.

MAGADINI, D.L. et al., 2020. Assessing the sorption of pharmaceuticals to microplastics through in-situ experiments in New York City waterways. *Science of the Total Environment*, 729, 138766.

MANDAL, D.K. et al., 2017. Optimization of acrylic acid grafting onto polypropylene using response surface methodology and its biodegradability. *Radiation Physics and Chemistry*, 132, pp. 71–81.

MANI, T. et al., 2015. Microplastics profile along the Rhine River. *Scientific Reports*, 5(December), pp. 1–7.

MARTENS, S., 2017. *Handbook of Cyanobacterial Monitoring and Cyanotoxin Analysis*. Edited by Jussi A.O. Meriluoto, Lisa Spooft and Geoffrey A. Cood. *Advances in Oceanography and Limnology*, vol. 8. Chichester: John Wiley & Sons.

MASON, S.A. et al., 2016. Pelagic plastic pollution within the surface waters of Lake Michigan, USA. *Journal of Great Lakes Research*, 42(4), pp. 753–759.

MCCORD, J. et al., 2018. pH dependent octanol–water partitioning coefficients of microcystin congeners. *Journal of Water and Health*, 16(3), pp. 340–345.

MCCORMICK, A.R. et al., 2016. Microplastic in surface waters of urban rivers: Concentration, sources, and associated bacterial assemblages. *Ecosphere*, 7(11), pp. 1–22.

- MENG, Y., KELLY, F.J. and WRIGHT, S.L., 2019. Advances and challenges of microplastic pollution in freshwater ecosystems: A UK perspective. *Environmental Pollution*, 256, 113445.
- MILLER, R.Z. et al., 2017. Mountains to the sea: River study of plastic and non-plastic microfiber pollution in the northeast USA. *Marine Pollution Bulletin*, 124, pp. 245–251.
- MINTENIG, S.M. et al., 2019. Low numbers of microplastics detected in drinking water from ground water sources. *Science of the Total Environment*, 648, pp. 631–635.
- MISUMI, 2011. *Glass transition temperature Tg of plastics*. [online]. Technical tutorial. Available from: <https://www.misumi-techcentral.com/tt/en/mold/2011/12/106-glass-transition-temperature-tg-of-plastics.html>.
- MOLAZADEH, M. et al., 2022. Buoyant microplastics in freshwater sediments – How do they get there? *Science of the Total Environment*, 860, 160489.
- MOURA, D.S. et al., 2022. Adsorption of cyanotoxins on polypropylene and polyethylene terephthalate: Microplastics as vector of eight microcystin analogues. *Environmental Pollution*, 303, 119135.
- MOURA, D.S. et al., 2023. Characterisation of microplastics is key for reliable data interpretation. *Chemosphere*, 331(January), 138691.
- MYLLÄRI, V., RUOKO, T.P. and SYRJÄLÄ, S., 2015. A comparison of rheology and FTIR in the study of polypropylene and polystyrene photodegradation. *Journal of Applied Polymer Science*, 132(28), pp. 1–6.
- NAKATUKA, Y. et al., 2015. The effect of particle size distribution on effective

zeta-potential by use of the sedimentation method. *Advanced Powder Technology*, 26(2), pp. 650–656.

NAPPER, I.E. and THOMPSON, R.C., 2019. Marine Plastic Pollution: Other Than Microplastic. In: *Waste*. Academic Press. pp. 425–442.

NCCOS, 2021. *Pharmaceuticals in the Environment*. [online]. Available from: <https://products.coastalscience.noaa.gov/peiar/search.aspx>.

NELMS, S.E. et al., 2018. Investigating microplastic trophic transfer in marine top predators. *Environmental Pollution*, 238, pp. 999–1007.

NEMATDOOST HAGHI, B. and BANAEI, M., 2017. Effects of micro-plastic particles on paraquat toxicity to common carp (*Cyprinus carpio*): biochemical changes. *International Journal of Environmental Science and Technology*, 14(3), pp. 521–530.

NIELSEN, M.E. and ROSLEV, P., 2018. Behavioral responses and starvation survival of *Daphnia magna* exposed to fluoxetine and propranolol. *Chemosphere*, 211, pp. 978–985.

NKOO, M. et al., 2019. Bioconcentration of the antiepileptic drug carbamazepine and its physiological and biochemical effects on *Daphnia magna*. *Ecotoxicology and Environmental Safety*, 172, pp. 11–18.

NURCHI, V.M. et al., 2019. Sorption of ofloxacin and chrysoidine by grape stalk. A representative case of biomass removal of emerging pollutants from wastewater. *Arabian Journal of Chemistry*, 12(7), pp. 1141–1147.

O'NEIL, J.M. et al., 2012. The rise of harmful cyanobacteria blooms: The potential roles of eutrophication and climate change. *Harmful Algae*, 14, pp. 313–334.

- OGONOWSKI, M. et al., 2016. The effects of natural and anthropogenic microparticles on individual fitness in daphnia magna. *PLoS ONE*, 11(5), pp. 1–20.
- OH, S., SHIN, W.S. and KIM, H.T., 2016. Effects of pH, dissolved organic matter, and salinity on ibuprofen sorption on sediment. *Environmental Science and Pollution Research*, 23(22), pp. 22882–22889.
- OSPAR COMMISSION, 2023. *Plastic particles in fulmars*. OSPAR: Quality Status Report 2023.
- PARK, J. et al., 2018. Sorption of pharmaceuticals to soil organic matter in a constructed wetland by electrostatic interaction. *Science of The Total Environment*, 635, pp. 1345–1350.
- PASCALL, M.A. et al., 2005. Uptake of Polychlorinated Biphenyls (PCBs) from an Aqueous Medium by Polyethylene, Polyvinyl Chloride, and Polystyrene Films. *Journal of Agricultural and Food Chemistry*, 53, pp. 164–169.
- PERKINELMER APPLICATION NOTE, n.d. *DSC as Problem Solving Tool: Measurement of Percent Crystallinity of Thermoplastics*. [online]. Available from: [https://resources.perkinelmer.com/corporate/content/applicationnotes/app\\_thermalcrystallinitythermoplastics.pdf](https://resources.perkinelmer.com/corporate/content/applicationnotes/app_thermalcrystallinitythermoplastics.pdf).
- PERSOONE, G. et al., 2009. Review on the acute Daphnia magna toxicity test - Evaluation of the sensitivity and the precision of assays performed with organisms from laboratory cultures or hatched from dormant eggs. *Knowledge and Management of Aquatic Ecosystems*, (393), pp. 1–29.
- PESTANA, C. et al., 2021. Potentially Poisonous Plastic Particles: Microplastics as a Vector for Cyanobacterial Toxins Microcystin-LR and Microcystin-LF.

*Environmental Science & Technology*, 55(23), pp. 15940–15949.

PETRIE, B. et al., 2014. Obtaining process mass balances of pharmaceuticals and triclosan to determine their fate during wastewater treatment. *Science of The Total Environment*, 497–498, pp. 553–560.

PETRIE, B. et al., 2023. Chiral pharmaceutical drug adsorption to natural and synthetic particulates in water and their desorption in simulated gastric fluid. *Journal of Hazardous Materials Advances*, 9, 100241.

PETRIE, B., BARDEN, R. and KASPRZYK-HORDERN, B., 2015. A review on emerging contaminants in wastewaters and the environment: Current knowledge, understudied areas and recommendations for future monitoring. *Water Research*, 72, pp. 3–27.

PHILIPP, C., UNGER, B. and SIEBERT, U., 2022. Occurrence of Microplastics in Harbour Seals (*Phoca vitulina*) and Grey Seals (*Halichoerus grypus*) from German Waters. *Animals*, 12(5), pp. 1–13.

PLASTIC EUROPE, 2022. *Plastics – the Facts 2022: An analysis of European plastics production, demand and waste data*. PlasticEurope.

PLASTICS EUROPE, 2020. *Plastics – the Facts 2020: An analysis of European plastics production, demand and waste data*. PlasticEurope.

PONIEWOZIK, M. and LENARD, T., 2022. Phytoplankton Composition and Ecological Status of Lakes with Cyanobacteria Dominance. *International Journal of Environmental Research and Public Health*, 19(7), 3832.

PRAJAPATI, A., NARAYAN VAIDYA, A. and KUMAR, A.R., 2022. Microplastic properties and their interaction with hydrophobic organic contaminants: a review. *Environmental Science and Pollution Research* 2022 29:33, 29(33), pp.

49490–49512.

PRATA, J.C. et al., 2019. Methods for sampling and detection of microplastics in water and sediment: A critical review. *TrAC Trends in Analytical Chemistry*, 110, pp. 150–159.

PUCKOWSKI, A. et al., 2021. Sorption of pharmaceuticals on the surface of microplastics. *Chemosphere*, 263, 127976.

RAGUSA, A. et al., 2021. Plasticenta: First evidence of microplastics in human placenta. *Environment International*, 146, 106274.

RAZEGHI, N. et al., 2021. Microplastic sampling techniques in freshwaters and sediments: a review. *Environmental Chemistry Letters*, 19(6), pp. 4225–4252.

RITCHIE, H. and ROSER, M., 2018. *Plastic pollution*. [online]. Our World in Data. Available from: <https://ourworldindata.org/plastic-pollution>.

RODRIGUES, M.O. et al., 2018. Spatial and temporal distribution of microplastics in water and sediments of a freshwater system (Antuã River, Portugal). *Science of the Total Environment*, 633, pp. 1549–1559.

ROMAN, L. et al., 2020. Plastic, nutrition and pollution; relationships between ingested plastic and metal concentrations in the livers of two Pachyptila seabirds. *Scientific Reports*, 10(1), pp. 1–14.

SAHA, D. and GRAPPE, H.A., 2017. Adsorption properties of activated carbon fibers. In: *Activated Carbon Fiber and Textiles*. Elsevier Inc. pp. 143–165.

SANTOS, L.H.M.L.M., RODRÍGUEZ-MOZAZ, S. and BARCELÓ, D., 2021. Microplastics as vectors of pharmaceuticals in aquatic organisms – An overview of their environmental implications. *Case Studies in Chemical and Environmental*



*Engineering*, 3, 100079.

SARIJAN, S. et al., 2021. Microplastics in freshwater ecosystems: a recent review of occurrence, analysis, potential impacts, and research needs. *Environmental Science and Pollution Research*, 28(2), pp. 1341–1356.

SCHINDLER, D.W., 1974. Eutrophication and recovery in experimental lakes: Implications for lake management. *Science*, 184(4139), pp. 897–899.

SCHINDLER, D.W., 2012. The dilemma of controlling cultural eutrophication of lakes. *Proceedings of the Royal Society B: Biological Sciences*, 279(1746), pp. 4322–4333.

SCHWARZENBACH, R.P. et al., 2010. Global water pollution and human health. *Annual Review of Environment and Resources*, 35, pp. 109–136.

SCHWARZER, M. et al., 2022. Shape, size, and polymer dependent effects of microplastics on *Daphnia magna*. *Journal of Hazardous Materials*, 426, 128136.

SEIDLITZ, H.K. et al., 2001. Solar radiation at the Earth's surface. *Comprehensive Series in Photosciences*, 3, pp. 705–738.

SEO, C. et al., 2022. Examination of Microcystin Adsorption by the Type of Plastic Materials Used during the Procedure of Microcystin Analysis, *toxins*, 14(9), 625.

SHARMA, R. and JAIN, S., 2009. UV-spectrophotometric estimation of venlafaxine hydrochloride. *Asian Journal of Chemistry*, 21(9), pp. 7440–7442.

SHAW, D.G., 1977. Pelagic tar and plastic in the gulf of alaska and bering sea: 1975. *Science of the Total Environment*, 8, pp. 13–20.

SIGHICELLI, M. et al., 2018. Microplastic pollution in the surface waters of Italian Subalpine Lakes. *Environmental Pollution*, 236, pp. 645–651.

- SORENSEN, R.M. and JOVANOVIĆ, B., 2021. From nanoplastic to microplastic: A bibliometric analysis on the presence of plastic particles in the environment. *Marine Pollution Bulletin*, 163, 111926.
- SOUZA, T. De et al., 2018. First evidence of microplastic ingestion by fishes from the Amazon River estuary. *Marine Pollution Bulletin*, 133, pp. 814–821.
- SPEIGHT, J.G., 2020. Sources of water pollution. *Natural Water Remediation*.
- STAMM, C. et al., 2016. Unravelling the Impacts of Micropollutants in Aquatic Ecosystems: Interdisciplinary Studies at the Interface of Large-Scale Ecology. *Advances in Ecological Research*, 55, pp. 183–223.
- STANIER, R.Y., 1977. The position of cyanobacteria in the world of phototrophs. *Carlsberg Research Communications*, 42(2), pp. 77–98.
- SU, L. et al., 2016. Microplastics in Taihu Lake, China. *Environmental Pollution*, 216, pp. 711–719.
- SU, X. et al., 2018. Evaluating the contamination of microcystins in Lake Taihu , China: The application of equivalent total MC-LR concentration. *Ecological Indicators*, 89, pp. 445–454.
- SUN, X. et al., 2017. Ingestion of microplastics by natural zooplankton groups in the northern. *Marine Pollution Bulletin*, 115, pp. 217–224.
- SVIRČEV, Z. et al., 2019. Global geographical and historical overview of cyanotoxin distribution and cyanobacterial poisonings. *Archives of Toxicology*, 93, pp. 2429–2481.
- TARPANI, R.R.Z. and AZAPAGIC, A., 2018. A methodology for estimating concentrations of pharmaceuticals and personal care products (PPCPs) in

wastewater treatment plants and in freshwaters. *Science of the Total Environment*, 622–623, pp. 1417–1430.

TAYLOR, T.N. and TAYLOR, E.L., 1993. *The Biology and Evolution of Fossil Plants*. New Jersey: Prentice Hall.

THE AMERICAN NUCLEAR SOCIETY, 2020. Natural and man-made radiation. In: *An Introduction to Radiation Protection*. National Council on Radiation and Measurement Reports. pp. 51–57.

THOMAS, K. V. and HILTON, M.J., 2004. The occurrence of selected human pharmaceutical compounds in UK estuaries. *Marine Pollution Bulletin*, 49(5–6), pp. 436–444.

THOMPSON, R.C. et al., 2009. Our plastic age. *Philosophical Transactions of the Royal Society B: Biological Sciences*, 364(1526), pp. 1973–1976.

TKACZYK, A. et al., 2021. Daphnia magna model in the toxicity assessment of pharmaceuticals: A review. *Science of the Total Environment*, 763, 143038.

TOLINSKI, M., 2015. Ultraviolet Light Protection and Stabilization. *Additives for Polyolefins*, pp. 32–43.

TOPPR, 2021. *Pseudo First Order Reaction*. [online]. Available from: [https://www.toppr.com/guides/chemistry/chemical-kinetics/pseudo-first-order-reaction/Difference Between Pseudo First Order,it a first order reaction](https://www.toppr.com/guides/chemistry/chemical-kinetics/pseudo-first-order-reaction/Difference%20Between%20Pseudo%20First%20Order,%20it%20a%20first%20order%20reaction).

TOURINHO, P.S. et al., 2019. Partitioning of chemical contaminants to microplastics: Sorption mechanisms, environmental distribution and effects on toxicity and bioaccumulation. *Environmental Pollution*, 252, pp. 1246–1256

TURNER, A. and HOLMES, L.A., 2015. Adsorption of trace metals by microplastic

- pellets in fresh water. *Environmental Chemistry*, 12(5), pp. 600–610.
- UNITED NATIONS ENVIRONMENT PROGRAMME, 1997. *Governing Council of the United Nations Environment Programme*. Nairobi.
- VARANO, V., FABBRI, E. and PASTERIS, A., 2017. Assessing the environmental hazard of individual and combined pharmaceuticals: acute and chronic toxicity of fluoxetine and propranolol in the crustacean *Daphnia magna*. *Ecotoxicology*, 26(6), pp. 711–728.
- VAUGHAN, R., TURNER, S.D. and ROSE, N.L., 2017. Microplastics in the sediments of a UK urban lake. *Environmental Pollution*, 229, pp. 10–18.
- VEERASINGAM, S. et al., 2021. Contributions of Fourier transform infrared spectroscopy in microplastic pollution research: A review. *Critical Reviews in Environmental Science and Technology*, 51(22), pp. 2681–2743.
- VELEZ, J.F.M. et al., 2018. Considerations on the use of equilibrium models for the characterisation of HOC-microplastic interactions in vector studies. *Chemosphere*, 210, pp. 359–365.
- VILLEGAS-NAVARRO, A. et al., 1999. Evaluation of *Daphnia magna* as an indicator of toxicity and treatment efficacy of textile wastewaters. *Environment International*, 25(5), pp. 619–624.
- VINCENT, W.F., 2009. Cyanobacteria. *Encyclopedia of Inland Waters*, pp. 226–232.
- WAGNER, J.R. et al., 2014. Polymer Overview and Definitions. In: *Extrusion*. William Andrew Publishing. pp. 209–224.
- WAGNER, N.D., SIMPSON, A.J. and SIMPSON, M.J., 2017. Metabolomic

responses to sublethal contaminant exposure in neonate and adult *Daphnia magna*. *Environmental Toxicology and Chemistry*, 36(4), pp. 938–946.

WAGSTAFF, A., LAWTON, L.A. and PETRIE, B., 2021. Polyamide microplastics in wastewater as vectors of cationic pharmaceutical drugs. *Chemosphere*, 288, 132578.

WAGSTAFF, A. and PETRIE, B., 2022. Enhanced desorption of fluoxetine from polyethylene terephthalate microplastics in gastric fluid and sea water. *Environmental Chemistry Letters* 2022, 1, pp. 1–8.

WANG, D. et al., 2021. Quantitative and qualitative determination of microplastics in oyster, seawater and sediment from the coastal areas in Zhuhai, China. *Marine Pollution Bulletin*, 164, 112000.

WANG, F. et al., 2019a. Adsorption characteristics of cadmium onto microplastics from aqueous solutions. *Chemosphere*, 235, pp. 1073–1080.

WANG, J. and WANG, S., 2016. Removal of pharmaceuticals and personal care products (PPCPs) from wastewater: A review. *Journal of Environmental Management*, 182, pp. 620–640.

WANG, W. et al., 2017. Microplastics pollution in inland freshwaters of China: A case study in urban surface waters of Wuhan, China. *Science of the Total Environment*, 575, pp. 1369–1374.

WANG, W. et al., 2018a. Microplastics in surface waters of Dongting Lake and Hong Lake, China. *Science of the Total Environment*, 633, pp. 539–545.

WANG, W. and WANG, J., 2018a. Comparative evaluation of sorption kinetics and isotherms of pyrene onto microplastics. *Chemosphere*, 193, pp. 567–573.

- WANG, W. and WANG, J., 2018b. Different partition of polycyclic aromatic hydrocarbon on environmental particulates in freshwater : Microplastics in comparison to natural sediment. *Ecotoxicology and Environmental Safety*, 147, pp. 648–655.
- WANG, Y. et al., 2019b. Bioaccumulation behaviour of pharmaceuticals and personal care products in a constructed wetland. *Chemosphere*, 222, pp. 275–285.
- WANG, Z. et al., 2018b. Sorption behaviors of phenanthrene on the microplastics identified in a mariculture farm in Xiangshan Bay, southeastern China. *Science of The Total Environment*, 628–629, pp. 1617–1626.
- WARD, C.J. and CODD, G.A., 1999. Comparative toxicity of four microcystins of different hydrophobicities to the protozoan, *Tetrahymena pyriformis*. *Journal of Applied Microbiology*, 86(5), pp. 874–882.
- WASEWAR, K.L., SINGH, S. and KANSAL, S.K., 2020. *Process intensification of treatment of inorganic water pollutants. Inorganic Pollutants in Water*. INC.
- WEITHMANN, N. et al., 2018. Organic fertilizer as a vehicle for the entry of microplastic into the environment. *Science Advances*, 4, eaap806
- WHO, 2021. *Toxic Cyanobacteria in Water*. 2nd ed. Edited by Ingrid Chorus and Martin Welker. *Taylor & Francis*. CRC Press.
- WILKINSON, J.L. et al., 2022. Pharmaceutical pollution of the world's rivers. *Proceedings of the National Academy of Sciences of the United States of America*, 119 (8) e2113947119
- WILLIAMS, A.T. and RANGEL-BUITRAGO, N., 2022. The past, present, and future of plastic pollution. *Marine Pollution Bulletin*, 176, 113429.

WU, C. et al., 2016a. Sorption of pharmaceuticals and personal care products to polyethylene debris. *Environmental Science and Pollution Research*, 23, pp. 8819–8826.

WU, C. et al., 2016b. Sorption of pharmaceuticals and personal care products to polyethylene debris. *Environmental Science and Pollution Research*, 23(9), pp. 8819–8826.

WU, J. et al., 2020a. Effects of polymer aging on sorption of 2,20,4,40-tetrabromodiphenyl ether by polystyrene microplastics. *Chemosphere*, 253, 126706.

WU, X. et al., 2020b. Adsorption of triclosan onto different aged polypropylene microplastics: Critical effect of cations. *Science of The Total Environment*, 717, 137033.

WU, X. et al., 2011. Mechanisms and factors affecting sorption of microcystins onto natural sediments. *Environmental Science and Technology*, 45, pp. 2641–2647.

XIANG, X. et al., 2022. Dual drive acute lethal toxicity of methylene blue to *Daphnia magna* by polystyrene microplastics and light. *Science of The Total Environment*, 840, 156681.

XIONG, X. et al., 2018. Sources and distribution of microplastics in China's largest inland lake – Qinghai Lake. *Environmental Pollution*, 235, pp. 899–906.

XU, B. et al., 2018a. Microplastics play a minor role in tetracycline sorption in the presence of dissolved organic matter. *Environmental Pollution*, 240, pp. 87–94.

XU, B. et al., 2018b. The sorption kinetics and isotherms of sulfamethoxazole with polyethylene microplastics. *Marine Pollution Bulletin*, 131, pp. 191–196.

- XU, X. et al., 2014. Establishment of a novel surface-imprinting system for melamine recognition and mechanism of template-matrix interactions. *Journal of Materials Science*, 49(7), pp. 2853–2863.
- YAKIMETS, I., LAI, D. and GUIGON, M., 2004. Effect of photo-oxidation cracks on behaviour of thick polypropylene samples. *Polymer Degradation and Stability*, 86(1), pp. 59–67.
- YAMINDAGO, A. et al., 2021. Fluoxetine in the environment may interfere with the neurotransmission or endocrine systems of aquatic animals. *Ecotoxicology and Environmental Safety*, 227, 112931.
- YANG, G.L. et al., 2013. The effect of specific surface area on the solid grafting reaction of maleic anhydride-grafted polypropylene. *Advanced Materials Research*, 781–784, pp. 385–389.
- YOUSIF, E. and HADDAD, R., 2013. Photodegradation and photostabilization of polymers, especially polystyrene: Review. *SpringerPlus*, 2(1), pp. 1–32.
- YOUSIF, E. and HASAN, A., 2015. Photostabilization of poly(vinyl chloride) – Still on the run. *Journal of Taibah University for Science*, 9(4), pp. 421–448.
- YU, F. et al., 2019. Adsorption behavior of organic pollutants and metals on micro/nanoplastics in the aquatic environment. *Science of The Total Environment*, 694, 133643.
- YU, F. et al., 2020. Adsorption behavior of the antibiotic levofloxacin on microplastics in the presence of different heavy metals in an aqueous solution. *Chemosphere*, 260, 127650.
- ZHAN, Z. et al., 2016. Sorption of 3,3',4,4'-tetrachlorobiphenyl by microplastics: A case study of polypropylene. *Marine Pollution Bulletin*, 110(1), pp. 559–563.



ZHANG, D. et al., 2020. Microplastic pollution in water, sediment, and fish from artificial reefs around the Ma'an Archipelago, Shengsi, China. *Science of the Total Environment*, 703, 134768.

ZHANG, H. et al., 2018a. Enhanced adsorption of oxytetracycline to weathered microplastic polystyrene: Kinetics, isotherms and influencing factors. *Environmental Pollution*, 243, pp. 1550–1557.

ZHANG, H. et al., 2018b. Enhanced adsorption of oxytetracycline to weathered microplastic polystyrene: Kinetics, isotherms and influencing factors. *Environmental Pollution*, 243, pp. 1550–1557.

ZHANG, H. et al., 2018c. Enhanced adsorption of oxytetracycline to weathered microplastic polystyrene: Kinetics, isotherms and influencing factors. *Environmental Pollution*, 243, pp 1550-1557

ZHANG, K. et al., 2015. Accumulation of floating microplastics behind the Three Gorges Dam. *Environmental Pollution*, 204, pp. 117–123.

ZHANG, K. et al., 2021. Understanding plastic degradation and microplastic formation in the environment: A review. *Environmental Pollution*, 274, 116554.

ZHAO, M. et al., 2022a. Characteristics and source-pathway of microplastics in freshwater system of China: A review. *Chemosphere*, 297, 134192.

ZHAO, W. et al., 2017. Deriving acute and chronic predicted no effect concentrations of pharmaceuticals and personal care products based on species sensitivity distributions. *Ecotoxicology and Environmental Safety*, 144, pp. 537–542.

ZHAO, X. et al., 2022b. Plastic waste upcycling toward a circular economy. *Chemical Engineering Journal*, 428, 131928.

ZHU, K. et al., 2020. Long-term phototransformation of microplastics under simulated sunlight irradiation in aquatic environments: Roles of reactive oxygen species. *Water Research*, 173, 115564.

ZIMMERMAN, L.R., THURMAN, E.M. and BASTIAN, K.C., 2000. Detection of persistent organic pollutants in the Mississippi Delta using semipermeable membrane devices. *Science of The Total Environment*, 248, pp. 169–179.

ZIMMERMANN, L. et al., 2020. What are the drivers of microplastic toxicity? Comparing the toxicity of plastic chemicals and particles to *Daphnia magna*. *Environmental Pollution*, 267, 115392.

## APPENDIX

**Table A3.1:** Wilcoxon rank sum test comparing the adsorption with each microplastic for each size with each microcystin analogue control. The significance level is set to 0.05. The colour red represents  $p > 0.05$ , therefore, not significantly different, the colour green represents  $p < 0.05$ , therefore, significantly different. Polyethylene terephthalate (PET), polypropylene (PP).

Solution with plastic	Control							
	MC-RR	MC-YR	MC-LR	MC-WR	MC-LA	MC-LY	MC-LW	MC-LF
Small PET	0.69000	0.36000	0.49000	0.00043	0.18000	0.00090	0.00000	0.00000
Large PET	0.89000	0.56000	0.46000	0.02500	0.09800	0.55000	0.00000	0.00000
Small PP	0.00000	0.00000	0.00000	0.00000	0.00000	0.00000	0.00000	0.00000
Large PP	1.00000	0.42000	0.38000	0.14000	0.21000	0.75000	0.00009	0.00000

**Table A3.2:** Wilcoxon rank sum test comparing the adsorption data of eight microcystin analogues with each other for adsorption onto polypropylene (PP) at the small size. The significance level is set to 0.05. The colour red represents  $p > 0.05$ , therefore, not significantly different, the colour green represents  $p < 0.05$ , therefore, significantly different.

Small PP	MC-RR	MC-YR	MC-LR	MC-WR	MC-LA	MC-LY	MC-LW	MC-LF
MC-RR	-	-	-	-	-	-	-	-
MC-YR	0.00000	-	-	-	-	-	-	-
MC-LR	0.00000	0.67000	-	-	-	-	-	-
MC-WR	0.00000	0.00000	0.00000	-	-	-	-	-
MC-LA	0.00000	0.00000	0.00000	0.00001	-	-	-	-
MC-LY	0.00000	0.00000	0.00000	0.00000	0.89000	-	-	-
MC-LW	0.00000	0.00001	0.00001	0.00000	0.35000	0.35000	-	-
MC-LF	0.00000	0.00000	0.00000	0.00000	0.89000	0.92000	0.37000	-

**Table A3.3:** Wilcoxon rank sum test comparing the adsorption of the eight microcystin variants with each other for polypropylene (PP) at the large size. The significance level is set to 0.05. The significance level is set on 0.05. The colour red represents  $p > 0.05$ , therefore, not significantly different, the colour green represents  $p < 0.05$ , therefore, significantly different.

Large PP	MC-RR	MC-YR	MC-LR	MC-WR	MC-LA	MC-LY	MC-LW	MC-LF
MC-RR	-	-	-	-	-	-	-	-
MC-YR	0.68984	-	-	-	-	-	-	-
MC-LR	0.68984	0.89362	-	-	-	-	-	-
MC-WR	0.21218	0.02923	0.02160	-	-	-	-	-
MC-LA	0.53300	0.68900	0.70000	0.01300	-	-	-	-
MC-LY	0.76299	1.00000	0.89362	0.02160	0.53300	-	-	-
MC-LW	0.06717	0.00042	0.00007	0.83579	0.00004	0.00012	-	-
MC-LF	0.02160	0.00003	0.00002	0.60483	0.00001	0.00002	0.53300	-

**Table A3.4:** Wilcoxon rank sum test comparing the adsorption of the eight microcystin variants with each other for polyethylene terephthalate (PET) at the small size. The significance level is set to 0.05. The colour red represents  $p > 0.05$ , therefore, not significantly different, the colour green represents  $p < 0.05$ , therefore, significantly different.

Small PET	MC-RR	MC-YR	MC-LR	MC-WR	MC-LA	MC-LY	MC-LW	MC-LF
MC-RR	-	-	-	-	-	-	-	-
MC-YR	0.61754	-	-	-	-	-	-	-
MC-LR	0.68984	0.87338	-	-	-	-	-	-
MC-WR	0.00024	0.00004	0.00008	-	-	-	-	-
MC-LA	0.76335	0.22554	0.20572	0.00000	-	-	-	-
MC-LY	0.76335	0.76299	1.00000	0.00000	0.17778	-	-	-
MC-LW	0.00000	0.00000	0.00000	0.25820	0.00000	0.00000	-	-
MC-LF	0.00006	0.00000	0.00001	0.61754	0.00000	0.00000	0.00018	-

**Table A3.5:** Wilcoxon rank sum test comparing the adsorption of the eight microcystin variants with each other for polyethylene terephthalate (PET) at the large size. The significance level is set to 0.05. The colour red represents  $p > 0.05$ , therefore, not significantly different, the colour green represents  $p < 0.05$ , therefore, significantly different.

Large PET	MC-RR	MC-YR	MC-LR	MC-WR	MC-LA	MC-LY	MC-LW	MC-LF
MC-RR	-	-	-	-	-	-	-	-
MC-YR	0.61754	-	-	-	-	-	-	-
MC-LR	0.68984	0.87338	-	-	-	-	-	-
MC-WR	0.00024	0.00004	0.00008	-	-	-	-	-
MC-LA	0.76335	0.22554	0.20572	0.00000	-	-	-	-
MC-LY	0.76335	0.76299	1.00000	0.00000	0.17778	-	-	-
MC-LW	0.00000	0.00000	0.00000	0.25820	0.00000	0.00000	-	-
MC-LF	0.00006	0.00000	0.00001	0.61754	0.00000	0.00000	0.00018	-

**Table A3.6:** Pearson correlation matrix of the amount of all microcystins adsorbed onto microplastic ( $\Sigma_{MC}$ ) of the experiment of section 3.3.2 and each microcystin analogue compared to the characterisation data of the virgin small and large microplastics. The characterisation data included the median size ( $D_{50}$ ), surface area ( $S_{BET}$ ), degree of crystallinity ( $X_C$ ), zeta potential measurement ( $\zeta$ ), and carbonyl index (CI). The correlation coefficient ( $r$ ) can vary between -1 (negative association) and 1 (positive association). A coefficient of  $< -0.7$  (■, red) was considered a strong the negative association, meanwhile a coefficient of  $> 0.7$  (■, green) was considered a strong positive association.

	$\Sigma$	$D_{50}$	$S_{BET}$	$X_C$	$\zeta$	CI	MC-RR	MC-YR	MC-LR	MC-WR	MC-LA	MC-LY	MC-LW	MC-LF
$\Sigma$	1.00													
$D_{50}$	-0.69	1.00												
$S_{BET}$	1.00	-0.66	1.00											
$X_C$	0.69	-0.06	0.71	1.00										
$\zeta$	0.46	-0.93	0.43	-0.29	1.00									
CI	-0.59	-0.06	-0.61	-0.99	0.41	1.00								
MC-RR	1.00	-0.66	1.00	0.70	0.44	-0.60	1.00							
MC-YR	1.00	-0.67	1.00	0.70	0.44	-0.60	1.00	1.00						
MC-LR	1.00	-0.66	1.00	0.70	0.44	-0.61	1.00	1.00	1.00					
MC-WR	1.00	-0.62	1.00	0.73	0.40	-0.64	1.00	1.00	1.00	1.00				
MC-LA	1.00	-0.66	1.00	0.71	0.43	-0.61	1.00	1.00	1.00	1.00	1.00			
MC-LY	1.00	-0.65	1.00	0.72	0.42	-0.62	1.00	1.00	1.00	1.00	1.00	1.00		
MC-LW	0.99	-0.57	0.99	0.79	0.31	-0.71	0.99	0.99	0.99	0.99	0.99	0.99	1.00	
MC-LF	1.00	-0.62	1.00	0.76	0.37	-0.67	1.00	1.00	1.00	1.00	1.00	1.00	1.00	1.00

**Table A3.7:** Pearson correlation matrix of the amount of all microcystins adsorbed onto microplastic ( $\Sigma_{MC}$ ) of the experiment of section 3.3.4 and each microcystin analogue compared to the characterisation data of the virgin small and large microplastics. The characterisation data included the median size ( $D_{50}$ ), surface area ( $S_{BET}$ ), degree of crystallinity ( $X_C$ ), zeta potential measurement ( $\zeta$ ), and carbonyl index (CI). The correlation coefficient ( $r$ ) can vary between -1 (negative association) and 1 (positive association). A coefficient of  $< -0.7$  (■, red) was considered a strong the negative association, meanwhile a coefficient of  $> 0.7$  (■, green) was considered a strong positive association.

	$\Sigma$	$D_{50}$	$S_{BET}$	$X_C$	$\zeta$	CI	MC-LR	MC-LW	MC-LF
$\Sigma$	1.00								
$D_{50}$	-0.49	1.00							
$S_{BET}$	0.89	-0.31	1.00						
$X_C$	0.40	0.08	0.66	1.00					
$\zeta$	0.02	0.10	-0.02	0.40	1.00				
CI	-0.27	-0.11	-0.12	0.43	0.14	1.00			
MC-LR	0.96	-0.39	0.91	0.45	-0.06	-0.23	1.00		
MC-LW	0.99	-0.54	0.84	0.34	0.00	-0.30	0.92	1.00	
MC-LF	0.99	-0.48	0.88	0.42	0.10	-0.26	0.94	0.98	1.00

**Table A4.1:** Pearson correlation matrix of the amount of all pharmaceuticals adsorbed onto microplastic ( $\Sigma_{PHA}$ ) compared to the characterisation data of the virgin and aged microplastics. The characterisation data included the median size ( $D_{50}$ ), surface area ( $S_{BET}$ ), degree of crystallinity ( $X_C$ ), zeta potential measurement ( $\zeta$ ), and carbonyl index (CI). Pearson correlation of log  $K_{OW}$  (related to pharmaceutical hydrophobicity) compared to the amount of each pharmaceutical adsorbed on virgin and aged particles of both sizes (small and large). A correlation coefficient ( $r$ ) can vary between -1 (negative association) and 1 (positive association). A coefficient of < -0.7 (■, red) was considered a strong the negative association, meanwhile a coefficient of > 0.7 (■, green), was considered a strong positive association.

<b>Virgin particles</b>	$\Sigma$	<i>Ofloxacin</i>	<i>Venlafaxine</i>	<i>Carbamazepine</i>	<i>Fluoxetine</i>	<i>Ibuprofen</i>	$D_{50}$	$S_{BET}$	$X_C$	$\zeta$	CI
$\Sigma$	1.00										
Ofloxacin	0.94	1.00									
Venlafaxine	0.97	0.99	1.00								
Carbamazepine	0.94	1.00	0.99	1.00							
Fluoxetine	0.71	0.61	0.61	0.61	1.00						
Ibuprofen	0.91	0.97	0.96	0.96	0.50	1.00					
$D_{50}$	-0.49	-0.32	-0.38	-0.31	-0.30	-0.44	1.00				
$S_{BET}$	0.97	0.99	1.00	0.99	0.58	0.97	-0.40	1.00			
$X_C$	0.26	0.46	0.38	0.47	0.43	0.39	0.09	0.35	1.00		
$\zeta$	-0.36	-0.14	-0.23	-0.13	-0.34	-0.15	0.78	-0.23	0.22	1.00	
CI	-0.14	-0.07	-0.08	-0.08	-0.31	-0.11	-0.12	-0.07	0.25	-0.11	1.00
<b>Aged particles</b>	$\Sigma$	<i>Ofloxacin</i>	<i>Venlafaxine</i>	<i>Carbamazepine</i>	<i>Fluoxetine</i>	<i>Ibuprofen</i>	$D_{50}$	$S_{BET}$	$X_C$	$\zeta$	CI
$\Sigma$	1.00										
Ofloxacin	0.82	1.00									
Venlafaxine	0.85	0.95	1.00								
Carbamazepine	0.80	0.85	0.74	1.00							
Fluoxetine	0.65	0.33	0.42	0.42	1.00						
Ibuprofen	0.64	0.67	0.49	0.94	0.37	1.00					
$D_{50}$	0.05	-0.29	-0.36	0.18	0.26	0.39	1.00				
$S_{BET}$	0.83	0.92	0.98	0.73	0.34	0.47	-0.39	1.00			
$X_C$	0.35	0.17	0.30	0.11	0.04	-0.04	-0.12	0.41	1.00		

ζ	-0.12	-0.34	-0.33	-0.15	-0.09	-0.06	0.68	-0.38	-0.14	1.00
CI	-0.25	-0.07	-0.09	-0.19	-0.65	-0.20	-0.32	-0.06	0.37	-0.06 1.00
<b>Log K<sub>ow</sub></b>	<b>Virgin small</b>	<b>Virgin large</b>	<b>Aged small</b>	<b>Aged large</b>	<b>Log D<sub>ow</sub></b>	<b>Virgin small</b>	<b>Virgin large</b>	<b>Aged small</b>	<b>Aged large</b>	
PP	-0.38	0.47	-0.09	0.47	PP	-0.81	-0.05	-0.52	-0.04	
PE	0.83	-	0.54	0.54	PE	0.48	-	0.00	0.00	
PET	-	-	0.21	0.21	PET	0.49	-	-0.14	-0.14	
PA	0.54	0.54	0.51	0.64	PA	0.00	0.00	0.07	0.25	
PS	0.52	-	0.36	0.37	PS	0.77	-	-0.10	-0.09	
PVC	0.49	-	0.38	0.38	PVC	-0.09	-	-0.14	-0.14	

**Table A5.1:** Pearson correlation matrix of density of the microplastics compared to size of the microplastics, the plastic concentration, the amount of fluoxetine adsorbed onto the microplastics, the amount of fluoxetine desorbed from the microplastics, the mortality of the neonates after 24 and 48 h. A correlation coefficient (r) can vary between -1 (negative association) and 1 (positive association). The correlation coefficient (r) can vary between -1 (negative association) and 1 (positive association). A coefficient of < -0.7 (■, red), was considered a strong the negative association, meanwhile a coefficient of > 0.7 (■, green) was considered a strong positive association.

	Density	Size	Plastic concentration	Amount adsorbed	Amount desorbed	Mortality (24 h)	Mortality (48 h)
Density	1.00						
Size	0.01	1.00					
Plastic concentration	0.49	0.12	1.00				
Amount adsorbed	-0.24	-0.16	-0.09	1.00			
Amount desorbed	-0.84	-0.20	-0.61	0.33	1.00		
Mortality (24 h)	-0.39	-0.41	-0.50	-0.02	0.62	1.00	
Mortality (48 h)	0.08	-0.27	-0.21	-0.16	0.20	0.40	1.00



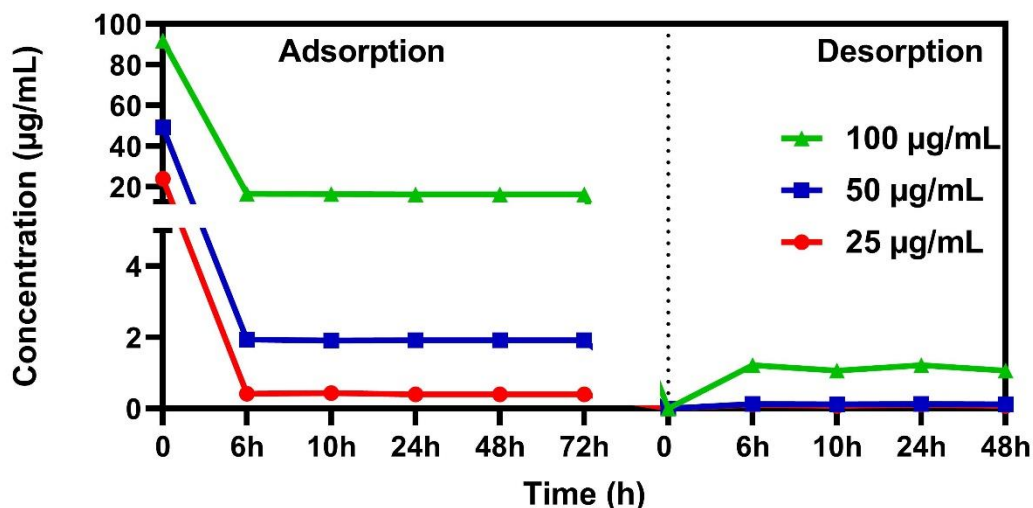


**Figure A4.1:** Concentration tests to evaluate the saturation of small PP and equilibrium time when exposed to the fluoxetine initial concentrations at 25, 50 and 100 µg mL<sup>-1</sup> in artificial freshwater + 0.02% (w/v) NaN<sub>3</sub> at 25 °C and 200 rpm.

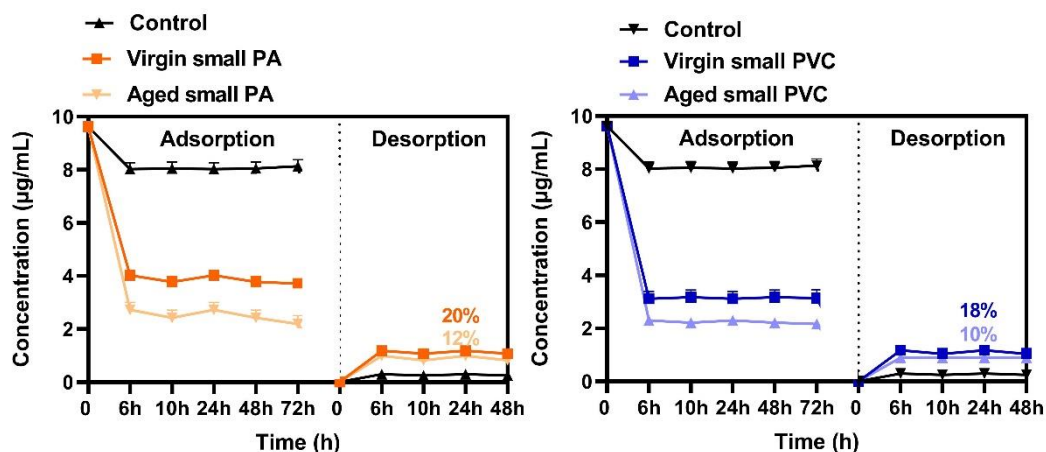


**Figure A4.2:** Concentration tests to evaluate the saturation of small PA and PVC and equilibrium time when exposed to the fluoxetine initial concentrations at 10 µg mL<sup>-1</sup> in artificial freshwater + 0.02% (w/v) NaN<sub>3</sub> at 25 °C and 200 rpm.